Late Tertiary tectonic uplift in the southern and central Appalachians

A Thesis Presented for the

Master of Science

Degree

The University of Tennessee, Knoxville

Mary Sheela Biswal

December 2015

ACKNOWLEDGMENTS

My academic endeavors in this project would not have been possible without the guidance and support of many people. I sincerely thank all my committee members. My academic advisor, Dr. Robert D. Hatcher, Jr., has been the most important person who guided me throughout this project and pushed me toward completion. Without his persistent backing and guidance, completion of this project wouldn't have been possible. Dr. Chris Fedo has provided me a lot of his time and support that have been a very key source of motivation for me. I thank him for his help and guidance in this project. Dr. Yingkui Li has been extremely helpful and kind to me, and has always been very approachable to talk and discuss anything about the project. Dr. David Prowell provided essential perspective in understanding complex aspects of this project; he has been very open in sharing his knowledge with me.

Many thanks to Andrew Wunderlich, without whose help and resourcefulness I would not have been able to complete the provisional terrace map and other digital work involving ArcGIS and Adobe Illustrator in this project. I thank Dr. Drew Coleman (UNC-Chapel Hill), Mark Pecha (Arizona LaserChron center) and Dominique Geisler (Arizona LaserChron Center) for providing their laboratory facilities and helping me with detrital zircon geochronology. I thank Latisha Brengman and Jason Muhlbauer for being helpful in my zircon analysis work. I thank Allen Patchen for helping me with catholuminescence imaging of my zircon samples. Thanks to Nancy Meadows for all her help with editing and proofreading. She has always been very kind to me and made me feel at home here. Her motivation and support have meant a lot to me. Hearty thanks to fellow Hatchlings

Kathleen Warrell, Annie Walker, Matt Huebner, Vade Scruggs, and Jake Glasbrenner for being great officemates.

Last but certainly not the least I thank my family, who have held me together in hard times. Being far away from home, my parents' strength and belief in me have given me the faith to keep moving forward and trying. I thank all my friends in Knoxville for always being there for me. My very special thank you to Ankush Singh without whose love and support I could never have made it through this journey.

ABSTRACT

The exposed Appalachian Mountains extend about 2500 km from Newfoundland to Alabama with the highest peaks >2000 m above sea level. The last orogeny that affected Appalachian crust was the 325-260 Ma Alleghanian. Even with minimal erosion rates, it is highly unlikely that the Appalachians could have sustained such elevations for over 200 m.y., suggesting that recent tectonic uplift has produced today's mountainous topography. The multiple phases of Tertiary uplift are related to poorly understood processes, but a large amount of data from today's mountain chain and the adjacent Coastal Plain indicate the present high topography is anomalous and clearly not related to Paleozoic crustal processes. Uplift signatures suggest that current topography and visible geomorphology are a product of the late Tertiary uplift.

Antecedent rivers flowing westward across very high topography in the Blue Ridge, westward-migrating drainage divide and anomalous drainage patterns are common in the southeastern Appalachians. A marked shift in high topography occurs northward from the Blue Ridge in Tennessee-North Carolina to the Valley and Ridge in Virginia-West Virginia. Evidence suggests a possible late Tertiary tectonic uplift in the southern and central Appalachians, although more data and evidence are needed to understand the uplift.

The main research problem of this project is to identify and analyze uplift signatures as recorded in lower Gulf Coastal Plain sediments and fluvial terraces along Douglas Lake, French Broad River. Detrital zircon geochronology of Miocene-Pliocene lower Gulf Coastal Plain sediments shows important age peaks at 1.0 Ga, 600 Ma, 480 Ma, 440 Ma and 300 Ma. Collective zircon data suggest a possible predominance of Appalachian provenance. This indicates occurrence of tectonic uplift in the source region during the Miocene-Pliocene,

producing exceptionally high sediment influx in the Coastal Plain during that time. Fluvial terrace mapping along Douglas Lake, Tennessee has been done with the help of vintage topographic maps and classic geologic mapping involving foot traverses. A provisional geologic terrace map at 1:24,000 scale has been produced as part of this study. Terrace mapping has helped identify five distinct terraces, resolve their relative chronology and understand the evolution of terraces along the river.

TABLE OF CONTENTS

Page Number

Page Number

Page Number

LIST OF TABLES

Page Number

LIST OF FIGURES

LIST OF ATTACHMENTS

CHAPTER I

INTRODUCTION

Brief geologic history of the southern and central Appalachians

The Appalachians extend 2500 km from Newfoundland to the north to Alabama to the south (Hatcher, 2010). The Appalachians formed during three Paleozoic orogenic events. The Appalachian Wilson cycle began in the Neoproterozoic and ended during the late Paleozoic (Hatcher, 2010). Hatcher (2010) presented a brief summary of processes, events, and elements that constitute the Appalachian Wilson cycle. The Taconic orogeny occurred during the Ordovician (480-440 Ma) and involved arc accretion (Hatcher, 1989; van Staal and Hatcher, 2010). The Acadian-Neoacadian orogeny occurred in the Late Devonian and early Mississippian (400-345 Ma), involving transpressional N-to-S zippered collision (Hatcher, 1989, 2010). During this orogenic event, the Carolina superterrane collided with the southern and central Appalachians with a coeval collision of the Avalon-Gander superterrane with the New England Appalachians (Hatcher, 1989, 2010). The third orogeny occurred during the late Paleozoic from the late Mississipian into the Permian (331-252 Ma), during which Laurentia, including all previously accreted Appalachian terranes, collided with Gondwana to create supercontinent Pangea (Hatcher, 1989, 2010). Breakup of Pangea occurred during the latest Triassic (~200 Ma), forming the Atlantic Ocean (Wilson, 1966; Phillips and Forsyth, 1972; Hatcher, 2010). The post-rift Appalachians went through multiple phases of tectonic uplift, intense weathering, and rapid erosion in the Triassic (Poag and Sevon, 1989). Even with minimal erosion rates, the

Appalachians are unlikely to have remained high for more than ~65 m.y. (Late Cretaceous to present).

Geologic and geomorphic setting

Southern Appalachian topography extends from south of the New River Valley in West Virginia southward to Alabama. The study area broadly includes part of the southern Appalachians and part of the Gulf Coastal Plain. The central Appalachians stretch from the Hudson Valley in New York to the New River Valley in Virginia and West Virginia. The southern Appalachians lie south of the New River Valley, consisting of the Piedmont, Blue Ridge, Valley and Ridge, and Cumberland Plateau physiographic provinces. The highest peak today in the Appalachians is Mt. Mitchell in North Carolina, 2042 m above sea level. The Appalachian Mountains have been a source of sediments carried by the westward-flowing rivers during and after the Mesozoic into the Gulf of Mexico basin (Galloway et al., 2011).

Cenozoic tectonism in southern and central Appalachians

Various kinds of geologic evidence in the Appalachians provide signatures of recent uplift and tectonic activity. The ruggedness and high elevations of the present-day southern and central Appalachians (Fig. 1-1) contradict the formerly widely accepted idea that the Appalachians are a slowly eroding mountain chain that has survived and persisted in a state of dynamic equilibrium since the late Paleozoic (Spotila et al., 2004). Debates that surround the idea of probable tectonic forces affecting the Cenozoic southern and central Appalachians (Pazzaglia and Brandon, 1996; Spotila et al., 2004; Gallen et al., 2011, 2013; Prince et al., 2011) suggest that the Appalachians are currently in a transient state of

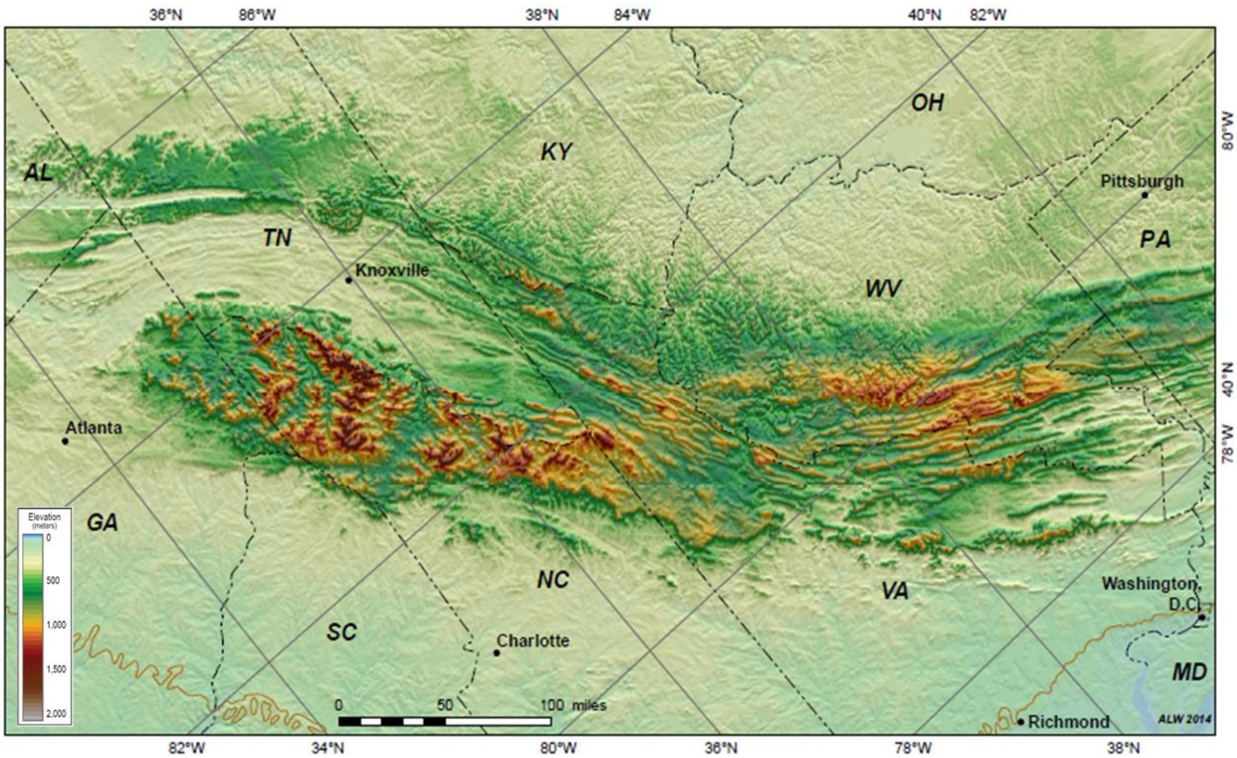

Figure 1-1. Digital Elevation Model (DEM) of the southern and central Appalachians. Note the overall high relief in the region and shift in high topography from TN-NC to VA-W VA. Compiled by Andrew. L. Wunderlich, 2014. Elevation data from USGS Global Topography dataset (GTOPO).

adjustment to a younger base level (Pazzaglia and Brandon, 1996; Gallen et al., 2011), and are still progressing toward dynamic equilibrium (Gallen et al., 2013).

Mean denudation rate is directly proportional to mean relief (Ahnert, 1970). With denudation processes and isostatic compensation, the relief of a region is reduced by ~90 percent in 18.5 m.y. (Ahnert, 1970). Consequently, the southeastern Appalachians should have acquired flat topography several times after the Paleozoic crustal processes ceased (Ahnert, 1970; Hack, 1982). There still, however, is an average relief of 1400 m in the Blue Ridge in Tennessee and North Carolina (Gallen et al., 2013), which indicates that there must be driving forces other than just isostatic compensation and denudation processes.

Research problem

The primary research goal of this project is to identify and analyze uplift signatures recorded in the lower Gulf Coastal Plain sediments and fluvial terraces along Douglas Lake, French Broad River. Uplift of the southern-central Appalachians is related to late Tertiary tectonic rejuvenation, and is possibly a product of lithospheric processes; present-day topography is only consequential (Hatcher et al., 2013). Previous literature documents geologic evidence and data related to the tectonic uplift in the southern and central Appalachians (Hack, 1982; Pavich, 1984; Prowell and Christopher, 2006, 2010); however, more data are needed to understand the uplift.

Goal of Gulf Coastal Plain study

The Gulf Coastal Plain has been the primary repository of sediments from the interior of the North American continent throughout the Mesozoic and Cenozoic. There were 14 depositional episodes, each lasting 3 ± 1 m.y., and five tectono-climatic episodes along five fluvio-deltaic axes over the last 65 m.y. that recorded differences in sedimentation patterns (Galloway et al., 2011). The Mississippi, Red, and Tennessee fluvio-deltaic axes were especially active during the late Tertiary, indicating an increased sediment influx into the Gulf Coastal Plain during this time. Sediment volume was calculated for each depositional episode; tectonism, climate change, and drainage basin evolution have been deciphered by Galloway et al. (2000) with the help of sedimentation history along the northern Gulf of Mexico basin margin.

Sediment volume was highest during the Late Cretaceous to early Paleocene, late Eocene, and Miocene. Tectonic disturbance in the source mountains is directly related to changes in sedimentation patterns, rates, and fluxes in the depositional basin. I analyzed late Tertiary sediment samples from the Gulf Coastal Plain in southern Mississippi, Alabama, and western Florida to determine the provenance of detrital zircons in the sediments. Identifying the source of the sediments has assisted in relating the late Tertiary deposition with the possible tectonic uplift in the source terrains. U-Pb geochronology was performed to determine ages of detrital zircons in sediment samples and decipher provenance of the sediments.

Goal of study in Douglas Lake, French Broad River, TN

Fluvial terraces are abandoned floodplains preserved at higher elevations as the river cuts its channel down as it flows downstream. Terrace deposits are usually composed of sedimentary material transported by the river. Formation of fluvial terraces is usually caused by a major climate change or a tectonic uplift (Pazzaglia, 2013). In the southern and southeastern Appalachian Mountains, fluvial terraces are indicators of the ongoing uplift produced by active tectonic processes. Fluvial terraces are landforms that integrate erosional and depositional processes as the river forms its valley. They are very common along the rivers in the southeastern Appalachians, and are an important place to study uplift history. Accurate dating of terrace deposits can delimit the incision rate of the stream system, timing of events that control incision rates, and response time of a fluvial system to uplift within the drainage basin (Repka et al., 1997). Because terraces form as a result of downcutting, the oldest age obtained on the terraces would be equal to or less than the age of the latest uplift event. This would again delimit the timing of uplift. Older terraces occur at a higher elevation than younger terraces. The goal was to map and correlate the fluvial terraces at Douglas Lake along the French Broad River to gain a perspective of the timing of the tectonic uplift of the southern and central Appalachians.

CHAPTER II

REVIEW: EVIDENCE OF LATE TERTIARY TECTONIC UPLIFT IN THE APPALACHIANS

Changes in southern and central Appalachians geomorphology

Topography and relief

Topographic profiles in the Blue Ridge and Piedmont in the southern and central Appalachians show an increase in steep gradients, migrating knick points, incised river gorges, frequent landslides/mass wasting events, and a 150 percent increase in relief since the Miocene (Gallen et al., 2013). Some geomorphic indicators of late Tertiary rejuvenation in the southern and central Appalachians are: (1) rugged youthful topographic expression of the eastern Blue Ridge escarpment (BRE) and other parts of the Blue Ridge and Valley and Ridge; (2) westward migration of the continental drainage divide (Fig. 2-1); (3) standard paleo-lake and sinkhole sediment traps suggesting inverted topography (Prowell and Christopher, 2006; Ochoa et al., 2012); (3) anomalous drainage patterns; (4) northward shift of high topography from the eastern Blue Ridge to the Valley and Ridge (see Fig. 1-1; Hatcher et al., 2013); and (5) high remnant river terraces in the southern and central Appalachians.

Continental drainage divide migration and stream capture

Major westward-draining rivers have headwaters in the eastern Blue Ridge and western Piedmont and drain across the high topography (Fig. 2-1); westward-migrating drainage divides and anomalous drainage patterns indicate that topography is not controlled by Paleozoic and early Mesozoic tectonics. High topography shifts from

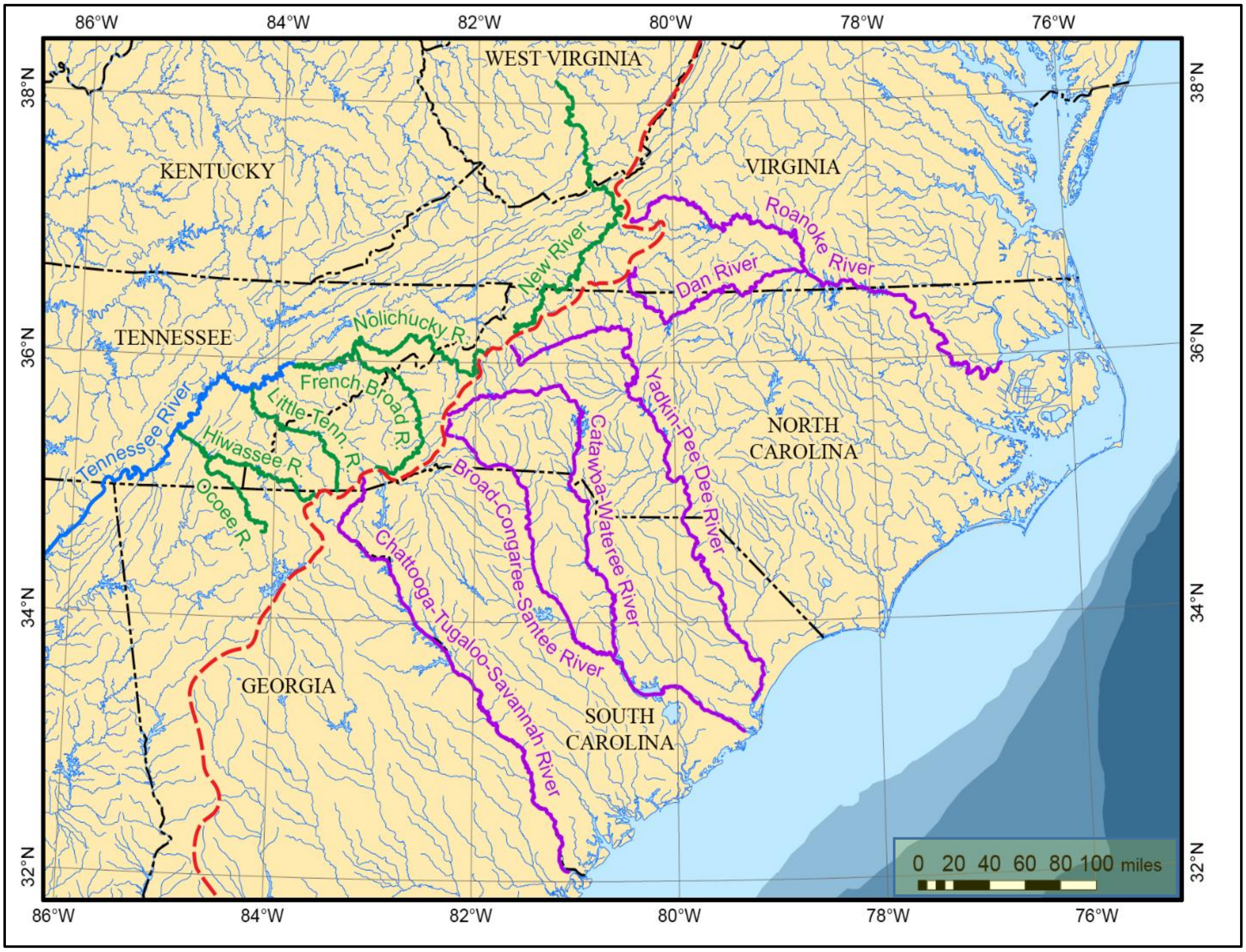

Figure 2-1. Rivers draining the southeastern Appalachians. Drainage divide is shown by dashed red line. Rivers on the westward side of the drainage divide drain into the Gulf Basin (shown in green). Rivers on the eastward side of the drainage divide drain into the Atlantic Basin (shown in magenta). Source: Hydrologic data from USGS, National Atlas, scale 1: 1,000,000. Graphic by Andrew L. Wunderlich.

the Blue Ridge in Tennessee-North Carolina to the Valley and Ridge in Virginia-West Virginia (see Fig. 1-1), and is a result of tectonic uplift.

Steep segments of topographic profiles in rivers draining the southern and central Appalachians are indicative of the active incision and youthful characteristics of the streams. As the uplift occurs in the eastern part of the southern Appalachians, the drainage divide progressively migrates westward (Fig. 2-1). Active uplift also impacts the valley gradient and overall topographic profiles of the eastward Atlantic draining rivers, which produce steeper slopes and sharp elevation drops in the headwaters regions (Fig. 2-2). Gulf Basin draining rivers, on the other hand, produce gentler slopes and lower valley gradients in their headwaters regions (Fig. 2-2).

Uplift-related occurrence of stream dissection and captures are common in the southern and central Appalachians. The Dan River drains northward into upland areas and captures the former headwaters of Reed Island Creek, which earlier flowed close to the Blue Ridge escarpment crest; anomalous stream patterns and relation to the crest of the escarpment suggest stream capture (Hack, 1982). Some other examples of stream capture in the southeastern Appalachian Blue Ridge are: capture of Chattooga River by the Tugaloo River; abrupt southeastern turn of the Chauga River where it cuts a steeper valley and deeper gorge; and capture of Laurel Creek where it enters Chauga River in an upstream direction (Acker and Hatcher, 1970). Terrace deposits are commonly present in areas of stream capture (Acker and Hatcher, 1970), indicating ongoing uplift of mountains.

Antecedent rivers, wherein rivers maintain their older course on a more recent uplifted surface, are seen in the Appalachian Mountains. The New River flows along a northwestward antecedent course in Virginia across the Valley and Ridge and then

Figure 2-2. Topographic profiles of rivers draining into the Gulf of Mexico basin (green) and Atlantic basin (purple). Topographic profiles generated by Andrew L. Wunderlich in ArcView using GTOPO30 DEM of the southern and central Appalachians.

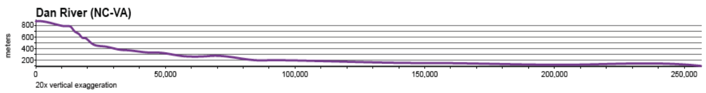
Dan River (NC-VA)
meters
20x vertical exaggeration

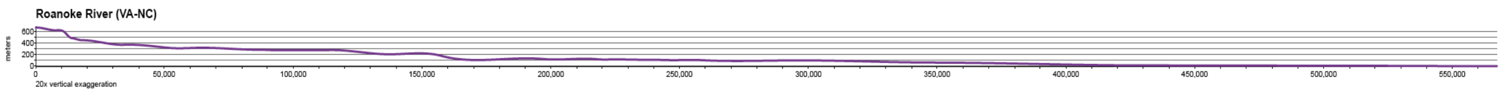
Roanoke River (VA-NC)
meters
20x vertical exaggeration

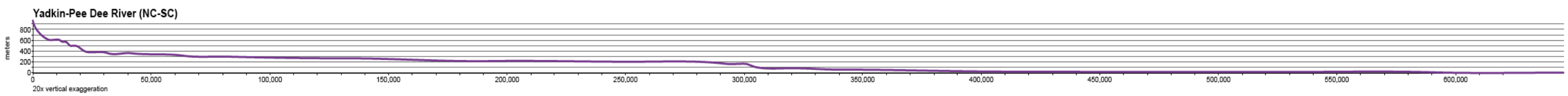
Yadkin-Pee Dee River (NC-SC)
meters
20x vertical exaggeration

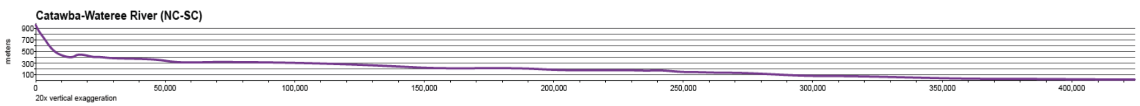
Catawba-Wateree River (NC-SC)
meters
20x vertical exaggeration

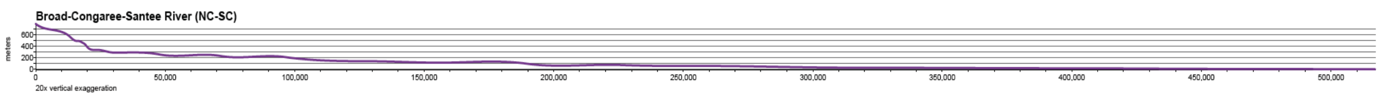
Broad-Congaree-Santee River (NC-SC)
meters
20x vertical exaggeration

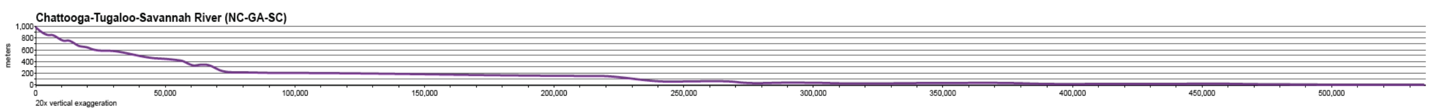
Chattooga-Tugaloo-Savannah River (NC-GA-SC)
meters
20x vertical exaggeration

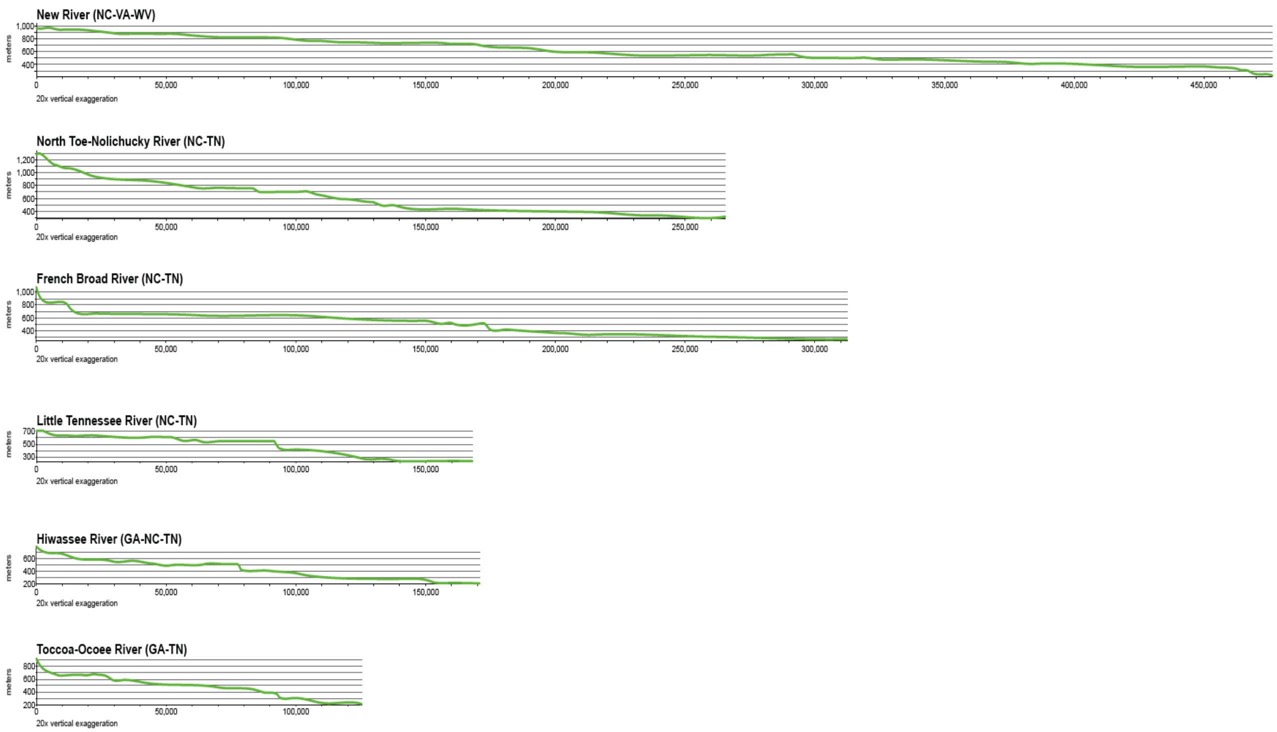
New River (NC-VA-WV)
meters
1,000
800
600
400
0
50,000
100,000
150,000
200,000
250,000
300,000
350,000
400,000
450,000
20x vertical exaggeration
North Toe-Nolichucky River (NC-TN)
meters
1,200
1,000
800
600
400
0
50,000
100,000
150,000
200,000
250,000
20x vertical exaggeration
French Broad River (NC-TN)
meters
1,000
800
600
400
0
50,000
100,000
150,000
200,000
250,000
300,000
20x vertical exaggeration
Little Tennessee River (NC-TN)
meters
700
500
300
0
50,000
100,000
150,000
20x vertical exaggeration
Hiwassee River (GA-NC-TN)
meters
600
400
200
0
50,000
100,000
150,000
20x vertical exaggeration
Toccoa-Ocoee River (GA-TN)
meters
800
600
400
200
0
50,000
100,000
20x vertical exaggeration

continues westward to join the Ohio River watershed. The French Broad River also flows along an antecedent path from southeast to northwest across high topography in the Appalachian Mountains. The Tennessee River originates at the confluence of the Holston and French Broad Rivers at Knoxville, in eastern Tennessee, and then flows southwestward toward the Gulf basin. The Tennessee River flows through regions of different topography and time; the complexity of the river course is explained either by superposition or an antecedent pattern, or a stream capture mechanism, which are all products of uplift (White, 1904; Milici, 1968). Westward migration of the regional drainage divide along the Blue Ridge Escarpment in Virginia is a result of inland escarpment retreat (Prince et al., 2010; Spotila and Prince, 2012), which is possibly related to uplift of mountains in the eastern part of the southern Appalachians. Abandoned river terrace deposits, pebbles, and gravel atop the Blue Ridge Escarpment suggest beheaded, underfed stream channels (Prince et al., 2011), and indicate major transient incision due to tectonic uplift. Relict terraces and the associated beheaded drainages indicate the role of large stream capture events in producing ongoing escarpment retreat through landward divide migration and subsequent topographic adjustment (Prince et al., 2010). Incision driven by stream capture in the Roanoke River basin has produced a rapid base-level drop, leading to migration of knick points and relict remnant surfaces to higher elevations (Prince et al., 2011; Spotila and Prince, 2012; Gallen et al., 2013).

Fluvial terraces

Cosmogenic ^{10}Be ages for New River, Virginia, river terraces at 10, 20, and 50 m above river yield are about 130, 600, and 950 ka, respectively (Ward et al., 2005). These ages yield an incision rate of 43 m/m.y., although the last one m.y. yields rates of about 100 m/m.y. (Ward et al., 2005). These data suggest an episodic nature of incision history. Extended periods of aggradation and terrace formation occurred between the events of high river incision. These ages indicate pulses of uplift that occurred during the Quaternary. The periodic nature of uplift might be indicative of intermittent tectonism (Ward et al., 2005). Oldest Optically Stimulated Luminescence (OSL) ages of terrace deposits at Douglas Lake, French Broad River are 203±13 ka, indicating that the uplift occurred at least 203±13 ka in this area (Hatcher et al., 2012).

Cosmogenic ^{10}Be and ^{26}Al ages of cave sediments along the western margin of the Cumberland Plateau correspond with terrace deposit ages along the Cumberland River (Anthony and Granger, 2004). These cave sediments are ~5.7 Ma and are in step with incision of the Upper Cumberland River (Anthony and Granger, 2004). Although there is no direct evidence that links the Cumberland Plateau with the uplift in the Blue Ridge and Piedmont, there may be some possibility that cave sediment age may be related to age of uplift in the southeastern Appalachians.

River incision rates and ages

River incision rates and strath terrace patterns in the Susquehanna and Potomac Rivers indicate that bedrock has been periodically incised at very fast rates (Reusser et al., 2004, 2006). Intermittently high river incision rates suggest periodic rejuvenation of the Appalachian Mountains during and after the late Tertiary.

Alternative ideas for the intermittent high river incision rates have been proposed; for instance, Reusser et al. (2004) suggested that glacial forebulge uplift could have helped maintain high rates of incision. However, inconsistency in the timing, patterns, and rates of bedrock incision suggest the activity may have been unrelated to glacial climate changes and more likely caused by tectonic uplift. Timing and rate of downcutting from ^{10}Be cosmogenic ages are similar on the glaciated Susquehanna and unglaciated Potomac Rivers, indicating that regional changes, not simply glacial meltwater, initiated incision (Reusser et al., 2004, 2006).

Westward- and southwestward-flowing rivers such as the French Broad and Tennessee exhibit meandering patterns throughout their course, indicating a mature stage of river development. The channel sides and beds, however, produce sharp downcutting valleys and deep gorges, which apparently are younger than the rivers. Occurrence of younger characteristics within older river valleys is indicative of probable tectonic uplift (Acker and Hatcher, 1970; Pazzaglia and Brandon, 1996; Spotila et al., 2004).

Thermochronologic and fission track ages of Coastal Plain sediments

Spotila et al. (2004) stated that an escarpment that has undergone tectonic uplift in the process of landscape evolution shows seaward-younging patterns of low-temperature cooling ages in the Coastal Plain, indicating a large amount (2-4 km) of exhumation and erosional origin rather than rift-related thermal transients. Apatite-He and apatite fission track ages are oldest atop the Blue Ridge Escarpment (200-120 m.y.) and decrease in age eastward (100-70 m.y.), suggesting denudation associated with erosional retreat of the escarpment. Significantly younger ages may have been caused by higher erosion rates that produced the high escarpment (Spotila et al., 2004). Apatite fission track ages indicate slow regional uplift in the northern Blue Ridge after the Early Jurassic (Naeser et al., 2005). Long-term erosional retreat and greater exhumation of younger ages in the region due to topographically warped isotherms prior to escarpment retreat suggest that the ages could be due either to a more rapid erosion rate or to recent resurgence of southeastern Appalachian topography (Spotila et al., 2004).

Sediment blanket in Appalachian Piedmont and Coastal Plain strata

Part or all of the outer Piedmont was covered by marine and non-marine clastic sediments of Cretaceous or younger age during the Cenozoic (Pavich, 1984). Examples of localities that record Late Cretaceous and Tertiary sediment thickness of at least 50-60 m deposited on Piedmont metamorphic rocks are: Warm Springs, Georgia and Fall Line, Virginia (Pavich, 1984; Prowell and Christopher, 2006). Hack (1982) suggested that the sediment blanket that existed in the early Cenozoic had been partially or fully removed in Alabama, Georgia, and South Carolina during the post-Paleocene. However, sediment cover in the Appalachian Piedmont of Virginia and Maryland were preserved until the late Tertiary; for example, marine Eocene limestone occurs at 150 m elevation in Raleigh, North Carolina, suggesting the region was at sea level during the early Tertiary, but later was uplifted (Hack, 1982; Prowell and Christopher, 2006). Differences in timing of removal of the sedimentary cover in various parts of the southern and central Appalachians indicate that processes responsible for removal of the sediment cover occurred selectively and in multiple episodes in the Tertiary (Hack, 1982; Pavich, 1984). This indicates Tertiary uplift in the southern and central Appalachians occurred in multiple episodes.

Configuration of the fall line between the Piedmont and Coastal Plain along with Cretaceous and younger marine deposits occurs up to 300 m above present sea level (Prowell and Christopher, 2006). In addition, terrestrial Cretaceous and early Tertiary sediment traps occur as high as 685 m can be found in northern Georgia, Alabama, eastern

Tennessee, western Virginia, and Pennsylvania (Prowell and Christopher, 2006), suggesting that a young sedimentary cover once covered the present Blue Ridge. This suggests that, as the ancestral mountains eroded, the modern Blue Ridge was tectonically uplifted to its present elevation. Coastal Plain strata were derived by regional erosion during the Mesozoic and Cenozoic, and pre-date the uplift that occurred in the late Cenozoic (Prowell and Christopher, 2006).

Cenozoic faults

Cenozoic faults are common in Coastal Plain strata and a few displace young sediments (Prowell, 1983). This is possibly produced by the late Tertiary tectonic uplift. The Washington, D.C., fault zone contains several examples of these faults. These faults vertically displace the contact between late Pliocene terrace gravels and Paleozoic crystalline rocks by a few meters in some areas, while they displace contacts between Paleozoic metamorphic rocks and Cretaceous deposits by a few meters in other places (Prowell and Christopher, 2010). A study of faults at Warm Springs, Georgia, shows that reverse faults displace both Paleocene non-marine sediments and Pliocene deposits by a few meters (Reinhardt et al., 1984). Sedimentation near Warm Springs, Georgia, forms an aggrading system; faulting and subsequent erosion developed in response to the tectonic environment and have changed the local drainage and depositional environment (Reinhardt et al., 1984).

Palynological record

Palynological age of pollen in sediment traps occurring at high elevations inland within the mountains, correlate with Coastal Plain formations suggesting that the Coastal Plain formations extended farther inland during the Tertiary period (Prowell and Christopher, 2006). Age of these sediments ranges from Late Cretaceous to Eocene (40 Ma) (Prowell and Christopher, 2006). These sediments traps are up to 100 m thick, which is greater than the minimum thickness that can be preserved with minimal erosion rates (3 m/ m.y.) over the time since they deposited (Prowell and Christopher, 2006). This indicates that they were possibly preserved in areas not subject to erosion and were uplifted much later than the Eocene (Prowell and Christopher, 2006). The palynological record from the Gray fossil site (karst lake), Tennessee, dates the oldest sediments at Paleocene-Eocene and youngest at Miocene-Pliocene (Ochoa et al., 2012), indicating that the most recent uplift possibly occurred during the Miocene-Pliocene.

Analysis: Implications of existing geomorphic evidence

Comprehensive evidence of the late Tertiary tectonic uplift in the southern and central Appalachians is complex and expansive. Even though there is substantial geomorphic evidence indicating possible tectonic uplift, it is not enough to unequivocally stand alone. Additional evidence is needed from various other geologic perspectives. Although the current geomorphic and other geologic evidence suggests late Tertiary tectonic uplift, I do not think it is entirely conclusive and does not provide an exclusively unique solution to the geomorphic anomalies observed in the southern and central Appalachians. Recent evidence (White, 1904; Milici, 1968; Acker and Hatcher, 1970; Hack, 1982; Prowell, 1983; Pavich, 1984; Reinhardt et al., 1984; Reusser et al., 2004, 2006; Spotila et al., 2004; Ward et al., 2005; Prowell and Christopher, 2006, 2010; Prince et al., 2010, 2011; Ochoa et al., 2012; Spotila and Prince, 2012; Gallen et al., 2013) strongly indicate that the late Tertiary Appalachians underwent uplift that has produced the topography we see today. The uplift is likely driven by tectonic forces or deep crustal lithospheric processes, although this requires more geologic evidence and additional geophysical data.

Steep headward topographic profiles in the southern and central Appalachians are related to very rapid erosion and fast incision of valleys, clearly representing an active and young mountain chain. Older, mature landscapes typically consist of gentler topographic profiles and broader valleys, unlike several parts of the southern and central Appalachians. Uneven young topography of the current Appalachians puts forth two possibilities: (1) the mountains have been in a constant state of formation since the Paleozoic; or (2) cessation of mountain building activities occurred at the end of the Paleozoic era, which was followed by subsequent erosion and flattening during the Mesozoic and early Tertiary. This was followed by several episodes of accelerated uplift and erosion that produced the uneven topography seen today.

The first possibility can be disregarded, because the mountain-building process ceased at the end of Alleghanian orogeny during the early Permian. Additionally, it is unlikely that any orogen remains in a continuous state of mountain-building and uplift with no erosion or other tectonic processes. Hence, the mountains have uplifted in episodes of accelerated and active phases of rejuvenation. Conspicuously high peaks in the Blue Ridge and Valley and Ridge are most likely a product of the latest episode of mountain uplift. Uplift definitely affects regional drainages and river valleys. Drainage network changes have been discussed in this chapter (e.g., stream captures, drainage divide migration). Uplift-related base-level changes produce accelerated incision in river valleys that subsequently produces fluvial terraces along the rivers draining the southern and central Appalachians. Fluvial terrace deposits also provide information about source regions located at much higher elevations upstream of the current floodplain.

There is no direct evidence of climate influencing these geomorphic anomalies, eliminating other possible causes of the uplift. Quantitative studies indicate most uplift-related sedimentation pulses during the Tertiary in the Atlantic margin basins have been produced by rapid, short-lived sources that do not relate to climatic episodes (Pazzaglia and Brandon, 1996). Inconsistencies in timing and rate of incision in glaciated and unglaciated rivers also suggest that uplift in this region is independent of climate (Reusser et al., 2004, 2006).

Tectonic displacements are sustainable evidence for uplift. Active uplift is likely to produce faulting in the preexisting terrane that would displace younger strata. This is observed in the areas discussed by Reinhardt et al. (1984) and Prowell and Christopher (2010).

Uplift inarguably displaces younger and raises older sedimentary deposits/fossils to higher elevations. This is observed in the older Cretaceous marine deposits discussed by Prowell and Christopher (2006). Isolated sediment trap ages correlate chronologically with Coastal Plain strata, which provide reasonable evidence for uplift.

Current regional and geomorphic evidence are certainly admissible in support of late Tertiary tectonic uplift, although additional data are required to fully understand the southern and central Appalachian uplift.

Analysis: Differential uplift in Blue Ridge and Piedmont

Landscape evolution

Various models of landscape evolution in the southern and central Appalachians were discussed by Verhoogen et al. (1970) and Hack (1982). Processes that produce adaptive landscapes are closely connected to evolving geomorphology of a geologic system. Equilibrium is the central concept around which all models of landscape evolution revolve as they try to attain absolute stability. Any combination of non-linear erosion and relatively constant or accelerated uplift is possible as long as erosion does not greatly exceed uplift for a very long time and the landscape eventually progresses toward equilibrium. Causes and duration of multiple phases of accelerated Tertiary uplift in the southern and central Appalachians are complicated and not presently understood. Erosion and uplift have been in and out of balance at various times and areal extent during the Cenozoic, producing the highly rugged topography inside the mountain chain. An important question to be addressed in the beginning of the Appalachian uplift research was whether the driving force of the southern and central Appalachian system was tectonic processes, or whether erosion and denudation were the driving force, producing isostatic uplift in response (Pavich, 1984). Another cause driving the uplift could be changes in the Cenozoic climate. However, the areal extent and timing of topographic rejuvenation does not support late Cenozoic (<4 myr) climate change to be the fundamental driver of relief enhancement in the southern Appalachians (Hack, 1982; Gallen et al., 2013).

Mean denudation rate is directly proportional to mean relief (Ahnert, 1970). With denudation processes and isostatic compensation, the relief of a region is reduced by 90 percent in 18.5 m.y. (Ahnert, 1970). Consequently, the southeastern Appalachians should have been peneplaned in the last 200 m.y. since the mid-Mesozoic (Ahnert, 1970; Hack, 1982). However, there still is relief of >1400 m in the Blue Ridge (Gallen et al., 2013), which indicates that there must be driving forces other than just isostatic compensation and denudation processes. This indicates that current uplift rates and amounts exceed uplift due to just isostatic compensation. Although conspicuously high areas in the Inner Piedmont do contain resistant units, the same units also occur in low relief areas; the relation between topographic forms and rock type suggests that both tectonic forces and rock control have operated to produce present landforms, tectonic forces playing a major role (Hack, 1982).

Comparison of relief in Blue Ridge and Piedmont

The southern and central Appalachians are not in steady-state equilibrium, as evidently seen in the high topography and uneven relief in the Valley and Ridge and the Blue Ridge; however, the Piedmont has relatively lower relief and topography that gives the impression that the Piedmont may be in steady state equilibrium. Isostatic compensation for mass lost by weathering and erosion has been a major component of continued uplift of the Piedmont through the Cenozoic (Pavich, 1984). A steady-state system of weathering, erosion, and isostatic uplift has operated since the end of the Mesozoic that has produced the lower relief and topography (Pavich, 1984). Average elevation in the Appalachian Piedmont is about 194 m, while average elevation in the Blue Ridge Mountains is 770 m.

It is unlikely that the late Tertiary uplift is locally confined only to the Blue Ridge and Valley and Ridge. Although surface relief in the Appalachian Piedmont is not as high and uneven as in the Blue Ridge Mountains, in all likelihood tectonic processes must affect the entire southern and central Appalachian region similarly. Therefore, it appears that short accelerated spans of regional uplift have affected but not produced a visible difference in the overall topography of the Piedmont. It follows that landscape evolution has been different in the Piedmont than the interior of the mountains possibly because of differential erosion and consequent equilibrium in the Piedmont. Significant erosion-uplift balance in the Piedmont has persisted despite the ongoing uplift, thus maintaining the overall uniform topography.

Uplift and erosion rates in Piedmont

Uplift rates in the southern and central Appalachians were 200 m/m.y. during the Paleozoic and about 25 m/m.y. in the Cenozoic (Pavich, 1984). The true average uplift rate for the Piedmont is 10-40 m/m.y. in the Cenozoic (Pavich, 1984). Fission track data of zircon, sphene and apatite (Durrant, 1978; Pavich, 1984) in the Piedmont indicate that there must have been 2-3 km of uplift during the Cenozoic, however, the highest elevation in today's Piedmont is only 500 m. Since the actual elevation is much less than the anticipated highest elevation, this indicates that erosion has exceeded uplift in the Piedmont (Pavich, 1984). Data also indicate that there is a crude mass balance between material eroded from the Appalachians and that trapped on the continental shelf (Pavich, 1984). Variable stream erosion (4.6-48 m/m.y.) can be seen in the Piedmont that is likely due to epeirogenic uplift relative to a eustatically fluctuating base; this is possibly related to the tectonic uplift in the Tertiary (Pavich, 1984). Based on sediment volume data, erosion of 1.6 km^3/km^2 occurred throughout the Cenozoic, indicating that average erosion rates in the Piedmont were 27 m/m.y. over the Cenozoic (Pavich, 1984). Similarity in the range of rates of uplift and erosion for the Appalachian Piedmont suggests a balance among weathering, erosion, and uplift rates (Pavich, 1984). Therefore, long-term uplift and erosion over the Cenozoic have been balanced in the Piedmont to produce the relatively uniform topography seen today.

CHAPTER III

PROVENANCE OF LOWER GULF COASTAL PLAIN SEDIMENTS AND ZIRCON SEPARATION FROM SEDIMENT SAMPLES

Why study Gulf Coastal Plain sediments?

The main reason for studying sediments from the lower Gulf Coastal Plain is that it is the sink for sediments transported from much of North America, thereby recording the Cenozoic history of sedimentation along the southern North American continental margin. Sedimentation history may be related to the tectonic processes. The Gulf of Mexico has been the principal repository of sediments derived from interior North America for 250 m.y., composed of North American clastic sediments and carbonates deposited during and after the Mesozoic. Although multiple sources across the North American continent have contributed to the sediment strata in the Gulf Coastal Plain, the southern and central Appalachians have been a major source of sediments from eastern North America. Influx of significant amounts of detrital material had largely ceased by the end of the Cretaceous and was essentially absent by the mid Cenozoic (Fig. 3-1), but it increased again in the Miocene (Fig. 3-1; Gibson, 1970). The increase in sedimentation during the Miocene was likely caused by increased sediment influx from the Appalachian source terranes, indicating greater erosion during that period; greater erosion may be related to the exposure of Appalachian source rocks caused by late Tertiary tectonic uplift.

Miocene-Pliocene age deposits were of interest for this study because distinct episodes of clastic sediment deposition occur during this time (Galloway et al., 2011) and very thick

Figure 3-1. Tertiary depositional history of the Gulf of Mexico (GOM). Figure shows active fluvio-deltaic axes, source and sink areas and various depositional episodes during the Tertiary. Fluvio-deltaic axes: Rio Bravo (RB), Rio Grande (RG), Guadalupe (G), Colorado (C), Houson-Brazos (HB), Red (R), Mississippi (MS), Tennessee (TN) (from Galloway et al., 2011). Time units from Geologic Society of America Geologic Time Scale, 2012.

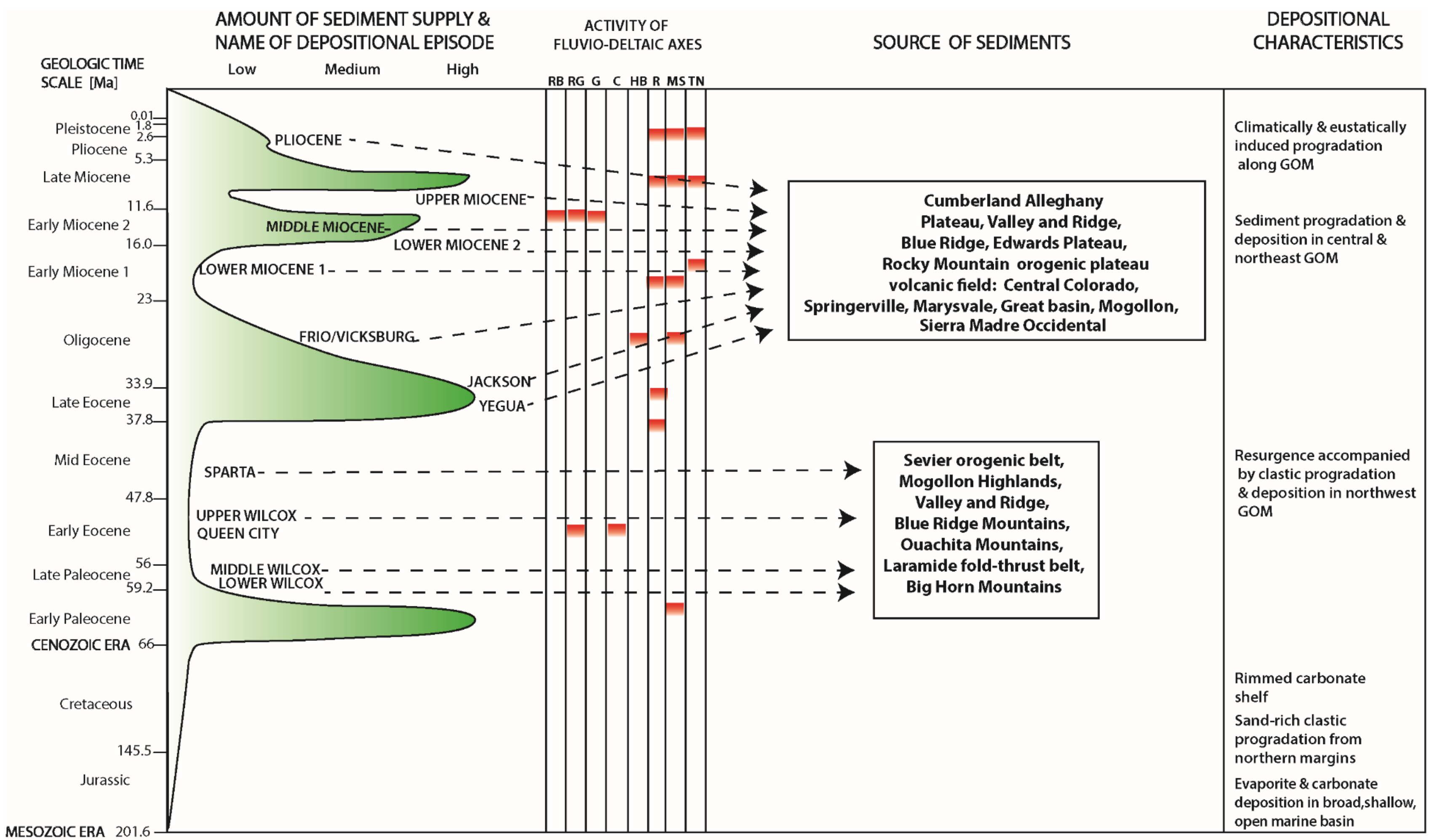
GEOLOGIC TIME SCALE [Ma]
AMOUNT OF SEDIMENT SUPPLY & NAME OF DEPOSITIONAL EPISODE
Low
Medium
High
ACTIVITY OF FLUVIO-DELTAIC AXES
RB RG G C HB R MS TN
SOURCE OF SEDIMENTS
DEPOSITIONAL CHARACTERISTICS
Pleistocene
Pliocene
Late Miocene
Early Miocene 2
Early Miocene 1
Oligocene
Late Eocene
Mid Eocene
Early Eocene
Late Paleocene
Early Paleocene
CENOZOIC ERA
Cretaceous
Jurassic
MESOZOIC ERA
0.01
1.8
2.6
5.3
11.6
16.0
23
33.9
37.8
47.8
56
59.2
66
145.5
201.6
PLIOCENE
UPPER MIOCENE
MIDDLE MIOCENE
LOWER MIOCENE 2
LOWER MIOCENE 1
FRIO/VICKSBURG
JACKSON
YEGUA
SPARTA
UPPER WILCOX
QUEEN CITY
MIDDLE WILCOX
LOWER WILCOX
Cumberland Alleghany Plateau, Valley and Ridge, Blue Ridge, Edwards Plateau, Rocky Mountain orogenic plateau volcanic field: Central Colorado, Springerville, Marysvale, Great basin, Mogollon, Sierra Madre Occidental
Sevier orogenic belt, Mogollon Highlands, Valley and Ridge, Blue Ridge Mountains, Ouachita Mountains, Laramide fold-thrust belt, Big Horn Mountains
Climatically & eustatically induced progradation along GOM
Sediment progradation & deposition in central & northeast GOM
Resurgence accompanied by clastic progradation & deposition in northwest GOM
Rimmed carbonate shelf
Sand-rich clastic progradation from northern margins
Evaporite & carbonate deposition in broad,shallow, open marine basin

Miocene-Pliocene sediment strata have been recorded to occur in the lower Gulf Coastal Plains. The depositional episodes are preceded by much quieter and longer periods of lower sediment influx. Quiescent periods of sediment deposition contain carbonate bank deposits that are common in both the Gulf and Atlantic Coastal Plains. Subsequent clastic depositional periods are very active with higher sediment influx that is rich in sand and other clastics (Galloway et al., 2011). Accelerated periods of clastic deposition can be related to tectonic uplift in the southern and central Appalachians.

Significance of provenance study of sediments

The goal of the provenance study is to reconstruct the history of sediments in a basin and understand characteristics of the source areas. Provenance interpretations can be used in conjunction with other evidence to test alternative paleogeographic and paleotectonic reconstructions (Fedo et al., 2003). Sediment dispersal is controlled by distribution of continental and oceanic basins and their varying tectonic character, diverse climatic regimes, changing patterns of seas and landmasses, configurations of subduction zones and associated orogenic belts, and locations of large rivers draining the source areas (Galloway et al., 2011).

Dominance of an Appalachian source signature in the late Tertiary Gulf Coastal Plain sediments would indicate increased erosional activity in the Appalachian source rocks. This is related to the uplift of the southern and central Appalachians during that time period. In this study, detrital zircon ages of late Tertiary sediments in the Gulf Coastal Plain of Mississippi (16 samples), Alabama (three samples) and Florida (one sample) have been used as proxies to determine sediment sources. Results of this study (discussed in later sections) show a predominance of Appalachian source rocks in the Miocene-Pliocene sediments analyzed, which indicates high sediment influx and erosion in the Appalachians during Miocene-Pliocene depositional periods, suggesting a major episode of late Tertiary tectonic uplift.

Depositional episodes and sediment supply in the Gulf of Mexico basin

A depositional episode is a time during which there were major sediment contributions (Frazier, 1974; Galloway et al., 2011). The sediment influx occurred via three major extra-basinal fluvial systems containing eight major fluvio-deltaic axes; the systems and axes are based on entry points of sediments along the margin and the location of main streams (Galloway et al., 2011). There were 14 depositional episodes, each lasting 3 ± 1 m.y., and five tectono-climatic eras along five fluvio-deltaic axes over the last 65 m.y. in the Gulf of Mexico basin that record differences in sedimentation patterns (Galloway et al., 2011). The eight major fluvial axes were: Rio Bravo, Rio Grande, Guadalupe, Colorado, Houston-Brazos, Red, Mississippi, and Tennessee. All fluvio-deltaic axes were active during the late Tertiary, suggesting increased erosional activity in the source mountains (Fig. 3-1). The Mississippi fluvio-deltaic axis was clearly the most active among Galloway's et al. (2011) eight axes, and shows prominent deposition phases during the early Eocene, late Miocene and Pliocene with medium to large amounts of sediment supply (Fig. 3-1). Sediment supply to the Gulf Coastal Plain via the paleo–Mississippi River was generally high during the Cenozoic (Craddock and Kylander-Clark, 2013).

Changes in topography were accompanied by drainage network readjustments affecting source areas for sediment fill (Galloway et al., 2011). The influx of significant amounts of detrital material into offshore areas largely ceased by the latest Cretaceous and was extremely low in the early Cenozoic. However, sediment fills increased considerably during the Miocene, especially along the Red, Mississippi, and Tennessee axes, indicating possible rejuvenation of the Appalachian source area (Galloway et al., 2011).

Late Tertiary stratigraphic units in lower Gulf Coastal Plain

Twenty samples collected from Mississippi (sixteen), Alabama (three) and Florida (one) were used for detrital zircon geochronology in this study. Most of these sediment samples were collected from the upper few meters of exposed sediments. Exact sample locations are described in Table 3-1 and located in Figure 3-2. Samples 1, 2, 4, 5, and 8 belong to the Hattiesburg-Pascagoula Formation (late Miocene); all other samples belong to either the Citronelle Formation (Pliocene-Pleistocene) or much younger deposits.

Cretaceous and Tertiary depositional units of the Gulf Coastal Plain in Mississippi (and some parts of Alabama and Florida) consist primarily of gravel, shale, limestone, sandstone, and clay (http://mrdata.usgs.gov/geology/state; McGlothlin, 1944). "Most of these deposits were laid down on the bottom of the sea as sand, clay, mud, or calcareous ooze, and many of them enclose different kinds of sea shells, sea urchins, or other marine fossils" (Adams et al., 1926). Some important stratigraphic index units are (Fig. 3-3): (1) Tuscaloosa and Eutaw Formations, and Selma Group (Gulf Series) (Late Cretaceous); (2) Midway, Wilcox, Claiborne, and Jackson Groups (Eocene); the oldest Cenozoic groups unconformably overlie the beveled surface of Upper Cretaceous rocks, this unconformity is possibly a very long interval of time (Adams et al., 1926); (3) Vicksburg Group (Oligocene); (4) Catahoula

Table 3-1. Detrital zircon sediment sample locations in the Gulf Coastal Plain. HT-Hattiesburg; PS-Pascagoula; CT-Citronelle.

Sample No.	Sample Name	Depositional Age	Contains marine/fluv-ial fossils	Formation	Latitude(N)	Longitude(W)
1.	W of Gravel Pit Rd-A,MS*	Miocene	Marine	HT-PS	31.32102	-89.4114
2.	W of Gravel Pit Rd-B,MS	Miocene	Marine	HT-PS	31.32112	-89.4109
3.	Red Bluff upper part, MS	Pliocene	No fossils	CT	31.32685	-89.9452
4.	Red Bluff middle part, MS	Miocene-Pliocene	No fossils	CT-HT-PS?	31.32685	-89.9452
5.	Red Bluff lower part, MS	Miocene-Pliocene	No fossils	HT-PS?	31.32685	-89.9452
6.	Dry Creek, near Maggie, MS	Pliocene	No fossils	CT	31.76807	-89.7569
7.	MS HWY 84 Collins, MS	Pliocene	No fossils	CT	31.63577	-89.5715
8.	MS HWY 49A Collins, MS*	Miocene	No fossils	HT-PS	31.63307	-89.56
9.	MS HWY 49B Collins, MS*	Pliocene	No fossils	CT	31.62862	-89.5517
10.	McCallum Landfill A, MS	Pliocene	No fossils	CT	31.23107	-89.2356
11.	McCallum Landfill B, MS	Pliocene	No fossils	CT	31.23112	-89.2363
12.	MS HWY 29 N of Runnels	Pliocene	No fossils	CT	31.40887	-89.0867
13.	MS HWY 42 W of Runnels	Pliocene	No fossils	CT	31.36505	-89.1348
14.	N of Petal, MS	Pliocene	No fossils	CT?	31.37542	-89.237
15.	Love Quarry, MS **	Pliocene	No fossils	CT?	34.75717	-89.9875
16.	Perry Quarry, MS **	Pliocene	No fossils	CT?	34.63667	-90.073
17.	Atmore Landfill, AL	Pliocene	No fossils	CT?	31.10365	-87.4871
18.	N of Jackson, AL	Miocene	No fossils	CT?	31.41427	-87.8909
19.	Citronelle, AL	Pliocene	No fossils	CT	31.08627	-88.219
20.	Alum Bluff, FL	Pleistocene	No fossils	HT-PS?	30.48167	-84.9758

***Sample not analyzed. **Sample collected by R. Cox, University of Memphis.**

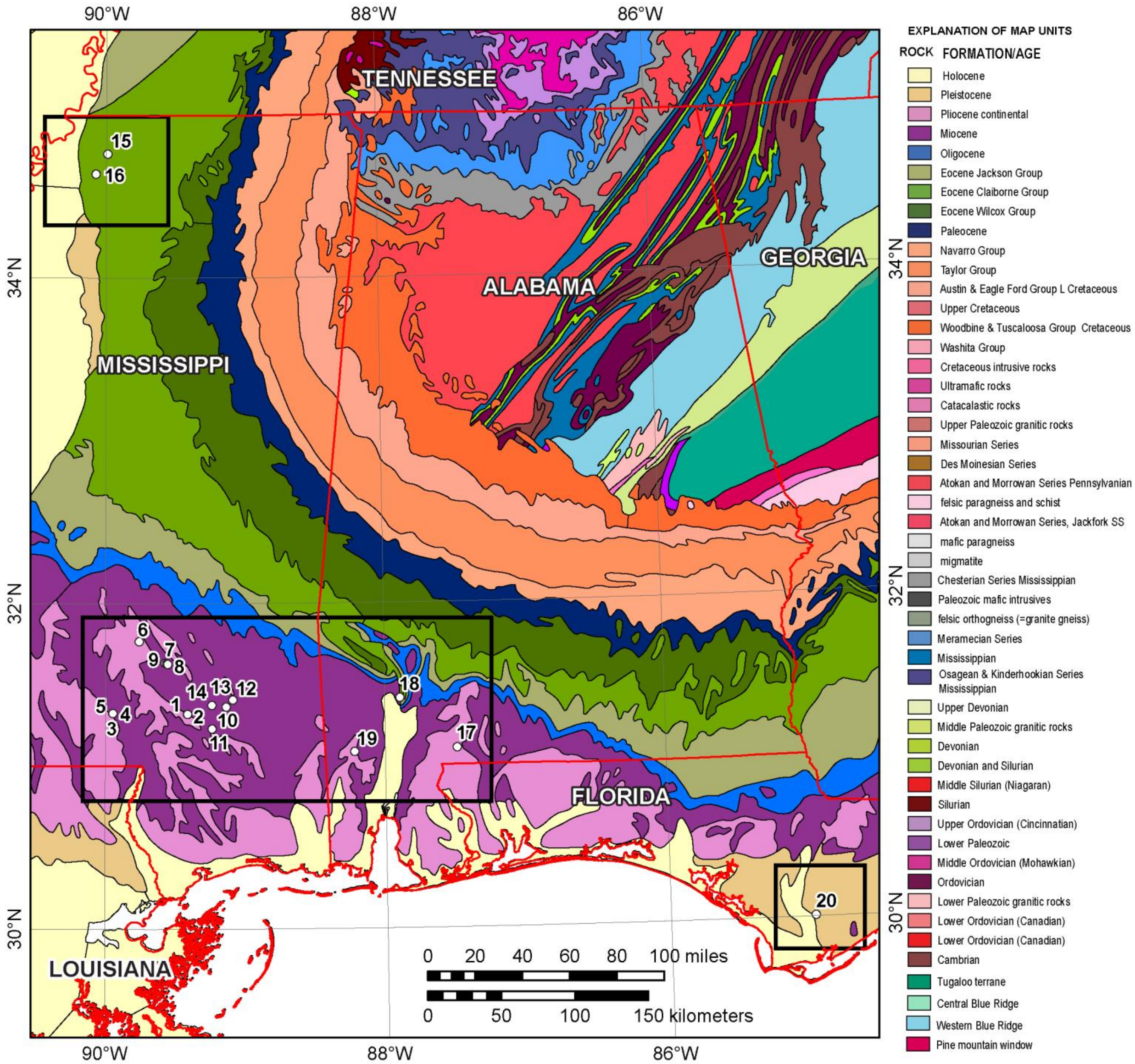

Figure 3-2. Geologic map of part of the southern and southeastern United States. Modified from Reed and Bush (2005). Black boxes highlight sample locations shown by respective sample numbers. See Table 3-1 for a detailed explanation of sample locations/numbers.

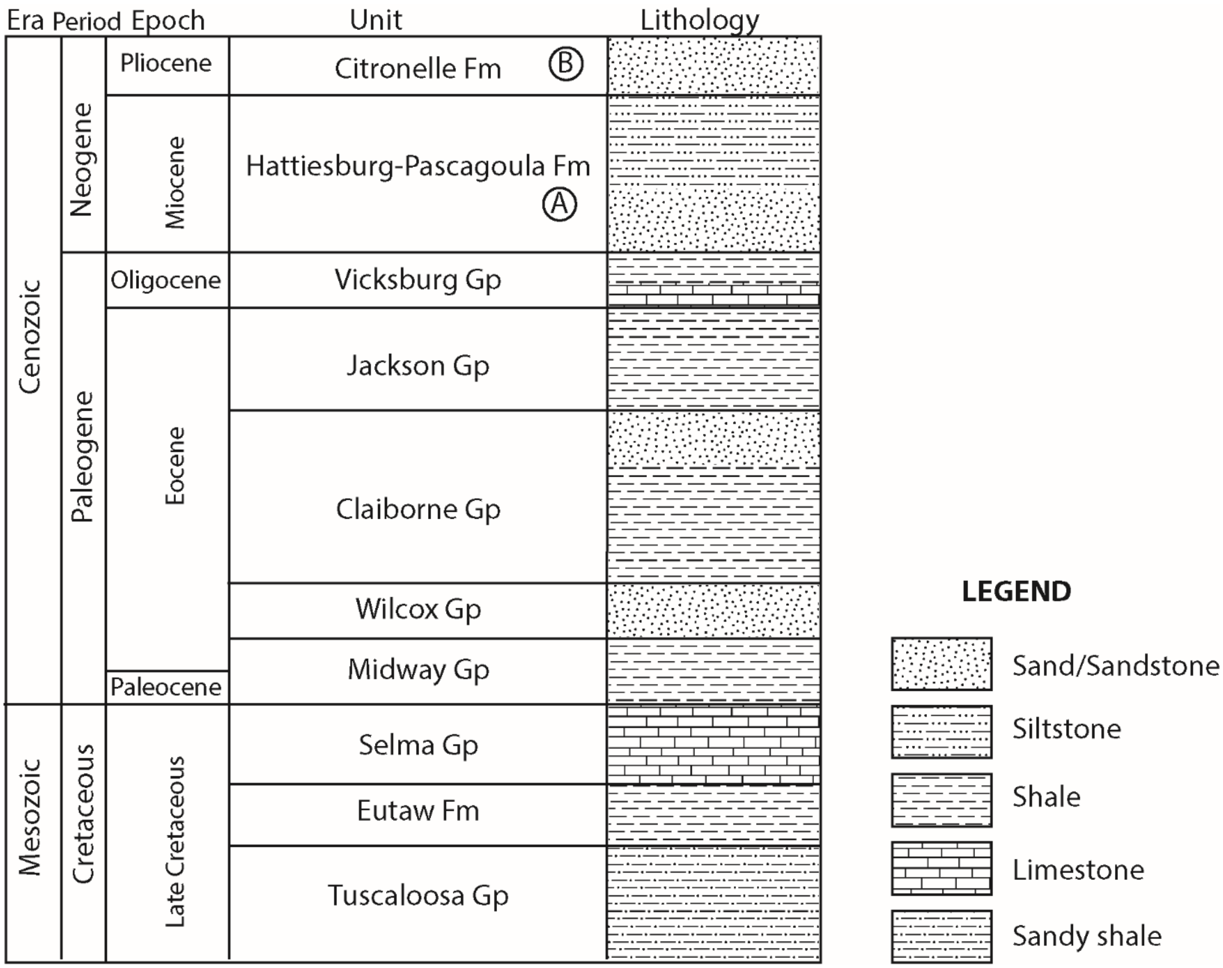

Figure 3-3. Generalized stratigraphic column showing Late Cretaceous and Tertiary units. Samples were collected from A- Miocene Hattiesburg-Pascagoula Formation (Samples 1, 2, 4, 5, and 8) and B- Pliocene Citronelle Formation (Samples 3, 6, 7, 9, 10, 11, 12, 13, 14, 15, 16, 17, 19, and 20). Modified after Harry and Londono, 2004.

Formation (Oligocene); (5) Hattiesburg-Pascagoula Formation (late Miocene); and (8) Citronelle Formation (Pliocene-Pleistocene and Recent) (Adams et al., 1926; McGlothlin, 1944; http://mrdata.usgs.gov/geology/state).

Alabama forms the transition zone between Miocene deposits of one facies in Mississippi and an entirely different facies in Florida (Adams et al., 1926). Miocene formations in Mississippi consist of Catahoula Sandstone, Hattiesburg Clay, and Pascagoula Clay (Adams et al., 1926). The Catahoula Formation contains irregularly bedded gray sand and sandstone; mottled red and gray, green, and chocolate-colored clay; some metaquartzite pebbles; and gravel (Adams et al., 1926; http://mrdata.usgs.gov/geology/state). The Hattiesburg-Pascagoula Formation can be up to 4900 feet (1493.5 m) thick and is locally fossiliferous and rich in green/bluish-green clay, sandy clay, sand, and gray siltstone (http://mrdata.usgs.gov/geology/state). Miocene formations in Florida consist of Choctawhatchee Marl, Alum Bluff Group, and Chattahoochee Formation (Adams et al., 1926). The Alum Bluff formation mainly consists of light-colored very fine-grained sand, and fossil shells (Adams et al., 1926). Miocene-Pliocene strata have a greater degree of induration than those of similar appearance in the area. Pliocene formations in Mississippi and Alabama mainly consist of the Citronelle Formation which gets its name from Citronelle, Mobile County, Alabama (Adams et al., 1926). The Citronelle Formation lies unconformably above the Hattiesburg Formation (Adams et al., 1926). The Citronelle Formation is 100 to 300 feet (30 to 91 m) thick in Mississippi and ranges from a thin veneer to 340 feet (103.6 m) in Alabama (Adams et al., 1926; http://mrdata.usgs.gov/geology/state). It crops out extensively across southern Mississippi and widely distributed as outliers in western Alabama (Adams et al., 1926). The

Citronelle formation predominantly contains cross-bedded red/purple/yellow-colored sand with lenses of clay, gravels, and may include terrace deposits, colluvium, and residuum (Adams et al., 1926; http://mrdata.usgs.gov/geology/state).

Study area in parts of Gulf Coastal Plain

The southern and southeastern parts of the Gulf Coastal Plain exposed in Mississippi, Alabama, and Florida provide an extensive stretch of low and flat-lying plains and cuestas extending along the coastline that are primarily made of sedimentary rocks and unconsolidated sediments.

The study area (insets in Fig. 3-2) is primarily underlain by Miocene, Pliocene, and Pleistocene Coastal Plain sedimentary deposits, which was the main reason for selecting the area for this study. Selection of sample sites was based on good and extensive exposures of sedimentary deposits. Such areas are usually sand pits/mines and can be identified in Google Earth™ images. Sample sites are located in Forest, Perry, Covington, and Jones Counties in southeastern Mississippi; Tate and Desoto Counties in northern Mississippi; Mobile, Escambia, and Clarke Counties in southwestern Alabama, and Franklin County in western Florida.

Sample collection in the field

Sixteen sediment samples were collected from Mississippi, three from Alabama and one from the Florida Gulf Coastal Plain. Although there are no strict guidelines for sample selection in detrital zircon studies, the nature of the study primarily dictates types of samples to be collected (Fedo et al., 2003). Mature and clastic sediments belonging to the late Tertiary, particularly Miocene-Pliocene strata, were collected for this study. Care was taken to avoid any bias in the sample collection process. Samples were collected from within first few feet/meters of exposed sediments using mattocks and shovels; special care was taken not to collect any colluvial or alluvial deposits. Colluvial deposits form as down-slope creep/gravity deposits and usually occur at the base of small slopes; they are loose and disintegrated and do not contain sedimentary structures (bedding, cross-beds, flaser bedding, etc.), unlike the partially lithified sediments that we collected for analysis.

Sample descriptions

Sample 1- W of Gravel Pit Rd-A, MS

Sample 1 was collected from a sand ridge within an abandoned construction site (refer to Table 3-1 for exact location). Some marine fossils were present in this sample suggesting that the depositional environment was marine. This sample belongs to the Hattiesburg-Pascagoula Formation that was deposited during the Miocene. Grain size is clay/fine silt and sorting is moderate. Color of the sample is dirty pale gray.

Sample 2- W of Gravel Pit Rd-B, MS

Sample 2 was collected from a few feet thick sand ridge in an abandoned construction pit (refer to Table 3-1 for exact location). Planar cross bedding is present in the strata. Strata contain some marine fossils indicating that the sediments were deposited in a marine environment. This sample belongs to the Hattiesburg-Pascagoula Formation that was deposited during the late Miocene. Grain size is very fine sand with mostly well-sorted grains. Granules and very fine pebbles are also present. Color of the sand/granules/pebbles ranges from dark pink to brown.

Sample 3- Red Bluff top part, MS

Sample 3 was collected from the top few meters of a deep erosion gulley (about 80 feet) at Red Bluff, Mississippi. Overall color of the sediments at this location is brick red. Grain size is fine-grained sand that is very well sorted with few cm-size chert and quartz clasts. Color of the sand varies between light pink to light brown. This sample belongs to the Citronelle Formation that was deposited during the Pliocene.

Sample 4- Red Bluff middle part, MS

Sample 4 was collected from the middle part of the same erosion gulley as sample 3, about 20 m below the ground surface. Grain size is fine sand that is very well sorted with some fine-medium grained chert pebbles. Color of this sample white to light brown. Cross stratification and graded bedding are common in this section of the exposure. This sample belongs to the Hattiesburg-Pascagoula Formation that was deposited during the Miocene.

Sample 5- Red Bluff lower section, MS

Sample 5 was collected from the bottom part of the same erosion gulley at Red Bluff as samples 3 and 4, about 30 m below the ground surface. Grain size is fine sand intermixed with medium/coarse pebbles. Sand is pinkish white and the color of pebbles varies from purple to orange to white. Overall sorting of the sample is poor-moderate. This sample is from the base of the Hattiesburg-Pascagoula Formation that was deposited during the Miocene.

Sample 6- Dry Creek, Maggie, MS

Sample 6 was collected from an old creek bed near the town of Maggie. Grain size is very fine sand, which is very well sorted. Color of the sand is pinkish brown. This sample belongs to the Citronelle Formation that was deposited during the Pliocene.

Sample 7- MS HWY 84 Collins

Sample 7 was collected from along HWY 84 near the town of Collins, Mississippi. Grain size is coarse silt-fine grained sand intermixed with coarse sand and granules. The sample is moderately sorted. Color of the sample is pinkish-brown to brown. Sample belongs to Citronelle Formation that was deposited during the Pliocene.

Sample 8- MS HWY 49 A Collins, MS

Sample 8 is collected along HWY 49 in Collins town, Mississippi. The sample is moderately sorted and grain size is mostly clay/silt. Color of the sample is dirty brownish gray. The sample belongs to the Hattiesburg-Pascagoula Formation that was deposited during the Miocene.

Sample 9- MS HWY 49 B Collins, MS

Sample 9 was also collected along HWY 49 in Collins, Mississippi, from a different place (refer to Table 3-1 for exact location). Sample is moderately sorted and grain size is fine sand with intermixed granules. Color of the sample is tan brown. Sample belongs to Citronelle Formation that was deposited during the Pliocene.

Sample 10- McCallum Landfill-A

Sample 10 was collected from a landfill in a construction sand pit at McCallum in southern Mississippi (refer to Table 3-1 for exact location). Grain size varies from fine sand to granules and fine to medium-sized pebbles. The grains are poorly sorted and color of the sample is reddish-brown, possibly because of iron oxidization. This sample belongs to the Citronelle Formation deposited during the Pliocene.

Sample 11- McCallum Landfill-B

Sample 11 was collected from a different place in the same landfill as sample 10. Grain size is medium to coarse silt and fine sand with some small-medium pebbles. The sample is poorly sorted and color of the sediments is dirty brown. This sample belongs to the Citronelle Formation deposited during the Pliocene.

Sample 12- MS HWY 29 N of Runnels

Sample 12 is collected along HWY 29 north of Runnels in Mississippi. Grain size is coarse silt and fine sand and few clasts with overall moderate sorting. Sample is light brown in color. The sample belongs to the Citronelle Formation deposited during the Pliocene.

Sample 13- MS HWY 42 W of Runnels

Sample 13 was collected along HWY 42 west of Runnels, Mississippi. Grain size is fine sand that is very well sorted. Sand is very clean, mature, and light pink. The sample belongs to the Citronelle Formation deposited during the Pliocene.

Sample 14- N of Petal, MS

Sample 14 was collected from a sand pit located north of Petal, Mississippi (refer to Table 3-1 for exact location). Grain size ranges from fine-medium sand with well-sorted texture. Color of the sample is reddish brown that is possibly related to iron oxidization. The sample belongs to the Citronelle Formation deposited during the Pliocene.

Sample 15- Love Quarry

Sample 15 was collected and sent to us by Prof. Randel T. Cox, University of Memphis. Grain size ranges from medium-coarse sand intermixed with some granules and fine pebbles. This sample is overall poorly sorted. Color of the sample is tan brown. This sample belongs to the Citronelle Formation deposited during the Pliocene.

Sample 16-Perry Quarry

Sample 15 was collected and sent to us by Prof. Randel T. Cox, University of Memphis. Grain size ranges from fine to medium sand with well-sorted grains. Color of the sample is light brick red. This sample belongs to the Citronelle Formation deposited during the Pliocene.

Sample 17- Atmore Landfill, AL

Sample 17 was collected from Atmore landfill in Alabama. Grain size is very fine sand that is very well sorted. The sand is very clean (little or no feldspar present) and yellowish brownish white. The sample belongs to the Citronelle Formation that was deposited during the Pliocene.

Sample 18- N of Jackson, AL

Sample 18 was collected from north of Jackson, Alabama. Grains are coarse silt and fine sand. Overall sorting is moderate in this sample. The sample looks very clean (little or no feldspar present) and has a pale orangish pinkish white color. The sample belongs to the Citronelle Formation that was deposited during the Pliocene.

Sample 19- Citronelle, AL

Sample 19 was collected from Citronelle, Alabama. Grain size is fine sand that is very well sorted. Sand is very clean (little or no feldspar present) and has a pale white color. Small black specks that are possibly a heavy mineral are present in very small quantities in the sample. The sample belongs to the Citronelle Formation that was deposited during the Pliocene.

Sample 20- Alum Bluff, FL

Sample 20 was collected from Alum Bluff, Florida. Grain size is fine sand with some medium pebbles. Sample has an overall well-sorted texture. Color of the sand is white with very few black specks that are possibly a heavy mineral. The sample belongs to the upper Citronelle Formation that was deposited during the Pleistocene.

Zircon separation procedure

Zircon (specific gravity 4.6-4.8) is heavier than most essential and accessory minerals in most rocks. Heavy minerals can be separated from minerals of lower density by gravity and magnetic methods. Separation of zircon grains by gravity methods was accomplished by (1) employing a Wilfley water table, (2) heavy liquid (methyl iodide, density 2.28 g/cc) funnel separation, and (3) magnetic separation by initially using a hand magnet and later running the sample through a Frantz magnetic separator. Since all samples were mostly loose sediment, there was no need to break or crush the samples, but some light hammering of the sediment lumps was needed for a few samples. Sieving of most samples was carried out to remove any cobbles, sharp clasts, pebbles, and gravel.

(1) Wilfley water table: The Wilfley water table is a shaking table that is used to separate heavier/larger grains from lighter/smaller grains. The basic principle of this table is to use the difference in density of the minerals to separate them into different parts with the flowing water and simultaneous shaking of the table. I used a slurry of each sediment sample on the Wilfley table to separate the heavy and light mineral fractions. The table has longitudinal grooves or riffles that act as barriers to slow down movement of the minerals. As water moves across the table, the longitudinal shaking action of the table deck causes the grains to be arranged according to their density. Water flow forces the light minerals to move slowly across the riffles down the small slope of the table. Due to the large inertia, heavy minerals/larger grains tend to move more effectively to the central grooves, while the light minerals move to the side grooves, thus collecting into separate containers placed at the end of the table.

(2) Heavy liquid (methyl iodide) separation: If a mixture of minerals with different densities is placed in a liquid with an intermediate density, the grains with higher densities will float, and grains with greater densities will sink. Methylene iodide (MeI) has a density of 2.28 g/cm^3 and is used for this step of zircon separation. While most minerals in the sediment samples are lighter than MeI, zircon is clearly heavier and sinks to the bottom.

Heavy liquid separation is carried out in separatory funnels. MeI is decanted into the separatory funnel followed by the sample. This setup is left undisturbed until the lighter minerals float to the top, while the heavier minerals sink to the bottom of the separatory funnel. After the minerals have been separated, the stopcock is carefully opened to allow the bottom material to quickly transfer into a flask; the stopcock is then quickly shut, leaving the lighter material in the separatory funnel. The MeI is drained from the heavy mineral separate, and the mineral separate is allowed to dry on a piece of weighing paper.

(3) Frantz magnetic separator: Ferromagnetic minerals are minerals that are themselves magnetic; they can be easily separated from other minerals as they stick to of a hand magnet that is brought close to the minerals. Non-magnetic detrital zircons ae used for geochronological purposes. A simple hand magnet is passed over the heavy mineral separate to remove any stray magnetic minerals. A Frantz magnetic separator is a more complex device that helps remove ferromagnetic minerals from the rest of the heavy mineral separate that is to be used for further analysis. It consists of a large electromagnet and a sloping metal trough that is divided near its exit. Two different metal bins/containers are placed at the end of the chute to separate magnetic and non-magnetic minerals. The sample is poured into the feeding funnel; as the mineral mixture is passed through the metal trough (chute), magnetic minerals move closer to the electromagnet and collect in the bin placed at the end of the chute. Separation is done at varying strengths of the magnetic field (by changing the electric current) and slope of the chute. A forward slope of the chute controls speed of movement of the grains, and a sideways tilt controls the separation of minerals based on their susceptibility. The process is repeated until the best results are obtained.

All samples were taken through these zircon separation processes. Preserving randomization of grain selection and avoiding any form of bias is essential to obtain best results. Any artificial bias or contamination during field sampling and zircon separation has been avoided by following necessary precautions and using extreme care. Hand picking of detrital zircons can introduce bias into the sample, so no microscopic handpicking of zircon was done except some basic microscopic scanning of the samples to remove any obvious non-zircon minerals such as opaque minerals and stray sediment grains. Samples were then sent to the University of Arizona LaserChron Center for mounting, imaging, and subsequent LA-ICP-MS age dating of the detrital zircon samples. Only 18 out of 20 samples were sent to the University of Arizona LaserChron Center for analysis due to lack of sufficient zircons separated from samples 1 and 8. Sample-9 was lost after the mail was sent to the University of Arizona LaserChron Center. Therefore, only 17 out of 20 that were collected were analyzed at the University of Arizona LaserChron Center.

CHAPTER IV

DETRITAL ZIRCON GEOCHRONOLOGY OF GULF COASTAL PLAIN SEDIMENTS

Overview of detrital zircon geochronology

"Detrital zircon geochronology is a very powerful tool for determining the provenance and maximum depositional age of clastic strata; rapid evolution of detrital zircon geochronology, also known as the DZ revolution, is a result of technical developments that have allowed researchers to efficiently determine U-Pb ages of individual zircon crystals" (Gehrels, 2012). For the last five decades, detrital zircon geochronology has been widely used to resolve problems and answer questions pertaining to the geologic history of depositional units. A detrital zircon geochronometer is commonly used to decipher formation, metamorphism, and provenance history of rocks. According to Fedo et al. (2003) and Gehrels (2012), common applications of detrital zircon geochronology are: (1) to determine provenance characteristics such as age and composition, where ages of detrital minerals are compared with ages of potential source terranes to determine ultimate sources of sediment; (2) to determine the oldest depositional age of a clastic unit. The youngest age component in a sedimentary unit is equivalent to the earliest possible/maximum depositional age of the unit. This method also is employed in recognizing intermittent intervals of time during which there was negligible sediment deposition; (3) to correlate sedimentary units, where ages of detrital minerals are compared to evaluate possible links between different sedimentary units; (4) to test paleogeographic reconstructions using provenance information contained in detrital zircons; and (5) to resolve complex problems in geologic history of the earth using information present in the mineral chemistry of detrital zircons. In this study, detrital zircon geochronology is used to determine the ultimate source of late Tertiary sediments in the Gulf Coastal Plain.

Zircon ($ZrSiO_4$) is commonly used for U-Th-Pb geochronology because zircon is present in most crustal rocks, contains moderate concentrations of U, Th and Pb, and is resistant to alteration and disturbance of the U-Th-Pb isotopic system (Fedo et al., 2003; Gehrels et al., 2008; Gehrels, 2012). Zircon is a very good geochronometer because of its ability to survive extreme pressure and temperature conditions during igneous, diagenetic, and metamorphic processes. Zircon is extremely difficult to destroy, even by multiple episodes of metamorphism/tectonism; the internal atomic structure of zircon makes it an extremely durable mineral. Zircon crystallizes in the tetragonal system; Zr and Si polyhedra form a strongly connected silicate structure producing a hardness of 7 on Mohs scale. Zircon is more resistant to weathering than any other accessory (heavy) mineral and preserves every geologic event as a distinct morphological segment with each passing period of zircon formation or consumption (Morton and Hallsworth, 1999; Gehrels et al., 2008; Gehrels, 2012). The closure temperature for the U-Th- Pb isotopic system in zircons is very high (> 900^0 C) (temperature below which there is no exchange of isotopes and zircon acts as a closed system), keeping the system isotopically closed through extended periods of high grade metamorphism and even partial melting of its host rock, which makes zircon a very powerful geochronometer.

LA-ICP-MS technique

Laser Ablation Inductively Coupled Plasma Mass Spectrometry (LA-ICP-MS) is a technique used to determine U-Pb ages of detrital zircons (Gehrels, 2012). "The LA-ICP-MS technique has been employed for geochronologic analyses since 1985" (Košler and Sylvester, 2003), although "a dramatic increase in amount of detrital zircon geochronology occurred in the late 1990s through early 2000s, when LA-ICP-MS was technologically developed to the point that U-Pb analyses could be conducted in a robust fashion" (Gehrels, 2012).

After the samples are taken through the traditional steps of zircon separation, the zircons are mounted in 1-inch epoxy mounts along with standards that are zircon crystals of known age and isotopic composition (Jackson et al., 1992; Košler and Sylvester, 2003; Gehrels, 2012). Sri Lankan (SL) standard zircons have been used in all of my analyses for this study. The mounts were abraded to a depth of 20 microns, followed by polishing, imaging and cleaning prior to isotopic analysis in the LA-ICP-MS machine at the Arizona LaserChron Center. Back-scattered electron (BSE) and/or cathodoluminescence (CL) imaging of zircons were completed prior to analysis in the LA-ICP-MS. CL and BSE imaging help separate cores from the rims. BSE imaging helps focus the laser beam on the desirable part (ideally core) of the zircon and avoid ablating across any zircon domain (core and rim) boundaries. Only BSE and reflected light images were used during analysis in this study. Mounted zircons are analyzed systematically, while skipping any metamict zircons/parts of zircons containing inclusions or imperfections (Fedo et al., 2003). Any obvious bias in the zircon selection on the mount was avoided by random selection of zircons from all sections of the mount.

A Photon Machines Analyte G2 excimer laser was used for ablation of zircons with a 30-micron spot diameter and 15 microns pit depth (Arizona LaserChron Center, 2014). A laser beam of wavelength ~1064 nm was focused onto the surface of the polished zircon grain, which resulted in ablation, leading to ejection of atoms, ions, molecules, and solid particles; these were transported directly into the ICP (inductively coupled plasma) from the laser system (Jackson et al., 1992; Košler and Sylvester, 2003). Analytical spots were concentrated only on undamaged parts of zircon grains so that metamict grains (radioactivity damaged grains/parts of grains) were avoided. Excited ions in the plasma torch were introduced into a mass spectrometer for elemental and isotopic analyses (Fig. 4-1; Košler and Sylvester, 2003). Ablated material was carried in helium into the plasma source of the mass spectrometer, which was equipped with a flight tube of sufficient width so that U, Th, and Pb isotopes were measured simultaneously (Arizona LaserChron Center, 2014). LA-ICP-MS produces ages with a precision and accuracy of 1-2 percent error (2-sigma) (Košler and Sylvester, 2003; Chang et al., 2006; Gehrels et al., 2008). Each analysis consists of one 15-second integration on peaks with the laser off, 15 one-second integrations with the laser firing, and a 30-second delay to purge the previous sample and prepare for the next analysis (Arizona LaserChron Center, 2014). Typical analysis time is only few minutes, thus producing a faster rate of ablation with quicker analysis time than other analytical instruments such as TIMS (Thermal Ionization Mass Spectrometry). This makes the LA-ICP-MS a very efficient instrument for detrital zircon analysis (Gehrels, 2012).

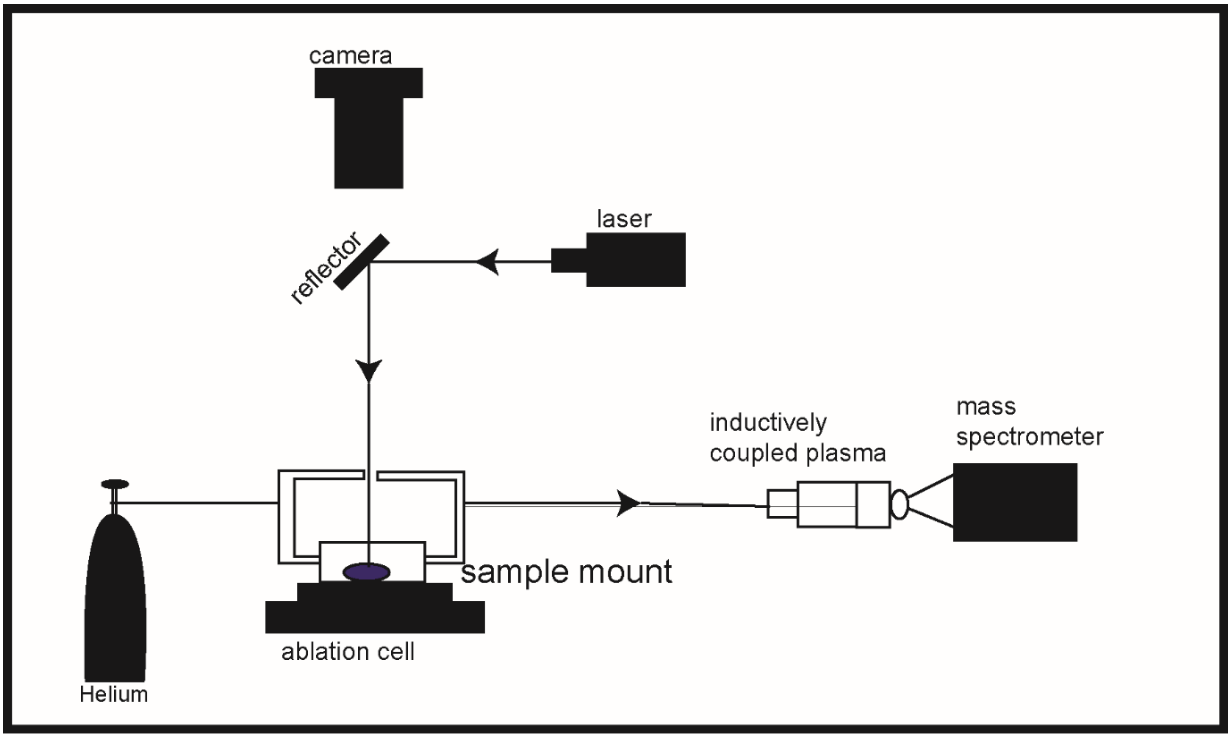

Figure 4-1: Schematic of the LA-ICP-MS set up modified from Arizona LaserChron Center webpage (http://www.geo.arizona.edu/alc).

U-Pb chronometer: Principle and age evaluation

U-Pb geochronology is by far the most powerful and common technique for extracting source information from detrital zircon grains (Fedo et al., 2003). The U-Pb radioactive decay system goes through two main disintegrations: (1) $^{238}U \rightarrow ^{206}Pb$, and (2) $^{235}U \rightarrow ^{207}Pb$, with a number of intermediate daughter products. The two decay reactions are linked because $^{238}U/^{235}U$ is constant through time (Gehrels, 2012). Mineral age is calculated by measurement and calculation of three geochronometers [Fig. 4-2(a) and (b)]: (1) $^{206}Pb/^{238}U$ (decreases with time); (2) $^{206}Pb/^{207}Pb$ (increases with time); and (3) $^{207}Pb/^{235}U$ (decreases with time; not measured directly and calculated from other two ratios) and plotting them against time (Gehrels, 2012). ^{204}Pb is a non-radiogenic isotope of Pb that is present since the time of formation of the mineral. Measurement of initial ^{204}Pb is important, because it is subtracted from U-Pb ratios in order to determine the correct age of the mineral. A graphical representation of these ratios as a function of age produces a concordia plot of $^{206}Pb/^{238}U$ versus $^{207}Pb/^{235}U$ [Fig. 4-2(a)]. Intersection of the three chronometer ratios as a function of age produces the concordia line passing through the origin [Fig. 4-2(a) and (b); Gehrels, 2012]. Slope of the concordia line represents $^{206}Pb/^{207}Pb$ sample concentration at a given time [Fig. 4-2(a); Gehrels, 2012]. Every point on the concordia line corresponds to a particular age during the growth history of the mineral [Fig. 4-2(a)].

Uncertainty values for each of the three chronometer ratios determine which chronometer will provide the best age. $^{206}Pb/^{238}U$ age is most precise and is commonly

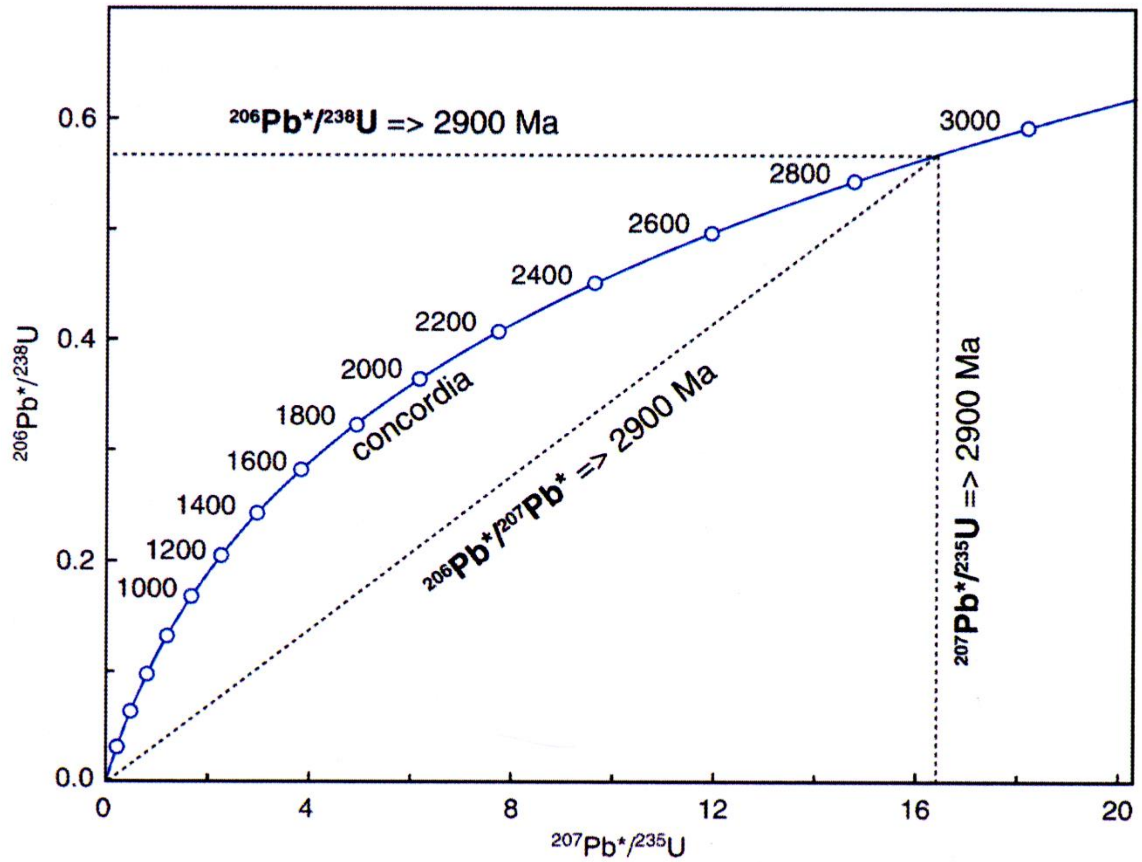

(a)

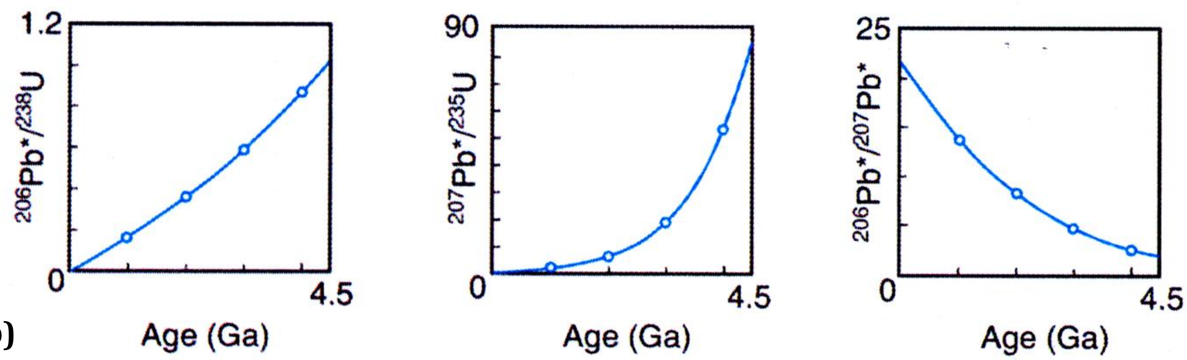

(b)

Figure 4-2(a) A representative U-Pb concordia diagram. **(b)** Most commonly used geochronometers for determining age of zircons. "*" means ^{204}Pb (originally present in mineral) has been subtracted. Source: Gehrels, 2012.

used for younger samples (< 1.0 m.y.); $^{206}Pb/^{207}Pb$ is used for older samples (> 1.0 m.y.). Age resolution for the U-Pb system is poorest at 1.4 m.y., because all three uncertainities have the same value at this age (Gehrels et al., 2008; Gehrels, 2012).

If all three ages ($^{206}Pb/^{238}U$, $^{207}Pb/^{235}U$, and $^{206}Pb/^{207}Pb$) are similar within allowed error, the analysis plots on the concordia line and is described as “concordant” (Gehrels, 2012). If the analysis plots below the concordia line it is called “discordant”; if the analysis plots above the concordia line it is called “reverse discordant.” Discordance usually occurs because of Pb loss during later events, causing the analysis results to shift below the concordia line. Reverse discordance may occur with Pb gain by inheritance of older material, in which case the analysis results moves above the concordia line.

Degree of discordance is expressed as a percentage of ($^{206}Pb/^{238}U$) age divided by ($^{206}Pb/^{207}Pb$) age. A perfectly concordant analysis will have 0 percent discordance, and therefore 100 percent concordance (Gehrels, 2012).

$$\text{Discordance} = 100 - 100*[(^{206}Pb/^{238}U)\text{ age} /(^{206}Pb/^{207}Pb)\text{ age}] \qquad \text{Eq. 4-1}$$

$$\text{Concordance} = 100* [(^{206}Pb/^{238}U)\text{ age}/(^{206}Pb/^{207}Pb)\text{ age}] \qquad \text{Eq. 4-2}$$

Zircons are susceptible to Pb loss with age (increasing lattice damage due to radioactivity), making older zircons commonly discordant (Gehrels, 2012). All three chronometers yield younger ages than the actual crystallization age in discordant zircons. However, it is more accurate to use $^{206}Pb/^{207}Pb$ age than the other two chronometers in case of discordant zircons, because $^{206}Pb/^{207}Pb$ age plots closest to the actual crystallization age (Gehrels, 2012). Inaccuracy of $^{206}Pb/^{207}Pb$ age increases as discordance increases; a discordance filter is essential to maintain zircon data accuracy (Gehrels, 2012).

Selection of the discordance filter depends on the purpose of the study; for example, a large 30 percent discordance filter may be used in a widely mixed zircon population to retain most ages; a tight 10 percent discordance filter may be used for a zircon population tested for a specific age population to obtain the best possible age resolution (Gehrels, 2012). It is always helpful to filter for clustered ages (2-sigma uncertainty) instead of more scattered ages. A reasonable strategy is to initially apply a moderate discordance filter (10-30%), and evaluate the accepted data in terms of clustering to highlight the most reliable age clusters (Gehrels, 2012). Frequency histograms of the detrital zircon ages help classify age populations and identify the most commonly occurring ages. A probability density plot (PDP) is a simple curve that connects the peaks of the highest frequencies in each age population group, and is based on the relative probability of age occurrence.

Errors and corrections in this study

The errors in determining $^{206}Pb/^{238}U$ and $^{206}Pb/^{204}Pb$, as well as $^{206}Pb/^{207}Pb$ and $^{206}Pb/^{204}Pb$, result in a measurement error of 1-2 percent (at 2-sigma level) in $^{206}Pb/^{238}U$ age (Arizona LaserChron Center, 2014). Because errors may be substantially larger for younger grains (< 1.0 Ga) due to low intensity of the ^{207}Pb signal, $^{206}Pb/^{238}U$ ratio is considered for younger grains. For most analyses, crossover in precision of $^{206}Pb/^{238}U$ and $^{206}Pb/^{207}Pb$ ages occurs at ~ 1.0 Ga (Arizona LaserChron Center, 2014). Analytical data in this study show an uncertainty at 1-sigma level and include only measurement errors (Arizona LaserChron Center, 2014). A discordance filter of 20 percent was used in this study, i.e, analyses that are >20 percent discordant (by $^{206}Pb/^{238}U$ and $^{206}Pb/^{207}Pb$ ages) or >5 percent reverse discordant were not used (Arizona LaserChron Center, 2014). Hg (mercury) correction is not significant for most analyses, as Hg backgrounds are low (Arizona LaserChron Center, 2014). Common Pb correction is accomplished by using Hg-corrected ^{204}Pb and assuming an initial Pb composition (Stacey and Kramers, 1975; Arizona LaserChron Center, 2014).

Results: *LA-ICP-MS detrital zircon data*

Appendix I contains LA-ICP-MS detrital zircon data for all 17 samples. Best age for each zircon grain was calculated using the ALC NUPMagecalc program that takes the various errors and discordance filter into account. Appendices II and III contain concordia plots and PDPs for all 17 samples, respectively. All samples are fairly similar in overall age populations and produce very concordant results. Sample 6 (Dry Creek near Maggie, MS) graphical plots are used as an example in this section to describe the overall analyses results. Most analyses (> 90%) in the representative sample (Sample 6) are concordant within analytical errors and filters used (Fig. 4-3). The concordia plot (Fig. 4-3) is generated from a total of 105 unknown zircon grain analyses with one standard SL zircon analyzed for every five unknown zircons. Almost all analyses are highly concordant (95-100% concordance) except for some discordance in grains older than 2.7 Ga. This may be due to radiation damage and Pb loss over a longer period of time, or a polycyclic transportation history of older grains.

The frequency histogram and PDP for the sample (Sample 6-Dry Creek near Maggie, MS) demonstrate the relative probability of occurrence (frequency) of each zircon age population and the major peaks (Fig. 4-4). A narrow bin width of 20 m.y. was used to better

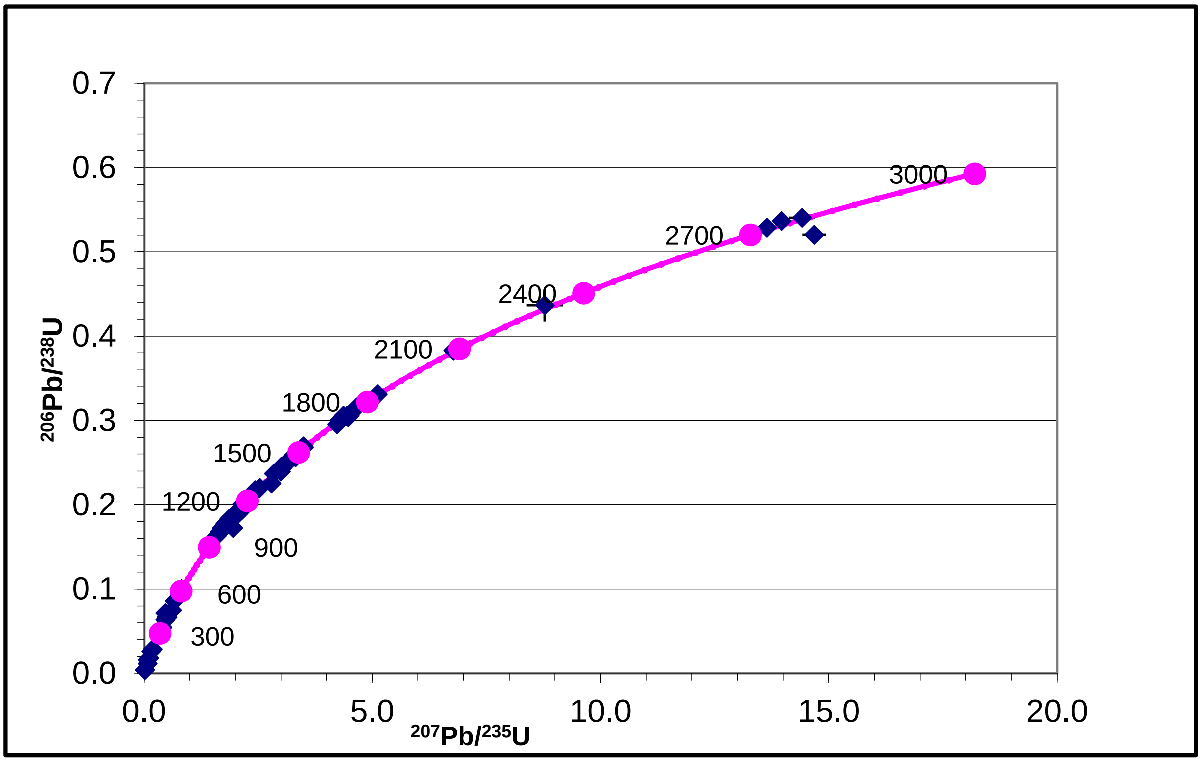

Figure 4-3. Sample 6-Dry Creek from near Maggie, MS (representative concordia plot). Blue diamonds are sample zircon ages. Cross axes through the diamonds show error range.

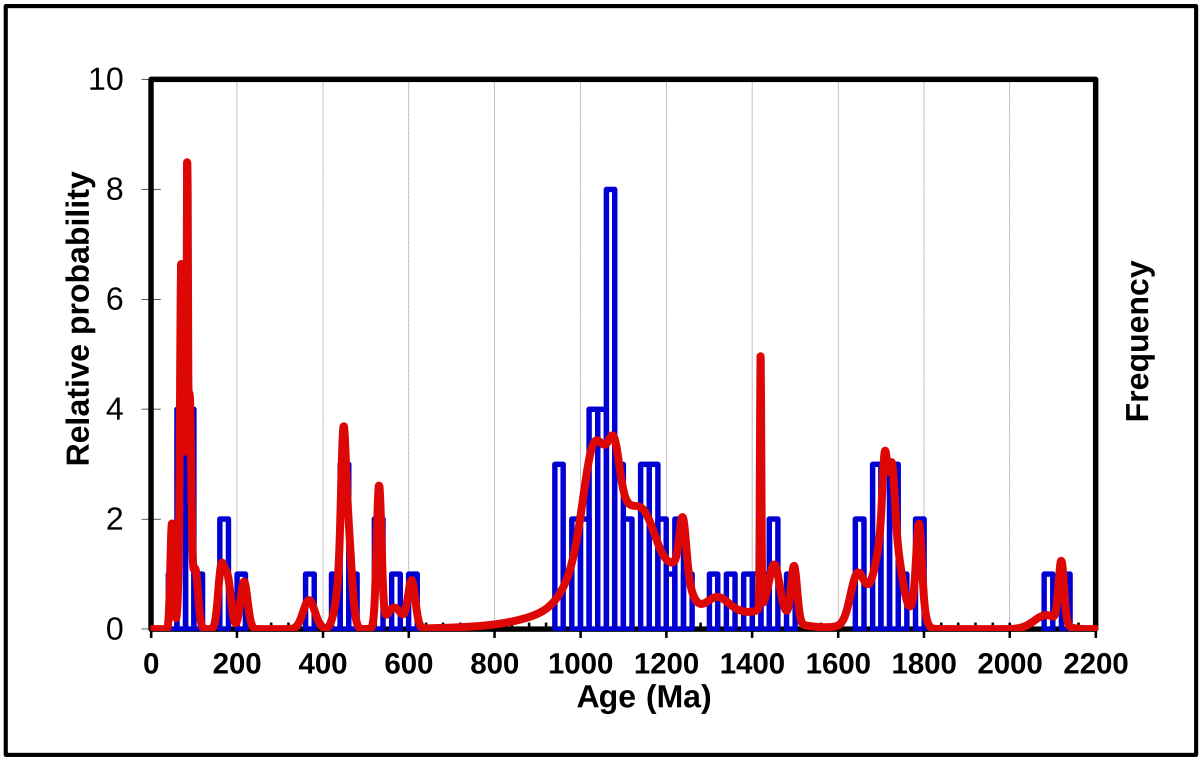

Figure 4-4. Sample 6-Dry Creek from near Maggie, MS. Representative frequency histogram (blue bars) and probability density plot (red curve). Bin width is 20 m.y.

classify the zircon ages. Prominent age populations readily seen in Figure 4-4 can be associated with source age.

Older zircons (≥ 1.0 Ga), Paleozoic zircons (542-260 Ma), and younger zircons (≤150 Ma) stand out in the frequency histogram; noticeable gaps in ages are also apparent, such as the age gap between 1.0 Ga-600 Ma and 400-200 Ma. Gaps in zircon ages may be related to a hiatus in deposition (Figs. 4-3 and 4-4). Age peaks and age gaps are important fingerprints of sedimentation history. An overall idea about results of samples 1-20 can be obtained from concordia and the frequency histogram/PDP plot of the representative sample (Figs. 4-3 and 4-4).

Miocene-Pliocene detrital zircon age data from the sediments in Mississippi, Alabama and Florida clearly demonstrate a dominance of mid-Paleozoic and early Neoproterozoic age populations. PDPs of all samples are stacked atop one another for quick visual interpretation of similarities and differences in age populations of the samples [Fig. 4-5 (a) and (b)]. Comprehensively, the data from Mississippi (13 samples), Alabama (three samples), and Florida (one sample) record four major zircon age populations:

(1) Very old > 2.0 Ga age peaks in most samples [Fig. 4-5 (a) and (b)].

(2) A major Grenville (1.2-1.0 Ga) age peak in all samples [Fig. 4-5 (a) and (b)].

(3) A ~600 Ma age peak in most samples and ~480, ~400, and ~300 Ma age peaks in all samples [Fig. 4-5 (a) and (b)].

(4) Late Cretaceous, Paleocene, Eocene, and Miocene ages peak in more than half of the samples [Fig. 4-5 (a) and (b)].

Figure 4-5 (a). Probability density plots (PDP) of U-Pb ages for detrital zircons from eight Miocene-Pliocene sediment samples from the lower Gulf Coastal Plain. **(b)** Probability density plots of U-Pb ages for detrital zircons from nine Miocene-Pliocene sediment samples from the lower Gulf Coastal Plain. Sample name and number is shown on top right corner of each individual PDP. Common age populations, frequency of ages, and similarity between overall sample results can be readily seen and compared through these figures. Mesoproterozoic (Grenville) age peaks are shown in yellow highlight; Neoproterozoic and Paleozoic age peaks are shown in blue highlight. Data not available for Samples 1, 8, and 9.

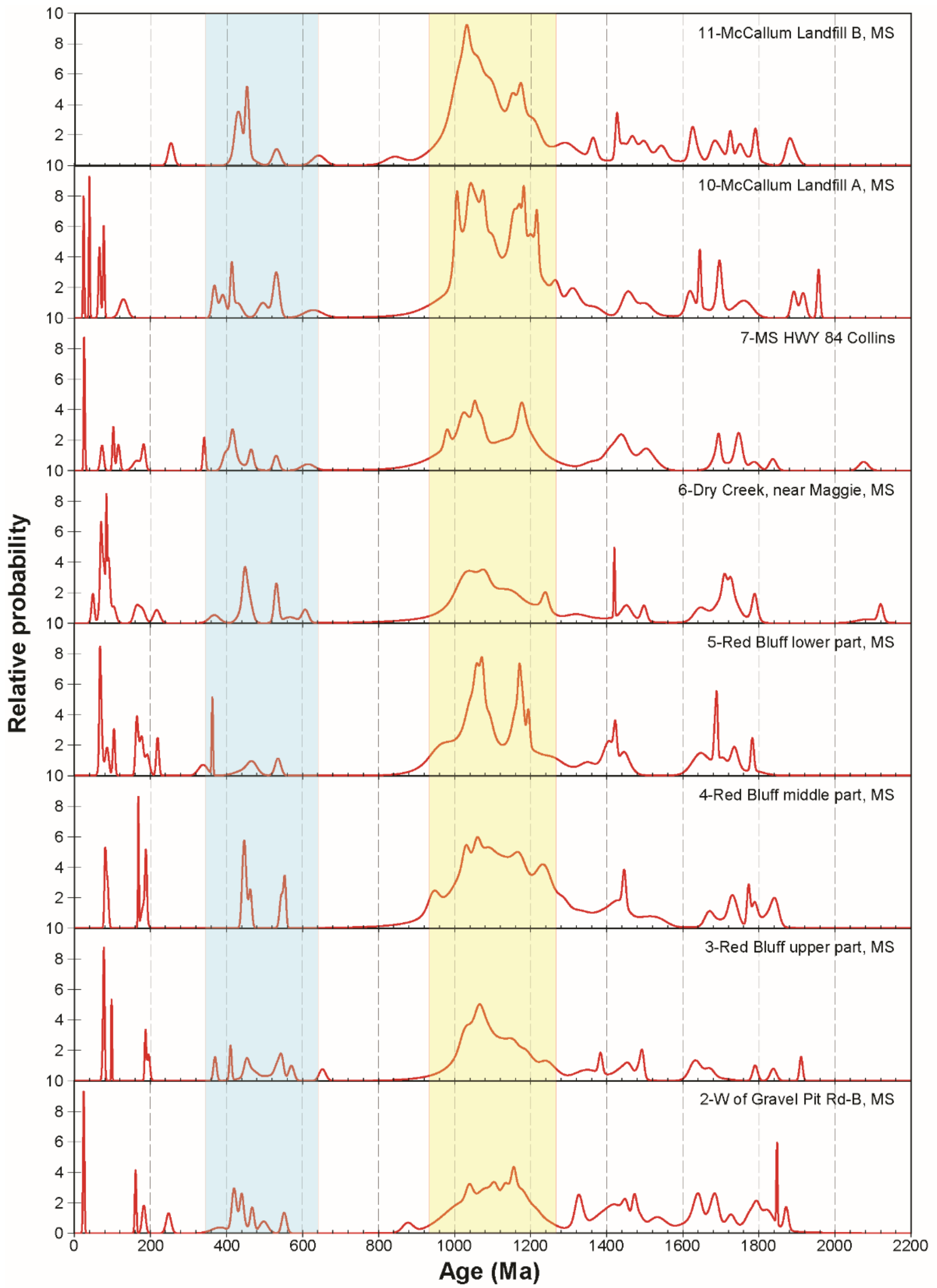
Relative probability
Age (Ma)
11-McCallum Landfill B, MS
10-McCallum Landfill A, MS
7-MS HWY 84 Collins
6-Dry Creek, near Maggie, MS
5-Red Bluff lower part, MS
4-Red Bluff middle part, MS
3-Red Bluff upper part, MS
2-W of Gravel Pit Rd-B, MS

(a)

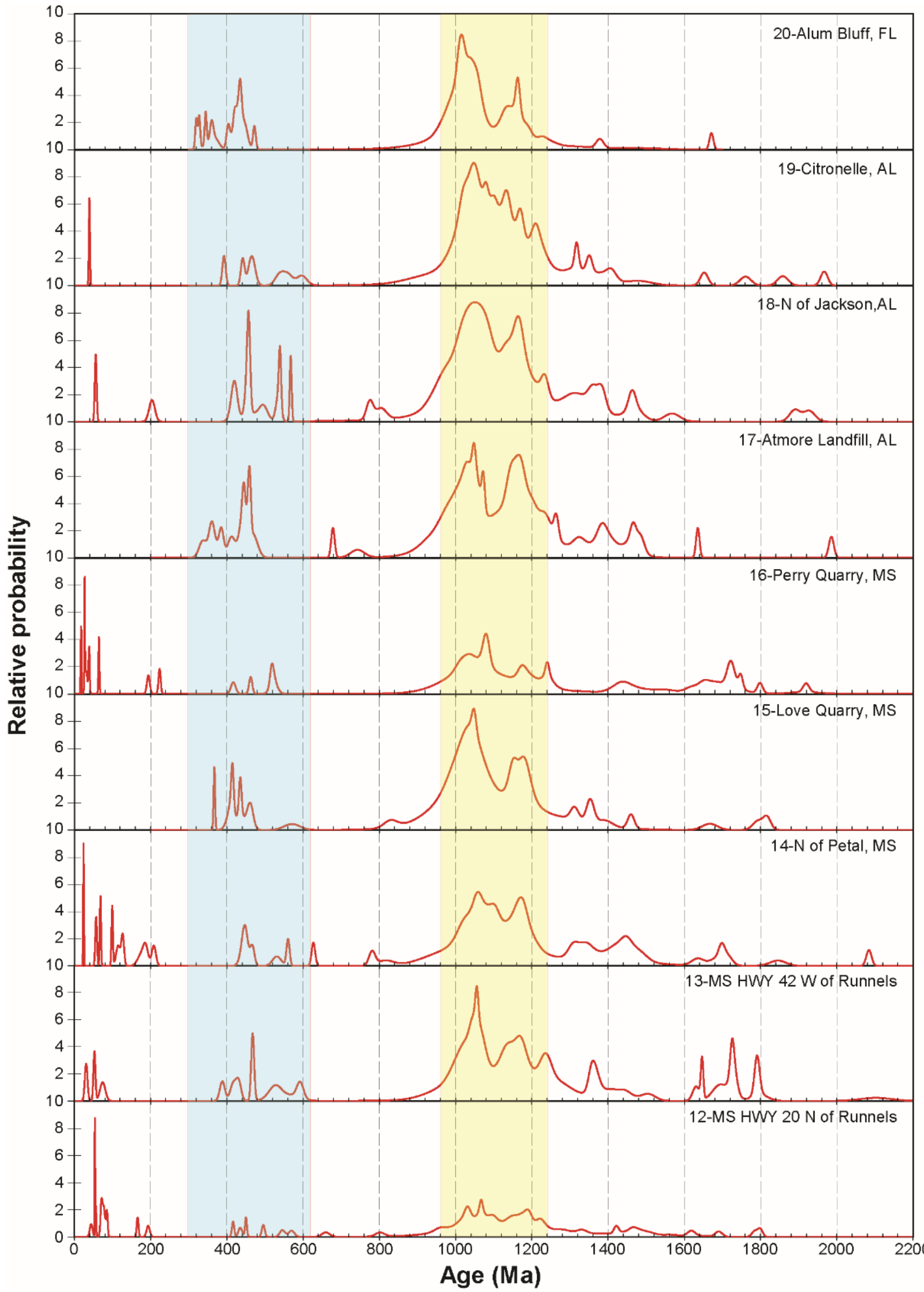
20-Alum Bluff, FL
19-Citronelle, AL
18-N of Jackson,AL
17-Atmore Landfill, AL
16-Perry Quarry, MS
15-Love Quarry, MS
14-N of Petal, MS
13-MS HWY 42 W of Runnels
12-MS HWY 20 N of Runnels
Relative probability
Age (Ma)

(b)

Statistical comparison between samples

There are two ways to analyze detrital zircon data: qualitative analysis and quantitative analysis (Fedo et al., 2003). Qualitative analysis is performed on the basis of morphology and texture of the mineral grains irrespective of their abundance among available grains; although this method can reveal provenance, analyzing the age proportions of the zircons is meaningless because true proportions are not represented (Fedo et al., 2003). Quantitative analysis is based on measurement of the number of zircons present for each age group. Statistical adequacy is the main principle used for quantitative analysis of detrital zircon data; results ensure that an analyzed sample is representative of the population (Fedo et al., 2003). Quantitative provenance analysis includes analytical, statistical, and numerical methods to characterize sediment properties, and is highly dependent on data acquisition (Weltje and Eynatton, 2004). Within the limits of this project, a quantitative analysis is useful to understand the results. Quantitative analysis of samples has helped in comparison and stochastic modeling of age proportions of multiple zircon populations.

Kolmogorov-Smirnov (K-S) and likeness metric tests are used to compare similarities or overlap of zircon age spectra, i.e., to examine degrees of sameness among detrital zircon age populations in space and time (Satkoski et al., 2013). I have used the K-S and the likeness metric tests in this project to compare the LA-ICP-MS detrital zircon age data of all samples. The likeness metric quantifies the degree of overlap between pairs of PDPs, while the K-S metric quantifies the statistical probability of indifference between the ages in a sample pair.

The likeness metric calculates the "sameness percent" between two unitized PDPs (Satkoski et al., 2013).

$$L = 1 - \left[\sum_{i=1}^{n} \frac{|a_1 - b_1|}{2} \right] \qquad \text{Eq. 4-3}$$

where n is the number of ages in both PDPs, and a and b are the frequency of any given age (Satkoski et al., 2013). One hundred percent likeness means the PDPs are exactly the same. Likeness greater than 60 percent indicates a very good overlap or sameness between the two samples and is highly desirable (Table 4-1). Most of the sample pairs depict a likeness of 65-75 percent, indicating a high degree of likeness between sample pairs (Fig. 4-6). Almost 85 percent of the individual sample pairs show likeness above 60 percent. This means that most (~85%) samples used in this study are alike and represent common provenance. Most samples lie within a 200-km geographic horizontal radius of each other and belong mostly to vertically conformable stratigraphic sections. It should be noted that there is no direct relationship between likeness and separation between the samples, perhaps because the distance between the samples is not great enough to produce a marked increasing or decreasing order in the age results.

Sample 20 (Alum Bluff, FL) shows poor likeness as compared to almost all other samples, suggesting a possible bias or sample collection problem. Sample 2 (W of Gravel Pit Rd-B, Miocene) shows a sudden drop in likeness with samples 15–19, which may be due to a difference in depositional ages of the samples or some other reason.

The Kolmogorov-Smirnov (or K-S) test determines if a statistically significant difference exists between two zircon populations (Satkoski et al., 2013). Probability (P) calculated by

Table 4-1. Individual likeness (%) between each sample pair.

Likeness (%) between individual sample pairs																				
	1	2	3	4	5	6	7	8	9	10	11	12	13	14	15	16	17	18	19	20
1	X	X	X	X	X	X	X	X	X	X	X	X	X	X	X	X	X	X	X	X
2	X							X	X											
3	X	60.7						X	X											
4	X	66	71.8					X	X											
5	X	64.3	70.5	70.5				X	X											
6	X	61.4	65.5	69.6	69.3			X	X											
7	X	63.8	62.8	68.5	70.5	66.4		X	X											
8	X	X	X	X	X	X	X	X	X	X	X	X	X	X	X	X	X	X	X	X
9	X	X	X	X	X	X	X	X	X	X	X	X	X	X	X	X	X	X	X	X
10	X	58.4	67.7	67.2	66.8	62.8	64.2	X	X											
11	X	66.7	71.9	72.7	68.8	64.9	70.2	X	X	72.6										
12	X	63.6	73.9	77.4	67.5	65.3	67.5	X	X	73.7	74.3									
13	X	60.4	69.6	72.8	69.3	66.6	65.4	X	X	71	70.5	72.4								
14	X	65.1	70	73.8	70.3	65.4	72.2	X	X	66.4	71.3	71.2	67.1							
15	X	56.2	64.5	68.3	65.7	55.6	63.5	X	X	67.1	76.3	69.2	67.2	66.4						
16	X	59.2	64.2	65.3	67.1	67.9	64.1	X	X	66.8	70.1	66.3	66.8	60.5	57.4					
17	X	56.5	63.8	66.9	63.9	55.8	65	X	X	65.5	68.8	68.2	65.9	63.5	74.3	57.4				
18	X	55.3	70.5	68.1	65.1	54.9	61.3	X	X	68.5	74.6	72.1	68.4	70.6	78.1	61.7	75.8			
19	X	55	69.3	69.9	64.3	56.5	59.3	X	X	72.1	73.9	69.2	67.9	67.7	77.3	62	70	73.8		
20	X	49.1	53.6	54.7	56.1	47.8	57.4	X	X	55	63.1	54.5	57.6	53.3	75.4	48.6	69.2	64.7	64	

Numbers in top row and far left column correspond to respective samples (Table 3-1 in Chapter 3). "X" means data not available. Highlighted results indicate a likeness of >60% (very good degree of likeness).

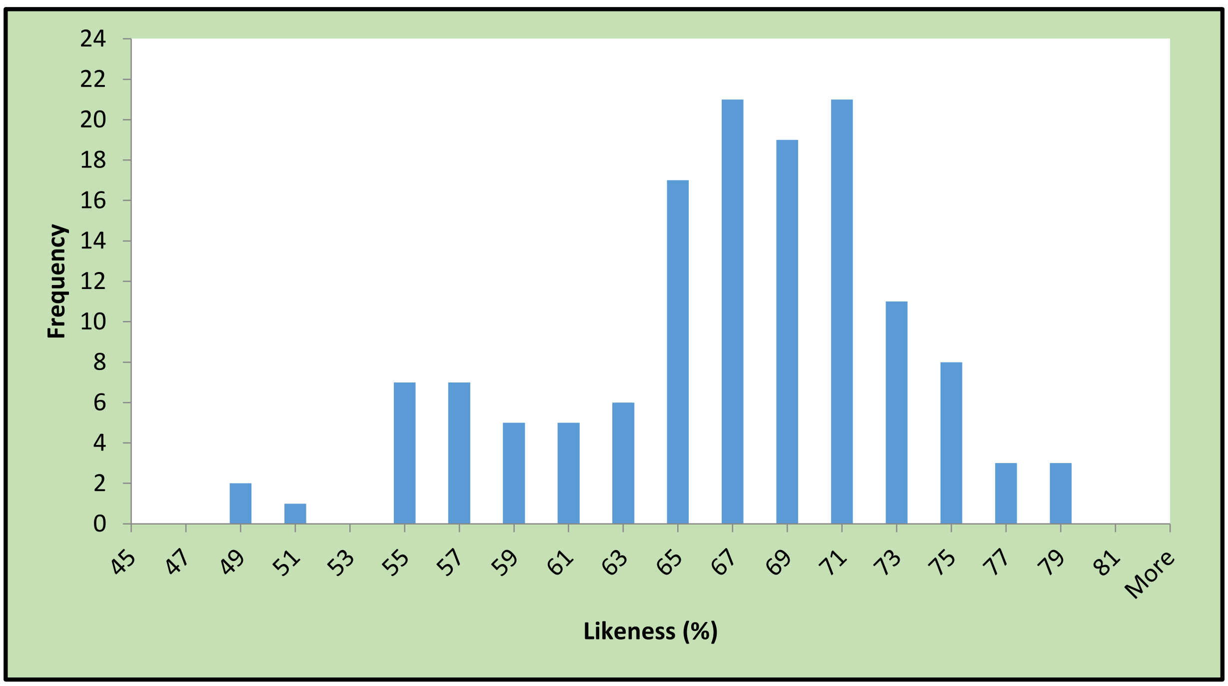

Figure 4-6. Frequency plot of likeness (%) between all sample pairs. Likeness >60% defines the acceptable range of results.

the K-S test represents the probability that the two populations could have been selected at random from the same parent population (Harris et al., 2012). P values of zero imply that any similarity between the two samples is likely due to random chance; P values near the maximum value of 1.0 suggest that there is a small likelihood that the similarity is due to random chance alone and that the two populations are likely from the same parent (Harris et al., 2012). P is calculated as the probability that the observed maximum difference is due to random sampling error versus a true difference between the populations; if P is high (typically $P \geq 0.05$, at 95 percent level of statistical confidence), it is unlikely that the two samples are from different populations (Satkoski et al., 2013). P greater than 0.05 is highly desirable, as it indicates that there is 95 percent chance that the two samples being compared do not belong to different source populations.

Most of the sample pairs (~78%) show $P \geq 0.05$ (Table 4-2), indicating that most samples belong to same source population, or do not belong to different source populations at 95 percent statistical confidence interval. Collective frequency of all samples with $P \geq 0.05$ has higher frequency compared to sample pairs with P less than 0.05 (Fig. 4-7), indicating most samples statistically do not belong to different populations. Sample 20 (Alum Bluff, FL) produces very low P values with all other samples; this may be because of a bias (e.g., selective grain loss during transportation of sediments) or a sample collection problem. Sample 2 (W of Gravel Pit Rd-B, Miocene) generates very low P values ($P \approx 0.0$), with samples 15–19 indicating an obvious disparity between the samples; this may be because of differences in the depositional age between samples or some other reason. These results are consistent with likeness metric results. Sample 16 (Love Quarry, MS) shows very low P-values with samples 17–19; this may be because of large spatial distance

Table 4-2. K-S test statistical probability (P) between each sample pair.

K-S test (P) for all sample pairs																				
	1	2	3	4	5	6	7	8	9	10	11	12	13	14	15	16	17	18	19	20
1	X	X	X	X	X	X	X	X	X	X	X	X	X	X	X	X	X	X	X	X
2	X							X	X											
3	X	0.05						X	X											
4	X	0.08	0.87					X	X											
5	X	0.05	1.00	0.83				X	X											
6	X	0.14	0.70	0.33	0.73			X	X											
7	X	0.45	0.76	0.96	0.79	0.85		X	X											
8	X	X	X	X	X	X	X	X	X	X	X	X	X	X	X	X	X	X	X	X
9	X	X	X	X	X	X	X	X	X	X	X	X	X	X	X	X	X	X	X	X
10	X	0.01	1.00	0.94	0.99	0.59	0.52	X	X											
11	X	0.17	0.89	1.00	0.52	0.17	0.77	X	X	0.97										
12	X	0.01	0.99	0.86	0.99	0.29	0.39	X	X	0.93	0.54									
13	X	0.28	0.74	0.99	0.74	0.44	0.99	X	X	0.76	0.99	0.38								
14	X	0.05	1.00	0.96	1.00	0.51	0.67	X	X	1.00	0.81	0.99	0.61							
15	X	0.00	0.84	0.23	0.52	0.18	0.08	X	X	0.77	0.35	0.53	0.16	0.81						
16	X	0.59	0.35	0.58	0.33	0.43	0.79	X	X	0.35	0.84	0.14	0.94	0.16	0.04					
17	X	0.00	0.43	0.22	0.38	0.03	0.02	X	X	0.31	0.08	0.52	0.04	0.42	0.80	0.00				
18	X	0.00	0.47	0.17	0.33	0.04	0.02	X	X	0.51	0.09	0.71	0.09	0.52	0.96	0.01	1.00			
19	X	0.00	0.75	0.38	0.51	0.12	0.06	X	X	0.86	0.24	0.52	0.23	0.74	0.78	0.02	0.56	0.72		
20	X	0.00	0.00	0.00	0.00	0.00	0.00	X	X	0.00	0.00	0.00	0.00	0.00	0.06	0.00	0.03	0.04	0.00	

Numbers in top row and far left column correspond to respective samples (Table 3-1 in Chapter 3). "X" means data not available. Highlighted results indicate P ≥ 0.05 (> 95% chance that the samples are not from different populations).

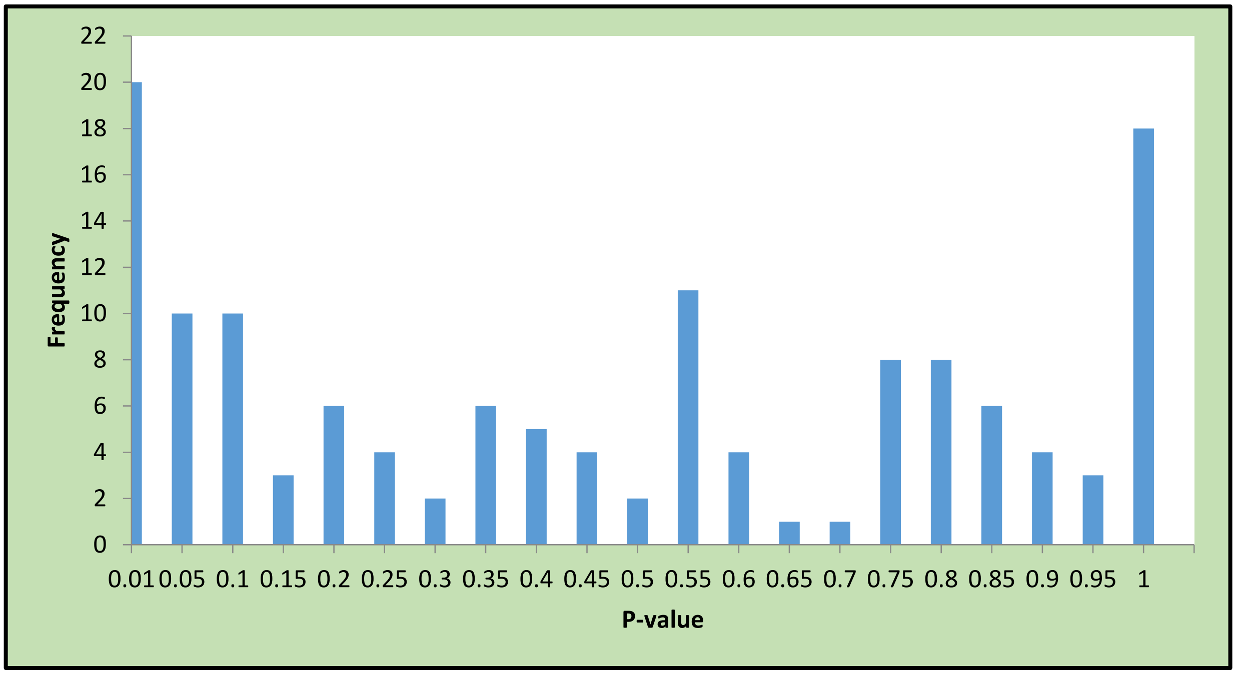

Figure 4-7. Frequency plot of P-values from K-S test of all sample pairs. P ≥ 0.05 defines the acceptable range of results.

or samples belonging to different stratigraphic units, even though there is no direct relationship between P-values and separation between samples. Most results from the K-S test are consistent with results of the likeness test, affirming that most of the samples are statistically alike and belong to the same source population.

Interpretation of results

Zircons that have ages of >2.0 Ga are likely derived from several North American basement regions that are largely made of Archean and Proterozoic rocks, e.g., Superior Province in the Canadian Shield. These zircons are commonly present in Appalachian rocks as a result of transportation and multiple recycling. Presence of these zircons in a basin implies they may have been directly derived from Appalachian source rocks and possibly ultimately derived from farther sources such as the Superior Province in the Canadian Shield. Although all samples contain this zircon population, samples 6, 7, 10, 13, 14, and 16 are especially rich in these old zircons. There is no particular reason for this, because this population is found in all samples in smaller or greater numbers.

Samples 1 through 20 contain an exceptionally high frequency of Grenville (1.2-1.0 Ga) zircon age populations. These may be derived from a Mesoproterozoic (1200–1000 Ma) Grenville basement and/or recycled Grenville zircons. An abundance of Grenville zircons has remained in the system for recycling and constitute widespread dominance of detrital populations throughout North America (Thomas, 2011). "Grenville-age detrital zircons were distributed across most of the Laurentian craton during Neoproterozoic and incorporated in Neoproterozoic-Cambrian sandstones in western North America" (Thomas, 2011). Similarly these zircons may have been incorporated in Appalachian rocks in eastern

North America. Erosion of these rocks has produced recycled Grenville zircons in addition to the primary Grenville zircons (Thomas, 2011). Therefore, primary and recycled Grenville zircons are commonly found throughout the North American continent, perhaps including the Appalachians.

Three major orogenies affected the Appalachian orogen during its development: the Taconic (490–440 Ma), Acadian (420–350 Ma), and Alleghanian (330–260 Ma) (Hatcher, 2010). Also, accreted peri-Gondwanan (680–530 Ma) terranes form the extensive Carolina superterrane in the southeastern Appalachians (Hatcher, 2010). The Paleozoic zircons in my samples are extremely important in determining provenance of the samples. Samples 1-20 contain age peaks from all three tectonothermal events. Samples 3, 4, 5, 11, 13, 15, 18, and 19 show an exceptionally high frequency of Taconic, Acadian, Alleghanian and peri-Gondwanan zircon populations. These zircons are possibly derived from the Appalachian source. Few samples, such as samples 7, 12, 13, 14, 15, 16, and 17, show a subdued frequency in the Alleghanian ages. Lack of the prominent Alleghanian age group may be attributed to an over-representation of other age groups, thus statistically understating the significance of the Alleghanian population.

Several samples contain Late Cretaceous and Tertiary zircons, indicating that the latest depositional episode occurred after the youngest grain (~24 Ma) was deposited. Late Cretaceous zircons range between 99 and 67 m.y., while Tertiary zircons range between 64 and 24 m.y. Although the source of these zircons is unknown, they may possibly be derived from the western part of the continent. Samples 2, 4, 5, 6, 7, 10, 12, 14, 16, 17, 18, and 19 contain a significant number of zircons belonging to these age populations. The high level of concordance in this age group indicates the ages may be closer to the crystallization age of the zircon grains and perhaps were deposited rapidly within a very short time period of their formation. These younger zircons are texturally very small and fragmented in size and shape, indicating that they may have been deposited by heavy aeolian transportation. The youngest igneous crystallization dates obtained on detrital zircons from a sedimentary rock sample will provide a maximum age for sediment deposition (Nelson, 2001). The age of the young zircons in my samples define the maximum age for the deposition of the sediments that contain them.

A possible Appalachian crustal provenance can be seen in the detrital zircons of the samples analyzed. An overall predominance of Appalachian source in all detrital zircon samples suggests uplift in the source Appalachian Mountains during Miocene-Pliocene. The uplift induced increased erosion and sedimentation during which the zircons were deposited in the lower Gulf Coastal Plain.

Unravelling the history of Gulf Coastal Plain sediments is a complex task that requires several other perspectives from sedimentary petrology, mineralogy, geochemistry, geochronology, stratigraphy, structural geology, and geomorphology. It is important to acknowledge that, although the provenance analysis done for this particular study indicates a possible Appalachian source, there may be more work needed to understand the uniqueness of these results. The age peaks identified in the results discussed above likely belong to an Appalachian source population, but in some cases may also be derived from other alternative sources. Complete and successful provenance analysis requires understanding of compositional and textural parameters in concert with the detrital zircon spectrum. Compositional and textural parameters are affected by chemical weathering, mechanical disaggregation, authigenic inputs, hydrodynamic sorting, and diagenesis (Johnson, 1993). Further studies through textural and geochemical analyses may help decipher a more complete picture of the provenance of late Tertiary Gulf Coastal Plain sediments. Although a more complete sediment analysis is desirable for analyzing the uniqueness of an Appalachian provenance for the current results within the limits of this project, it is absolutely acceptable to infer that there is a strong possibility of Appalachian source in the detrital zircons analyzed for this study, which can be related to the late Tertiary tectonic uplift of the Appalachian Mountains.

Discussion and Conclusions

Previous studies involving detrital zircon geochronology of rocks/sediments derived from eastern and western North America have commonly been used to help solve a variety of geologic problems, e.g., to test for tectonomagmatic events and crustal melting during specific ages in the geologic past (Eriksson et al., 2003); to understand sediment provenance in the Tertiary Mississippi River (Craddock et al., 2013); to compare age frequency data in time and space from multiple sediment samples (Satkoski et al., 2013); and to compare variations in sediment ages from different sections of a river (Hietpas et al., 2011). No previous study had been performed to understand the late Tertiary Appalachian uplift with the use of detrital zircon geochronology of sediments in the lower Gulf Coastal Plain. Current research method used to test Appalachian uplift with detrital zircon geochronology is unique, and new detrital zircon age data through this study have provided a fresh perspective to view the late Tertiary Appalachian uplift.

Two main conclusions of the detrital zircon age data in this study are: (1) Major age peaks have been identified in the zircon data and related with provenance information. Based on results from this study, the ultimate source of late Tertiary sediments in the lower Gulf Coastal Plain is concluded to be possibly southern and central Appalachians. (2) Zircon age data from each sample have been compared with every other sample. Statistical comparisons show high similarity of results between the samples, indicating a high likelihood of a common provenance regardless of the nature of the source.

In summary, major zircon age populations from the LA-ICP-MS data obtained in all 17 samples are:

- very old 2.5 Ga age peaks in 14 samples.
- a marked Grenville (1.0 Ga) peak in all samples.
- age peaks at 480 Ma, 400 Ma, and 300 Ma in almost all samples, indicating Taconic, Acadian, and Alleghanian orogen source rocks in the Appalachians for zircons in the sediments.
- a marked 600 Ma age peak in 14 samples indicating the presence of Carolina superterrane source rocks in the sediments (peri-Gondwanan rocks east of the Central Piedmont suture).
- Late Cretaceous and Tertiary (Paleocene, Eocene, Miocene) age peaks in ten samples.

Paleozoic age peaks in the zircon data clearly indicate a possible Appalachian source. Also, pre-Proterozoic and Grenville zircons may be derived from the Appalachians. Recognizing a possible Appalachian signature in these results has been useful to understand provenance of these Miocene-Pliocene sediments. Predominance of an

Appalachian source is likely related to the tectonic changes, perhaps a tectonic uplift in the southeastern Appalachians during the same time. Likeness and K-S metric results indicate great similarity in the zircon age data of all 17 samples, implying very little to insignificant differences between the 17 sets of detrital zircons data. In other words, irrespective of what the provenance is for the results of this study, it is safe to say that it stands similar for all 17 individual sets of data and that they are mutually alike.

While I appreciate the significance of provenance analysis in this study, I do not disregard the complexities involved in accurate provenance analysis. “Provenance encompasses all factors related to the production of sediment, with specific reference to the composition and location of the parent rocks as well as the physiography and climate of the source area from which the sediment is derived” (Weltje and Eynatten, 2004). Resolving the history of Gulf Coastal Plain sediments is a complex task, and accurate reconstruction of sedimentary history of zircons from the source to deposition demands further study and data from sedimentary petrology, mineralogy, geochemistry, geochronology, stratigraphy, structural geology, and geomorphology. To establish a complete and unarguable source for the sediments in this study, we need compositional and textural data in addition to detrital zircon spectrum. If not the Appalachians, there may be alternative sources of sediments, which must be determined as an essential next step in this project. Such a task could start with critical areas that need to be tested first, e.g., missing Paleozoic age peaks, paucity of Taconic peaks relative to Acadian age peaks, over-representation of other age peaks as compared to Alleghanian, etc. Critical analysis of the detrital zircon age data and precise understanding of a complete dispersal system from source to deposition are needed for identification of a unique provenance of sediment samples in this study.

CHAPTER V

RIVER TERRACE MAPPING: UPLIFT-RELATED TERRACES ALONG THE FRENCH BROAD RIVER

Why study fluvial terraces?

Fluvial terraces may be closely related to regional uplift, the main reason for studying them as a part of this project. Fluvial terraces in the southern and central Appalachians are indicators of ongoing uplift possibly produced by active tectonic processes. These are landforms that integrate erosional and depositional processes as a river forms its valley. In the southeastern Appalachians terraces are commonly found along all rivers and are an important part of tectonic uplift history.

Morphology of fluvial terraces

"Fluvial terraces are abandoned floodplains forming at a higher elevation than at present" (Ritter et al., 2011). This section is a summary of morphology of terraces based on Ritter et al. (2011). Tread of a terrace is the flatter base that was previously occupied by an older floodplain, and the scarp of a terrace is the steep slope face that connects the tread to a lower segment of the valley. Terrace deposits are commonly composed of sediments transported by the river as it flowed through its channel previously. There are two types of fluvial terraces based on a genetic classification: 1) erosional and 2) depositional.

In erosional terraces, the tread has been formed by lateral erosion. If lateral erosion cuts/truncates the local bedrock in the region, it produces a strath, or a rock-cut terrace. Shifting of channel position back and forth in a valley and occasional scouring eventually produce a beveled surface, resulting in an erosional terrace. Such terraces are commonly formed in mountain-uplift related areas. Major erosional terrace straths form as a result of tectonism and are tectonically controlled stream-terrace landforms. Erosional terraces are usually capped by a thin layer of alluvium formed by riverbed scouring, and the layer is underlain by hard bedrock along a smooth surface. Repetitive erosion and accretion by the river on the valley bottom produces lateral accretion features (point bars) on the flat eroded surface of the underlying bedrock. Later scouring can remove/erode this alluvial material and expose the underlying surface.

Depositional terraces form by extensive periods of valley fill and aggradation due to depositional processes. Cyclic periods of valley fill and entrenchment occur as alluvium is deposited and the depositional terrace subsequently forms. Valley filling occurs because the amount of sediment produced in the basin exceeds the amount that can be carried by the river. Alluvial cover is very thick in a depositional terrace with an irregular bedrock surface underlying the fill of the depositional terrace. Alluvium under the tread can vary in thickness and is not controlled by riverbed scouring. Depositional terraces are mainly driven by climatically induced aggradation, e.g., glacial outwash or sea-level rise affecting base level. Besides climate, local changes in lithologic controls and drainage distribution in main stream tributaries can produce depositional terraces. Sudden influx of coarse sediments into the valley of the stream-capturing tributary causes an excess of sediment load and debris to flow into the main stream. The main stream has difficulty carrying the bedload and the resulting valley fill forms a depositional terrace.

Study Area

The study area is located in the Appalachian Valley and Ridge foreland fold-thrust belt and consists of multiple Quaternary terraces in a ~150 km^2 area around part of Douglas Reservoir in eastern Tennessee [Fig. 5-1(a)]. Douglas Lake is an artificial reservoir on the French Broad River, located ~50 km E of Knoxville, Tennessee [Fig. 5-1(a) and (b)]. Dandridge, Tennessee, is in the northern part of the study area. This study area was chosen because of the excellent exposure of terrace and bedrock deposits, and many exposed areas along the shores of the TVA Douglas Lake during late fall-winter-early spring drawdowns. Most previous mapping was concentrated on bedrock (Hatcher, 1965; Hardeman, 1966; Hatcher and Bridge, 1974; Shanmugam and Walker, 1980), so knowledge of the Quaternary geology (terraces) is mostly lacking in this area. The study area consists of parts of four 7.5-minute quadrangles along the French Broad River in Jefferson and Sevier Counties (parts of Jefferson City, Shady Grove, Douglas Dam, Chestnut Grove, and White Pine quadrangles). A 1:24,000-scale provisional geologic map of fluvial terraces along Douglas Lake has been produced as a major part of this study, and has been useful to resolve relative chronology of terraces and better understand the history of the French Broad River drainage as part of the Tennessee River system.

Bedrock geology of the study area consists of Upper Cambrian-Lower Ordovician Knox Group unconformably overlain by Middle Ordovician Chickamauga Group (thin Lenoir Limestone and overlying Sevier Shale, a mixed clastic unit of calcareous turbiditic shale and sandstone (Hatcher, 1965; Hardeman, 1966; Hatcher and Bridge, 1974; Shanmugam and

Figure 5-1. (a) Location of the study area (red rectangle east of Knoxville) in the Appalachian Valley and Ridge foreland fold-thrust belt. **(b)** Generalized geologic, topographic, shaded-relief map of the study area showing the location of Douglas Lake and the French Broad River channel. Q–Prominent Quaternary river deposits visible at this scale. Source: USGS topographic maps of Jefferson City, Shady Grove, Douglas Dam, Chestnut Grove, and White Pine quadrangles. Graphic by Andrew L. Wunderlich.

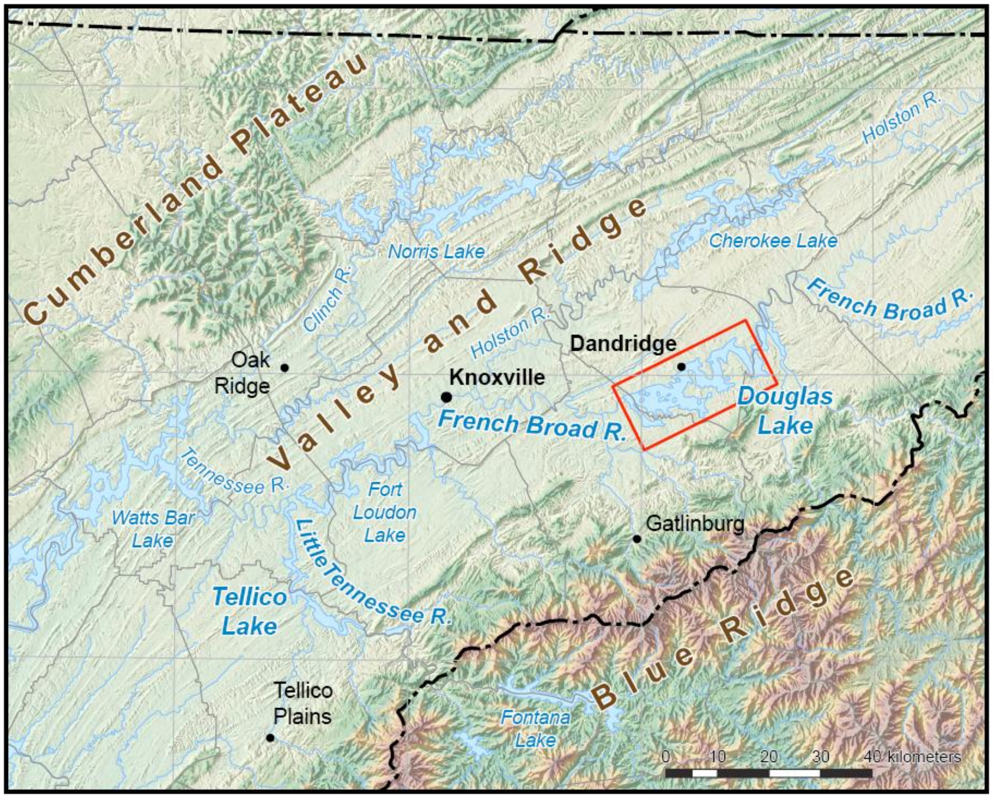
84°W
83°W
Cumberland Plateau
Valley and Ridge
Blue Ridge
Norris Lake
Cherokee Lake
Holston R.
Clinch R.
French Broad R.
Dandridge
Oak Ridge
Knoxville
Douglas Lake
Tennessee R.
Watts Bar Lake
Fort Loudon Lake
LittleTennessee R.
Gatlinburg
Tellico Lake
Tellico Plains
Fontana Lake
36°N
0 10 20 30 40 kilometers

(a)

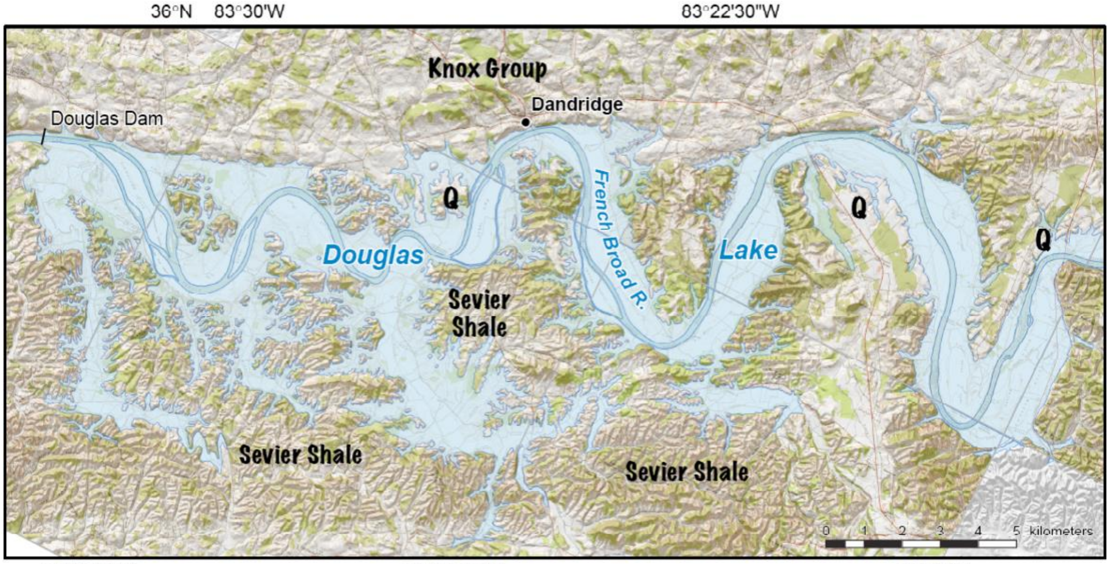
36°N 83°30'W
83°22'30"W
Knox Group
Dandridge
Douglas Dam
Q
Douglas
Lake
French Broad R.
Sevier Shale
0 1 2 3 4 5 kilometers
35°52'30"N
83°22'30"W
83°15'W

(b)

Walker, 1980). These bedrock units are overlain by latest Tertiary(?)-Quaternary river sediments (mostly erosional terraces) of the French Broad drainage, which formed as the river cut a channel, isolating segments of older floodplains (Hatcher, 1965; Hardeman, 1966; Hatcher and Bridge, 1974; Shanmugam and Walker, 1980).

The French Broad River headwaters are located in the Piedmont and Blue Ridge northwest of Brevard, North Carolina, where tributaries flow east from the Blue Ridge into the westernmost Piedmont to form the French Broad River. The French Broad River then flows northeast near Asheville, North Carolina, turns westward and crosses the highest part of Blue Ridge, then flows into the Valley and Ridge and joins the Holston River at Knoxville to form the Tennessee River. Other major westward-flowing tributaries of the Tennessee River, e.g., the Ocoee, Hiwassee, Little Tennessee, and Pigeon, follow patterns similar to the French Broad River and have headwaters on the east side of the Blue Ridge, suggesting these are ancient (pre-Quaternary) superposed streams.

Mapping methodology

Classical geologic mapping techniques were employed including extensive foot traverses using Google™ images and topographic base maps at 1:12,000 scale, with locations provided by a GPS. An airborne drone was also employed on an experimental basis to evaluate the utility of this technology to investigate areas otherwise not accessible; results to date are mixed. The mapping data were used to construct shapefiles in ArcGIS™ to assist in constructing a provisional geologic map of much of the study area. River terrace deposits have been mapped in parts of Jefferson City, Shady Grove, Douglas Dam, Chestnut Grove, and White Pine 7.5-minute quadrangles in Tennessee using Google™ images and

1:12,000-scale topographic base maps. Use of vintage maps is reflected in the current provisional geologic map (Plate 1). The modern floodplain (T0) and the lowermost terrace (T1) are generally visible on the vintage topographic base but are physically inaccessible, since they are continually covered by the reservoir.

Classical geologic mapping that involves separation of terraces during foot traverses is the primary method of data collection. Locations of contacts are recorded on paper maps assisted by a GPS unit. Basic field data consist of visible and approximately located contacts between separate river terraces, bedrock and lower contacts of river terraces, and composition and distribution of single traceable terraces. The resulting map has been compiled in ArcGIS using field data exported to Adobe Illustrator™. At least five terraces have been separated along the French Broad River in the study area, and it is very likely that several higher terraces exist that have not yet been mapped.

Results and interpretation

The provisional terrace map resolves relative chronology of terraces and helps to better understand the history of the French Broad River drainage as part of the Tennessee River system. Higher terraces are older than lower terraces (age of T5 > T4 >. . .T0) (Plate 1). At least five younger (Tertiary(?) to Quaternary) terraces were recognized in the study area. Terraces range 300–500 m in elevation and are individually 5-8 m thick (height) at various places. Pebble compositions and textural maturity indicate provenance at least 100 km or greater from where they presently reside. Mature terrace deposits indicate a lengthy and complex history of development of the French Broad (-Tennessee) River system.

Mapping of fluvial terraces at Douglas Lake along the French Broad River has been useful to understand the relative chronology of terraces and get a preliminary idea of the relations between terraces and development of the river valley as uplift occurred. Nature and distribution of the fluvial terraces and available Optically Stimulated Luminescence (OSL) age dates (Hatcher et al., 2012) suggest that the modern French Broad River has undergone a long developmental history. Oldest OSL ages of terrace deposits at Douglas Lake, French Broad River are 203±13 ka, indicating that the uplift occurred at least 203±13 ka in this area (Hatcher et al., 2012).

Terraces mostly consist of a basal coarse pebble to boulder gravel layer that fines upward into sand and then into red clay [Fig. 5-2(a) and (b)]. Pebbles to boulders are dominantly composed of vein quartz (all terraces) and chert (mixed with quartz in lower terraces) with lesser amounts of quartzite and granitoid, and rare amphibolite and calc-silicate (confined to higher terraces). Quartzite is likely derived from the frontal Blue Ridge, whereas the granitoid is derived from plutons in the eastern Blue Ridge or basement in the western and central Blue Ridge. Amphibolite and calcsilicate are likely derived from the eastern Blue Ridge. Unique characteristics of the clasts indicate a Blue Ridge source, suggesting a long and complex transportation history. Intense weathering of the clasts indicates antiquity of the river system. Quartzite and other clasts, except vein quartz, in higher terraces are more weathered than those in lower terraces. Individual terrace elevations increase upstream. The terraces unconformably overlie Paleozoic Sevier Shale and Knox Dolomite. Terrace mapping along the French Broad River has provided a better perspective of the terraces in the Tertiary uplift process.

Figure 5-2. (a) Terraces in the upper part of Douglas Lake distinguished by the basal gravel layer overlain by a fining-upward sequence of sand and clay. Note that bedrock is exposed in the creek bed; the flat area immediately above the person in the mid-ground is the top of another terrace. **(b)** Terrace deposits on the south side of Douglas Lake W of Dandridge, TN, that exhibit both channeling and cross bedding. Trough cross beds occur in channeled sand immediately above a contact marked by a zone of Mn-Fe oxides. The cross-bedded sand is truncated by less prominently bedded, finer-grained sand overlain by red clay that may have moved as part of a colluvium. Photographs by RDH.

(a)

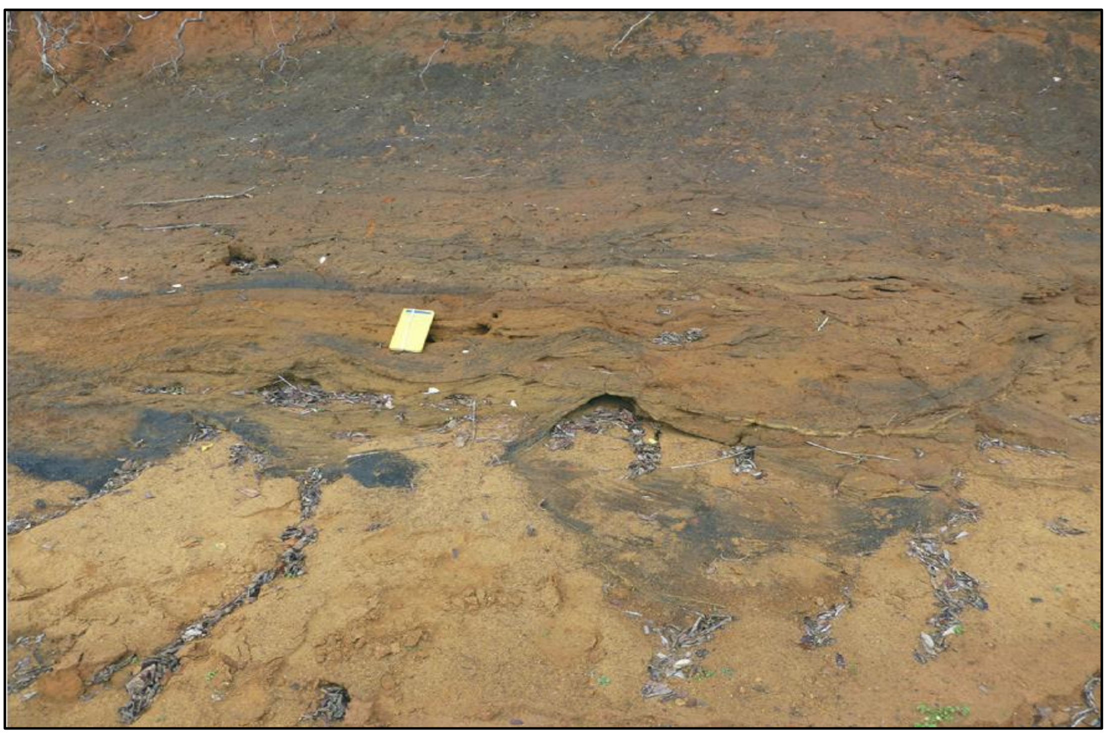

(b)

Occurrence of relict terrace gravels on some of the high ridges on the French Broad River and possibly other rivers systems several km from the present-day river channel is an interesting observation. These gravels have been observed 100 to 150 m above the present-day channel in the Douglas Lake area northwest of Dandridge, and also downstream at least as far as west Knoxville (Hatcher, 1965). Clasts are predominantly vein quartz and chert, quartzite, pegmatite, and granitic basement rocks. The quartzite may be derived from the Longarm Quartzite (Snowbird Group) and one or more of the Chilhowee Group quartzites in the Blue Ridge, as are the vein quartz and basement pebbles; most of the granitic rocks in higher terraces are partially to mostly decomposed, and the quartzite may also be partially decomposed, particularly if it is feldspathic. Occurrence of these gravels/pebbles indicates accelerated incision of the river valley due to base level changes caused by the late Tertiary tectonic uplift.

Significance of age dating terrace deposits

Accurately dating terrace deposits can provide ages that constrain the incision rate of the stream system, timing of events that control incision rates, and response time of a fluvial system to uplift within the drainage basin (Repka et al., 1997). Ages of these terraces can be determined using cosmogenic nuclide dating and optically stimulated luminescence (OSL) dating. OSL dates of terrace deposits from four sites around Douglas Lake are oldest at 203,010 ± 13,035 yr and youngest at 73,440 yr (Hatcher et al., 2012). Since the terraces formed as a result of uplift, the oldest age obtained on the terraces is equal to or less than the age of the uplift in this area. Old OSL age dates of terrace deposits in this region also indicate that the French Broad River has had a long developmental history spanning many thousands of years. The oldest age recorded is from the highest terrace in this area. Older ages can be expected from terrace deposits that occur at higher elevation, because higher terraces are older than lower terraces. Incision rates can also be calculated using vertical distance and age interval between consecutive terraces. Cosmogenic age dating of terrace deposits from Tellico Lake southwest of Knoxville are currently being performed as part of another related study; results of this study should prove to be very significant in understanding timing of the uplift. It is important that a large number of samples are used for dating terrace deposits to ensure accurate and precise ages, and to reduce any age scatter effect that may have been caused by exposure time differences between surface clasts and buried clasts (Repka et al., 1997).

Discussion: Implications from fluvial terrace mapping

No previous studies that include terrace mapping have been done in the current study area; the provisional geologic terrace map produced in this study is new and unmodified. An archeological report and fluvial terrace mapping by Paul A. Delcourt (1980) along Tellico Lake, 107 km southwest of Knoxville, have been useful references in mapping fluvial terraces along Douglas Lake. Vintage topographic maps made prior to construction of Douglas Reservoir in 1943 show the extent of floodplains and lower terraces. All terraces higher than T0 are older than the current floodplain. Terrace mapping has shown the relative position of older terraces to the current channel.

Historically, the river flowed at a much higher elevation than the current channel position. The highest historical position of the river is indicated by the position of the highest terrace occurring along the river. The amount of material that has been removed during the process of the river cutting through its valley is equivalent to the amount of erosion that has taken place during this time. In this case, an uplift-related base level change has probably driven the rapid river incision. Each terrace is indicative of a phase during which the river was adjusting to the changing base level. Mapping terraces has been useful to retrospectively see the track of changes in the channel slopes during periods of uplift. Changes in spatial and temporal position of terraces in landscape evolution occur as responses to regional tectonic uplift. Quantification of total uplift is possible using interrelationships of a landscape evolution model described here. Equations (5-1) to (5-6) show the relationships between total base level drop and total uplift. Total drop in base level in a region is a cumulative sum of individual base drops over a period of time (Eq. 5-1). Each individual base level drop is directly proportional to amount of tectonic uplift during that time; therefore, total base level drop is directly proportional to total uplift during that time (Eq. 5-2). As discussed in this chapter, fluvial terraces are an integral part and indicator of tectonic uplift and related to the drop in base level. Total drop in base level over a period of time is directly proportional to vertical separation between the highest terrace and current floodplain (Eq. 5-3). Thus it follows that total uplift at a given point of time is directly proportional to the vertical separation between the highest terrace and current floodplain (Eq. 5-4). Total uplift is a sum of multiple individual uplifts at different time periods (Eq. 5-5). A corollary from this is that the total drop in base level in a region is the product of cumulative sum of individual tectonic uplifts at various times and a constant that accounts for other relatively stable factors during the given period of time (Eq. 5-6). Quantification of total uplift is possible using these equations and recording the required variables in these equations.

Assuming that all uplift in the southeastern Appalachians has been driven by tectonic uplift,

$$D = BL_0 + BL_1 + BL_2 + \ldots + BL_n \quad \text{Eq. 5-1}$$

$$D \propto Total\ uplift \quad \text{Eq. 5-2}$$

$$H \propto D \quad \text{Eq. 5-3}$$

$$H \propto Total\ uplift \quad \text{Eq. 5-4}$$

$$Total\ uplift = UTi_n + UTi_{n-1} + \ldots + UTi_3 + UTi_2 + UTi_1 + UTi_0$$

$$Total\ uplift = \sum_{k=0}^{n} (UTi)_k$$

Eq. 5-5

$$D \propto \sum_{k=0}^{n} (UTi)_k$$

$$D = \in * \sum_{k=0}^{n} (UTi)_k$$

Eq. 5-6

where BL_n = Base level drop during time n

D= Total drop in base level from beginning of mountain uplift till now

H= Vertical distance between highest terrace and current floodplain

T_0........T_n = Terraces

UTi_n= Uplift during time *n*

$\epsilon =$ physical constant accounting for volume of material eroded, velocity of water, and rate of incision.

Landscape evolution is a slow adaptive process during which changes responsive to a climatic or tectonic event are progressively recorded in time. Stratigraphic and geomorphic evidence of regional tectonic uplift is preserved through fluvial terraces.

Contour intervals on the base vintage maps decide the maximum resolution at which terrace contacts can be placed in the fluvial terrace map. Vintage maps used in this study have 20 ft contours with supplementary contours of 10 ft for the floodplain and gentler slopes.

Transverse cross sections demonstrate the relative position of terraces along the river [Fig. 5-3(a) and (b)]. The transverse cross sections of the river indicate [Fig. 5-3(b)]: (1) higher older terraces occur uphill from the current floodplain, (2) terraces increase in elevation from mouth to source of the river i.e. the same terrace occurs at a higher elevation closer to the source of the river.

Relative elevations of river terraces along Douglas Lake were determined through mapping and are shown in Table 5-1. Longitudinal profiles of terraces along Douglas Lake illustrate the relationship between multiple terraces within a part of the French Broad River valley (Table 5-1; Fig. 5-4). Longitudinal profiles of river terraces upstream help to understand interrelationships, evolution, and change in the gradient of terraces with distance from mouth to source. Longitudinal profiles of all terraces were produced using data in Table 5-1 and additional data from the provisional geologic map of fluvial terraces (Fig. 5-4; Plate 1).

The main observations that stand out from the longitudinal profiles are: (1) a marked upstream increase in height of the same terrace, and (2) prominently greater elevation of younger terraces (Fig. 5-4). Additionally, topographic gradients of terraces are steeper for lower and younger terraces, indicative of higher observable incision in younger terraces (Table 5-1, Fig. 5-4).

Figure 5-3. (a) Part of Douglas Lake and French Broad River showing locations of the transverse cross sections. Numbers on the French Broad River indicate river mileage. **(b)** Transverse cross sections showing relative positions of terraces along Douglas Lake and French Broad River. Terraces (shown in red) lie uncomformably over Paleozoic bedrock (shown in lavender). Bedrock in this region is comprised of Ordovician Sevier Shale and Knox Dolomite.

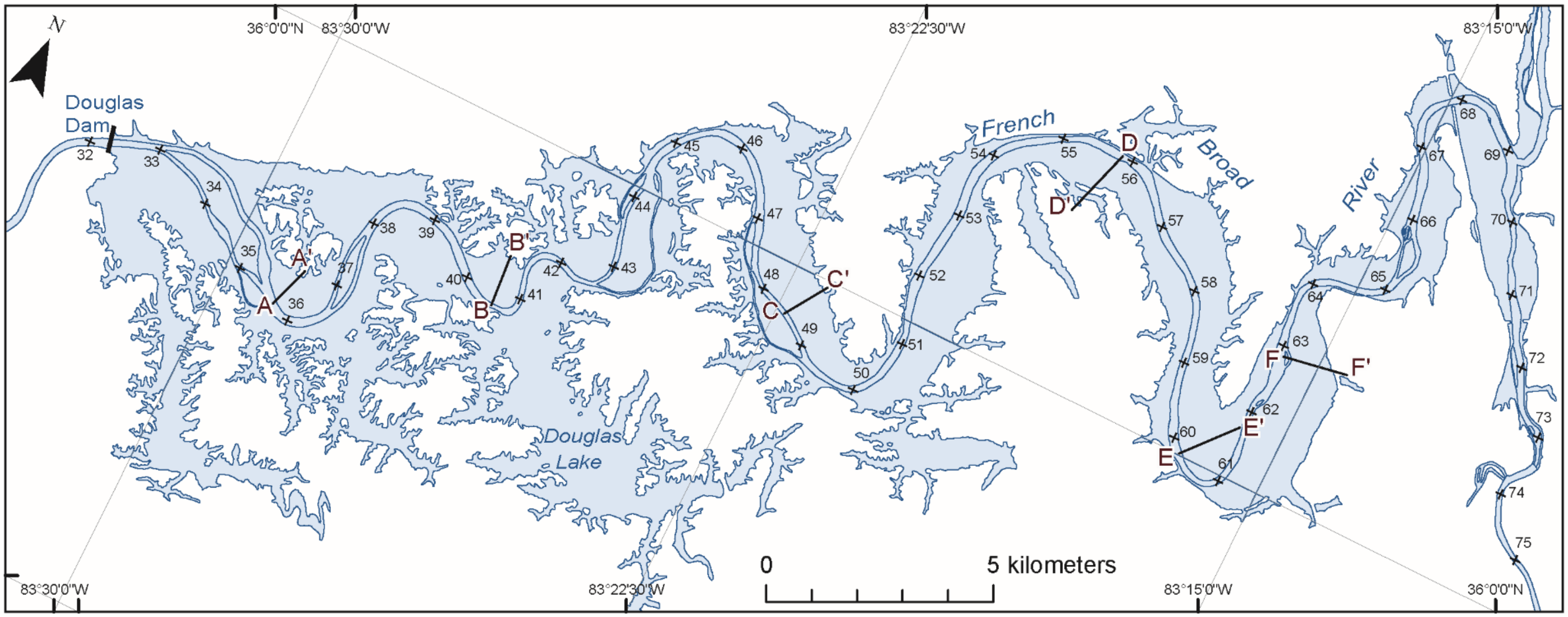

Douglas
Dam
French
Broad
River
Douglas
Lake
36°0'0"N
83°30'0"W
83°22'30"W
83°15'0"W
0
5 kilometers
A
A'
B
B'
C
C'
D
D'
E
E'
F
F'

(a)

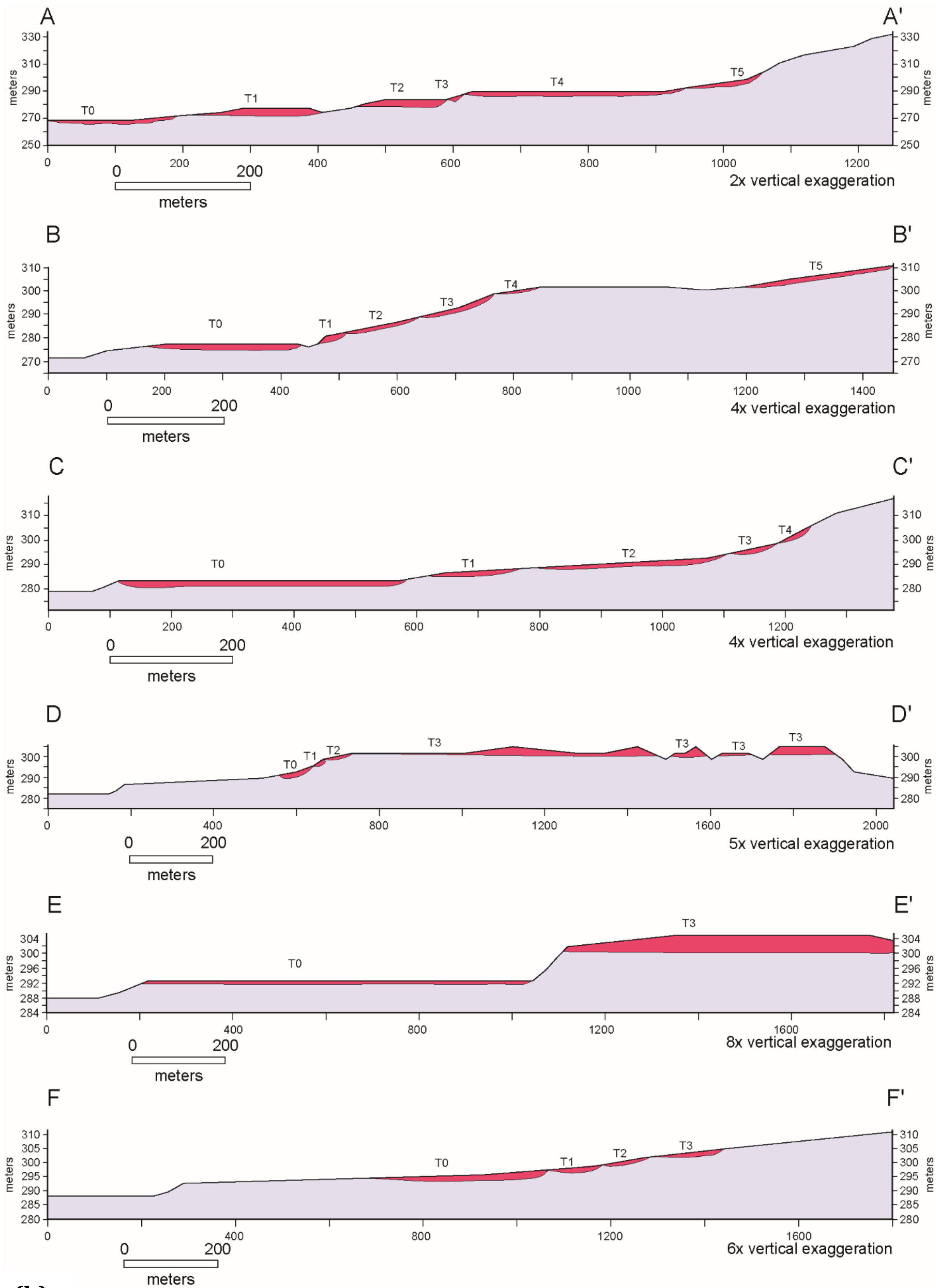

A
A'
T0
T1
T2
T3
T4
T5
meters
2x vertical exaggeration
B
B'
T0
T1
T2
T3
T4
T5
meters
4x vertical exaggeration
C
C'
T0
T1
T2
T3
T4
meters
4x vertical exaggeration
D
D'
T0
T1
T2
T3
meters
5x vertical exaggeration
E
E'
T0
T3
meters
8x vertical exaggeration
F
F'
T0
T1
T2
T3
meters
6x vertical exaggeration

(b)

Table 5-1. Height and longitudinal gradient (slope) of fluvial terraces along Douglas Lake, French Broad River.

Terrace Surface	Difference between highest and lowest elevation of terrace (ft)	Elevation above msl (ft)	Longitudinal distance upstream (river miles)	Gradient of longitudinal profile (ft/mile)
T5	30	1020	16	1.88
T4	80	1015	29	2.93
T3	65	990	31	2.09
T2	120	1035	41	2.92
T1	205	1090	43	4.77
T0	225	1100	44	5.11

Five discreet terraces identified and mapped in this part of the valley include the current modern floodplain T0 and older terraces at topographically higher elevations T1, T2, T3, T4 and T5. The gradient on younger terraces is steeper than on older terraces (Table 5-1, Fig. 5-4), indicating that erosion of higher terraces and progressive incision of the valley over time has resulted in the current longitudinal profiles. Upstream longitudinal gradients (slopes) of T5 to T0 systematically increase from 1.88 ft/river mile to 5.11 ft/river mile, respectively (measured from 32 river miles to 76 river miles; Table 5-1, Fig. 5-4). Progressive incision of the river valley over time indicates lowering of local base level for the French Broad River during the Quaternary, which is likely related to the ongoing tectonic uplift. In other words, mountain-uplift driven base-level changes have produced progressive incision of the French Broad River valley in this part of the southeastern Appalachians, creating vertically separated geomorphic features (terraces) along the length of the valley. Terrace longitudinal profiles are parallel to each other and are vertically

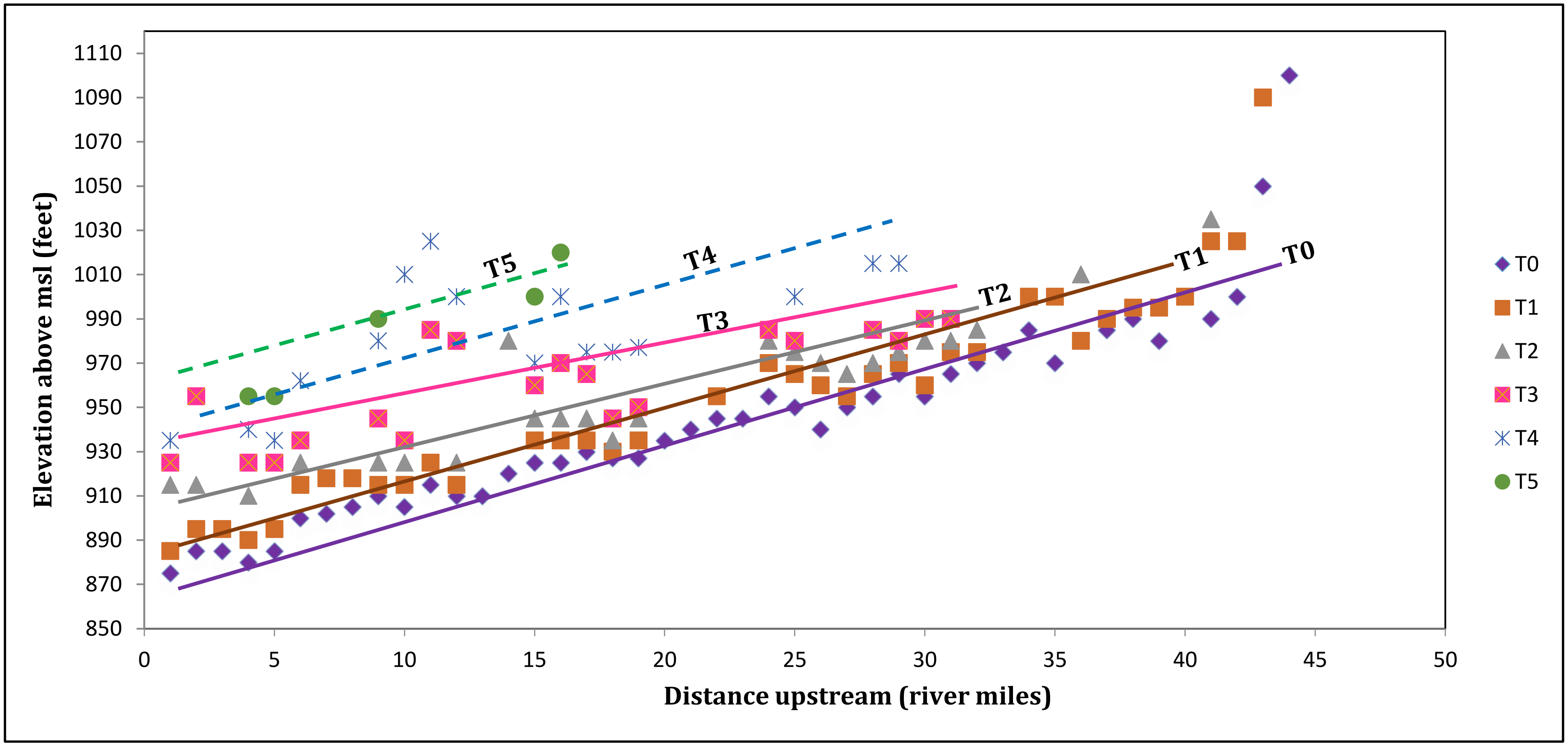

Figure 5-4. Longitudinal profiles of terraces (T0, T1, T2, T3, T4, and T5) along Douglas Lake, French Broad River. Data points are fitted to a best fit linear regression line that represents the terrace profile. Linear regression lines were not generated for T4 and T5 due to limited data available. Dotted line means estimated best fit line.

separated from one another (Fig. 5-4), suggesting that each terrace developed independently of the other terraces and no two terraces formed at a single point in time.

The primary geologic control operative over the entire time scale of valley incision and terrace development is most likely mountain rejuvenation by tectonic uplift. Erosion of channel walls, subsequent aggradation, deposition of river load, and reworking of sediments brought downslope from topographically higher regions have produced the final terrace deposits we see today. Further study and analysis of the terrace deposits is required to fully understand composition of terrace deposits and formation of the uplift-related terraces. Periods of accelerated tectonic uplift occurred multiple times during the late Tertiary period, producing phases of accelerated and intense incision in the river channels. Peak rates for valley aggradation occurred during these accelerated periods of uplift, as sedimentation rates increased due to higher erosion rates. Accurate ages of the terrace deposits (currently done as part of another related project) are a future prospect of this project and will be very helpful in recognizing timing of the periods of uplift.

CHAPTER VI

CONCLUSIONS

1. High elevations in the Blue Ridge and western Piedmont indicate active tectonic uplift in the southeastern Appalachians. Anomalous drainage networks including steep topographic profiles, deep incision of river valleys, stream captures, and westward-migrating drainage divides support the idea of recent tectonic uplift in the southern and central Appalachians.

2. LA-ICP-MS age dates of detrital zircons from Miocene-Pliocene sediment samples contain the following age peaks: (1) Archean: >2.5 Ga; (2) Mesoproterozoic (Grenville): 1.2-1.0 Ga; (3) Neoproterozoic: ~600 Ma; (4) Paleozoic: 480 Ma, 400 Ma, 300 Ma; and (5) Late Cretaceous and Tertiary: 99-67 Ma and 64-24 Ma.

3. Detrital zircon geochronology of sediment samples from the Gulf Coastal Plain show a likely dominant Appalachian provenance. This is based on the major age populations of the detrital zircons. A possible Appalachian provenance for Miocene-Pliocene sediments suggests a late Tertiary tectonic uplift in the southern and central Appalachians during Miocene-Pliocene. .

4. Statistical comparison of detrital zircon results from different samples using likeness and K-S metrics indicates common provenance because of a high degree of uniformity between the detrital zircon results of all samples. The likeness test produces a > 60 percent likeness among samples, implying that provenance of most samples is alike. The K-S test produces a ≥ 0.05 probability between sample results, suggesting that most samples have a high probability of being derived from a common source.

5. The provisional geologic map of fluvial terraces along the Douglas Lake reveals five distinct terraces: T0, T1, T2, T3, T4, and T5. T0 is the current floodplain and T5 is the oldest and highest terrace mapped.

6. River terrace profiles reveal an upstream increase in elevation of individual terraces. Younger terraces have steeper topographic profiles and greater recordable heights than older terraces. Topographic profiles of terraces suggests that progressive incision and erosion have influenced the evolution the valley affecting the current position of the terraces.

7. Maturity and composition of terrace deposits suggest they have been transported over very long distances and possibly derived from frontal Blue Ridge, basement in western and central Blue Ridge, and plutons in eastern Blue Ridge. Source of the clasts indicates a long and complex transportation history, and intense weathering of the deposits indicates antiquity of the river system.

REFERENCES CITED

Acker, L. L., and Hatcher, R. D., Jr., 1970, Relationships between structure and topography in northwest South Carolina: South Carolina Division of Geology, Geologic Notes, v. 14, p. 35-48.

Adams, G. I., Butts, C., Stephenson, L. W., and Cooke, W., 1926, Geology of Alabama: Geological Survey of Alabama, Special Report no. 14, 312 p.

Ahnert, F., 1970, Functional relationships between denudation, relief and uplift in large mid-latitude drainage basins: American Journal of Science, v. 268, p. 243-263.

Anthony, D. M., and Granger, D. E., 2004, A Late Tertiary origin for multilevel caves along the western escarpment of the Cumberland Plateau, Tennessee and Kentucky, established by cosmogenic ^{26}Al and ^{10}Be: Journal of Cave and Karst Studies, v. 66, p. 46-55.

Arizona LaserChron Center, Department of Geosciences, University of Arizona, http://www.geo.arizona.edu/alc (accessed June 2015).

Arizona LaserChron Center, 2014, Notes from ALC.

Chang, Z., Vervoort, J. D., McClelland, W. C., and Knaack, C, 2006, U-Pb dating of zircon by LA-ICP-MS: Geochemistry, Geophysics, Geosystems, v. 7, no. 5, doi: 10.1029/2005GC001100.

Craddock, W. H., and Kylander-Clark, A. R. C., 2013, U-Pb ages of detrital zircons from the Tertiary Mississippi River Delta in central Louisiana: Insights into sediment provenance: Geosphere, v. 9, no. 6, p. 1832-1851, doi:10.1130/GES00917.1.

Delcourt, P. A., 1980, Quaternary alluvial terraces of the Little Tennessee River Valley, east Tennessee, *in* Chapman, J., ed., The 1979 archaeological and geological investigations in the Tellico Reservoir: University of Tennessee Department of Anthropology Report of Investigations 29, p. 110–121.

Durrant, J. M., 1978, Structural and metamorphic history of the Eastern Virginia Piedmont province near Richmond, Va. [unpub. Master's thesis]: Columbus, The Ohio State University, 116 p.

Eriksson, K. A., Campbell, I. H., Palin, M. J., and Allen, C. M., 2003, Predominance of Grenvillian magmatism recorded in detrital zircons from modern Appalachian rivers: Journal of Geology, v. 111, p. 707-717.

Fedo, C. M., Sircombe, K. N., and Rainbird, R. H., 2003, Detrital zircon analysis of the sedimentary record: Reviews in Mineralogy and Geochemistry, v. 53, p. 277-303.

Frazier, D. E., 1974, Depositional-Episodes: Their Relationship to the Quaternary Stratigraphic Framework in the Northwestern Portion of the Gulf Basin: Bureau of

Economic Geology, The University of Texas at Austin, Austin, Texas-78712, Geological Circular 74-1.

Gallen, S. F., Wegmann, K. W., and Bohnenstiehl, D. R., 2013, Miocene rejuvenation of topographic relief in the southern Appalachians: GSA Today, v. 23, p. 4-10, doi: 10.1130/GSATG163A.1.

Gallen, S. F., Wegmann, K. W., Frankel, K. L., Hughes, S., Lewis, R. Q., Lyons, N., Paris, P., Ross, K., Bauer, J. B., and Witt, A. C., 2011, Hillslope response to knickpoint migration in the southern Appalachians: Implications for the evolution of post-orogenic landscapes: Earth Surface Processes and Landforms, v. 36, p. 1254-1267, doi: 10.1002/esp.2150; doi: 10.1130/GSATG163A.1.

Galloway, W. E., Ganey-Curry, P. E., Li, X., and Buffler, R. T., 2000, Cenozoic depositional history of the Gulf of Mexico Basin: American Association of Petroleum Geologists Bulletin, v. 84, p. 1743-1774.

Galloway, W. E., Whiteaker, T. L., and Ganey-Curry, P., 2011, History of Cenozoic North American drainage basin evolution, sediment yield, and accumulation in the Gulf of Mexico Basin: Geosphere, v. 7, p. 938-973, doi: 10.1130/GES00647.1.

Gehrels, G., 2012, Detrital zircon U-Pb geochronology: current methods and new opportunities, *in* Busby, C. and Azor, A., eds., Recent Advances in Tectonics of Sedimentary Basins: Hoboken, New Jersey, Wiley-Blackwell, p. 46-62.

Gehrels, G. E., Valencia, V. A., and Ruiz, J., 2008, Enhanced precision, accuracy, efficiency, and spatial resolution of U-Pb ages by laser ablation-multicollector-inductively coupled plasma-mass spectrometry: Geochemistry, Geophysics, Geosystems, v. 9, no. 3, doi: 10.1029/2007GC00 1805.

Gibson, T. G., 1970, Late Mesozoic-Cenozoic tectonic aspects of the Atlantic coastal margin: Geological Society of America Bulletin, v. 81, p. 1813-1822.

Hack, J. T., 1982, Physiographic divisions and differential uplift in the Piedmont and Blue Ridge: U.S. Geological Survey Professional Paper 1265, 49 p.

Hardeman, W. D., 1966, Geologic map of Tennessee: Tennessee Division of Geology, scale 1:250,000.

Harris, D. B., Toro, J., and Prokopiev, A. V., 2012, Detrital zircon U-Pb geochronology of Mesozoic sandstones from the Lower Yana River, northern Russia: Lithosphere, v. 5, no. 1, p. 98-108, doi: 10.1130/L250.1.

Harry, D. L, and Londono, J., 2004, Structure and evolution of the central Gulf of Mexico continental margin and coastal plain, southeast United States: Geological Society of America Bulletin, v. 116, no. ½, p. 188-199, doi: 10.1130/B25237.1.

Hatcher, R. D., Jr., 1965, Structure of the northern portion of the Dumplin Valley fault zone in East Tennessee [unpub. Ph.D. dissertation]: Knoxville, University of Tennessee, 168 p.

Hatcher, R. D., Jr., 1989, Tectonic synthesis of the U.S. Appalachians, *in* Hatcher, R. D., Jr., Thomas, W. A., and Viele, G. W., eds., The Appalachian-Ouachita orogen in the United States: Boulder, Colorado, Geological Society of America, The Geology of North America, v. F-2, p. 511-535.

Hatcher, R. D., Jr., 2010, The Appalachian orogen: A brief summary, *in* Tollo, R. P., Batholomew, M. J., Hibbard, J. P., and Karabinos, P. M., eds., From Rodinia to Pangea: The Lithotectonic Record of the Appalachian Region: Boulder, Colorado, Geological Society of America Memoir 206, p. 1-19, doi: 10.1130/2010.1206(01).

Hatcher, R. D., Jr., and Bridge, J., 1974, Geologic map of the Jefferson City quadrangle, Tennessee: Tennessee Division of Geology, GM 163-SW, scale 1:24,000.

Hatcher, R. D., Jr., Prowell, D. C., and Biswal, M. S., 2013, Lithospheric processes and the late Cenozoic origin of the Appalachian Mountains: Geological Society of America Abstracts with Programs, Annual Meeting, v. 45, no. 7, p. 60.

Hatcher, R. D., Jr., Vaughn, J. D., and Obermeier, S. F., 2012, Large earthquake paleoseismology in the East Tennessee seismic zone: Results of an 18-month pilot study, *in* Cox, R. T., Boyd, O. L., and Locat, J., eds., Recent Advances in North American Paleoseismology and Neotectonics East of the Rockies: Boulder, Colorado, Geological Society of America, Special Paper 493, p. 111-142.

Hietpas, J., Samson, S., Moecher, D., and Chakraborty, S., 2011, Enhancing tectonic and provenance information from detrital zircon studies: assessing terrane-scale sampling and grain-scale characterization: Journal of the Geological Society, London, v. 168, p. 309-318.

Jackson, S. E., Longerich, H. P., Dunning, G. R., and Fryer, B. J., 1992, The application of laser-ablation microprobe-inductively coupled plasma-mass spectrometry (LAM-ICP-MS) to *in situ* trace-element determinations in minerals: Canadian Mineralogist, v. 30, p. 1049-1064.

Johnson, M. J., 1993, The system controlling the composition of clastic sediments, *in* Johnsson, M. J., and Basu, A., eds., Processes Controlling the Composition of Clastic Sediments: Boulder, Colorado, Geological Society of America, Special Paper 284, p. 1-20.

Košler, J., and Sylvester, P. J., 2003, Present trends and the future of zircon in geochronology: laser ablation ICPMS: Reviews in Mineralogy and Geochemistry, v. 53, p. 243-275, doi: 10.2113/0530243.

McGlothlin, T., 1944, General geology of Mississippi: Bulletin of the American Association of Petroleum Geologists, v. 28, p. 29-62.

Milici, R. C., 1968, Mesozoic and Cenozoic physiographic development of the lower Tennessee River: In terms of the dynamic equilibrium concept: Journal of Geology, v. 76, p. 472-479.

Mineral Resource Data System, http://mrdata.usgs.gov/geology/state (accessed May 2015).

Morton, A. C., and Hallsworth, C. R., 1999, Processes controlling the composition of heavy mineral assemblages in sandstones: Sedimentary Geology, v. 124, p. 3-29.

Naeser, C. W., Naeser, N. D., and Southworth, S., 2005, Tracking across the southern Appalachians, *in* Hatcher, R. D., Jr., and Merschat, A. J., eds., Blue Ridge geology geotraverse east of the Great Smoky Mountains National Park, western North Carolina: North Carolina Geological Survey, Carolina Geological Society Annual Field Trip Guidebook, p. 67-71.

Nelson, D. R., 2001, An assessment of the determination of depositional ages for Precambrian clastic sedimentary rocks by U-Pb dating of detrital zircons: Sedimentary Geology, v. 141-142, p. 37-60, doi: 10.1016/S0037-0738(01)00067-7.

Ochoa, D., Whitelaw, M., Liu, Y., and Zavada, M., 2012, Palynology of Neogene sediments at the Gray fossil site, Tennessee, USA: Floristic implications: Review of Palaeobotany and Palynology, v. 184, p. 36-48, doi: 0.1016/j.revpalbo.2012.03.006.

Pavich, M. J., 1984, Appalachian Piedmont morphogenesis: weathering, erosion and Cenozoic uplift, *in* Morisawa, M., and Hack, J. T., eds., Tectonic geomorphology: The Binghamton Symposia in Geomorphology: International Series, no. 15, p. 299-319.

Pazzaglia, F. J., 2013, Fluvial terraces, *in* Wohl, E., ed., Treatise of Geomorphology: San Diego, Reference Module in Earth Systems and Environmental Sciences, v. 9, p. 379-412. doi:10.1016/B978-0-12-374739-6.00248-7.

Pazzaglia, F. J., and Brandon, M. T., 1996, Macrogeomorphic evolution of the post-Triassic Appalachian Mountains determined by deconvolution of the offshore basin sedimentary record: Basin Research, v. 8, p. 255-278.

Phillips, J. D., and Forsyth, D., 1972, Plate tectonics, paleomagnetism, and the opening of the Atlantic: Geological Society of America Bulletin, v. 83, p. 1579-1600.

Poag, C. W., and Sevon, W. D., 1989, A record of Appalachian denudation in postrift Mesozoic and Cenozoic sedimentary deposits of the U.S. Middle Atlantic continental margin: Geomorphology, v. 2, p. 119-157.

Prince, P. S. , Spotila, J. A., and Henika, W. S., 2010, New physical evidence of the role of stream capture in active retreat of the Blue Ridge escarpment, southern Appalachians: Geomorphology, v. 123, p. 305-319, doi: 10.1016/j.geomorph.2010.07.023.

Prince, P. S., Spotila, J. A., and Henika, W. S., 2011, Stream capture as driver of transient landscape evolution in a tectonically quiescent setting: Geology, v. 39, no. 9, p. 823-826, doi: 10.1130/G32008.1.

Prowell, D. C., 1983, Index of faults of Cretaceous and Cenozoic age in the eastern United States: U.S. Geological Survey Miscellaneous Field Studies Map MF-1269, scale 1: 2,500,000.

Prowell, D. C., and Christopher, R. A., 2006, Evidence of the Late Cenozoic uplift in the southern Appalachian Mountains from isolated sediment traps: Geological Society of America Abstracts with Programs, Southeastern Section Meeting, v. 38, no. 3, p. 67.

Prowell, D. C., and Christopher, R. A., 2010, The fault with the White House: A study of Late Cenozoic tectonism in Washington, D.C.: Geological Society of America Abstracts with Programs, Northeastern and Southeastern Sections Joint Meeting, v. 42, no. 1, p. 100.

Reed, J. C., and Bush, C. A., 2005, Generalized geologic map of the conterminous United States: U. S. Geological Survey, v. 1.2, scale: 1:7,500,000 (http://pubs.usgs.gov/atlas/geologic).

Reinhardt, J. R., Prowell, D. C., and Christopher, R. A., 1984, Evidence for Cenozoic tectonism in the southwest Georgia Piedmont: Geological Society of America Bulletin, v. 95, p. 1176-1187.

Repka, J. L., Anderson, R. S., and Finkel, R. C., 1997, Cosmogenic dating of fluvial terraces, Fremont River, Utah: Earth and Planetary Science Letters, v. 152, p. 59-73.

Reusser, L. J., Bierman, P. R., Pavich, M. J., Larsen, J., and Finkel, R., 2006, An episode of rapid bedrock channel incision during the last glacial cycle, measured with ^{10}Be: American Journal of Science, v. 306, p. 69-102.

Reusser, L. J., Bierman, P. R., Pavich, M. J., Zen, E., Larsen, J., and Finkel, R., 2004, Rapid late Pleistocene incision of Atlantic passive-margin river gorges: Science, v. 305, p. 499-502.

Ritter, D. F., Kochel, R. C., and Miller, J. R., 2011, Process Geomorphology, 5th ed.: Long Grove, IL, Waveland Press, Inc., 652 p.

Satkoski, A. M., Wilkinson, B. H., Hietpas, J., and Samson, S. D., 2013, Likeness among detrital zircon populations-An approach to the comparison of age frequency data in time and space: Geological Society of America Bulletin, v. 125, p. 1783-1799, doi:10.1130/B30888.1.

Shanmugam, G., and Walker, K. R., 1980, Sedimentation, subsidence, and evolution of a foredeep basin in the Middle Ordovician, southern Appalachians: American Journal of Science, v. 280, p. 479-496.

Spotila, J. A., and Prince, P., 2012, Disequilibrium in landscape evolution of the southern Appalachian Mountains: Field Trip Guidebook, Field Trip 409, Geological Society of America Annual Meeting, Charlotte, NC, 39 p.

Spotila, J. A., Bank, G. C., Reiners, P. W., Naeser, C. W., Naeser, N. D., and Henika, B. S., 2004, Origin of the Blue Ridge escarpment along the passive margin of eastern North America: Basin Research, v. 16, p. 41-63, doi: 10.1046/j.1365-2117.2003.00219.x.

Stacey, J. S., and Kramers, J. D., 1975, Approximation of terrestrial lead isotope evolution by a two-stage model: Earth and Planetary Science Letters, v. 26, p. 207-221.

Thomas, W. A., 2011, Detrital zircon geochronology and sedimentary provenance: Lithosphere, v. 3, no. 4, p. 304-308, doi: 10.1130/RF.L001.1.

Van Staal, C. R., and Hatcher, R. D., Jr., 2010, Global setting of Ordovician orogenesis: Geological Society of America Special Paper 466, p. 1-11.

Verhoogen, J., Turner, F. J., and Weiss, L. E., 1970, The Earth, An Introduction to Physical Geology: Chicago, Holt, Reinhart and Winston, Inc., 748 p.

Ward, D. J., Spotila, J. A., Hancock, G. S., and Galbraith, J. M., 2005, New constraints on the Cenozoic incision history of the New River, Virginia: Geomorphology, v. 72, p. 54-72, doi:10.1016/j.geomorph.2005.05.002.

Warrell, K. F., 2013, Detailed geologic studies of paleoseismic features exposed at sites in the East Tennessee seismic zone: Evidence for large, prehistoric earthquakes [unpub. Master's thesis]: Knoxville, University of Tennessee, 120 p.

Weltje, G. J., and Eynatten, H. V., 2004, Quantitative provenance analysis of sediments: review and outlook: Sedimentary Geology, v. 171, p. 1-11.

White, C. H., 1904, The Appalachian River versus a Tertiary trans-Appalachian River in eastern Tennessee: Journal of Geology and Research, v. 12, p. 34-39.

Wilson, J. T., 1966, Did the Atlantic close and then re-open?: Nature, v. 211, p. 676-681.

APPENDICES

APPENDIX I

LA-ICP-MS DATA OF DETRITAL ZIRCON SAMPLES

SAMPLE 2- W of Gravel Pit Rd B, MS

Grain No.	U (ppm)	$^{206}Pb/^{204}Pb$	U/Th	$^{206}Pb^*/^{207}Pb^*$	Error (±%)	$^{207}Pb^*/^{235}U^*$	Error (±%)	$^{206}Pb^*/^{238}U$	Error (±%)	Best Age (Ma)	Error (± Ma)	Concordance (%)
1-1	38	22712	2.1	11.1779	1.6	3.0651	2.2	0.2485	1.5	1414.1	30.5	101.2
1-2	378	121437	3.2	12.5694	0.7	2.2299	3.8	0.2033	3.7	1186.1	13.5	100.6
1-3	169	53075	4.0	5.5912	0.2	11.9012	0.6	0.4826	0.6	2642.2	2.9	96.1
1-4	82	34205	1.1	11.7068	0.9	2.6348	1.5	0.2237	1.2	1325.1	17.8	98.2
1-5	581	78274	0.6	20.1989	2.4	0.1730	2.7	0.0253	1.3	161.3	2.0	NA
1-6	165	43790	10.7	8.9792	2.3	4.9598	2.5	0.3230	0.9	1821.9	41.5	99.0
1-7	70	43938	0.8	13.1288	2.9	1.9088	3.7	0.1818	2.4	1099.5	57.2	97.9
1-8	9	13509	1.0	10.0454	5.4	3.8358	5.7	0.2795	1.9	1615.6	100.8	98.3
1-9	65	54455	2.2	11.3835	1.1	2.8715	2.7	0.2371	2.4	1379.1	21.8	99.4
1-10	83	50850	2.9	13.9338	1.7	1.5676	2.0	0.1584	1.1	979.3	33.7	96.8
1-12	245	304722	2.6	9.9007	0.5	4.0527	1.7	0.2910	1.6	1642.6	8.5	100.2
1-13	72	169520	1.3	12.7604	1.8	2.1136	3.0	0.1956	2.4	1156.2	35.5	99.6
1-14	150	40867	1.0	18.2534	3.0	0.5340	3.2	0.0707	1.1	440.3	4.8	109.1
1-15	66	64899	1.0	5.8399	0.3	11.4069	1.6	0.4831	1.6	2569.7	5.6	98.9
1-16	44	80758	0.9	10.4438	1.1	3.3966	2.5	0.2573	2.2	1542.9	19.9	95.7
1-17	109	1838	0.6	9.4860	3.9	3.7551	4.9	0.2583	3.1	1721.6	71.0	86.0
1-18	78	72811	1.9	12.7741	1.0	2.1334	2.2	0.1977	2.0	1154.1	19.1	100.7
1-19	62	52581	1.1	13.1188	2.4	1.9184	2.8	0.1825	1.5	1101.0	47.5	98.2
1-20	64	43900	3.2	13.3294	2.5	1.8513	3.4	0.1790	2.3	1069.1	50.4	99.3
1-21	336	264064	6.2	18.0139	1.5	0.5145	2.0	0.0672	1.3	419.4	5.4	96.9
1-22	86	43372	2.0	11.1816	1.4	2.9808	1.9	0.2417	1.3	1413.4	26.1	98.7
1-23	143	74589	2.2	13.3022	1.2	1.8771	1.5	0.1811	0.9	1073.2	23.3	100.0
1-24	53	9120	2.0	11.3821	2.7	2.5955	3.8	0.2143	2.7	1379.3	51.1	90.7
1-25	70	114093	0.9	9.6816	0.8	4.2736	2.3	0.3001	2.1	1684.0	15.6	100.5
1-27	121	40576	2.1	13.7019	1.6	1.6681	1.9	0.1658	1.0	1013.4	31.4	97.6
1-29	185	33419	1.6	18.3891	3.0	0.5068	3.5	0.0676	1.7	421.6	7.0	109.0
1-30	171	110400	1.7	12.4123	0.7	2.3055	3.1	0.2075	3.0	1210.9	14.2	100.4
1-31	55	63211	3.0	10.8051	1.8	3.2119	2.2	0.2517	1.2	1478.7	33.4	97.9
1-32	997	88662	3.1	8.8537	0.1	5.3564	1.1	0.3440	1.1	1847.3	1.5	103.2
1-33	85	44518	1.4	13.2111	1.3	1.8733	2.2	0.1795	1.8	1087.0	26.9	97.9
1-34	288	160637	1.7	13.5321	0.4	1.7741	1.3	0.1741	1.3	1038.7	8.5	99.6
1-35	207	138754	1.9	11.6830	0.6	2.7056	1.8	0.2293	1.7	1329.0	10.9	100.1
1-36	92	48031	2.0	11.1005	1.2	3.0249	2.6	0.2435	2.3	1427.3	23.1	98.4

Grain No.	U (ppm)	$^{206}Pb/^{204}Pb$	U/Th	$^{206}Pb^{*}/^{207}Pb^{*}$	Error (±%)	$^{207}Pb^{*}/^{235}U^{*}$	Error (±%)	$^{206}Pb^{*}/^{238}U$	Error (±%)	Best Age (Ma)	Error (± Ma)	Concordance (%)
1-37	62	127990	1.9	10.0437	1.6	3.9280	2.0	0.2861	1.2	1615.9	29.1	100.4
1-38	139	1369	0.6	13.8173	40.5	0.6119	41.0	0.0613	6.0	383.7	22.4	NA
1-39	18	20219	1.2	11.1901	3.5	3.0530	5.0	0.2478	3.6	1412.0	67.4	101.1
1-40	177	25555	2.1	13.2230	0.8	1.8717	1.5	0.1795	1.3	1085.2	16.2	98.1
1-43	100	7758	1.0	19.4987	23.3	0.2036	23.5	0.0288	2.6	183.0	4.6	NA
1-44	111	269457	2.6	10.7797	0.6	3.2729	1.8	0.2559	1.8	1483.1	10.6	99.0
1-45	52	101526	1.4	5.3021	0.4	13.5384	1.8	0.5206	1.8	2730.0	6.0	99.0
1-46	269	223907	6.1	12.7664	0.3	2.1642	1.8	0.2004	1.7	1155.2	5.9	101.9
1-47	198	88743	2.6	10.8414	0.3	3.2416	1.6	0.2549	1.5	1472.3	5.7	99.4
1-48	43	94846	1.5	3.6177	0.3	25.8572	1.7	0.6784	1.7	3342.8	4.0	99.9
1-49	114	87540	2.0	11.1074	1.0	3.1186	2.6	0.2512	2.4	1426.2	19.0	101.3
1-50	37	48220	2.2	13.6220	4.0	1.7466	5.5	0.1726	3.8	1025.3	81.5	100.1
1-51	101	38895	3.7	12.7503	0.8	2.0405	1.3	0.1887	1.0	1157.8	15.9	96.2
1-52	145	176357	1.3	9.9462	0.6	3.7290	2.6	0.2690	2.6	1634.1	10.4	94.0
1-53	47	42266	0.8	9.1684	1.6	4.8821	1.9	0.3246	1.0	1783.9	29.3	101.6
1-54	40	52508	1.3	8.9632	1.1	5.0758	2.6	0.3300	2.3	1825.1	19.2	100.7
1-55	221	34823	1.1	18.0045	2.8	0.5764	3.0	0.0753	1.1	467.8	5.2	107.8
1-56	61	45461	0.6	13.4837	2.7	1.7614	2.8	0.1722	1.0	1045.9	53.8	97.9
1-57	57	34552	0.7	13.8219	1.9	1.6486	2.7	0.1653	2.0	995.8	38.2	99.0
1-58	167	331078	1.7	5.9210	1.3	10.0827	2.0	0.4330	1.6	2546.7	21.7	91.1
1-59	74	47465	2.9	13.6718	1.6	1.6932	4.3	0.1679	4.0	1017.9	33.3	98.3
1-60	133	178894	1.0	8.7353	0.3	5.3532	1.7	0.3391	1.6	1871.7	5.6	100.6
1-61	305	5575	0.7	27.7978	35.1	0.0196	35.7	0.0039	6.4	25.4	1.6	NA
1-62	191	13482	3.5	5.5051	0.3	12.6233	1.0	0.5040	1.0	2668.0	4.5	98.6
1-63	242	22040	2.4	10.1173	4.0	3.9580	6.2	0.2904	4.6	1602.3	75.5	102.6
1-64	42	14366	1.9	13.2967	2.6	1.9175	3.1	0.1849	1.7	1074.0	51.8	101.8
1-65	84	69083	2.2	12.7358	1.0	2.0680	1.7	0.1910	1.4	1160.0	20.4	97.1
1-66	248	249971	1.8	11.7047	0.4	2.6100	1.6	0.2216	1.5	1325.4	8.2	97.3
1-67	136	320977	2.4	9.6701	0.4	4.2180	1.1	0.2958	1.0	1686.2	8.0	99.1
1-68	26	4161	2.5	9.7375	4.1	4.1082	7.3	0.2901	6.1	1673.4	75.3	98.1
1-69	149	710168	2.7	9.1156	0.4	4.8689	1.0	0.3219	0.9	1794.4	8.1	100.3
1-70	190	79674	1.1	10.9726	0.4	3.0256	1.1	0.2408	1.0	1449.4	7.9	96.0

Grain No.	U (ppm)	$^{206}Pb/^{204}Pb$	U/Th	$^{206}Pb^{*}/^{207}Pb^{*}$	Error (±%)	$^{207}Pb^{*}/^{235}U^{*}$	Error (±%)	$^{206}Pb^{*}/^{238}U$	Error (±%)	Best Age (Ma)	Error (± Ma)	Concordance (%)
1-71	34	17075	1.2	13.1010	3.1	1.7972	3.6	0.1708	1.8	1103.7	62.0	92.1
1-72	145	87271	2.4	13.2823	1.8	1.8433	3.9	0.1776	3.4	1076.2	35.4	97.9
1-73	146	123823	1.9	12.6301	0.7	2.1753	3.4	0.1993	3.3	1176.6	14.3	99.6
1-75	63	74027	3.1	12.9346	0.9	1.9794	2.5	0.1857	2.3	1129.2	18.9	97.2
1-76	193	38280	1.9	19.5125	4.8	0.2773	5.5	0.0392	2.7	248.1	6.5	NA
1-77	178	23071	0.8	9.4620	0.6	4.3602	1.9	0.2992	1.8	1726.3	10.1	97.8
1-78	70	47174	2.1	13.6251	1.5	1.7379	1.6	0.1717	0.7	1024.8	29.8	99.7
1-79	27	13284	0.6	13.5617	6.2	1.7174	6.6	0.1689	2.2	1034.3	125.9	97.3
1-80	253	5417	1.8	19.0684	104	0.0279	104.4	0.0039	7.2	24.8	1.8	NA
1-81	29	30807	2.5	12.2726	2.4	2.3133	3.2	0.2059	2.0	1233.1	46.9	97.9
1-82	87	69116	1.3	14.3523	2.2	1.3998	2.8	0.1457	1.7	876.9	13.7	95.4
1-84	54	1772	1.2	16.8060	7.6	0.6589	7.9	0.0803	2.3	498.0	10.9	85.0
1-85	160	49459	1.4	17.1577	3.2	0.7183	3.4	0.0894	1.2	551.9	6.3	102.1
1-86	61	80620	1.9	12.2679	1.9	1.9700	2.8	0.1753	2.0	1233.9	37.8	84.4
1-87	128	118211	0.8	9.7199	0.6	4.1822	1.1	0.2948	1.0	1676.7	10.9	99.3
1-88	111	45055	1.1	12.2733	1.4	2.3425	1.8	0.2085	1.1	1233.0	27.3	99.0
1-89	340	62946	3.9	12.9125	0.5	2.0642	2.0	0.1933	1.9	1132.6	9.2	100.6
1-91	68	5803	1.3	11.3358	1.9	2.4163	2.6	0.1987	1.8	1387.2	37.0	84.2
1-94	133	7595	0.9	10.5348	1.0	3.4691	1.4	0.2651	1.0	1526.5	18.8	99.3
1-95	90	183643	3.7	9.1995	0.6	4.7959	1.8	0.3200	1.7	1777.8	10.8	100.7
1-96	43	4210	0.6	8.9065	5.9	4.5343	6.1	0.2929	1.8	1836.6	106.4	90.2
1-98	91	84570	1.8	14.1048	1.8	1.5490	2.0	0.1585	0.9	954.5	36.1	99.3
1-99	171	299163	2.0	13.0882	0.4	1.9225	0.7	0.1825	0.5	1105.7	9.0	97.7
1-100	77	72662	1.8	13.3205	2.5	1.8028	2.7	0.1742	1.2	1070.5	49.3	96.7
1-101	229	12591	1.6	8.9849	0.7	4.2149	1.2	0.2747	0.9	1820.7	13.6	85.9
1-102	61	46787	1.4	9.9286	1.1	4.0337	1.3	0.2905	0.6	1637.4	20.9	100.4
1-103	67	54430	1.8	13.1523	2.6	1.9112	2.7	0.1823	0.9	1095.9	51.7	98.5
1-104	64	27677	1.7	17.5682	7.4	0.5565	7.8	0.0709	2.5	441.6	10.7	90.4
1-105	48	5922	2.0	12.5489	1.9	2.1616	2.6	0.1967	1.8	1189.3	36.7	97.3

SAMPLE 3- Red Bluff upper part, MS												
Grain No.	U (ppm)	$^{206}Pb/^{204}Pb$	U/Th	$^{206}Pb^*/^{207}Pb^*$	Error (±%)	$^{207}Pb^*/^{235}U^*$	Error (±%)	$^{206}Pb^*/^{238}U$	Error (±%)	Best Age (Ma)	Error (± Ma)	Concordance (%)
3-2	139	83455	3.4	13.5795	0.8	1.7801	0.9	0.1753	0.4	1031.6	15.4	100.9
3-3	46	17674	1.6	11.1639	2.4	2.9091	2.6	0.2355	1.0	1416.4	46.6	96.3
3-4	60	73584	1.7	12.9445	1.3	2.0308	1.9	0.1907	1.4	1127.7	26.7	99.8
3-5	36	33320	3.1	12.4346	4.6	2.2857	5.4	0.2061	2.8	1207.3	91.3	100.1
3-6	147	112390	1.9	12.9302	0.9	1.9558	1.9	0.1834	1.7	1129.9	17.2	96.1
3-7	233	159866	2.7	10.7219	0.3	3.3680	0.6	0.2619	0.6	1493.3	4.9	100.4
3-8	178	73394	1.1	9.1379	0.4	4.6547	0.9	0.3085	0.8	1790.0	6.4	96.8
3-9	54	29006	2.0	12.8957	2.2	2.1151	2.4	0.1978	0.9	1135.2	43.8	102.5
3-10	62	48734	2.1	13.4861	1.5	1.7871	2.4	0.1748	1.9	1045.6	30.4	99.3
3-11	55	28368	1.5	13.0881	2.4	1.9737	2.6	0.1874	1.0	1105.7	47.7	100.1
3-12	25	7020	0.8	16.1223	8.1	0.6392	10.9	0.0747	7.2	464.7	32.2	68.8
3-13	112	45563	3.4	13.5142	1.3	1.8608	2.4	0.1824	2.0	1041.3	27.2	103.7
3-14	35	26798	2.9	13.4602	4.8	1.8168	5.3	0.1774	2.4	1049.5	96.2	100.3
3-15	58	53813	0.9	5.4287	0.3	13.4068	1.9	0.5279	1.9	2691.1	4.7	101.5
3-16	94	53324	0.8	13.4856	2.0	1.8006	2.4	0.1761	1.3	1045.7	41.3	100.0
3-17	139	78752	1.1	13.2251	0.8	1.9164	1.1	0.1838	0.8	1084.9	15.4	100.3
3-20	77	69712	0.6	11.6450	1.3	2.7026	1.6	0.2283	0.9	1335.3	24.8	99.3
3-21	335	99806	2.4	17.2333	1.1	0.7059	1.5	0.0882	1.0	545.0	5.4	102.7
3-22	49	14619	5.0	10.9870	1.5	3.2592	6.3	0.2597	6.1	1446.9	27.7	102.9
3-23	16	18945	1.1	12.6255	9.5	2.1549	10.2	0.1973	3.7	1177.3	189.2	98.6
3-24	167	88683	2.2	13.6239	0.6	1.7458	0.8	0.1725	0.6	1025.0	11.3	100.1
3-25	92	48030	2.0	12.8449	1.7	2.0917	1.9	0.1949	0.8	1143.1	33.8	100.4
3-26	61	58454	1.6	9.9413	1.1	4.0240	1.3	0.2901	0.7	1635.0	20.0	100.4
3-27	46	10962	0.8	13.1611	3.0	1.8707	4.1	0.1786	2.8	1094.6	59.3	96.8
3-31	75	41899	1.6	13.7480	2.9	1.7242	3.2	0.1719	1.4	1006.6	58.9	101.6
3-32	48	59680	2.0	13.2692	4.1	1.9432	4.5	0.1870	1.9	1078.2	82.3	102.5
3-33	44	96334	1.5	5.0442	0.6	14.9929	1.0	0.5485	0.8	2811.8	9.4	100.3
3-34	154	175787	4.5	11.0309	0.8	3.1119	1.3	0.2490	1.0	1439.3	15.8	99.6
3-35	260	160872	4.1	9.9321	0.7	3.9295	0.9	0.2831	0.6	1636.7	13.1	98.2
3-36	119	43684	0.9	17.8348	4.9	0.5628	5.1	0.0728	1.5	453.0	6.4	99.5
3-38	54	14412	3.5	17.4420	4.5	0.6681	6.3	0.0845	4.3	523.0	21.8	103.7
3-39	63	55753	2.3	13.7703	4.2	1.6956	4.3	0.1693	0.6	1003.4	85.4	100.5

Grain No.	U (ppm)	$^{206}Pb/^{204}Pb$	U/Th	$^{206}Pb^*/^{207}Pb^*$	Error (±%)	$^{207}Pb^*/^{235}U^*$	Error (±%)	$^{206}Pb^*/^{238}U$	Error (±%)	Best Age (Ma)	Error (± Ma)	Concordance (%)
3-40	82	78789	2.4	13.1219	1.7	1.9111	1.9	0.1819	0.9	1100.6	34.5	97.9
3-41	49	20989	1.6	13.3370	3.6	1.8635	3.9	0.1803	1.5	1068.0	73.1	100.0
3-42	174	85685	3.0	12.2785	0.7	2.3502	0.8	0.2093	0.3	1232.2	14.0	99.4
3-44	270	7834	2.2	22.1406	14.2	0.0755	14.4	0.0121	2.2	77.7	1.7	NA
3-46	62	29935	2.0	13.1876	2.5	1.9432	3.2	0.1859	1.9	1090.5	50.7	100.8
3-47	92	22893	1.0	10.9254	0.6	3.1595	1.3	0.2504	1.2	1457.6	10.7	98.8
3-48	157	87357	1.8	13.3471	1.1	1.8198	1.4	0.1762	0.8	1066.4	22.9	98.1
3-49	64	15393	2.9	13.3847	3.0	1.7959	3.3	0.1743	1.3	1060.8	60.3	97.7
3-50	45	25825	1.4	13.6699	1.9	1.8020	2.7	0.1787	1.9	1018.2	38.4	104.1
3-R50	494	129833	4.5	17.0109	0.8	0.7504	1.5	0.0926	1.2	570.8	6.8	102.1
3-51	126	33104	1.5	16.4118	2.6	0.8945	2.9	0.1065	1.4	652.3	8.5	102.4
3-52	188	119427	1.3	12.4490	0.7	2.3095	1.0	0.2085	0.7	1205.0	13.9	101.3
3-54	184	302569	0.7	9.7525	0.6	4.1755	1.3	0.2953	1.1	1670.5	11.7	99.9
3-55	136	10471	1.7	21.0014	7.8	0.2017	8.0	0.0307	1.9	195.1	3.7	NA
3-56	184	151201	1.3	10.7610	0.4	3.2989	2.7	0.2575	2.6	1486.4	7.6	99.4
3-57	46	27651	1.1	13.1322	3.1	1.9594	3.3	0.1866	1.3	1099.0	62.1	100.4
3-60	74	22742	3.7	13.3917	1.9	1.9320	2.9	0.1876	2.2	1059.7	37.9	104.6
3-61	84	35532	2.8	13.1580	2.0	1.9999	2.7	0.1909	1.8	1095.1	39.3	102.8
3-62	47	25701	1.6	13.2395	2.3	1.8888	3.0	0.1814	2.0	1082.7	46.5	99.2
3-63	41	23091	1.3	9.7007	1.8	4.2309	2.1	0.2977	1.1	1680.4	33.6	100.0
3-64	189	8461	3.4	17.4209	4.5	0.5941	5.4	0.0751	3.0	466.6	13.4	92.0
3-67	100	83691	0.9	13.1754	1.5	1.9400	1.6	0.1854	0.6	1092.4	30.2	100.4
3-68	29	7004	3.5	20.9894	14.7	0.5681	14.8	0.0865	1.5	534.7	7.5	655.6
3-69	146	302344	1.3	5.2533	0.3	14.0434	0.5	0.5351	0.5	2745.2	4.2	100.6
3-70	90	12190	3.0	12.7425	1.8	2.0778	2.0	0.1920	0.8	1159.0	36.3	97.7
3-72	266	31197	1.6	20.5786	1.8	0.1971	2.1	0.0294	1.1	186.9	2.0	NA
3-73	142	80453	2.5	12.7410	0.9	2.0872	1.5	0.1929	1.2	1159.2	17.0	98.1
3-74	219	157902	2.1	12.0931	0.9	2.4640	3.7	0.2161	3.6	1261.9	17.6	99.9
3-75	222	356303	2.0	8.5480	0.2	5.5777	0.6	0.3458	0.5	1910.7	4.1	100.2
3-76	114	4697	2.3	21.2942	41.3	0.0772	41.5	0.0119	3.5	76.4	2.7	NA
3-77	203	65371	1.5	18.1700	1.8	0.4991	2.0	0.0658	0.7	410.7	2.8	99.3
3-78	176	22054	0.6	18.8282	3.3	0.4324	3.5	0.0591	1.1	369.9	4.1	NA
3-80	38	43587	0.8	13.0733	4.0	1.8455	4.2	0.1750	1.5	1108.0	79.2	93.8
3-81	78	47136	2.0	11.5001	2.2	2.7281	2.6	0.2275	1.4	1359.5	42.2	97.2

Grain No.	U (ppm)	$^{206}Pb/^{204}Pb$	U/Th	$^{206}Pb^{*}/^{207}Pb^{*}$	Error (±%)	$^{207}Pb^{*}/^{235}U^{*}$	Error (±%)	$^{206}Pb^{*}/^{238}U$	Error (±%)	Best Age (Ma)	Error (± Ma)	Concordance (%)
3-84	135	57406	1.7	13.5613	1.3	1.7945	1.8	0.1765	1.2	1034.3	26.6	101.3
3-85	84	74050	2.0	8.9010	0.5	5.1598	0.6	0.3331	0.4	1837.7	8.2	100.9
3-86	96	284751	1.6	5.1562	0.4	14.4892	0.8	0.5418	0.7	2775.9	5.9	100.6
3-87	54	31653	1.6	11.4935	1.4	2.8640	1.5	0.2387	0.5	1360.6	26.2	101.4
3-88	19	16506	0.9	13.3575	4.7	1.8933	5.2	0.1834	2.1	1064.9	94.7	101.9
3-89	334	91524	2.2	12.7657	0.7	2.0177	1.1	0.1868	0.9	1155.4	13.2	95.6
3-90	129	6791	1.8	24.5456	24.3	0.0681	24.5	0.0121	2.8	77.7	2.2	NA
3-91	102	48795	1.0	13.3845	1.1	1.8192	3.1	0.1766	2.9	1060.8	22.8	98.8
3-92	388	119953	2.5	13.3622	0.5	1.8330	1.0	0.1776	0.8	1064.2	9.6	99.0
3-93	41	49814	3.1	13.8120	4.6	1.7296	4.9	0.1733	1.8	997.2	93.8	103.3
3-94	41	76234	1.6	5.4830	0.7	12.6040	1.4	0.5012	1.2	2674.6	11.5	97.9
3-95	46	39394	1.3	12.2237	3.1	2.3472	3.6	0.2081	1.9	1240.9	60.8	98.2
3-96	294	536324	2.9	13.3440	0.6	1.8340	0.9	0.1775	0.7	1066.9	12.0	98.7
3-97	122	113679	1.1	9.9802	0.7	3.9404	0.8	0.2852	0.4	1627.8	12.7	99.4
3-98	229	131739	3.8	12.5717	0.6	2.1956	1.0	0.2002	0.8	1185.7	11.9	99.2
3-99	46	32880	2.0	13.5847	2.1	1.7732	2.5	0.1747	1.4	1030.8	42.7	100.7
3-101	171	59614	2.7	12.1965	0.8	2.4077	2.9	0.2130	2.8	1245.3	15.3	100.0
3-102	335	11106	2.1	21.2095	7.6	0.0998	7.6	0.0153	1.0	98.2	1.0	NA
3-103	93	40910	1.5	12.5650	1.0	2.2361	1.2	0.2038	0.5	1186.8	20.5	100.7
3-104	58	16080	1.2	13.1702	2.6	1.9478	2.8	0.1860	0.8	1093.2	52.9	100.6
3-105	420	227913	1.3	11.3579	0.3	2.9076	1.9	0.2395	1.8	1383.4	4.8	100.1

SAMPLE 4- Red Bluff middle part, MS

Grain No.	U (ppm)	$^{206}Pb/^{204}Pb$	U/Th	$^{206}Pb^*/^{207}Pb^*$	Error (±%)	$^{207}Pb^*/^{235}U^*$	Error (±%)	$^{206}Pb^*/^{238}U$	Error (±%)	Best Age (Ma)	Error (± Ma)	Concordance (%)
4-31	206	9095	1.7	22.0559	18.6	0.0791	18.8	0.0127	2.7	81.0	2.2	NA
4-78	203	1008	0.9	18.6896	18.9	0.0998	19.3	0.0135	3.7	86.6	3.2	NA
4-35	427	35385	1.2	19.3439	4.4	0.1886	4.4	0.0265	0.7	168.4	1.1	NA
4-93	166	5497	1.4	18.7929	7.9	0.2107	8.7	0.0287	3.7	182.5	6.6	NA
4-44	257	18471	1.7	20.3621	4.6	0.2007	4.7	0.0296	1.3	188.3	2.4	NA
4-3	134	78551	3.7	18.3076	5.1	0.5351	5.2	0.0710	0.9	442.5	3.7	111.5
4-30	158	21784	1.4	17.9507	2.9	0.5515	3.0	0.0718	0.8	447.0	3.4	101.4
4-71	190	13051	3.0	17.9006	2.2	0.5582	2.4	0.0725	1.0	451.0	4.3	100.9
4-54	197	27708	1.1	17.3856	2.8	0.5901	2.9	0.0744	0.9	462.6	4.1	90.4
4-33	157	31622	0.7	17.0933	2.5	0.7109	2.6	0.0881	0.9	544.5	4.7	99.2
4-14	365	144388	2.7	17.0757	1.3	0.7238	1.4	0.0896	0.6	553.4	3.2	100.5
4-81	496	146987	3.6	14.1737	0.6	1.4945	3.0	0.1536	2.9	944.5	12.1	97.5
4-83	207	93179	3.0	14.1666	1.0	1.5240	1.1	0.1566	0.5	945.5	20.1	99.2
4-57	64	56056	0.9	13.8666	2.5	1.6776	4.0	0.1687	3.2	989.2	49.9	101.6
4-75	49	19920	1.6	13.7897	3.1	1.7308	3.2	0.1731	1.0	1000.5	62.6	102.9
4-1	33	13734	1.9	13.7789	3.9	1.7066	5.4	0.1706	3.8	1002.1	78.8	101.3
4-73	34	8739	2.0	13.7731	7.7	1.6427	7.8	0.1641	1.3	1002.9	156.8	97.7
4-67	82	30860	1.1	13.7234	2.8	1.7516	3.1	0.1743	1.2	1010.3	57.0	102.5
4-79	33	8098	2.0	13.7184	4.5	1.6801	4.9	0.1672	2.0	1011.0	90.3	98.6
4-43	69	47716	2.7	13.6754	1.7	1.7787	2.1	0.1764	1.1	1017.4	35.2	102.9
4-65	23	6382	1.0	13.6310	4.7	1.8176	5.7	0.1797	3.2	1024.0	95.3	104.0
4-82	113	47469	2.1	13.6110	2.2	1.7713	2.4	0.1749	0.7	1026.9	45.2	101.2
4-103	27	9748	0.8	13.6108	6.8	1.7401	7.9	0.1718	4.0	1027.0	137.3	99.5
4-91	84	25018	1.6	13.5964	2.9	1.7714	3.0	0.1747	0.7	1029.1	58.5	100.8
4-11	263	87933	3.6	13.5954	0.4	1.7842	0.8	0.1759	0.7	1029.3	8.0	101.5
4-69	176	95865	2.8	13.5916	1.2	1.8002	1.5	0.1775	0.9	1029.8	24.7	102.3
4-95	77	31688	31.6	13.5903	1.6	1.7541	2.0	0.1729	1.2	1030.0	32.6	99.8
4-63	28	17727	1.0	13.5246	5.2	1.8667	5.4	0.1831	1.3	1039.8	105.5	104.2
4-100	72	24074	0.9	13.4535	1.9	1.8177	5.5	0.1774	5.1	1050.5	38.7	100.2
4-5	316	12563	2.5	13.3986	2.1	1.7373	2.6	0.1688	1.5	1058.7	41.8	95.0
4-77	114	5829	1.9	13.3977	2.2	1.7714	2.3	0.1721	0.7	1058.8	44.2	96.7
4-26	492	211586	3.3	13.3946	0.4	1.8345	0.7	0.1782	0.6	1059.3	8.3	99.8

Grain No.	U (ppm)	$^{206}Pb/^{204}Pb$	U/Th	$^{206}Pb^*/^{207}Pb^*$	Error (±%)	$^{207}Pb^*/^{235}U^*$	Error (±%)	$^{206}Pb^*/^{238}U$	Error (±%)	Best Age (Ma)	Error (± Ma)	Concordance (%)
4-9	133	51725	1.3	13.3910	1.6	1.8219	1.8	0.1769	0.9	1059.8	32.2	99.1
4-84	92	64770	1.6	13.3841	1.7	1.8543	1.9	0.1800	0.8	1060.9	34.4	100.6
4-105	16	13878	0.9	13.3754	9.6	1.8328	9.8	0.1778	2.0	1062.2	193.3	99.3
4-56	89	56450	0.8	13.3064	1.7	1.9134	1.8	0.1847	0.6	1072.6	33.2	101.8
4-64	107	49422	1.0	13.2380	1.8	1.9037	2.1	0.1828	0.9	1082.9	37.1	99.9
4-6	89	60075	0.9	13.2199	2.8	1.8565	3.0	0.1780	0.8	1085.7	56.9	97.3
4-94	134	42837	1.2	13.2070	0.8	1.9005	1.1	0.1820	0.7	1087.6	16.5	99.1
4-92	137	45399	2.3	13.1511	1.0	1.8993	1.6	0.1812	1.3	1096.1	20.8	97.9
4-34	58	47944	1.7	13.1415	3.4	1.8431	3.8	0.1757	1.7	1097.6	68.0	95.1
4-21	118	28787	2.5	13.1369	1.4	1.7947	3.7	0.1710	3.4	1098.2	28.8	92.7
4-17	25	7696	0.9	13.0482	9.6	1.8254	9.8	0.1727	1.9	1111.8	191.5	92.4
4-52	42	33697	1.9	13.0444	3.0	2.0887	3.4	0.1976	1.4	1112.4	60.5	104.5
4-45	64	39672	3.0	13.0012	1.3	2.0085	1.9	0.1894	1.5	1119.0	25.5	99.9
4-88	181	140353	1.6	12.9379	0.9	2.0389	1.3	0.1913	1.0	1128.8	17.4	100.0
4-101	15	5746	2.2	12.9356	9.2	2.0401	9.8	0.1914	3.3	1129.1	184.4	100.0
4-24	52	30174	1.9	12.9126	1.8	2.1379	4.1	0.2002	3.7	1132.6	35.4	103.9
4-85	58	94581	2.1	12.8550	2.1	2.1126	2.4	0.1970	1.1	1141.5	42.3	101.5
4-104	133	74338	1.4	12.8292	1.2	2.1600	1.8	0.2010	1.4	1145.5	24.5	103.1
4-46	35	8914	1.4	12.8197	5.1	2.0295	5.3	0.1887	1.7	1147.0	100.6	97.1
4-41	107	81109	1.0	12.7955	1.4	2.1748	2.9	0.2018	2.5	1150.7	27.6	103.0
4-19	185	97206	2.2	12.7300	0.9	2.1575	1.2	0.1992	0.9	1160.9	17.3	100.9
4-18	189	135894	3.3	12.6584	0.7	2.1284	1.7	0.1954	1.6	1172.1	14.4	98.2
4-70	37	21810	1.7	12.6465	3.1	2.1808	3.3	0.2000	1.1	1174.0	61.6	100.1
4-89	104	69421	2.3	12.6432	0.9	2.1501	1.5	0.1972	1.2	1174.5	17.9	98.8
4-2	40	26848	2.7	12.5982	4.4	2.3030	5.0	0.2104	2.4	1181.6	86.2	104.2
4-80	73	33847	1.6	12.5297	1.7	2.2232	1.8	0.2020	0.5	1192.3	34.3	99.5
4-42	58	3385	1.2	12.5172	3.1	2.2575	3.3	0.2049	1.0	1194.3	61.3	100.6
4-16	66	40956	0.4	12.4151	3.2	2.3432	3.3	0.2110	0.8	1210.4	62.7	102.0
4-76	67	52010	1.2	12.4014	2.1	2.3374	3.3	0.2102	2.5	1212.6	41.9	101.4
4-86	262	15808	6.0	12.3952	2.4	2.1004	3.2	0.1888	2.1	1213.6	48.0	91.9
4-39	55	23287	1.3	12.3658	3.1	2.2440	3.4	0.2012	1.5	1218.2	60.2	97.0
4-36	67	35268	2.0	12.3402	1.6	2.1879	2.2	0.1958	1.4	1222.3	31.8	94.3
4-53	64	36046	2.0	12.3084	1.0	2.4372	1.6	0.2176	1.3	1227.4	19.1	103.4

Grain No.	U (ppm)	$^{206}Pb/^{204}Pb$	U/Th	$^{206}Pb^{*}/^{207}Pb^{*}$	Error (±%)	$^{207}Pb^{*}/^{235}U^{*}$	Error (±%)	$^{206}Pb^{*}/^{238}U$	Error (±%)	Best Age (Ma)	Error (± Ma)	Concordance (%)
4-13	51	23739	1.6	12.2526	1.9	2.4892	2.2	0.2212	1.2	1236.3	37.5	104.2
4-87	198	26285	0.6	12.2523	0.9	2.3223	1.2	0.2064	0.8	1236.4	18.0	97.8
4-8	414	10384	3.2	12.2322	0.9	2.2298	6.3	0.1978	6.2	1239.6	17.5	93.9
4-48	106	65549	3.3	12.1701	1.5	2.4403	1.7	0.2154	0.8	1249.5	30.0	100.6
4-66	40	9366	0.7	12.1093	10.0	2.0711	11.7	0.1819	6.0	1259.4	195.6	85.5
4-102	161	79461	3.2	11.9499	0.8	2.5218	1.6	0.2186	1.4	1285.2	14.8	99.2
4-27	25	12876	1.9	11.8277	5.0	2.5315	6.3	0.2172	3.9	1305.2	96.8	97.1
4-29	96	54807	2.4	11.6898	1.2	2.7295	1.3	0.2314	0.6	1327.9	23.4	101.1
4-20	58	64268	2.8	11.5322	2.4	2.6866	7.2	0.2247	6.8	1354.1	45.8	96.5
4-47	16	14045	1.4	11.4908	6.0	2.7718	7.6	0.2310	4.7	1361.1	115.9	98.4
4-72	85	80409	2.3	11.2767	1.3	2.9162	1.6	0.2385	0.9	1397.2	24.7	98.7
4-28	60	45742	1.2	11.1948	2.3	2.9733	2.3	0.2414	0.4	1411.2	44.3	98.8
4-10	78	42360	1.0	11.0911	1.0	3.1174	1.2	0.2508	0.7	1429.0	19.7	100.9
4-55	137	112453	2.3	11.0282	1.0	3.1374	1.7	0.2509	1.4	1439.8	19.5	100.2
4-51	41	17397	1.6	11.0049	2.2	3.2587	2.5	0.2601	1.2	1443.8	42.2	103.2
4-15	292	346446	3.9	10.9942	0.2	3.1574	0.9	0.2518	0.8	1445.7	4.4	100.1
4-25	81	82653	1.7	10.6756	1.3	3.3966	1.6	0.2630	1.0	1501.5	24.5	100.2
4-4	67	42651	0.5	10.4708	1.2	3.4718	6.3	0.2637	6.2	1538.0	23.0	98.1
4-58	157	19213	1.3	9.7620	0.6	3.5109	2.2	0.2486	2.1	1668.8	11.2	85.8
4-22	90	126278	0.9	9.5777	1.2	4.3223	9.0	0.3002	8.9	1703.9	22.6	99.3
4-40	135	99895	2.4	9.4604	0.5	4.4569	0.8	0.3058	0.6	1726.6	8.5	99.6
4-74	156	124417	2.6	9.3998	0.5	4.5848	0.9	0.3126	0.7	1738.4	9.7	100.9
4-99	258	220310	2.5	9.3486	4.1	4.0891	4.6	0.2772	2.0	1748.4	75.6	90.2
4-98	172	192496	1.4	9.2258	0.2	4.7678	1.7	0.3190	1.7	1772.5	4.0	100.7
4-32	107	83832	1.3	9.1478	0.4	4.8403	0.7	0.3211	0.5	1788.0	7.5	100.4
4-49	268	29926	8.1	9.0338	1.1	4.4570	5.3	0.2920	5.2	1810.8	19.5	91.2
4-68	103	183761	3.3	8.9102	0.7	5.0149	1.2	0.3241	1.0	1835.8	12.6	98.6
4-38	108	110647	1.9	8.8724	0.5	5.1550	0.6	0.3317	0.3	1843.5	9.4	100.2
4-59	174	328952	0.9	5.8669	0.2	10.2011	2.0	0.4341	2.0	2562.0	3.7	90.7
4-7	209	308993	1.6	5.6364	0.7	11.6677	4.8	0.4770	4.7	2628.9	11.3	95.6
4-96	44	125414	0.7	5.4384	0.6	13.2471	1.2	0.5225	1.0	2688.1	10.5	100.8
4-50	119	96553	0.5	5.3167	0.1	13.4342	1.3	0.5180	1.3	2725.5	2.2	98.7
4-62	55	32670	0.6	5.3126	0.5	13.9655	0.9	0.5381	0.7	2726.8	8.2	101.8
4-90	66	105908	1.1	4.9730	0.4	15.1896	0.6	0.5478	0.5	2835.0	6.0	99.3

SAMPLE 5- Red Bluff lower part, MS												
Grain No.	U (ppm)	$^{206}Pb/^{204}Pb$	U/Th	$^{206}Pb^{*}/^{207}Pb^{*}$	Error (±%)	$^{207}Pb^{*}/^{235}U^{*}$	Error (±%)	$^{206}Pb^{*}/^{238}U$	Error (±%)	Best Age (Ma)	Error (± Ma)	Concordance (%)
5-89	192	8366	0.5	22.3968	19.7	0.0647	19.9	0.0105	2.6	67.4	1.7	NA
5-17	186	8090	2.1	20.3866	26.1	0.0738	26.4	0.0109	3.8	69.9	2.7	NA
5-39	247	10732	1.6	20.4830	7.7	0.0740	10.2	0.0110	6.8	70.5	4.8	NA
5-19	130	6252	2.1	24.6109	14.4	0.0754	15.4	0.0135	5.4	86.2	4.7	NA
5-64	118	9238	1.5	22.3279	32.0	0.1009	32.1	0.0163	2.7	104.5	2.8	NA
5-12	104	11785	0.9	24.1730	25.6	0.1470	25.7	0.0258	1.9	164.1	3.1	NA
5-11	249	39390	1.3	20.1050	5.4	0.1820	6.2	0.0265	3.1	168.9	5.2	NA
5-7	232	41261	1.2	19.6338	4.0	0.1965	4.6	0.0280	2.3	177.9	4.1	NA
5-50	145	8104	2.3	20.8465	6.9	0.1995	7.6	0.0302	3.3	191.5	6.2	NA
5-90	157	21342	6.0	19.9376	3.9	0.2392	4.2	0.0346	1.6	219.2	3.4	NA
5-103	254	58944	34.4	18.1857	4.6	0.4090	5.9	0.0539	3.7	338.7	12.1	NA
5-54	293	61520	6.7	18.9653	1.7	0.4213	1.7	0.0580	0.5	363.2	1.6	NA
5-51	15	5689	0.7	22.2295	19.8	0.4473	20.6	0.0721	5.7	448.9	24.6	NA
5-22	36	13997	2.0	18.6627	14.6	0.5561	14.9	0.0753	2.8	467.8	12.4	132.3
5-80	84	25488	4.9	16.8478	4.7	0.7089	5.0	0.0866	1.5	535.5	7.6	92.3
5-53	60	41020	2.0	14.1777	2.3	1.5273	2.9	0.1570	1.8	943.9	47.3	99.6
5-84	251	110267	5.1	14.0890	1.1	1.4144	2.6	0.1445	2.4	956.7	22.5	91.0
5-96	144	79211	4.1	13.9798	2.2	1.4320	2.7	0.1452	1.5	972.7	45.3	89.9
5-55	86	118817	3.8	13.9706	1.4	1.5856	1.6	0.1607	0.7	974.0	28.2	98.6
5-28	72	51781	1.9	13.9694	2.2	1.6403	2.4	0.1662	0.8	974.1	45.4	101.7
5-52	50	78059	2.1	13.8729	3.4	1.5682	5.3	0.1578	4.1	988.3	68.9	95.6
5-16	64	30347	0.5	13.8119	2.3	1.6675	3.2	0.1670	2.3	997.2	46.1	99.9
5-20	56	44212	1.8	13.7446	1.8	1.6296	2.5	0.1624	1.7	1007.1	36.6	96.3
5-34	35	24584	1.1	13.7356	4.8	1.7184	5.5	0.1712	2.7	1008.5	96.7	101.0
5-82	58	64982	2.4	13.6193	2.4	1.7472	2.7	0.1726	1.2	1025.7	48.3	100.1
5-25	30	64113	1.2	13.5983	3.9	1.8332	4.5	0.1808	2.2	1028.8	79.3	104.1
5-71	76	95359	1.7	13.5550	1.8	1.7702	2.2	0.1740	1.4	1035.3	35.6	99.9
5-105	162	157046	1.8	13.5402	1.0	1.7933	1.2	0.1761	0.8	1037.5	19.5	100.8
5-70	182	210033	1.8	13.5282	1.0	1.7669	2.6	0.1734	2.4	1039.3	19.6	99.2
5-86	196	145603	2.2	13.5147	0.6	1.7790	2.0	0.1744	2.0	1041.3	11.8	99.5
5-99	42	30961	2.4	13.5067	4.0	1.7776	4.2	0.1741	1.3	1042.5	80.5	99.3
5-42	228	155078	3.3	13.4880	0.5	1.8050	0.9	0.1766	0.8	1045.3	10.8	100.3

Grain No.	U (ppm)	^{206}Pb/ ^{204}Pb	U/Th	^{206}Pb*/ ^{207}Pb*	Error (±%)	^{207}Pb*/ ^{235}U*	Error (±%)	^{206}Pb*/ ^{238}U	Error (±%)	Best Age (Ma)	Error (± Ma)	Concordance (%)
5-23	86	65361	1.4	13.4367	1.4	1.7520	1.5	0.1707	0.5	1053.0	28.1	96.5
5-36	67	81861	1.6	13.4253	2.8	1.7930	3.3	0.1746	1.6	1054.7	57.1	98.4
5-61	251	428038	2.0	13.4080	0.3	1.8473	1.4	0.1796	1.4	1057.3	5.7	100.7
5-74	330	375004	1.7	13.3740	0.5	1.9028	2.2	0.1846	2.2	1062.4	9.4	102.8
5-49	276	91882	1.8	13.3684	0.4	1.8613	1.0	0.1805	0.9	1063.2	8.1	100.6
5-44	158	32909	2.9	13.3520	1.3	1.4653	4.1	0.1419	3.9	1065.7	26.2	80.3
5-40	72	32632	1.4	13.3281	2.0	1.8023	2.6	0.1742	1.7	1069.3	40.8	96.8
5-43	398	199028	4.7	13.3065	0.2	1.8921	2.0	0.1826	2.0	1072.6	4.7	100.8
5-14	310	185364	5.3	13.2991	0.3	1.8720	2.1	0.1806	2.1	1073.7	6.9	99.7
5-6	74	48473	2.4	13.2566	1.6	1.9154	2.0	0.1842	1.1	1080.1	32.7	100.9
5-63	183	17795	1.2	13.2495	1.0	1.8787	1.8	0.1805	1.5	1081.2	19.1	99.0
5-8	50	4379	0.9	13.2097	4.0	1.8510	4.7	0.1773	2.5	1087.2	79.7	96.8
5-38	24	22758	0.7	13.2066	3.7	1.8753	3.9	0.1796	1.2	1087.7	74.1	97.9
5-31	297	154945	2.6	13.1905	0.4	1.9443	0.8	0.1860	0.7	1090.1	8.9	100.9
5-21	193	99479	1.7	13.1528	0.9	1.9609	1.5	0.1871	1.2	1095.8	18.3	100.9
5-1	71	49169	1.1	13.1386	1.6	1.9340	3.2	0.1843	2.8	1098.0	31.7	99.3
5-76	18	12348	1.4	13.0647	5.2	2.0143	5.7	0.1909	2.3	1109.3	104.1	101.5
5-73	77	84734	1.4	12.8155	1.5	2.0625	3.5	0.1917	3.1	1147.6	29.1	98.5
5-5	140	64687	1.7	12.7698	0.9	2.1355	1.8	0.1978	1.6	1154.7	18.2	100.7
5-18	236	118943	3.7	12.7303	0.5	2.1605	1.5	0.1995	1.4	1160.9	9.1	101.0
5-59	105	65878	2.1	12.7278	0.9	2.1653	2.1	0.1999	1.9	1161.3	17.5	101.2
5-35	787	87709	6.0	12.6707	0.2	2.1469	0.5	0.1973	0.5	1170.2	3.5	99.2
5-45	236	237807	4.1	12.6686	0.7	2.1483	0.9	0.1974	0.6	1170.5	14.3	99.2
5-94	269	92615	9.4	12.6534	0.5	2.1710	1.0	0.1992	0.8	1172.9	10.3	99.9
5-24	23	9805	2.1	12.6369	4.8	2.0849	5.0	0.1911	1.5	1175.5	95.2	95.9
5-3	284	173902	7.3	12.6225	0.2	2.0915	2.4	0.1915	2.4	1177.8	4.6	95.9
5-62	39	34702	1.6	12.5964	2.1	2.2806	3.1	0.2084	2.3	1181.8	41.4	103.2
5-4	70	66400	1.8	12.5726	1.3	2.0957	3.4	0.1911	3.2	1185.6	25.3	95.1
5-81	38	34720	1.7	12.5367	2.5	2.1490	2.7	0.1954	1.1	1191.2	48.4	96.6
5-92	35	65465	1.0	12.5226	3.4	2.1870	3.8	0.1986	1.7	1193.4	66.5	97.9
5-56	537	244251	4.4	12.5194	0.2	2.1726	0.8	0.1973	0.8	1193.9	3.8	97.2
5-9	18	18909	3.0	12.5020	7.0	2.2759	7.4	0.2064	2.5	1196.7	137.7	101.1
5-57	29	92213	1.7	12.4711	3.9	2.2526	4.7	0.2037	2.6	1201.6	76.8	99.5

Grain No.	U (ppm)	$^{206}Pb/^{204}Pb$	U/Th	$^{206}Pb^*/^{207}Pb^*$	Error (±%)	$^{207}Pb^*/^{235}U^*$	Error (±%)	$^{206}Pb^*/^{238}U$	Error (±%)	Best Age (Ma)	Error (± Ma)	Concordance (%)
5-97	127	82898	2.0	12.3912	1.2	2.2689	2.6	0.2039	2.3	1214.2	24.4	98.5
5-37	85	120358	1.5	12.1152	1.1	2.4591	1.6	0.2161	1.2	1258.4	21.2	100.2
5-47	20	17621	1.4	12.0178	4.7	2.4031	5.5	0.2095	2.8	1274.1	92.2	96.2
5-72	159	44403	1.5	11.9838	1.9	2.4343	2.6	0.2116	1.8	1279.6	37.4	96.7
5-66	99	57971	1.6	11.5656	0.9	2.7505	2.2	0.2307	2.0	1348.5	17.5	99.2
5-77	26	27511	1.8	11.3979	2.9	2.7496	3.0	0.2273	1.0	1376.7	55.2	95.9
5-48	59	122040	1.6	11.2661	1.5	2.9443	1.9	0.2406	1.2	1399.0	28.7	99.3
5-100	104	123100	2.1	11.2461	0.7	2.9886	1.3	0.2438	1.2	1402.4	13.1	100.3
5-98	125	99468	2.1	11.2321	0.8	3.0502	3.3	0.2485	3.2	1404.8	15.9	101.8
5-10	91	56619	2.1	11.1909	0.7	3.0545	1.7	0.2479	1.5	1411.8	12.6	101.1
5-83	794	782083	3.7	11.1291	0.2	3.0465	0.5	0.2459	0.4	1422.4	4.0	99.6
5-87	160	169401	2.4	11.0025	0.5	3.1116	1.2	0.2483	1.1	1444.3	10.0	99.0
5-30	117	69868	1.0	10.9412	0.8	3.1604	1.3	0.2508	1.0	1454.9	14.3	99.2
5-27	436	378303	3.1	9.9375	1.0	3.5776	1.3	0.2578	0.7	1635.7	19.3	90.4
5-101	67	67673	1.5	9.9127	1.1	4.0438	1.3	0.2907	0.7	1640.4	20.1	100.3
5-15	104	71399	1.3	9.8443	0.8	4.0755	2.1	0.2910	2.0	1653.2	15.0	99.6
5-46	34	56005	1.2	9.7402	2.4	4.1665	2.9	0.2943	1.6	1672.9	44.1	99.4
5-60	244	181345	4.7	9.6774	0.2	4.2932	0.9	0.3013	0.9	1684.8	3.3	100.8
5-13	52	47783	1.6	9.6753	0.8	4.2902	3.1	0.3010	3.0	1685.2	14.3	100.7
5-32	805	1256030	3.1	9.6526	0.1	4.2514	1.4	0.2976	1.4	1689.6	2.5	99.4
5-67	140	332550	3.3	9.5618	0.6	4.4454	4.0	0.3083	4.0	1707.0	10.9	101.5
5-2	141	130566	3.9	9.4198	0.5	4.4987	2.7	0.3073	2.7	1734.5	8.3	99.6
5-78	87	108301	2.5	9.4004	0.7	4.5044	0.8	0.3071	0.5	1738.3	12.1	99.3
5-85	314	1054828	2.4	9.1748	0.2	4.7504	0.5	0.3161	0.5	1782.7	4.0	99.3
5-69	31	65860	1.0	9.1702	1.5	4.8127	3.1	0.3201	2.7	1783.6	28.2	100.4
5-93	68	155132	0.8	5.4510	0.2	12.5863	0.9	0.4976	0.9	2684.3	2.7	97.0
5-104	39	6076	0.8	5.4494	0.7	13.1735	1.0	0.5207	0.7	2684.8	12.0	100.6
5-91	35	108344	1.1	5.2435	0.6	14.2158	1.5	0.5406	1.4	2748.3	10.2	101.4

SAMPLE 6- Dry Creek near Maggie, MS

Grain No.	U (ppm)	$^{206}Pb/^{204}Pb$	U/Th	$^{206}Pb^*/^{207}Pb^*$	Error (±%)	$^{207}Pb^*/^{235}U^*$	Error (±%)	$^{206}Pb^*/^{238}U$	Error (±%)	Best Age (Ma)	Error (± Ma)	Concordance (%)
6-1	82	65530	1.7	13.3081	1.2	1.8724	1.8	0.1807	1.3	1072.3	23.7	99.9
6-2	31	26578	1.1	11.5027	3.4	2.7778	3.7	0.2317	1.5	1359.1	65.6	98.9
6-3	35	26263	0.8	13.4829	4.0	1.8275	4.3	0.1787	1.4	1046.1	81.4	101.3
6-5	131	32831	2.0	9.6072	1.2	4.4041	2.1	0.3069	1.8	1698.2	21.4	101.6
6-6	313	15338	1.7	18.7425	9.9	0.2063	10.8	0.0280	4.5	178.3	7.9	NA
6-7	42	7268	2.0	13.2315	7.1	1.7606	7.5	0.1690	2.3	1083.9	143.0	92.8
6-9	99	86183	2.1	13.5923	1.3	1.7765	1.7	0.1751	1.2	1029.7	25.5	101.0
6-10	80	32298	2.9	12.8601	1.5	2.0814	1.7	0.1941	0.8	1140.7	30.4	100.3
6-11	56	20616	2.6	11.7439	1.3	2.6373	1.6	0.2246	0.9	1319.0	25.3	99.0
6-12	83	73759	2.4	13.2523	1.5	1.9312	2.0	0.1856	1.2	1080.7	31.1	101.6
6-13	156	3068	1.7	23.3288	18.7	0.0842	19.0	0.0142	3.6	91.1	3.2	NA
6-14	301	2517	0.8	15.8758	1.9	0.7981	3.9	0.0919	3.4	566.7	18.6	80.1
6-15	26	43701	2.6	12.1877	4.2	2.3662	4.5	0.2092	1.6	1246.7	82.2	98.2
6-16	77	131856	1.4	9.5476	1.0	4.3448	2.1	0.3009	1.9	1709.7	18.0	99.2
6-17	129	63185	2.9	13.6043	1.4	1.7195	2.6	0.1697	2.2	1027.9	27.5	98.3
6-18	108	58127	7.5	13.5948	0.8	1.7579	1.5	0.1733	1.2	1029.3	16.8	100.1
6-19	113	35519	2.0	12.9949	1.2	2.0259	2.7	0.1909	2.3	1120.0	24.5	100.6
6-20	50	22622	0.9	17.5069	10.9	0.5552	11.2	0.0705	2.6	439.2	11.2	88.5
6-21	63	7017	2.4	9.3907	1.3	4.6301	2.4	0.3153	1.9	1740.1	24.7	101.5
6-22	102	99768	1.8	9.4651	0.3	4.3938	1.4	0.3016	1.4	1725.7	6.3	98.5
6-23	26	47193	0.9	9.6931	2.8	4.2082	3.1	0.2958	1.4	1681.8	51.7	99.3
6-24	47	30664	2.8	11.0816	3.7	2.9401	5.0	0.2363	3.4	1430.6	70.4	95.6
6-25	27	15140	2.3	14.0976	7.1	1.5064	7.9	0.1540	3.4	955.5	145.9	96.6
6-26	100	3606	2.2	27.8840	40.7	0.0553	41.4	0.0112	7.7	71.6	5.5	NA
6-27	101	2787	1.4	24.6674	28.2	0.0642	29.0	0.0115	6.7	73.6	4.9	NA
6-29	62	31444	2.9	13.8425	1.7	1.6690	4.0	0.1676	3.6	992.7	35.5	100.6
6-30	33	14244	0.9	13.3640	5.6	1.8339	5.9	0.1778	1.9	1063.9	112.1	99.1
6-32	327	10408	1.9	23.3131	8.8	0.0814	10.0	0.0138	4.7	88.2	4.1	NA
6-33	84	61073	1.8	10.9730	1.1	3.0755	1.3	0.2448	0.7	1449.4	21.2	97.4
6-36	106	81072	1.9	12.8638	1.1	2.0942	3.6	0.1954	3.4	1140.2	21.5	100.9
6-38	1820	695511	8.0	11.1443	0.1	3.0626	1.2	0.2475	1.2	1419.8	1.6	100.4
6-39	101	47520	1.6	13.3687	1.4	1.8854	2.6	0.1828	2.2	1063.2	27.8	101.8

Grain No.	U (ppm)	^{206}Pb/ ^{204}Pb	U/Th	^{206}Pb*/ ^{207}Pb*	Error (±%)	^{207}Pb*/ ^{235}U*	Error (±%)	^{206}Pb*/ ^{238}U	Error (±%)	Best Age (Ma)	Error (± Ma)	Concordance (%)
6-40	89	6534	2.2	13.2515	2.6	1.7920	3.1	0.1722	1.8	1080.9	51.8	94.8
6-41	280	7709	0.8	23.4060	16.8	0.0642	17.1	0.0109	3.1	69.8	2.2	NA
6-42	47	21330	2.2	12.8011	4.0	2.0332	4.8	0.1888	2.7	1149.9	78.5	96.9
6-43	170	24009	2.2	5.4320	0.3	13.0524	2.5	0.5142	2.4	2690.1	4.9	99.4
6-45	44	22459	2.2	14.1200	3.7	1.5901	4.2	0.1628	1.9	952.3	76.3	102.1
6-46	108	63271	1.5	9.5620	0.9	4.3103	1.7	0.2989	1.5	1706.9	16.4	98.8
6-47	38	23379	1.2	12.5234	3.4	2.1873	3.5	0.1987	0.9	1193.3	66.2	97.9
6-48	175	43483	2.6	13.6587	1.4	1.6990	2.2	0.1683	1.6	1019.8	29.0	98.3
6-49	100	128051	1.5	13.4796	1.4	1.7645	1.6	0.1725	0.6	1046.6	29.1	98.0
6-50	285	126754	2.6	12.2380	0.4	2.3542	1.1	0.2090	1.0	1238.7	7.7	98.8
6-51	252	35055	0.5	15.0017	26.4	0.5399	26.7	0.0587	3.8	368.0	13.6	NA
6-52	127	64070	2.0	10.6966	0.4	3.3284	1.1	0.2582	1.0	1497.8	7.0	98.9
6-53	85	5463	1.1	5.2269	0.2	13.2266	1.8	0.5014	1.8	2753.5	4.0	95.1
6-54	121	150074	2.1	10.9578	0.6	3.1155	1.0	0.2476	0.8	1452.0	11.3	98.2
6-55	68	27697	1.1	12.6236	3.0	2.1323	3.1	0.1952	0.8	1177.6	59.0	97.6
6-56	53	31562	2.7	12.5960	1.9	2.2864	6.7	0.2089	6.5	1181.9	37.4	103.5
6-57	155	205639	1.8	12.2376	0.9	2.4113	2.3	0.2140	2.1	1238.7	17.8	100.9
6-58	90	202128	1.9	13.6798	1.0	1.7641	1.5	0.1750	1.2	1016.7	19.8	102.3
6-59	54	52541	0.4	9.9013	0.8	4.1038	1.5	0.2947	1.3	1642.5	14.4	101.4
6-60	57	58170	0.9	13.6429	4.8	1.7909	5.2	0.1772	1.9	1022.2	97.5	102.9
6-61	132	61929	2.1	9.5504	0.3	4.4954	1.8	0.3114	1.8	1709.2	5.6	102.2
6-62	204	82567	0.8	17.5531	1.7	0.5749	2.8	0.0732	2.2	455.4	9.8	92.9
6-63	87	183654	1.1	9.4616	1.2	4.5030	1.5	0.3090	0.8	1726.3	22.0	100.5
6-65	332	127248	1.8	17.3154	1.4	0.6828	1.8	0.0858	1.1	530.4	5.8	101.9
6-66	41	3345	1.2	11.3642	4.2	2.7933	4.9	0.2302	2.4	1382.4	81.4	96.6
6-67	187	140325	0.9	7.5954	0.4	7.0278	1.5	0.3871	1.4	2120.2	6.3	99.5
6-68	179	200831	2.2	9.1443	0.3	4.8178	1.3	0.3195	1.2	1788.7	6.0	99.9
6-69	383	147199	1.3	5.1815	0.2	13.9682	1.6	0.5249	1.6	2767.8	3.5	98.3
6-70	51	53633	3.1	9.6031	1.8	4.2621	2.1	0.2968	1.1	1699.0	32.5	98.6
6-71	101	171101	1.1	12.3918	1.3	2.3195	1.9	0.2085	1.3	1214.1	26.2	100.5
6-72	190	8391	2.4	7.7478	1.6	6.5211	2.7	0.3664	2.2	2085.3	28.0	96.5
6-73	181	119978	0.6	5.9453	0.2	9.2661	1.5	0.3995	1.5	2539.8	2.9	85.3
6-74	81	37084	0.9	13.3776	2.4	1.8876	2.7	0.1831	1.4	1061.8	47.8	102.1

Grain No.	U (ppm)	^{206}Pb/ ^{204}Pb	U/Th	^{206}Pb*/ ^{207}Pb*	Error (±%)	^{207}Pb*/ ^{235}U*	Error (±%)	^{206}Pb*/ ^{238}U	Error (±%)	Best Age (Ma)	Error (± Ma)	Concordance (%)
6-75	76	55780	0.8	9.8555	1.0	4.0243	2.5	0.2877	2.2	1651.1	19.3	98.7
6-76	60	82732	0.8	5.3400	0.3	13.7428	1.9	0.5322	1.8	2718.3	5.4	101.2
6-77	184	65337	1.4	17.4709	3.7	0.5851	4.2	0.0741	1.9	461.0	8.3	92.1
6-78	109	96045	2.6	12.7238	1.0	2.2341	1.8	0.2062	1.4	1161.9	20.7	104.0
6-79	282	161732	0.6	13.2600	0.6	1.9175	2.0	0.1844	1.9	1079.6	11.5	101.1
6-80	117	102966	2.6	13.3946	1.1	1.7589	2.7	0.1709	2.5	1059.3	22.4	96.0
6-81	168	4588	1.6	20.9371	55.4	0.0500	55.9	0.0076	7.6	48.8	3.7	NA
6-82	134	49295	0.5	18.1230	2.8	0.5489	3.3	0.0721	1.7	449.1	7.3	107.1
6-83	84	2175	1.1	33.1622	59.1	0.0496	59.9	0.0119	9.4	76.4	7.2	NA
6-84	113	290217	3.6	9.1467	0.6	4.7503	1.3	0.3151	1.2	1788.2	10.8	98.7
6-85	79	25582	0.8	12.6132	1.7	2.1753	1.9	0.1990	0.8	1179.2	33.7	99.2
6-86	75	16531	2.3	16.7213	6.1	0.8143	6.3	0.0988	1.5	607.1	8.5	101.8
6-87	22	11350	1.4	14.1020	8.9	1.6322	9.6	0.1669	3.6	954.9	181.7	104.2
6-88	54	5700	0.5	19.9343	20.2	0.2363	20.5	0.0342	3.9	216.6	8.3	NA
6-89	96	5056	1.0	25.1074	39.7	0.0686	40.4	0.0125	7.6	80.0	6.0	NA
6-90	144	229230	1.6	9.4167	0.7	4.3966	2.5	0.3003	2.4	1735.1	13.7	97.6
6-91	37	28342	1.7	13.4382	3.6	1.9104	4.1	0.1862	2.1	1052.8	72.6	104.6
6-93	89	29663	2.4	13.8075	1.9	1.6995	2.3	0.1702	1.2	997.9	38.5	101.5
6-94	164	13157	1.4	17.4106	2.2	0.5696	2.5	0.0719	1.1	447.7	5.0	88.1
6-96	61	13651	1.8	13.0287	1.7	2.0354	2.9	0.1923	2.3	1114.8	34.8	101.7
6-97	110	232023	0.7	13.2973	1.9	1.8633	2.2	0.1797	1.2	1074.0	37.9	99.2
6-98	77	10804	1.4	16.9537	5.8	0.6992	5.9	0.0860	1.0	531.7	5.3	93.9
6-99	113	7474	1.5	21.8284	13.1	0.1618	13.8	0.0256	4.3	163.1	7.0	NA
6-100	299	7500	2.0	22.8284	12.6	0.0797	12.7	0.0132	1.4	84.5	1.2	NA
6-101	155	40739	1.1	5.8191	0.2	11.2016	2.2	0.4728	2.2	2575.7	3.8	96.9
6-102	114	74936	2.0	13.2668	1.7	1.8551	3.0	0.1785	2.4	1078.5	34.4	98.2
6-104	125	8564	1.7	23.0696	18.2	0.0961	19.3	0.0161	6.4	102.9	6.5	NA
6-105	85	59946	1.9	13.3632	2.4	1.8061	2.8	0.1750	1.4	1064.0	48.4	97.7

SAMPLE 7- MS HWY 84 Collins, MS

Grain No.	U (ppm)	$^{206}Pb/^{204}Pb$	U/Th	$^{206}Pb^*/^{207}Pb^*$	Error (±%)	$^{207}Pb^*/^{235}U^*$	Error (±%)	$^{206}Pb^*/^{238}U$	Error (±%)	Best Age (Ma)	Error (± Ma)	Concordance (%)
7-1	309	4072	0.5	35.0107	64.9	0.0157	65.1	0.0040	4.9	25.6	1.3	NA
7-89	328	3907	0.7	27.5457	45.4	0.0209	45.8	0.0042	6.2	26.8	1.7	NA
7-51	143	4713	1.7	19.6197	17.6	0.0798	18.5	0.0113	5.8	72.7	4.2	NA
7-42	173	15208	1.9	26.7519	19.2	0.0826	19.4	0.0160	2.4	102.4	2.4	NA
7-101	78	3407	2.7	21.3657	22.3	0.1170	22.6	0.0181	3.6	115.9	4.1	NA
7-77	93	10956	1.4	23.1174	22.0	0.1547	22.9	0.0259	6.6	165.0	10.7	NA
7-70	158	7804	1.9	20.9264	14.0	0.1891	14.2	0.0287	2.5	182.4	4.5	NA
7-52	580	94416	2.5	18.7414	0.9	0.4001	1.3	0.0544	1.0	341.4	3.2	NA
7-78	88	26416	1.4	18.7259	5.4	0.4671	5.7	0.0634	2.0	396.5	7.6	NA
7-81	52	19799	0.8	18.5184	11.2	0.4953	11.5	0.0665	2.6	415.2	10.5	111.9
7-93	186	63138	1.5	17.9316	3.7	0.5124	3.9	0.0666	1.4	415.9	5.5	93.9
7-40	87	31476	1.2	18.5689	7.3	0.4969	7.9	0.0669	2.8	417.6	11.3	114.4
7-3	19	4922	0.8	21.1815	20.5	0.4658	21.2	0.0716	5.1	445.6	21.9	743.9
7-94	131	5404	1.0	16.9070	7.5	0.6100	7.6	0.0748	1.3	465.0	6.0	81.2
7-67	121	29851	1.9	17.6407	3.3	0.6707	3.6	0.0858	1.4	530.7	7.1	110.7
7-65	45	12062	1.4	16.7475	6.8	0.8229	7.4	0.1000	2.9	614.2	16.9	103.5
7-57	62	30116	2.6	14.0277	3.6	1.6042	4.2	0.1632	2.3	965.7	72.7	100.9
7-24	280	117264	3.5	13.9319	0.3	1.6639	0.8	0.1681	0.7	979.6	6.4	102.3
7-47	58	33881	1.8	13.9230	2.7	1.7027	3.1	0.1719	1.5	981.0	55.1	104.3
7-35	66	44652	1.6	13.8410	3.4	1.7036	4.0	0.1710	2.2	993.0	69.3	102.5
7-15	63	40370	11.1	13.7751	3.5	1.7070	3.6	0.1705	0.9	1002.6	71.2	101.2
7-4	82	48102	2.5	13.7723	1.8	1.7084	1.9	0.1706	0.8	1003.1	36.0	101.3
7-91	26	12272	0.9	13.7616	4.5	1.7687	5.0	0.1765	2.2	1004.6	90.6	104.3
7-49	94	17088	2.9	13.7456	2.9	1.7837	7.1	0.1778	6.4	1007.0	59.7	104.8
7-14	140	134349	2.3	13.6964	1.4	1.7238	1.9	0.1712	1.3	1014.3	28.1	100.5
7-17	25	17548	2.1	13.6522	6.8	1.7566	7.0	0.1739	1.5	1020.8	137.7	101.3
7-82	525	356232	2.3	13.6499	0.5	1.7348	0.8	0.1717	0.6	1021.2	9.5	100.1
7-55	285	256487	1.6	13.6273	0.8	1.7669	1.1	0.1746	0.8	1024.5	15.6	101.3
7-5	51	28688	1.9	13.6015	4.1	1.7634	4.4	0.1740	1.5	1028.3	83.2	100.5
7-102	42	15417	2.2	13.5936	2.7	1.7602	2.9	0.1735	1.0	1029.5	55.4	100.2
7-21	67	33564	0.8	13.5936	2.8	1.7914	3.3	0.1766	1.7	1029.5	57.1	101.8
7-95	17	7784	2.1	13.5831	9.9	1.8203	10.2	0.1793	2.5	1031.1	200.5	103.1

Grain No.	U (ppm)	$^{206}Pb/^{204}Pb$	U/Th	$^{206}Pb^*/^{207}Pb^*$	Error (±%)	$^{207}Pb^*/^{235}U^*$	Error (±%)	$^{206}Pb^*/^{238}U$	Error (±%)	Best Age (Ma)	Error (± Ma)	Concordance (%)
7-45	25	8280	0.9	13.5822	6.9	1.8037	7.0	0.1777	1.5	1031.2	139.3	102.2
7-48	135	54381	0.6	13.5348	1.3	1.8691	1.5	0.1835	0.8	1038.3	26.3	104.6
7-11	162	67472	2.8	13.5035	0.8	1.8103	1.3	0.1773	0.9	1042.9	16.7	100.9
7-97	41	23577	0.9	13.4987	3.2	1.8267	3.8	0.1788	2.0	1043.7	64.8	101.6
7-105	170	91815	3.3	13.4803	1.0	1.8078	1.2	0.1767	0.8	1046.5	19.5	100.3
7-76	58	35433	1.2	13.4705	3.3	1.8323	3.6	0.1790	1.5	1047.9	67.0	101.3
7-56	48	40302	1.0	13.4535	3.1	1.7916	3.4	0.1748	1.4	1050.5	62.6	98.9
7-53	679	548770	1.7	13.4413	0.3	1.8121	0.5	0.1767	0.5	1052.3	5.6	99.7
7-100	40	44089	0.5	13.4322	4.6	1.8587	5.5	0.1811	2.9	1053.7	93.0	101.8
7-2	69	9767	2.5	13.3970	2.9	1.7936	3.2	0.1743	1.3	1058.9	58.4	97.8
7-28	210	300017	2.6	13.3477	0.6	1.8731	1.7	0.1813	1.6	1066.4	11.8	100.7
7-32	472	290739	3.6	13.3283	0.4	1.9010	1.1	0.1838	1.0	1069.3	8.9	101.7
7-60	120	104921	1.6	13.2710	1.3	1.8692	1.5	0.1799	0.7	1077.9	27.0	98.9
7-58	21	14091	1.7	13.2539	9.3	1.8663	9.9	0.1794	3.4	1080.5	186.8	98.4
7-34	138	59359	2.2	12.9548	0.9	2.0121	1.7	0.1891	1.4	1126.2	18.8	99.1
7-71	96	30510	2.3	12.8945	2.0	2.0084	2.5	0.1878	1.5	1135.4	39.0	97.7
7-12	39	19615	1.5	12.8875	3.9	2.0058	4.2	0.1875	1.6	1136.5	77.2	97.5
7-27	57	36459	1.5	12.8651	2.6	2.1491	2.9	0.2005	1.3	1140.0	51.8	103.4
7-39	38	10485	1.8	12.8256	1.9	2.0943	2.7	0.1948	2.0	1146.1	37.2	100.1
7-88	86	49236	2.2	12.7154	1.6	2.0796	2.0	0.1918	1.1	1163.2	32.6	97.2
7-63	112	55847	2.0	12.6604	1.9	2.1495	2.0	0.1974	0.8	1171.8	37.0	99.1
7-43	131	63172	1.4	12.6513	1.1	2.1851	1.7	0.2005	1.2	1173.2	22.1	100.4
7-6	729	359641	5.4	12.6482	0.4	2.0665	1.4	0.1896	1.3	1173.7	8.1	95.3
7-33	267	90931	2.1	12.6190	0.4	2.2505	1.1	0.2060	1.1	1178.3	8.4	102.5
7-103	69	41322	2.2	12.6164	1.2	2.2410	1.7	0.2051	1.2	1178.7	24.5	102.0
7-10	21	19018	3.6	12.6043	6.5	2.1912	6.8	0.2003	2.0	1180.6	128.3	99.7
7-7	136	122211	0.8	12.5951	1.1	2.1919	1.8	0.2002	1.5	1182.1	20.9	99.5
7-79	89	49750	1.2	12.5280	1.0	2.2534	1.3	0.2047	0.8	1192.6	20.1	100.7
7-37	76	79883	6.7	12.5005	1.7	2.1312	2.6	0.1932	2.0	1196.9	34.4	95.1
7-44	89	41060	2.6	12.4570	1.4	2.3340	1.5	0.2109	0.7	1203.8	27.1	102.5
7-96	33	19440	3.0	12.3999	4.1	2.2452	4.4	0.2019	1.6	1212.8	80.5	97.8
7-18	37	26605	2.2	12.3224	1.6	2.4323	1.9	0.2174	1.0	1225.1	31.3	103.5
7-41	77	32582	0.8	12.1935	1.8	1.9502	3.6	0.1725	3.2	1245.8	35.2	82.3

Grain No.	U (ppm)	$^{206}Pb/^{204}Pb$	U/Th	$^{206}Pb^*/^{207}Pb^*$	Error (±%)	$^{207}Pb^*/^{235}U^*$	Error (±%)	$^{206}Pb^*/^{238}U$	Error (±%)	Best Age (Ma)	Error (± Ma)	Concordance (%)
7-62	32	9305	1.5	11.9665	3.3	2.5332	4.2	0.2199	2.6	1282.5	64.2	99.9
7-72	139	102177	2.0	11.4987	1.0	2.8423	1.4	0.2370	1.0	1359.7	20.1	100.8
7-90	94	55850	1.6	11.2067	0.8	3.0124	1.1	0.2448	0.8	1409.1	15.4	100.2
7-8	91	154307	2.2	11.1723	1.1	2.9782	2.6	0.2413	2.4	1415.0	20.7	98.5
7-87	70	26580	0.7	11.1371	1.9	3.0051	2.1	0.2427	0.8	1421.0	36.3	98.6
7-20	67	16581	2.6	11.1340	2.0	2.7903	2.4	0.2253	1.4	1421.6	38.5	92.1
7-86	70	7806	1.2	11.1171	1.8	3.0261	2.0	0.2440	0.9	1424.5	33.5	98.8
7-92	180	273957	0.7	11.0332	0.6	3.0892	1.4	0.2472	1.2	1438.9	12.4	99.0
7-73	74	38243	1.2	11.0224	1.0	3.1362	1.1	0.2507	0.5	1440.8	19.3	100.1
7-68	108	112080	1.5	11.0128	0.8	2.9957	1.2	0.2393	0.9	1442.5	14.7	95.9
7-38	60	39989	1.1	10.8688	1.4	3.2790	1.5	0.2585	0.7	1467.5	26.2	101.0
7-84	44	25615	0.6	10.7477	1.3	3.3631	1.7	0.2622	1.1	1488.7	24.0	100.8
7-26	87	52018	2.0	10.6657	0.7	3.3159	1.1	0.2565	0.9	1503.2	12.6	97.9
7-25	77	47093	13.5	10.6298	1.4	3.4932	2.2	0.2693	1.7	1509.6	25.8	101.8
7-30	68	88567	1.5	10.5562	1.0	3.4991	1.1	0.2679	0.6	1522.7	18.1	100.5
7-54	114	159533	0.8	9.6624	0.5	4.2806	0.9	0.3000	0.8	1687.7	9.5	100.2
7-16	59	36741	1.6	9.6470	1.1	4.3690	2.3	0.3057	2.0	1690.6	21.2	101.7
7-74	493	457462	1.6	9.6280	0.3	4.2297	1.8	0.2954	1.8	1694.3	5.0	98.5
7-46	39	43945	1.8	9.4673	1.1	4.4446	4.1	0.3052	3.9	1725.2	21.0	99.5
7-29	168	11960	2.2	9.3636	0.6	4.4733	1.2	0.3038	1.1	1745.4	10.8	98.0
7-85	350	384693	3.8	9.3590	0.4	4.5027	1.0	0.3056	0.9	1746.3	7.6	98.4
7-23	117	57608	2.9	9.3460	0.5	4.6554	1.4	0.3156	1.3	1748.9	9.7	101.1
7-31	103	243897	1.1	9.1525	0.7	4.8438	1.0	0.3215	0.7	1787.1	12.4	100.6
7-80	185	322860	0.5	8.9084	0.5	5.1234	0.9	0.3310	0.7	1836.2	9.2	100.4
7-64	63	75036	2.0	7.7932	0.7	6.7753	1.2	0.3830	0.9	2075.0	12.2	100.7
7-104	51	92205	0.9	6.8607	0.8	8.7767	4.5	0.4367	4.4	2296.7	14.1	101.7
7-9	59	237169	0.8	5.3396	0.4	13.6458	0.9	0.5285	0.8	2718.4	7.3	100.6
7-13	26	57865	1.3	5.2954	1.0	13.9668	1.4	0.5364	1.0	2732.1	15.9	101.3
7-61	39	58413	1.5	5.1684	0.7	14.4149	2.0	0.5403	1.9	2772.0	11.9	100.5
7-50	40	38112	1.2	4.8853	0.5	14.6824	1.8	0.5202	1.7	2864.0	8.4	94.3

SAMPLE 10- Mc Callum Landfill A, MS

Grain No.	U (ppm)	$^{206}Pb/^{204}Pb$	U/Th	$^{206}Pb^{*}/^{207}Pb^{*}$	Error (±%)	$^{207}Pb^{*}/^{235}U^{*}$	Error (±%)	$^{206}Pb^{*}/^{238}U$	Error (±%)	Best Age (Ma)	Error (± Ma)	Concordance (%)
10-96	378	3464	0.9	24.9315	28.8	0.0210	29.4	0.0038	5.8	24.4	1.4	NA
10-58	1286	20941	0.6	21.0420	4.5	0.0404	5.6	0.0062	3.2	39.6	1.3	NA
10-11	287	14131	1.4	21.6640	17.8	0.0655	18.3	0.0103	4.0	66.1	2.6	NA
10-94	280	6095	1.1	24.7974	10.7	0.0670	11.1	0.0121	2.6	77.3	2.0	NA
10-57	196	1523	1.2	17.1696	27.1	0.1622	28.2	0.0202	7.8	128.9	9.9	NA
10-25	269	22634	1.3	18.2641	1.9	0.4437	2.5	0.0588	1.6	368.1	5.9	NA
10-73	240	21338	1.6	17.6408	4.8	0.4874	5.2	0.0624	2.2	390.0	8.2	NA
10-59	349	9518	10.4	17.9726	2.0	0.5086	2.2	0.0663	1.0	413.8	3.8	94.5
10-34	102	4584	1.6	17.2111	4.4	0.5508	5.4	0.0688	3.0	428.7	12.4	80.3
10-85	73	15812	1.4	17.7856	5.6	0.6196	6.1	0.0799	2.6	495.7	12.3	107.5
10-15	383	95995	3.4	17.1456	1.2	0.6894	2.3	0.0857	1.9	530.2	9.7	97.8
10-36	314	77945	2.8	17.4230	1.5	0.6798	2.0	0.0859	1.4	531.2	7.1	104.8
10-65	91	2682	1.2	15.7320	6.2	0.8966	7.4	0.1023	4.0	627.9	24.1	86.3
10-82	103	53775	2.6	14.1298	1.9	1.5400	2.5	0.1578	1.5	950.9	39.4	99.3
10-3	68	40132	2.0	13.8819	4.1	1.7195	4.6	0.1731	2.1	986.9	84.2	104.3
10-24	23	15094	2.2	13.8565	8.9	1.7402	9.9	0.1749	4.4	990.7	181.4	104.9
10-13	34	17582	1.4	13.8025	4.7	1.5192	5.1	0.1521	2.1	998.6	94.8	91.4
10-4	461	188127	2.7	13.7648	0.5	1.6947	1.3	0.1692	1.2	1004.2	9.2	100.3
10-75	144	49621	2.1	13.7550	0.4	1.6889	1.3	0.1685	1.2	1005.6	8.9	99.8
10-7	408	269889	4.0	13.7542	0.2	1.7040	1.3	0.1700	1.3	1005.7	4.5	100.6
10-51	77	97314	2.7	13.7180	1.9	1.6943	2.7	0.1686	1.8	1011.1	39.0	99.3
10-28	286	103326	3.1	13.6614	0.4	1.7284	1.6	0.1712	1.5	1019.4	8.8	100.0
10-30	52	26548	0.7	13.6594	2.6	1.6963	2.8	0.1681	1.2	1019.7	52.0	98.2
10-100	46	24061	1.7	13.6025	2.2	1.7630	2.7	0.1739	1.6	1028.2	44.4	100.5
10-31	71	15374	0.7	13.5604	2.6	1.6976	2.9	0.1670	1.4	1034.5	52.0	96.2
10-14	887	803328	3.3	13.5392	0.3	1.7633	1.4	0.1731	1.4	1037.6	7.1	99.2
10-61	215	136221	1.8	13.5130	0.6	1.7859	2.0	0.1750	1.9	1041.5	12.0	99.8
10-37	100	105586	3.9	13.5110	2.0	1.7334	3.4	0.1699	2.7	1041.8	39.8	97.1
10-99	131	47575	1.1	13.5033	0.9	1.7688	1.9	0.1732	1.7	1043.0	18.5	98.7
10-18	340	160143	3.7	13.4786	0.5	1.8008	1.2	0.1760	1.1	1046.7	10.7	99.9
10-27	65	12046	2.0	13.4760	2.1	1.6951	2.6	0.1657	1.5	1047.1	43.3	94.4
10-67	131	44765	1.8	13.4411	2.1	1.7980	2.5	0.1753	1.3	1052.3	42.6	98.9

Grain No.	U (ppm)	$^{206}Pb/^{204}Pb$	U/Th	$^{206}Pb^*/^{207}Pb^*$	Error (±%)	$^{207}Pb^*/^{235}U^*$	Error (±%)	$^{206}Pb^*/^{238}U$	Error (±%)	Best Age (Ma)	Error (± Ma)	Concordance (%)
10-12	162	140483	2.0	13.4252	0.8	1.8440	1.4	0.1795	1.1	1054.7	17.1	100.9
10-19	110	50646	1.3	13.4027	1.2	1.8869	3.0	0.1834	2.8	1058.1	24.3	102.6
10-90	80	39627	0.8	13.3967	1.4	1.8692	2.2	0.1816	1.6	1059.0	28.5	101.6
10-105	41	17763	1.8	13.3556	6.2	1.7792	6.4	0.1723	1.7	1065.2	123.8	96.2
10-102	311	26374	5.2	13.3498	0.6	1.8876	1.2	0.1828	1.0	1066.0	12.6	101.5
10-47	435	33845	4.0	13.3469	0.8	1.8216	2.3	0.1763	2.1	1066.5	15.9	98.2
10-40	180	187983	1.9	13.3081	1.2	1.8719	3.2	0.1807	2.9	1072.3	24.5	99.8
10-81	473	88526	8.9	13.2857	0.3	1.8348	1.2	0.1768	1.1	1075.7	5.7	97.6
10-9	117	113677	1.3	13.2517	1.7	1.8996	2.1	0.1826	1.3	1080.8	34.4	100.0
10-87	21	10175	1.6	13.1533	7.2	1.8367	8.0	0.1752	3.7	1095.8	143.4	95.0
10-84	177	37094	2.4	13.1512	1.6	1.9367	2.4	0.1847	1.8	1096.1	32.6	99.7
10-43	452	163298	3.1	13.1378	0.5	1.8750	3.2	0.1787	3.1	1098.1	11.0	96.5
10-72	481	344974	7.0	13.1253	0.7	1.8853	3.3	0.1795	3.3	1100.1	13.7	96.7
10-91	67	39555	1.7	12.9615	2.2	2.0356	2.4	0.1914	0.8	1125.1	43.8	100.3
10-86	134	43876	2.0	12.9573	0.9	2.0407	1.4	0.1918	1.1	1125.8	18.3	100.5
10-35	114	51567	2.0	12.8981	1.2	2.0500	2.1	0.1918	1.8	1134.9	22.9	99.7
10-6	23	41641	2.3	12.8786	3.5	2.1279	4.1	0.1988	2.1	1137.9	69.0	102.7
10-104	142	72929	2.4	12.8128	1.0	2.1126	4.1	0.1963	4.0	1148.1	19.5	100.6
10-88	456	109615	1.4	12.7839	0.4	1.9765	2.2	0.1833	2.1	1152.5	7.9	94.1
10-98	149	53258	3.5	12.7501	1.0	2.1673	2.3	0.2004	2.0	1157.8	19.9	101.7
10-48	454	86178	21.7	12.7252	0.4	2.1560	3.6	0.1990	3.5	1161.7	7.8	100.7
10-20	191	27242	3.2	12.7237	0.9	2.0799	1.4	0.1919	1.0	1161.9	18.1	97.4
10-33	364	183826	1.7	12.6605	0.3	2.1843	1.6	0.2006	1.6	1171.8	5.5	100.6
10-41	40	26869	3.8	12.6564	2.1	2.1075	2.5	0.1934	1.4	1172.4	41.5	97.2
10-42	115	5401	2.4	12.6258	3.4	2.0803	4.0	0.1905	2.1	1177.2	67.4	95.5
10-95	401	232646	3.1	12.5959	0.2	2.1743	1.3	0.1986	1.3	1181.9	3.6	98.8
10-10	361	4192	8.7	12.5902	1.3	1.8063	3.8	0.1649	3.6	1182.8	24.8	83.2
10-79	70	53263	2.3	12.5669	1.7	2.1896	2.9	0.1996	2.3	1186.5	34.5	98.9
10-76	209	126391	1.5	12.5428	0.6	2.2517	1.9	0.2048	1.8	1190.3	11.4	100.9
10-97	142	60992	2.8	12.4948	0.7	2.2340	1.4	0.2024	1.2	1197.8	13.8	99.2
10-1	64	34503	1.4	12.4566	2.5	2.3256	3.3	0.2101	2.1	1203.8	50.2	102.1
10-16	200	85088	1.0	12.4388	0.5	2.2617	2.0	0.2040	1.9	1206.7	9.4	99.2
10-62	134	13737	2.4	12.4091	1.5	2.1724	1.8	0.1955	1.0	1211.4	29.4	95.0

Grain No.	U (ppm)	$^{206}Pb/^{204}Pb$	U/Th	$^{206}Pb^*/^{207}Pb^*$	Error (±%)	$^{207}Pb^*/^{235}U^*$	Error (±%)	$^{206}Pb^*/^{238}U$	Error (±%)	Best Age (Ma)	Error (± Ma)	Concordance (%)
10-78	1029	36200	6.6	12.3774	0.2	2.3129	1.2	0.2076	1.2	1216.4	3.9	100.0
10-101	76	58305	3.7	12.2926	2.2	2.2939	4.1	0.2045	3.5	1229.9	42.4	97.5
10-17	163	158730	0.9	12.2681	1.0	2.3900	1.5	0.2127	1.1	1233.8	20.0	100.7
10-2	67	21680	2.0	12.2571	1.7	2.3756	2.6	0.2112	2.0	1235.6	32.5	100.0
10-49	297	93311	2.8	12.0649	0.5	2.4697	2.4	0.2161	2.4	1266.5	10.0	99.6
10-93	89	64183	1.3	11.8466	1.3	2.5355	2.0	0.2179	1.5	1302.1	25.3	97.6
10-26	625	101933	1.8	11.7991	0.7	2.5627	4.1	0.2193	4.0	1309.9	14.3	97.6
10-45	94	34227	0.9	11.7106	1.2	2.6912	2.8	0.2286	2.6	1324.5	22.5	100.2
10-39	142	57206	1.2	11.4397	1.1	2.9034	1.9	0.2409	1.6	1369.6	20.4	101.6
10-83	105	54757	2.0	10.9440	0.8	3.2168	1.8	0.2553	1.6	1454.4	14.5	100.8
10-50	93	58850	1.5	10.9288	0.9	3.1490	1.0	0.2496	0.4	1457.0	17.0	98.6
10-5	217	3157	0.8	10.6803	2.8	2.9126	4.7	0.2256	3.8	1500.7	53.8	87.4
10-60	112	57697	1.3	10.6800	0.9	3.4147	2.5	0.2645	2.4	1500.7	17.2	100.8
10-103	139	95155	1.2	10.0333	0.5	3.9346	2.2	0.2863	2.1	1617.9	9.4	100.3
10-69	65	49799	0.8	9.9235	1.3	3.7291	1.7	0.2684	1.2	1638.3	23.4	93.5
10-29	243	146534	4.9	9.8909	0.2	4.0421	2.6	0.2900	2.6	1644.4	3.2	99.8
10-46	43	42128	1.1	9.6737	2.4	4.2221	3.4	0.2962	2.4	1685.5	44.3	99.2
10-44	183	84939	3.1	9.6189	0.6	4.3146	1.6	0.3010	1.5	1696.0	10.2	100.0
10-68	227	431012	0.8	9.6183	0.3	4.3284	1.7	0.3019	1.6	1696.1	5.4	100.3
10-56	81	86367	1.8	9.3430	1.2	4.5649	2.1	0.3093	1.7	1749.5	22.3	99.3
10-23	292	23758	3.3	9.2457	1.0	4.5240	4.6	0.3034	4.5	1768.6	19.1	96.6
10-70	228	544635	2.2	8.6388	0.4	5.3862	2.9	0.3375	2.9	1891.7	7.1	99.1
10-80	157	170329	0.7	8.5222	0.4	5.7020	1.2	0.3524	1.2	1916.1	7.5	101.6
10-63	372	658564	1.1	8.3309	0.2	5.6313	1.6	0.3403	1.6	1956.7	3.8	96.5
10-89	122	172204	1.1	5.5588	0.3	12.0320	1.3	0.4851	1.3	2651.9	4.6	96.1
10-38	323	60306	0.9	5.5509	0.3	12.3556	1.2	0.4974	1.1	2654.2	5.0	98.1
10-74	83	215939	1.2	5.3690	0.4	13.7900	2.5	0.5370	2.4	2709.3	6.0	102.3
10-55	35	22601	1.3	5.3324	0.5	13.4982	2.2	0.5220	2.1	2720.6	7.9	99.5

SAMPLE 11- Mc Callum Landfill B, MS

Grain No.	U (ppm)	$^{206}Pb/^{204}Pb$	U/Th	$^{206}Pb^*/^{207}Pb^*$	Error (±%)	$^{207}Pb^*/^{235}U^*$	Error (±%)	$^{206}Pb^*/^{238}U$	Error (±%)	Best Age (Ma)	Error (± Ma)	Concordance (%)
11-1	81	32500	4.2	13.9609	1.9	1.6244	2.1	0.1645	1.0	975.4	38.3	100.6
11-2	25	1575	0.5	10.3282	3.5	3.2434	4.1	0.2429	2.3	1563.8	65.1	89.7
11-3	152	96705	1.6	13.2255	0.9	1.9093	1.0	0.1831	0.5	1084.8	18.1	99.9
11-4	490	276970	1.9	12.6468	0.3	2.1335	0.5	0.1957	0.3	1173.9	6.7	98.1
11-5	174	140235	2.1	13.5824	0.8	1.7489	1.2	0.1723	0.9	1031.2	16.8	99.4
11-7	31	18091	1.5	10.8252	2.3	3.3067	3.1	0.2596	2.2	1475.1	43.1	100.9
11-8	330	306940	2.7	13.4920	0.5	1.7809	1.2	0.1743	1.1	1044.7	10.7	99.1
11-10	26	51854	2.7	5.2054	1.1	14.2709	1.7	0.5388	1.3	2760.3	17.3	100.7
11-11	43	35435	0.7	10.7229	1.9	3.3861	4.1	0.2633	3.6	1493.1	35.2	100.9
11-12	175	180175	2.0	9.4717	0.3	4.2391	0.8	0.2912	0.8	1724.4	5.5	95.5
11-13	126	96224	1.6	10.8754	0.5	3.2844	1.6	0.2591	1.5	1466.4	9.0	101.3
11-14	200	47758	2.8	13.6620	1.0	1.7527	1.2	0.1737	0.6	1019.4	21.1	101.3
11-15	393	139723	4.6	13.1263	0.6	1.9320	1.2	0.1839	1.0	1099.9	12.0	99.0
11-16	35	10991	2.2	16.0174	4.9	0.9004	5.6	0.1046	2.7	641.3	16.6	93.1
11-17	223	129050	6.1	13.5325	1.1	1.7600	1.4	0.1727	0.8	1038.6	22.6	98.9
11-18	78	37977	2.4	11.6217	1.9	2.6940	2.0	0.2271	0.7	1339.2	37.0	98.5
11-19	81	41330	1.4	13.5614	1.7	1.7388	1.9	0.1710	0.8	1034.3	34.0	98.4
11-20	60	16867	1.1	13.1606	1.6	1.9323	2.3	0.1844	1.7	1094.7	32.3	99.7
11-21	41	25850	1.8	12.6850	4.1	2.0950	4.8	0.1927	2.3	1167.9	82.2	97.3
11-22	138	230081	1.5	8.7016	0.5	5.2357	1.2	0.3304	1.1	1878.6	9.2	98.0
11-23	217	170975	2.5	13.7894	1.0	1.6473	1.2	0.1647	0.6	1000.5	20.5	98.3
11-25	97	40394	6.7	13.2951	1.4	1.8978	1.7	0.1830	0.9	1074.3	28.4	100.8
11-26	48	12316	2.2	12.7364	3.4	2.0682	3.7	0.1910	1.5	1159.9	66.5	97.2
11-27	80	112472	2.1	9.9561	0.6	4.0459	3.3	0.2921	3.2	1632.2	11.5	101.2
11-28	265	64197	2.1	12.6872	0.7	2.0915	1.4	0.1925	1.2	1167.6	14.0	97.2
11-29	14	6729	3.6	12.4110	8.0	2.2563	8.6	0.2031	3.2	1211.1	158.5	98.4
11-30	180	46461	2.3	18.1992	2.4	0.5520	5.0	0.0729	4.4	453.4	19.1	110.6
11-31	103	61609	1.6	12.8893	1.9	2.0806	2.2	0.1945	1.0	1136.3	38.1	100.8
11-32	149	24052	2.3	10.7030	0.6	3.3495	1.0	0.2600	0.8	1496.6	11.9	99.5
11-33	35	13331	2.0	18.0449	25.7	0.5217	25.9	0.0683	3.1	425.8	12.9	99.2
11-34	149	66659	1.4	13.1148	1.8	1.8298	3.2	0.1740	2.7	1101.7	35.1	93.9
11-35	49	20952	2.5	12.6517	2.6	2.1836	3.6	0.2004	2.4	1173.2	51.8	100.4

Grain No.	U (ppm)	^{206}Pb/ ^{204}Pb	U/Th	^{206}Pb*/ ^{207}Pb*	Error (±%)	^{207}Pb*/ ^{235}U*	Error (±%)	^{206}Pb*/ ^{238}U	Error (±%)	Best Age (Ma)	Error (± Ma)	Concordance (%)
11-36	60	5790	2.4	13.2673	3.0	1.8390	3.5	0.1770	1.6	1078.5	61.2	97.4
11-38	323	54622	6.1	17.8448	1.1	0.5660	1.5	0.0733	1.0	455.8	4.3	100.4
11-39	35	41928	3.1	13.5558	2.9	1.6920	3.3	0.1664	1.6	1035.1	57.9	95.8
11-42	193	23117	1.7	13.2879	0.7	1.7136	2.8	0.1651	2.7	1075.4	13.5	91.6
11-43	65	20260	1.8	11.9136	1.6	2.5317	1.8	0.2188	0.8	1291.1	32.1	98.8
11-44	61	34398	1.5	14.0368	2.4	1.5966	2.6	0.1625	0.9	964.4	48.7	100.7
11-45	111	47896	1.8	11.9112	1.1	2.3335	2.6	0.2016	2.4	1291.5	21.0	91.7
11-46	439	332597	3.9	11.1072	0.2	3.1100	0.8	0.2505	0.7	1426.2	4.1	101.1
11-47	169	53482	1.1	18.3102	2.6	0.5139	3.1	0.0682	1.6	425.6	6.5	107.4
11-48	81	47515	1.5	13.3701	1.8	1.8697	2.4	0.1813	1.6	1063.0	35.3	101.0
11-49	23	16790	2.6	13.0682	6.8	2.0374	7.1	0.1931	2.1	1108.7	136.4	102.7
11-50	35	44165	1.1	13.0821	5.1	2.0310	5.2	0.1927	1.1	1106.6	101.6	102.7
11-51	112	132160	1.5	14.3292	1.7	1.3391	3.3	0.1392	2.9	840.0	22.5	91.1
11-52	30	38362	4.9	13.2309	5.1	1.7988	5.8	0.1726	2.6	1084.0	103.2	94.7
11-53	65	55234	1.4	13.7006	2.1	1.7699	2.4	0.1759	1.3	1013.6	41.7	103.0
11-54	159	53440	0.5	13.5548	1.1	1.7574	2.3	0.1728	2.0	1035.3	22.8	99.2
11-55	217	86787	2.3	11.4747	0.4	2.8685	1.0	0.2387	0.9	1363.8	8.3	101.2
11-56	64	102778	1.3	5.0374	1.7	14.3091	4.5	0.5228	4.2	2814.0	28.4	96.3
11-57	101	29650	1.1	17.3195	3.9	0.6831	4.3	0.0858	2.0	530.7	10.0	102.1
11-58	76	11480	1.1	17.3577	6.5	0.5551	6.7	0.0699	1.6	435.4	6.7	84.6
11-59	89	242796	3.4	8.6453	0.7	5.4632	3.3	0.3425	3.3	1890.3	12.6	100.5
11-60	297	51993	2.4	4.6876	0.2	13.0922	1.9	0.4451	1.9	2931.0	3.0	81.0
11-61	46	55022	1.1	9.1850	1.2	4.7311	1.5	0.3152	0.9	1780.6	21.6	99.2
11-62	72	42314	0.7	13.1430	1.9	1.9212	3.6	0.1831	3.0	1097.3	38.2	98.8
11-63	19	11721	0.9	13.2670	7.6	1.9268	8.5	0.1854	3.7	1078.5	153.0	101.7
11-64	288	74734	1.3	10.0002	0.4	3.8434	2.4	0.2788	2.4	1624.0	7.1	97.6
11-65	22	22367	1.6	12.8182	5.9	2.2098	6.3	0.2054	2.2	1147.2	117.8	105.0
11-66	75	35594	1.0	13.6115	1.7	1.7180	2.8	0.1696	2.2	1026.9	34.8	98.3
11-67	72	47442	0.9	13.7245	2.9	1.7068	3.0	0.1699	0.8	1010.1	59.5	100.1
11-68	130	34018	1.8	17.3797	3.8	0.5749	3.9	0.0725	0.9	451.0	3.9	88.0
11-69	90	68696	1.1	10.4381	0.7	3.4529	1.6	0.2614	1.5	1543.9	12.3	97.0
11-70	332	121352	2.8	13.7871	0.7	1.6477	1.3	0.1648	1.1	1000.9	14.0	98.2
11-72	550	30820	10.5	9.6988	0.6	4.1062	1.0	0.2888	0.8	1680.8	10.2	97.3

Grain No.	U (ppm)	^{206}Pb/ ^{204}Pb	U/Th	^{206}Pb*/ ^{207}Pb*	Error (±%)	^{207}Pb*/ ^{235}U*	Error (±%)	^{206}Pb*/ ^{238}U	Error (±%)	Best Age (Ma)	Error (± Ma)	Concordance (%)
11-73	207	157307	4.4	12.4047	0.7	2.3220	2.0	0.2089	1.9	1212.1	13.3	100.9
11-74	81	37651	0.9	13.6607	2.8	1.7935	2.9	0.1777	0.8	1019.6	56.5	103.4
11-75	57	42753	1.4	12.7420	2.4	2.0229	2.5	0.1869	0.9	1159.0	46.9	95.3
11-76	112	190804	3.1	9.3446	0.5	4.3497	2.7	0.2948	2.6	1749.2	9.3	95.2
11-77	188	149855	2.3	13.6297	0.7	1.7399	1.5	0.1720	1.3	1024.1	14.7	99.9
11-78	324	127397	10.8	13.3824	0.5	1.7648	2.9	0.1713	2.9	1061.1	9.3	96.0
11-79	207	90712	0.7	12.5457	0.8	2.1824	1.6	0.1986	1.4	1189.8	16.8	98.1
11-80	109	64241	5.7	13.8957	2.3	1.6957	2.7	0.1709	1.4	985.0	46.6	103.3
11-81	202	158848	1.9	11.0254	0.6	3.0863	1.1	0.2468	1.0	1440.3	11.0	98.7
11-82	105	77117	1.9	9.1353	0.3	4.7844	1.2	0.3170	1.1	1790.5	5.6	99.1
11-83	92	58431	1.5	13.3585	1.9	1.9081	2.7	0.1849	1.9	1064.7	38.5	102.7
11-84	22	29628	0.8	13.0036	9.4	1.9348	9.5	0.1825	1.4	1118.7	188.0	96.6
11-86	31	19237	1.5	12.5815	3.0	2.2291	4.5	0.2034	3.3	1184.2	59.2	100.8
11-87	50	35749	1.5	12.6101	2.1	2.1973	2.4	0.2010	1.1	1179.7	41.5	100.1
11-88	237	120407	2.4	12.7931	0.4	2.1083	1.2	0.1956	1.1	1151.1	8.7	100.1
11-89	79	29146	2.9	13.6612	2.0	1.7233	2.5	0.1707	1.6	1019.5	39.5	99.7
11-90	64	55995	1.2	12.7464	2.4	2.0838	2.6	0.1926	1.0	1158.4	46.6	98.0
11-91	125	77837	2.7	13.6512	0.8	1.7206	1.5	0.1704	1.2	1021.0	16.8	99.3
11-92	67	20408	1.1	18.4521	14.5	0.2988	14.8	0.0400	3.0	252.8	7.3	NA
11-96	33	29609	2.6	13.3301	5.1	1.7693	5.4	0.1711	2.0	1069.0	102.3	95.2
11-98	61	37618	2.2	12.5058	2.8	2.3249	3.2	0.2109	1.6	1196.1	55.0	103.1
11-99	72	70207	1.5	13.4861	2.1	1.7939	3.0	0.1755	2.2	1045.6	42.1	99.7
11-100	22	13718	1.8	11.5280	5.3	2.7110	5.6	0.2267	1.8	1354.8	102.3	97.2
11-101	64	101171	1.8	12.9382	1.9	1.9420	2.2	0.1822	1.2	1128.7	36.9	95.6
11-102	564	277465	2.0	13.5850	0.3	1.7750	0.7	0.1749	0.7	1030.8	6.7	100.8
11-103	28	17661	0.7	9.8346	4.0	4.1205	4.3	0.2939	1.3	1655.0	75.0	100.4
11-105	63	73161	1.9	9.6082	0.8	4.2994	2.4	0.2996	2.3	1698.1	14.0	99.5

SAMPLE 12- MS HWY 29 N of Runnels, MS												
Grain No.	U (ppm)	$^{206}Pb/^{204}Pb$	U/Th	$^{206}Pb^*/^{207}Pb^*$	Error (±%)	$^{207}Pb^*/^{235}U^*$	Error (±%)	$^{206}Pb^*/^{238}U$	Error (±%)	Best Age (Ma)	Error (± Ma)	Concordance (%)
12-83	153	3267	1.0	19.6341	23.9	0.0484	25.3	0.0069	8.2	44.3	3.6	NA
12-86	1349	58125	3.1	20.8399	5.4	0.0556	5.4	0.0084	0.8	54.0	0.4	NA
12-2	222	4622	2.1	24.4070	19.3	0.0494	19.4	0.0087	2.2	56.1	1.3	NA
12-7	146	5012	1.6	22.4807	38.6	0.0678	38.7	0.0111	2.9	70.9	2.1	NA
12-97	203	9243	1.2	21.0473	10.9	0.0757	12.2	0.0116	5.5	74.1	4.1	NA
12-93	164	6226	1.7	21.6994	20.7	0.0760	21.7	0.0120	6.7	76.7	5.1	NA
12-59	143	8343	2.9	19.1860	19.3	0.0872	19.8	0.0121	4.5	77.7	3.5	NA
12-55	144	3780	1.3	20.6440	23.2	0.0894	23.3	0.0134	2.3	85.7	2.0	NA
12-25	189	10772	1.5	20.2238	9.5	0.1779	9.6	0.0261	1.4	166.0	2.4	NA
12-26	95	9501	3.5	22.1458	10.2	0.1900	10.4	0.0305	2.2	193.8	4.2	NA
12-85	190	9889	1.8	18.3676	1.8	0.5009	2.0	0.0667	0.7	416.4	3.0	106.9
12-36	120	10888	1.5	17.8164	5.1	0.5407	5.2	0.0699	1.2	435.4	5.0	95.2
12-48	221	21253	1.6	17.7636	2.2	0.5616	2.2	0.0724	0.6	450.3	2.4	97.0
12-43	186	9876	4.0	17.4666	1.7	0.6310	1.8	0.0799	0.8	495.7	3.9	98.9
12-35	62	4895	1.1	17.1332	6.5	0.7110	6.7	0.0884	1.3	545.8	6.9	100.4
12-34	65	15294	0.8	17.0478	5.1	0.7475	5.3	0.0924	1.4	569.8	7.6	102.8
12-5	123	47297	0.9	15.3018	1.8	0.9704	2.4	0.1077	1.7	659.4	10.5	83.9
12-69	183	85356	4.2	14.4343	1.5	1.2652	2.1	0.1325	1.6	801.8	11.9	88.4
12-73	297	167353	2.2	14.0692	0.7	1.5833	1.4	0.1616	1.1	959.6	14.8	100.6
12-57	32	13192	2.6	13.9490	4.6	1.6770	4.8	0.1697	1.3	977.1	93.9	103.4
12-99	23	10712	16.4	13.9380	7.1	1.6417	7.2	0.1660	1.4	978.7	145.2	101.1
12-13	80	57769	2.2	13.8507	2.3	1.6987	2.5	0.1706	1.0	991.5	46.5	102.4
12-15	51	22284	3.7	13.7422	2.3	1.7208	2.4	0.1715	0.7	1007.5	46.3	101.3
12-75	49	5095	1.7	13.6946	6.3	1.6491	6.6	0.1638	1.8	1014.5	128.8	96.4
12-45	281	201656	3.1	13.6827	0.6	1.7108	1.0	0.1698	0.8	1016.3	13.0	99.5
12-58	49	28422	2.9	13.6616	5.7	1.8192	5.8	0.1803	1.2	1019.4	115.7	104.8
12-3	77	52270	1.4	13.6513	2.7	1.6086	2.9	0.1593	0.9	1020.9	55.0	93.3
12-6	365	219262	4.0	13.5898	0.4	1.7135	0.7	0.1689	0.6	1030.1	7.9	97.7
12-50	429	281984	5.0	13.5740	0.4	1.7666	0.5	0.1739	0.4	1032.4	7.3	100.1
12-103	51	39818	2.1	13.5718	2.3	1.7805	2.8	0.1753	1.6	1032.8	45.5	100.8
12-67	156	109101	1.4	13.5294	1.2	1.7866	1.3	0.1753	0.6	1039.1	23.7	100.2
12-37	35	14301	1.5	13.5195	3.1	1.8689	3.7	0.1833	2.0	1040.6	62.6	104.2

Grain No.	U (ppm)	$^{206}Pb/^{204}Pb$	U/Th	$^{206}Pb^*/^{207}Pb^*$	Error (±%)	$^{207}Pb^*/^{235}U^*$	Error (±%)	$^{206}Pb^*/^{238}U$	Error (±%)	Best Age (Ma)	Error (± Ma)	Concordance (%)
12-71	92	73599	0.8	13.5124	3.3	1.7026	3.4	0.1669	0.7	1041.6	66.2	95.5
12-44	93	32895	2.1	13.4729	1.6	1.5834	5.4	0.1547	5.2	1047.6	32.7	88.5
12-95	85	31904	1.1	13.4646	2.2	1.8377	2.3	0.1795	0.8	1048.8	43.7	101.4
12-46	30	14438	1.9	13.4526	3.9	1.7685	4.3	0.1726	1.8	1050.6	78.8	97.7
12-66	68	64496	0.9	13.4499	2.4	1.8263	2.5	0.1781	0.7	1051.0	48.4	100.6
12-100	34	18784	1.4	13.4062	4.7	1.8211	4.8	0.1771	1.0	1057.6	94.4	99.4
12-68	21	11337	1.4	13.3777	6.0	1.8634	6.2	0.1808	1.2	1061.8	121.4	100.9
12-77	103	46673	1.7	13.3741	0.9	1.8441	1.0	0.1789	0.4	1062.4	17.7	99.9
12-62	514	139201	12.3	13.3429	0.2	1.8601	0.6	0.1800	0.6	1067.1	4.1	100.0
12-41	174	120961	1.5	13.3394	0.4	1.8677	1.2	0.1807	1.1	1067.6	8.6	100.3
12-54	29	31773	1.3	13.2698	5.6	1.8574	6.0	0.1788	2.1	1078.1	112.7	98.3
12-91	30	19245	1.8	13.2432	5.4	1.8847	5.6	0.1810	1.4	1082.1	108.8	99.1
12-105	118	39217	1.0	13.1983	1.4	1.9561	1.6	0.1872	0.8	1088.9	27.4	101.6
12-11	129	17563	1.4	13.1502	1.3	1.8964	1.7	0.1809	1.2	1096.2	25.3	97.8
12-14	293	257199	2.9	13.1420	0.5	1.9242	0.7	0.1834	0.5	1097.5	10.0	98.9
12-60	53	36846	3.0	13.1119	2.0	1.9051	2.7	0.1812	1.9	1102.1	39.6	97.4
12-70	59	72535	1.2	13.0699	2.2	1.9424	2.5	0.1841	1.3	1108.5	44.1	98.3
12-23	36	8097	0.8	13.0488	3.6	1.7988	4.2	0.1702	2.3	1111.7	71.2	91.2
12-61	46	12664	1.0	12.9871	3.6	1.9201	3.8	0.1809	1.2	1121.2	71.7	95.6
12-27	26	19191	1.4	12.9591	4.7	2.0509	5.0	0.1928	1.4	1125.5	94.7	101.0
12-9	18	26444	1.4	12.8945	3.0	2.0325	4.0	0.1901	2.7	1135.4	59.5	98.8
12-28	248	119154	2.5	12.8398	0.6	2.1117	0.8	0.1966	0.5	1143.9	12.3	101.2
12-65	37	15786	1.7	12.8380	4.1	2.1134	4.4	0.1968	1.7	1144.2	81.4	101.2
12-88	41	20492	1.3	12.8307	2.5	2.1337	2.7	0.1986	1.2	1145.3	49.2	101.9
12-104	180	136141	2.1	12.7597	0.9	2.0535	1.2	0.1900	0.7	1156.3	18.6	97.0
12-90	182	265877	2.5	12.7149	0.9	2.1584	1.0	0.1990	0.5	1163.3	17.4	100.6
12-56	117	47832	1.4	12.6790	1.0	2.1706	1.1	0.1996	0.5	1168.9	19.4	100.4
12-96	88	63446	1.7	12.6394	2.0	2.1526	2.1	0.1973	0.6	1175.1	40.4	98.8
12-47	194	20268	3.9	12.6068	0.6	2.1251	0.9	0.1943	0.6	1180.2	12.8	97.0
12-101	33	21578	1.9	12.5767	3.4	2.0845	3.9	0.1901	2.0	1184.9	66.3	94.7
12-42	276	296281	3.1	12.5576	0.6	2.2135	1.1	0.2016	0.9	1187.9	12.1	99.7
12-1	277	205407	1.9	12.5301	0.4	2.1597	1.1	0.1963	1.0	1192.2	7.7	96.9
12-38	114	66172	2.3	12.5297	1.3	2.2277	1.9	0.2024	1.5	1192.3	25.4	99.7

Grain No.	U (ppm)	$^{206}Pb/^{204}Pb$	U/Th	$^{206}Pb^*/^{207}Pb^*$	Error (±%)	$^{207}Pb^*/^{235}U^*$	Error (±%)	$^{206}Pb^*/^{238}U$	Error (±%)	Best Age (Ma)	Error (± Ma)	Concordance (%)
12-87	57	1702	0.8	12.5208	6.3	2.0672	7.9	0.1877	4.8	1193.7	125.3	92.9
12-31	96	62363	2.1	12.4131	1.6	2.3117	2.5	0.2081	1.9	1210.7	31.2	100.7
12-29	39	17448	2.2	12.3934	2.5	2.2565	2.8	0.2028	1.0	1213.9	50.2	98.1
12-82	221	118169	1.7	12.3418	0.5	2.2788	1.0	0.2040	0.9	1222.0	9.5	97.9
12-8	149	74898	1.3	12.3110	2.0	2.2503	2.1	0.2009	0.5	1227.0	39.2	96.2
12-30	96	55544	2.3	12.3085	0.7	2.3360	1.0	0.2085	0.7	1227.4	14.1	99.5
12-24	32	32639	2.5	12.0805	3.6	2.5384	3.8	0.2224	1.1	1264.0	70.3	102.4
12-52	37	20882	0.8	11.9686	3.4	2.5728	3.6	0.2233	1.2	1282.1	66.8	101.4
12-98	98	9575	6.5	11.9667	1.0	2.4179	1.7	0.2099	1.4	1282.4	19.2	95.8
12-12	29	15779	1.8	11.7589	2.8	2.6660	2.9	0.2274	0.7	1316.5	55.1	100.3
12-74	58	64696	1.2	11.7299	2.9	2.6497	3.0	0.2254	0.5	1321.3	56.6	99.2
12-89	158	18910	1.7	11.6686	0.6	2.8212	1.2	0.2388	1.0	1331.4	12.5	103.7
12-18	43	34523	3.4	11.3400	1.4	2.8647	1.8	0.2356	1.0	1386.5	27.8	98.4
12-20	374	40117	1.2	11.1350	0.3	3.0111	0.7	0.2432	0.7	1421.4	6.2	98.7
12-102	41	38290	1.9	11.0554	2.0	3.1249	2.2	0.2506	0.9	1435.1	37.8	100.4
12-16	119	124305	1.2	11.0091	0.8	3.0596	1.2	0.2443	0.9	1443.1	14.9	97.6
12-72	77	66655	3.2	10.8931	0.5	3.2142	0.7	0.2539	0.5	1463.3	10.1	99.7
12-63	151	46584	0.8	10.8147	0.6	3.3294	0.8	0.2611	0.5	1477.0	12.3	101.3
12-53	104	84734	1.6	10.7194	0.8	3.3895	1.3	0.2635	1.0	1493.7	16.1	100.9
12-79	70	65305	1.9	10.6170	0.9	3.5038	1.4	0.2698	1.0	1511.9	17.7	101.8
12-49	330	11018	5.6	10.3507	1.2	3.6368	1.5	0.2730	0.9	1559.7	22.8	99.8
12-76	117	124079	1.3	10.0309	0.5	3.8998	1.3	0.2837	1.2	1618.3	9.3	99.5
12-81	179	3544	1.7	9.9633	1.9	3.1453	6.3	0.2273	6.0	1630.9	35.8	81.0
12-4	95	193940	2.0	9.6485	0.5	4.2680	1.2	0.2987	1.1	1690.4	9.1	99.7
12-40	196	104873	1.1	9.1625	0.4	4.9128	1.3	0.3265	1.2	1785.1	7.9	102.0
12-78	156	252506	4.2	9.0909	0.3	4.9378	0.7	0.3256	0.6	1799.4	6.4	101.0
12-19	43	28839	0.9	6.0767	0.8	10.6774	1.2	0.4706	1.0	2503.1	13.0	99.3
12-92	149	352788	6.8	5.4157	0.2	13.2538	0.7	0.5206	0.7	2695.0	2.9	100.2
12-10	66	199271	1.0	5.3832	0.3	13.1366	0.6	0.5129	0.6	2705.0	4.8	98.7
12-64	22	4187	1.5	5.3687	1.4	10.4812	1.9	0.4081	1.3	2709.4	22.4	81.4
12-32	26	33517	1.4	5.1789	1.0	14.4946	2.2	0.5444	1.9	2768.6	16.3	101.2

SAMPLE 13- MS HWY 42 W of Runnels, MS

Grain No.	U (ppm)	$^{206}Pb/^{204}Pb$	U/Th	$^{206}Pb^*/^{207}Pb^*$	Error (±%)	$^{207}Pb^*/^{235}U^*$	Error (±%)	$^{206}Pb^*/^{238}U$	Error (±%)	Best Age (Ma)	Error (± Ma)	Concordance (%)
13-58	143	5520	0.7	10.7446	79.2	0.0621	80.0	0.0048	11.3	31.1	3.5	NA
13-83	305	5514	1.9	25.9735	33.7	0.0436	34.0	0.0082	5.0	52.8	2.6	NA
13-33	87	4412	0.8	22.3825	30.0	0.0715	31.5	0.0116	9.5	74.4	7.0	NA
13-60	66	9463	12.1	17.6943	9.3	0.4838	9.5	0.0621	1.8	388.3	6.6	NA
13-18	99	19339	3.0	17.8746	6.5	0.5150	6.8	0.0668	1.9	416.7	7.7	92.6
13-9	189	59929	1.2	17.9073	2.2	0.5324	2.7	0.0691	1.6	431.0	6.8	96.6
13-65	130	19549	1.3	18.0653	5.1	0.5739	5.2	0.0752	0.8	467.3	3.7	109.6
13-56	129	26910	7.9	17.5807	5.0	0.5910	5.1	0.0754	0.9	468.4	4.0	96.2
13-71	94	4153	4.1	15.8882	3.9	0.7330	5.5	0.0845	3.9	522.8	19.3	74.0
13-14	41	19180	1.4	17.0660	9.2	0.6918	9.7	0.0856	3.0	529.6	15.3	95.9
13-6	32	8833	1.6	16.9506	8.5	0.7557	9.5	0.0929	4.2	572.7	22.9	101.0
13-63	68	58350	1.3	16.1232	3.6	0.8231	3.9	0.0962	1.5	592.4	8.5	87.8
13-45	71	40244	1.6	14.1933	2.1	1.5615	2.3	0.1607	0.9	941.7	43.3	102.0
13-35	46	4816	2.1	13.8310	2.8	1.6411	3.0	0.1646	1.3	994.4	56.0	98.8
13-53	98	39711	1.3	13.8109	1.9	1.7539	2.1	0.1757	1.1	997.4	37.9	104.6
13-86	30	17356	1.6	13.8019	6.6	1.7166	6.9	0.1718	2.0	998.7	133.6	102.4
13-59	226	142366	1.7	13.7986	0.9	1.6769	1.0	0.1678	0.5	999.2	18.8	100.1
13-7	79	51550	2.1	13.6877	1.3	1.6768	3.5	0.1665	3.2	1015.6	26.6	97.7
13-72	149	65223	2.0	13.6830	1.4	1.7361	1.5	0.1723	0.5	1016.2	28.4	100.8
13-75	63	53779	2.1	13.6751	2.8	1.7645	3.0	0.1750	1.2	1017.4	56.4	102.2
13-94	820	14059	3.2	13.6405	0.8	1.6871	1.3	0.1669	1.1	1022.5	15.6	97.3
13-23	205	9056	4.1	13.6384	1.1	1.7516	2.4	0.1733	2.1	1022.9	22.9	100.7
13-68	66	10720	1.7	13.6246	2.8	1.7235	3.2	0.1703	1.6	1024.9	57.1	98.9
13-11	31	18697	1.5	13.5764	3.7	1.7657	4.1	0.1739	1.9	1032.1	74.4	100.1
13-80	50	26148	1.5	13.5362	3.3	1.7745	3.5	0.1742	1.3	1038.1	66.3	99.7
13-96	130	144531	2.5	13.4948	1.3	1.7933	1.5	0.1755	0.6	1044.2	26.3	99.8
13-73	239	100947	2.7	13.4943	0.9	1.8056	1.0	0.1767	0.6	1044.3	17.4	100.4
13-47	580	267497	4.2	13.4909	0.4	1.8081	0.7	0.1769	0.5	1044.8	8.4	100.5
13-105	110	98678	1.1	13.4317	1.3	1.8673	1.6	0.1819	0.9	1053.7	25.7	102.2
13-54	298	232383	2.3	13.4253	0.9	1.8545	1.0	0.1806	0.4	1054.7	18.5	101.5
13-41	981	369855	3.3	13.4179	0.2	1.8343	0.8	0.1785	0.8	1055.8	4.0	100.3
13-39	75	54928	2.3	13.3840	1.3	1.8375	1.4	0.1784	0.5	1060.9	26.0	99.7

Grain No.	U (ppm)	$^{206}Pb/^{204}Pb$	U/Th	$^{206}Pb^*/^{207}Pb^*$	Error (±%)	$^{207}Pb^*/^{235}U^*$	Error (±%)	$^{206}Pb^*/^{238}U$	Error (±%)	Best Age (Ma)	Error (± Ma)	Concordance (%)
13-15	253	132426	2.3	13.3672	0.6	1.8802	3.0	0.1823	2.9	1063.4	12.0	101.5
13-104	181	190736	2.2	13.3531	0.7	1.8480	1.2	0.1790	1.0	1065.5	14.5	99.6
13-1	45	22723	1.5	13.3344	3.4	1.8069	3.6	0.1747	1.0	1068.4	68.5	97.2
13-78	172	77424	2.6	13.3278	0.8	1.8147	1.1	0.1754	0.8	1069.4	16.1	97.4
13-92	65	37765	3.6	13.2604	3.1	1.8751	3.2	0.1803	0.9	1079.5	62.5	99.0
13-38	44	28458	1.3	13.1690	3.2	1.8422	3.4	0.1759	1.1	1093.4	63.7	95.6
13-50	63	3915	1.2	13.0075	3.1	1.9669	3.2	0.1856	0.6	1118.1	62.5	98.1
13-77	113	45962	1.9	12.9841	1.0	2.0582	1.6	0.1938	1.3	1121.7	20.0	101.8
13-48	65	45845	1.1	12.9169	2.2	1.9665	2.3	0.1842	0.9	1132.0	43.0	96.3
13-76	311	125116	1.4	12.9045	0.7	1.9846	2.7	0.1857	2.6	1133.9	14.0	96.9
13-19	130	71112	2.1	12.8389	1.5	2.1249	2.1	0.1979	1.3	1144.0	30.8	101.7
13-85	53	48683	1.5	12.8315	2.1	2.1684	2.9	0.2018	2.0	1145.2	42.4	103.5
13-69	111	76764	0.9	12.8263	1.1	2.1111	1.4	0.1964	0.9	1146.0	22.0	100.9
13-74	83	43371	1.7	12.8014	1.4	2.1194	2.4	0.1968	1.9	1149.8	27.7	100.7
13-51	86	88063	1.9	12.7804	2.2	2.1409	2.7	0.1984	1.6	1153.1	42.7	101.2
13-21	179	234987	1.4	12.7483	1.4	2.1423	1.9	0.1981	1.3	1158.1	27.0	100.6
13-52	42	35059	2.2	12.6684	2.6	2.1944	2.8	0.2016	1.2	1170.5	51.0	101.2
13-66	183	206986	1.4	12.6674	0.6	2.1946	0.8	0.2016	0.5	1170.7	12.7	101.1
13-25	226	122629	3.9	12.6564	0.7	2.2055	1.3	0.2024	1.1	1172.4	14.4	101.4
13-2	105	62064	2.0	12.6489	1.2	2.1157	1.8	0.1941	1.4	1173.6	23.9	97.4
13-84	47	33278	1.6	12.6121	2.8	2.1818	3.0	0.1996	1.0	1179.4	55.1	99.5
13-102	60	45374	1.6	12.5329	2.0	2.0946	2.2	0.1904	0.9	1191.8	38.7	94.3
13-31	27	25569	1.5	12.4704	6.9	2.2189	7.1	0.2007	1.8	1201.6	136.1	98.1
13-79	85	48829	0.8	12.4340	1.6	2.3169	1.7	0.2089	0.6	1207.4	31.0	101.3
13-61	104	47074	2.4	12.4136	1.4	2.2250	1.6	0.2003	0.7	1210.7	28.1	97.2
13-82	102	87708	1.7	12.2589	0.8	2.3893	1.5	0.2124	1.2	1235.3	15.3	100.5
13-44	109	74214	2.3	12.2519	0.8	2.3686	0.9	0.2105	0.5	1236.4	15.2	99.6
13-62	284	285991	1.0	12.2455	0.7	2.2972	1.0	0.2040	0.6	1237.5	14.4	96.7
13-3	90	50047	0.8	12.1484	1.2	2.3481	1.5	0.2069	0.9	1253.0	22.9	96.7
13-88	64	27465	1.5	12.0134	1.3	2.5829	1.6	0.2250	0.9	1274.8	26.3	102.6
13-46	139	3705	3.6	11.9446	1.4	2.2535	1.8	0.1952	1.1	1286.0	27.2	89.4
13-22	32	13118	1.7	11.7878	3.3	2.6861	3.6	0.2296	1.4	1311.7	64.7	101.6
13-5	37	22324	1.3	11.6682	2.5	2.7951	2.7	0.2365	0.9	1331.5	48.3	102.8

Grain No.	U (ppm)	$^{206}Pb/^{204}Pb$	U/Th	$^{206}Pb^*/^{207}Pb^*$	Error (±%)	$^{207}Pb^*/^{235}U^*$	Error (±%)	$^{206}Pb^*/^{238}U$	Error (±%)	Best Age (Ma)	Error (± Ma)	Concordance (%)
13-55	270	221428	3.4	11.5185	0.4	2.8237	0.6	0.2359	0.3	1356.4	8.5	100.7
13-24	161	128011	2.6	11.4651	0.6	2.9539	1.8	0.2456	1.7	1365.4	11.1	103.7
13-90	148	70600	2.6	11.4552	0.6	2.7831	0.8	0.2312	0.5	1367.0	12.2	98.1
13-36	124	62100	1.7	11.2342	1.1	2.9609	1.3	0.2412	0.6	1404.4	20.5	99.2
13-29	110	84434	1.2	11.2149	2.3	2.9105	8.9	0.2367	8.5	1407.7	44.6	97.3
13-13	135	120868	3.1	10.9986	0.9	3.1888	2.1	0.2544	1.9	1444.9	17.8	101.1
13-100	60	64041	1.5	10.6573	1.0	3.4550	1.3	0.2671	0.7	1504.7	19.2	101.4
13-64	167	47487	1.5	9.9639	0.5	3.9371	1.0	0.2845	0.9	1630.8	9.1	99.0
13-30	449	273017	1.9	9.8800	0.2	4.1258	1.0	0.2956	1.0	1646.5	3.3	101.4
13-57	82	111195	1.7	9.6659	0.9	4.3168	1.2	0.3026	0.7	1687.0	17.3	101.0
13-28	73	105911	1.5	9.5718	1.1	4.2948	1.3	0.2981	0.7	1705.1	20.4	98.7
13-67	88	94817	1.4	9.5537	1.6	4.3886	1.7	0.3041	0.7	1708.5	28.6	100.2
13-4	684	50028	12.8	9.4666	0.3	4.3528	0.5	0.2989	0.4	1725.4	4.9	97.7
13-27	309	26825	2.5	9.4536	0.5	3.5423	5.8	0.2429	5.8	1727.9	8.6	81.1
13-20	137	101861	1.3	9.4452	0.5	4.3693	2.1	0.2993	2.0	1729.5	9.3	97.6
13-42	245	172029	1.5	9.1364	0.4	4.4879	2.1	0.2974	2.0	1790.3	6.5	93.7
13-32	127	133675	1.1	9.1313	0.4	4.7817	0.7	0.3167	0.6	1791.3	6.7	99.0
13-103	76	141524	0.7	9.0955	1.1	4.9472	1.5	0.3264	1.0	1798.5	20.2	101.2
13-101	25	26753	0.6	7.6735	2.4	6.9971	2.7	0.3894	1.3	2102.2	42.0	100.9
13-87	110	230419	0.8	6.9100	0.8	8.3176	1.7	0.4168	1.5	2284.4	13.7	98.3
13-81	181	165814	2.1	5.5813	2.2	12.8793	5.2	0.5213	4.8	2645.2	36.1	102.3
13-26	71	136510	2.6	5.4860	0.4	13.1581	0.7	0.5235	0.5	2673.7	6.3	101.5
13-97	60	142477	0.6	5.4448	0.5	13.1853	0.6	0.5207	0.5	2686.2	7.7	100.6
13-10	97	71918	0.5	5.4277	0.6	10.8962	8.3	0.4289	8.3	2691.4	9.1	85.5
13-89	124	346508	1.7	5.3945	0.2	13.4857	0.5	0.5276	0.5	2701.5	3.0	101.1
13-40	29	36582	0.4	5.3759	0.6	13.3804	1.0	0.5217	0.8	2707.2	10.1	100.0
13-98	36	48314	1.7	5.3453	0.6	13.3581	0.7	0.5179	0.4	2716.7	10.6	99.0

SAMPLE 14- N of Petal, MS

Grain No.	U (ppm)	$^{206}Pb/^{204}Pb$	U/Th	$^{206}Pb^*/^{207}Pb^*$	Error (±%)	$^{207}Pb^*/^{235}U^*$	Error (±%)	$^{206}Pb^*/^{238}U$	Error (±%)	Best Age (Ma)	Error (± Ma)	Concordance (%)
14-22	414	4062	1.2	25.2992	39.8	0.0203	40.0	0.0037	3.7	24.0	0.9	NA
14-39	280	5157	1.7	20.8906	21.2	0.0585	21.5	0.0089	3.9	56.9	2.2	NA
14-57	234	6695	1.5	20.6960	18.7	0.0709	18.8	0.0106	2.3	68.2	1.5	NA
14-72	620	20690	1.1	21.5846	4.1	0.0990	4.5	0.0155	1.9	99.1	1.8	NA
14-88	178	6076	2.6	22.3236	15.0	0.1109	15.8	0.0180	4.8	114.8	5.4	NA
14-54	176	11980	6.5	21.1183	13.3	0.1294	13.6	0.0198	2.9	126.5	3.6	NA
14-105	62	8409	1.5	24.6132	41.2	0.1545	41.6	0.0276	5.7	175.4	9.8	NA
14-62	87	5061	2.2	19.8698	18.7	0.2040	19.0	0.0294	3.6	186.8	6.5	NA
14-103	125	11729	4.0	20.6334	8.6	0.2194	9.0	0.0328	2.7	208.3	5.5	NA
14-46	68	10038	1.1	19.0844	6.5	0.5153	6.9	0.0713	2.2	444.2	9.5	146.7
14-100	97	18718	0.7	17.8105	4.6	0.5548	5.0	0.0717	1.9	446.2	8.4	97.4
14-12	168	12337	0.9	18.2266	5.8	0.5441	6.0	0.0719	1.5	447.8	6.6	110.1
14-75	160	13948	2.1	17.8860	3.2	0.5788	3.5	0.0751	1.2	466.7	5.6	104.0
14-9	113	29017	1.0	17.3421	2.7	0.6825	3.5	0.0858	2.3	530.9	11.5	102.7
14-63	1448	217108	0.4	16.8862	0.3	0.7415	0.8	0.0908	0.8	560.4	4.1	97.4
14-14	173	48370	3.9	16.4866	2.6	0.8540	2.7	0.1021	0.8	626.8	4.7	100.0
14-92	75	32115	1.4	15.0939	3.4	1.1761	3.6	0.1288	1.1	780.7	8.1	95.9
14-79	114	60133	1.6	14.1696	2.5	1.3121	3.8	0.1348	2.9	815.4	22.0	86.3
14-61	92	44566	3.0	14.2938	2.0	1.5018	2.2	0.1557	1.0	927.2	41.3	100.6
14-77	49	35269	2.2	14.0871	2.3	1.6081	2.5	0.1643	0.8	957.0	48.0	102.5
14-93	59	25674	1.8	14.0587	4.4	1.5741	4.5	0.1605	1.0	961.2	90.2	99.8
14-19	85	21927	1.8	14.0206	1.8	1.6353	2.1	0.1663	1.1	966.7	36.2	102.6
14-82	221	145522	3.0	13.6693	0.8	1.7340	0.8	0.1719	0.2	1018.3	15.3	100.4
14-49	142	109550	2.1	13.6588	1.2	1.7511	1.6	0.1735	1.0	1019.8	25.3	101.1
14-4	96	53975	1.8	13.6530	1.5	1.6982	1.9	0.1682	1.1	1020.7	31.1	98.2
14-58	105	53741	0.9	13.5709	2.2	1.8014	2.3	0.1773	0.7	1032.9	43.9	101.9
14-89	68	42397	2.1	13.5200	1.9	1.7906	2.0	0.1756	0.7	1040.5	38.8	100.2
14-56	219	66580	1.8	13.5156	1.0	1.8112	1.2	0.1775	0.7	1041.1	19.4	101.2
14-5	38	16158	1.8	13.4898	5.0	1.7532	5.3	0.1715	1.9	1045.0	100.0	97.7
14-18	58	29395	1.1	13.4806	2.4	1.7629	2.8	0.1724	1.5	1046.4	48.5	98.0
14-8	64	8341	0.6	13.4514	2.5	1.8226	2.7	0.1778	1.1	1050.8	49.7	100.4
14-50	138	78908	2.2	13.4432	1.1	1.7530	1.3	0.1709	0.6	1052.0	22.2	96.7

Grain No.	U (ppm)	^{206}Pb/ ^{204}Pb	U/Th	^{206}Pb*/ ^{207}Pb*	Error (±%)	^{207}Pb*/ ^{235}U*	Error (±%)	^{206}Pb*/ ^{238}U	Error (±%)	Best Age (Ma)	Error (± Ma)	Concordance (%)
14-48	172	64114	1.2	13.4187	1.4	1.8350	1.5	0.1786	0.4	1055.7	29.2	100.3
14-95	60	27011	1.5	13.4178	4.2	1.7948	4.3	0.1747	0.9	1055.8	84.2	98.3
14-25	630	244874	3.7	13.4106	0.5	1.7939	1.8	0.1745	1.8	1056.9	9.5	98.1
14-3	98	49138	2.7	13.3859	1.7	1.8208	2.5	0.1768	1.8	1060.6	34.1	98.9
14-20	174	79360	2.1	13.3808	0.7	1.8119	1.4	0.1758	1.2	1061.4	14.3	98.4
14-7	39	14967	1.0	13.3615	4.0	1.7843	6.1	0.1729	4.5	1064.3	81.0	96.6
14-36	69	55500	1.6	13.3463	2.1	1.8289	2.2	0.1770	0.7	1066.6	42.5	98.5
14-97	68	28712	2.7	13.3257	3.3	1.8757	3.4	0.1813	0.8	1069.7	66.0	100.4
14-29	106	26014	1.6	13.2876	1.5	1.8624	1.8	0.1795	1.0	1075.4	29.9	98.9
14-34	146	61156	0.7	13.2379	1.0	1.8712	1.2	0.1797	0.7	1082.9	19.1	98.4
14-60	32	21411	1.5	13.1961	4.6	1.8745	4.7	0.1794	1.3	1089.3	91.5	97.7
14-102	159	11630	2.4	13.1914	1.0	1.9351	1.8	0.1851	1.5	1090.0	20.4	100.5
14-66	59	33539	1.7	13.1873	2.8	1.8264	3.1	0.1747	1.5	1090.6	55.4	95.2
14-76	102	48747	0.9	13.1598	1.4	1.9486	1.8	0.1860	1.1	1094.8	28.3	100.4
14-74	151	68745	2.4	13.1421	1.3	1.9463	1.5	0.1855	0.8	1097.5	26.5	100.0
14-70	278	200331	1.5	13.1049	0.5	1.9023	0.8	0.1808	0.5	1103.1	11.0	97.1
14-28	56	3937	1.7	13.0497	3.9	1.8381	5.1	0.1740	3.3	1111.6	78.2	93.0
14-99	70	52769	1.4	12.9398	1.5	2.0882	1.6	0.1960	0.7	1128.5	29.7	102.2
14-32	20	10270	1.1	12.9137	6.6	2.1367	6.9	0.2001	1.8	1132.5	132.0	103.8
14-24	106	42600	3.7	12.9070	1.7	2.0554	1.9	0.1924	0.8	1133.5	33.6	100.1
14-37	75	3548	2.1	12.8505	4.5	1.8208	6.0	0.1697	4.0	1142.2	89.4	88.5
14-98	98	32226	2.3	12.8261	2.1	2.1457	2.3	0.1996	0.8	1146.0	42.4	102.4
14-10	79	72220	2.7	12.7913	1.1	2.1320	1.6	0.1978	1.2	1151.4	21.8	101.0
14-13	46	14870	1.2	12.7883	2.7	2.1644	2.9	0.2007	1.2	1151.8	52.7	102.4
14-43	66	22665	2.2	12.7217	1.7	2.1420	1.8	0.1976	0.7	1162.2	33.7	100.0
14-17	79	40995	2.2	12.7166	2.1	2.1745	2.8	0.2006	1.8	1163.0	41.7	101.3
14-41	57	29575	2.8	12.6980	2.9	2.1365	3.2	0.1968	1.3	1165.9	57.7	99.3
14-11	119	103710	2.5	12.6971	1.1	2.1729	1.3	0.2001	0.7	1166.0	21.4	100.8
14-83	262	147223	1.5	12.6927	0.7	2.1547	0.9	0.1984	0.6	1166.7	13.5	100.0
14-90	148	110138	0.9	12.6913	0.9	2.1762	1.0	0.2003	0.5	1166.9	18.2	100.9
14-23	171	46396	2.7	12.6302	0.8	2.1868	1.4	0.2003	1.2	1176.5	15.8	100.0
14-40	248	89435	1.6	12.6227	0.6	2.1915	0.7	0.2006	0.4	1177.7	11.4	100.1
14-6	54	42283	1.8	12.6039	1.5	2.1351	1.7	0.1952	0.8	1180.7	30.5	97.3

Grain No.	U (ppm)	$^{206}Pb/^{204}Pb$	U/Th	$^{206}Pb^*/^{207}Pb^*$	Error (±%)	$^{207}Pb^*/^{235}U^*$	Error (±%)	$^{206}Pb^*/^{238}U$	Error (±%)	Best Age (Ma)	Error (± Ma)	Concordance (%)
14-15	43	17902	1.0	12.5670	2.6	2.1428	2.9	0.1953	1.4	1186.5	50.8	96.9
14-86	146	43704	1.3	12.4717	0.9	2.2863	1.0	0.2068	0.4	1201.4	17.4	100.9
14-21	37	21646	1.7	12.3553	4.8	2.3912	5.9	0.2143	3.5	1219.9	94.5	102.6
14-51	30	15568	1.3	12.1198	2.9	2.3493	3.2	0.2065	1.2	1257.7	57.6	96.2
14-101	26	28572	1.5	11.8684	5.5	2.7316	5.8	0.2351	1.8	1298.5	106.7	104.8
14-94	210	148334	1.2	11.8121	0.6	2.6211	1.0	0.2246	0.7	1307.7	12.5	99.9
14-16	112	77285	1.3	11.7439	1.0	2.5865	1.5	0.2203	1.0	1319.0	20.2	97.3
14-64	26	11343	3.4	11.7119	4.0	2.7039	7.9	0.2297	6.8	1324.2	77.7	100.6
14-81	8	3880	1.5	11.6875	8.0	2.2869	9.0	0.1939	4.2	1328.3	154.4	86.0
14-31	130	112061	1.3	11.5961	0.8	2.7503	1.1	0.2313	0.7	1343.5	15.7	99.8
14-55	83	41423	0.9	11.5918	1.3	2.7402	1.5	0.2304	0.6	1344.2	25.8	99.4
14-38	95	13369	1.3	11.4803	1.9	2.7041	2.5	0.2252	1.6	1362.8	37.2	96.1
14-68	42	21183	1.8	11.3217	1.9	2.8816	2.2	0.2366	1.2	1389.6	36.0	98.5
14-26	99	18654	3.2	11.1278	1.1	3.0821	1.6	0.2487	1.2	1422.6	20.3	100.7
14-67	59	46055	2.7	11.1130	2.3	2.9207	3.8	0.2354	3.0	1425.2	43.5	95.6
14-45	95	80465	0.5	11.0569	1.3	2.9767	1.6	0.2387	0.9	1434.8	25.1	96.2
14-53	74	33014	1.1	11.0162	1.8	3.1068	1.9	0.2482	0.8	1441.9	34.1	99.1
14-96	120	71855	1.5	10.9799	0.7	3.1677	0.8	0.2523	0.5	1448.2	12.6	100.1
14-85	97	69684	1.8	10.8886	1.2	3.1918	1.7	0.2521	1.2	1464.1	22.4	99.0
14-1	42	10100	1.9	10.7720	3.0	3.2509	3.2	0.2540	1.2	1484.5	56.9	98.3
14-87	208	3254	1.8	10.7673	1.1	2.9073	1.9	0.2270	1.5	1485.3	20.1	88.8
14-47	21	1317	0.8	10.3008	9.3	3.5912	12.6	0.2683	8.5	1568.7	174.0	97.7
14-27	104	71687	0.6	9.9374	0.9	4.0542	1.2	0.2922	0.8	1635.7	16.1	101.0
14-71	53	42093	1.2	9.6838	0.9	4.3209	1.7	0.3035	1.5	1683.6	16.0	101.5
14-73	243	51149	3.8	9.6102	0.4	4.2043	1.1	0.2930	1.0	1697.7	7.8	97.6
14-44	157	90348	3.8	9.5268	0.6	4.4088	1.0	0.3046	0.7	1713.7	11.9	100.0
14-104	42	61803	1.2	8.8629	1.2	5.1748	1.7	0.3326	1.2	1845.5	21.1	100.3
14-33	50	67978	1.4	7.7535	0.4	6.7915	1.6	0.3819	1.5	2084.0	6.9	100.1
14-84	59	58726	1.5	6.3152	0.5	9.9030	0.7	0.4536	0.5	2438.1	8.6	98.9
14-2	58	70779	1.2	5.4636	0.5	12.9877	1.2	0.5146	1.1	2680.5	7.6	99.8
14-52	38	4507	1.1	5.3915	0.8	12.8538	2.0	0.5026	1.9	2702.5	13.4	97.1
14-30	50	101949	0.6	5.3314	0.7	13.4587	0.9	0.5204	0.6	2720.9	11.8	99.3
14-59	30	25576	1.6	5.2948	1.0	13.8006	1.3	0.5300	0.8	2732.3	16.2	100.3

SAMPLE 15- Love Quarry, MS

Grain No.	U (ppm)	^{206}Pb/ ^{204}Pb	U/Th	^{206}Pb*/ ^{207}Pb*	Error (±%)	^{207}Pb*/ ^{235}U*	Error (±%)	^{206}Pb*/ ^{238}U	Error (±%)	Best Age (Ma)	Error (± Ma)	Concordance (%)
15-77	391	54894	27.4	18.7233	2.2	0.4314	2.3	0.0586	0.5	367.0	1.9	NA
15- 24	146	89380	0.9	18.2490	5.5	0.4919	6.0	0.0651	2.3	406.6	9.2	100.7
15-81	76	11806	1.4	18.2793	5.1	0.4992	5.4	0.0662	1.7	413.1	6.7	103.2
15-61	204	28019	1.0	18.1518	2.1	0.5045	2.2	0.0664	0.8	414.5	3.1	99.7
15-73	56	9954	1.3	18.5985	6.6	0.5161	6.9	0.0696	1.9	433.9	7.9	120.1
15-76	99	16758	2.1	17.8947	7.7	0.5379	7.8	0.0698	0.8	435.0	3.4	97.2
15-42	147	30234	1.6	18.6178	2.9	0.5428	3.7	0.0733	2.3	455.9	9.9	127.0
15- 10	38	12419	1.8	17.2868	15.1	0.5927	15.2	0.0743	1.6	462.1	7.3	88.2
15- 2	122	15411	3.1	15.0337	2.5	0.8489	4.5	0.0926	3.8	570.7	20.7	69.4
15-44	93	23635	2.1	14.4858	3.0	1.3067	3.8	0.1373	2.2	829.3	17.4	92.2
15- 23	67	23544	1.6	14.1822	3.6	1.5073	3.8	0.1550	1.0	943.2	73.9	98.5
15-83	34	8344	0.2	14.0524	3.9	1.6431	4.4	0.1675	2.0	962.1	79.7	103.7
15-40	60	46315	1.7	14.0451	2.3	1.6294	2.5	0.1660	1.0	963.2	46.4	102.8
15-51	61	53379	2.0	14.0366	2.7	1.6380	2.9	0.1668	1.1	964.4	54.9	103.1
15-78	89	52230	2.3	13.9604	2.4	1.6211	2.6	0.1641	1.0	975.5	48.6	100.4
15-55	59	30175	2.5	13.9551	5.4	1.5173	5.5	0.1536	1.4	976.3	109.2	94.3
15-71	57	54265	2.1	13.9048	4.3	1.6864	4.4	0.1701	1.0	983.6	87.2	102.9
15-62	25	10230	1.3	13.8842	3.2	1.6535	3.7	0.1665	1.8	986.7	65.8	100.6
15-53	87	32743	3.1	13.8666	2.1	1.6730	2.2	0.1683	0.8	989.2	42.7	101.3
15-70	50	26203	2.2	13.8472	5.0	1.6457	5.0	0.1653	0.9	992.1	100.8	99.4
15-100	186	57449	5.8	13.8424	1.0	1.5960	2.5	0.1602	2.2	992.8	21.1	96.5
15-28	45	39863	1.9	13.8025	4.0	1.7088	4.1	0.1711	0.9	998.6	81.9	101.9
15-97	111	40062	4.8	13.7164	1.5	1.7234	1.7	0.1714	0.8	1011.3	30.4	100.9
15-64	80	25437	0.8	13.7105	2.5	1.6536	2.7	0.1644	1.1	1012.2	50.2	97.0
15-95	209	134546	2.3	13.7042	1.2	1.7402	1.7	0.1730	1.1	1013.1	25.3	101.5
15-54	130	11612	0.4	13.6922	1.4	1.6992	1.6	0.1687	0.7	1014.9	28.3	99.0
15- 16	81	35470	1.2	13.6892	2.4	1.6990	2.4	0.1687	0.6	1015.3	48.2	99.0
15- 19	71	20149	4.0	13.6725	2.0	1.6994	2.2	0.1685	0.9	1017.8	40.4	98.6
15-104	145	48648	1.2	13.6618	1.9	1.7386	3.8	0.1723	3.3	1019.4	39.4	100.5
15-50	55	44891	1.8	13.6567	3.2	1.7381	3.3	0.1722	0.8	1020.1	64.3	100.4
15- 5	84	31499	1.8	13.6350	2.4	1.7487	2.7	0.1729	1.1	1023.4	49.5	100.5
15-84	166	67416	1.5	13.6320	0.8	1.7685	0.9	0.1749	0.3	1023.8	16.7	101.5

Grain No.	U (ppm)	^{206}Pb/ ^{204}Pb	U/Th	^{206}Pb*/ ^{207}Pb*	Error (±%)	^{207}Pb*/ ^{235}U*	Error (±%)	^{206}Pb*/ ^{238}U	Error (±%)	Best Age (Ma)	Error (± Ma)	Concordance (%)
15- 20	101	64103	0.4	13.6318	1.4	1.7504	1.5	0.1731	0.7	1023.8	27.9	100.5
15-49	91	65243	3.4	13.6190	1.9	1.6851	2.2	0.1664	1.1	1025.7	38.2	96.8
15-29	149	40474	1.3	13.5599	1.1	1.7232	1.4	0.1695	0.9	1034.5	21.2	97.5
15-90	157	61715	2.9	13.5589	0.9	1.7696	1.0	0.1740	0.4	1034.7	18.3	100.0
15-63	68	6445	2.3	13.5506	2.3	1.7292	3.0	0.1699	1.8	1035.9	47.3	97.7
15- 7	156	74059	2.3	13.5337	1.6	1.7659	1.6	0.1733	0.4	1038.4	31.4	99.2
15-66	243	172369	1.9	13.5123	0.8	1.7951	0.8	0.1759	0.3	1041.6	15.4	100.3
15-32	83	39712	1.4	13.5081	2.4	1.7321	2.8	0.1697	1.3	1042.2	49.4	96.9
15-69	42	17571	13.0	13.5006	5.6	1.6484	5.8	0.1614	1.6	1043.4	112.1	92.4
15-57	424	162642	2.0	13.4682	0.3	1.7951	0.5	0.1753	0.5	1048.3	5.7	99.4
15- 6	78	43468	0.5	13.4625	1.8	1.7691	2.0	0.1727	0.9	1049.1	36.4	97.9
15-38	31	36704	2.0	13.4605	2.9	1.7977	3.4	0.1755	1.7	1049.4	59.3	99.3
15- 4	115	51147	1.6	13.4501	1.0	1.7033	1.2	0.1662	0.7	1051.0	19.7	94.3
15-67	288	25461	0.8	13.3747	0.8	1.7856	1.1	0.1732	0.7	1062.3	16.2	96.9
15-82	130	67688	2.5	13.3491	1.6	1.8538	1.7	0.1795	0.5	1066.1	32.3	99.8
15-60	51	49530	3.4	13.3441	3.5	1.8214	3.7	0.1763	1.1	1066.9	70.1	98.1
15-103	210	146616	5.0	13.3202	1.2	1.8559	1.3	0.1793	0.4	1070.5	25.1	99.3
15-36	173	91100	2.3	13.2519	1.1	1.8759	1.5	0.1803	1.0	1080.8	22.2	98.9
15- 25	116	94965	0.6	13.2246	2.4	1.8470	3.1	0.1772	2.0	1085.0	47.1	96.9
15-89	88	27648	1.1	13.1832	1.6	1.8996	1.9	0.1816	1.1	1091.2	31.1	98.6
15- 15	34	9350	0.9	13.1263	2.6	1.9741	2.9	0.1879	1.4	1099.9	51.5	100.9
15-30	17	11821	5.1	13.1096	6.1	1.9839	6.3	0.1886	1.4	1102.4	122.6	101.0
15-48	31	11691	7.5	13.0024	8.0	1.8589	8.2	0.1753	1.7	1118.8	160.3	93.1
15-33	69	31684	2.4	12.9521	2.4	2.0159	2.6	0.1894	0.8	1126.6	48.7	99.2
15-102	75	53155	2.0	12.8461	2.3	2.1186	2.4	0.1974	0.7	1142.9	44.8	101.6
15-27	82	52216	1.7	12.8279	1.5	1.9191	1.9	0.1785	1.1	1145.7	30.3	92.4
15-34	138	88708	1.9	12.8247	0.5	2.0630	1.0	0.1919	0.8	1146.2	10.6	98.7
15-92	525	213799	2.8	12.7866	0.5	1.9866	6.5	0.1842	6.5	1152.1	9.0	94.6
15-85	136	93793	1.9	12.7512	1.0	2.0964	1.5	0.1939	1.1	1157.6	20.3	98.7
15- 21	36	20371	0.9	12.7169	5.0	1.9481	5.4	0.1797	2.2	1163.0	98.6	91.6
15-75	42	29221	2.4	12.7162	1.2	2.0510	1.5	0.1892	0.9	1163.1	24.0	96.0
15-105	163	77482	1.3	12.6421	0.7	2.1639	0.9	0.1984	0.6	1174.7	13.8	99.3
15-47	43	18809	1.5	12.6356	4.5	2.1394	4.6	0.1961	0.8	1175.7	88.6	98.2

Grain No.	U (ppm)	$^{206}Pb/^{204}Pb$	U/Th	$^{206}Pb^*/^{207}Pb^*$	Error (±%)	$^{207}Pb^*/^{235}U^*$	Error (±%)	$^{206}Pb^*/^{238}U$	Error (±%)	Best Age (Ma)	Error (± Ma)	Concordance (%)
15-37	47	39761	2.2	12.6304	2.2	2.2338	4.7	0.2046	4.1	1176.5	44.2	102.0
15-101	42	13008	1.4	12.6297	3.2	1.9455	3.5	0.1782	1.5	1176.6	63.1	89.8
15-91	169	26448	0.9	12.6291	0.6	1.9213	1.4	0.1760	1.2	1176.7	12.6	88.8
15-31	149	52015	2.4	12.6105	0.8	2.0860	1.0	0.1908	0.6	1179.6	16.6	95.4
15-80	80	45877	1.7	12.5958	1.8	2.1623	2.1	0.1975	1.2	1181.9	34.9	98.3
15-88	101	62191	1.5	12.5537	0.7	2.2298	1.0	0.2030	0.8	1188.5	13.3	100.3
15-93	29	23414	2.4	12.5452	7.0	2.2881	7.6	0.2082	3.0	1189.9	138.6	102.5
15-58	98	88535	1.2	12.5342	1.0	2.1777	1.2	0.1980	0.6	1191.6	20.5	97.7
15- 3	22	10752	3.0	12.3309	4.2	2.2669	5.3	0.2027	3.1	1223.8	82.9	97.2
15-87	47	61894	2.2	12.3227	3.3	2.2706	3.5	0.2029	1.3	1225.1	64.5	97.2
15-94	51	31544	1.8	12.3139	2.1	2.3392	2.5	0.2089	1.4	1226.5	40.8	99.7
15- 13	19	14017	1.9	12.2052	6.2	2.1433	6.9	0.1897	3.0	1243.9	121.9	90.0
15-39	64	31196	1.3	12.1787	2.7	2.2585	5.2	0.1995	4.4	1248.1	52.5	93.9
15-74	285	45199	1.3	11.7872	0.5	2.5635	1.0	0.2192	0.9	1311.8	10.2	97.4
15- 12	66	56914	1.3	11.7862	1.5	2.6561	1.8	0.2270	0.8	1312.0	30.1	100.5
15- 22	238	324231	1.5	11.5399	0.5	2.7361	1.2	0.2290	1.1	1352.8	9.0	98.3
15- 18	188	142932	1.0	11.5362	0.6	2.7244	0.8	0.2279	0.6	1353.5	11.6	97.8
15-99	20	11610	2.0	11.3495	3.7	3.0403	4.0	0.2503	1.5	1384.9	71.0	104.0
15-68	125	30527	4.9	11.3105	1.0	2.5811	2.1	0.2117	1.8	1391.5	19.2	89.0
15-56	256	138466	2.1	10.9121	0.5	3.2193	0.7	0.2548	0.5	1459.9	8.6	100.2
15-98	96	50593	1.0	9.7721	1.1	3.8374	1.9	0.2720	1.6	1666.8	19.9	93.0
15-45	158	10388	5.3	9.1235	0.7	5.0158	1.3	0.3319	1.1	1792.9	13.5	103.1
15- 9	95	69575	0.9	9.0042	0.5	4.9695	0.8	0.3245	0.6	1816.8	9.9	99.7
15-52	59	93118	0.9	4.4794	0.2	18.2124	0.7	0.5917	0.7	3004.2	3.1	99.7

SAMPLE 16- Perry Quarry, MS												
Grain No.	U (ppm)	^{206}Pb/ ^{204}Pb	U/Th	^{206}Pb*/ ^{207}Pb*	Error (±%)	^{207}Pb*/ ^{235}U*	Error (±%)	^{206}Pb*/ ^{238}U	Error (±%)	Best Age (Ma)	Error (± Ma)	Concordance (%)
16-56	779	5445	1.9	27.0703	15.3	0.0137	15.9	0.0027	4.0	17.4	0.7	NA
16-50	636	8955	0.9	24.1979	17.9	0.0239	18.0	0.0042	2.4	26.9	0.7	NA
16-59	170	1708	0.5	25.0406	45.8	0.0264	46.9	0.0048	9.9	30.9	3.0	NA
16-85	150	1141	0.7	17.7616	37.4	0.0464	37.6	0.0060	3.7	38.4	1.4	NA
16-40	425	15218	4.5	21.0108	8.7	0.0657	8.9	0.0100	1.9	64.2	1.2	NA
16-76	595	51552	1.9	19.7531	2.1	0.2132	2.9	0.0305	2.0	193.9	3.8	NA
16-95	186	25069	1.1	19.6728	6.7	0.2471	6.8	0.0353	1.3	223.4	2.8	NA
16-77	148	25939	1.4	18.4619	4.0	0.4987	4.3	0.0668	1.5	416.7	6.1	110.3
16-45	105	2087	1.3	16.7265	3.7	0.6129	3.8	0.0743	0.9	462.3	4.2	77.6
16-42	211	20308	2.9	17.0454	2.3	0.6764	2.4	0.0836	0.9	517.7	4.4	93.3
16-55	96	25901	1.8	17.3906	3.3	0.6686	3.6	0.0843	1.4	521.9	7.1	102.2
16-78	71	24968	1.8	16.2464	6.6	0.7176	6.9	0.0846	2.1	523.3	10.5	79.5
16-32	50	23709	1.8	14.1569	2.2	1.5779	2.6	0.1620	1.4	946.9	44.8	102.2
16-74	40	40794	1.7	13.9116	2.0	1.6792	2.2	0.1694	1.0	982.6	40.2	102.7
16-60	92	126604	2.3	13.7872	2.4	1.6843	3.0	0.1684	1.8	1000.9	48.7	100.3
16-89	107	18214	1.3	13.7538	2.0	1.6872	2.3	0.1683	1.0	1005.8	41.5	99.7
16-96	200	104603	2.4	13.7212	1.4	1.6618	1.6	0.1654	0.7	1010.6	28.8	97.6
16-16	340	200230	1.7	13.7127	0.7	1.7342	1.6	0.1725	1.4	1011.8	13.3	101.4
16-18	30	21397	1.2	13.7093	4.1	1.7141	5.5	0.1704	3.7	1012.4	84.0	100.2
16-51	68	44732	2.1	13.7016	2.8	1.7661	3.6	0.1755	2.2	1013.5	56.5	102.9
16-8	149	99405	3.3	13.6731	0.9	1.7327	1.5	0.1718	1.2	1017.7	17.8	100.4
16-73	80	129785	1.6	13.6191	2.7	1.7736	3.6	0.1752	2.4	1025.7	54.2	101.5
16-31	76	35577	2.2	13.5751	2.4	1.7504	2.6	0.1723	1.1	1032.3	47.7	99.3
16-57	96	39548	2.4	13.5618	2.1	1.7923	2.6	0.1763	1.6	1034.2	42.5	101.2
16-70	258	59182	2.1	13.5601	0.8	1.7965	1.5	0.1767	1.3	1034.5	15.7	101.4
16-64	192	94973	4.7	13.5443	0.7	1.7831	1.9	0.1752	1.8	1036.9	13.6	100.3
16-75	44	20675	1.2	13.5125	3.9	1.7647	4.5	0.1729	2.3	1041.6	78.3	98.7
16-21	50	30467	1.1	13.4515	3.4	1.7966	3.7	0.1753	1.6	1050.8	67.6	99.1
16-94	179	50183	2.7	13.4333	1.8	1.8107	2.9	0.1764	2.2	1053.5	35.3	99.4
16-46	122	94411	1.2	13.4328	1.2	1.7509	1.4	0.1706	0.8	1053.6	23.7	96.4
16-92	180	59344	1.2	13.4247	0.7	1.8196	1.0	0.1772	0.7	1054.8	14.9	99.7
16-80	33	23142	0.8	13.4135	5.8	1.8525	6.1	0.1802	2.0	1056.5	116.2	101.1

Grain No.	U (ppm)	^{206}Pb/ ^{204}Pb	U/Th	^{206}Pb*/ ^{207}Pb*	Error (±%)	^{207}Pb*/ ^{235}U*	Error (±%)	^{206}Pb*/ ^{238}U	Error (±%)	Best Age (Ma)	Error (± Ma)	Concordance (%)
16-61	41	36962	1.6	13.4081	5.4	1.7825	5.5	0.1733	1.0	1057.3	107.9	97.5
16-5	39	25962	1.5	13.3918	3.5	1.7554	3.9	0.1705	1.5	1059.7	71.3	95.8
16-4	38	18017	0.8	13.3765	3.6	1.7843	4.0	0.1731	1.6	1062.0	73.2	96.9
16-67	43	28371	1.2	13.2944	5.4	1.9477	5.7	0.1878	1.7	1074.4	108.8	103.3
16-102	266	519610	3.0	13.2915	0.4	1.8668	1.1	0.1800	1.1	1074.8	8.6	99.2
16-2	379	204881	1.6	13.2728	0.3	1.8602	1.1	0.1791	1.1	1077.6	5.9	98.5
16-13	198	144791	0.9	13.2619	0.8	1.8959	1.7	0.1824	1.5	1079.3	16.5	100.1
16-105	251	90011	2.3	13.2572	0.6	1.9072	0.8	0.1834	0.5	1080.0	12.2	100.5
16-26	30	12264	1.0	13.2258	4.9	1.9526	5.4	0.1873	2.3	1084.8	97.8	102.0
16-83	314	153602	1.4	13.2219	0.3	1.8798	0.7	0.1803	0.6	1085.3	6.1	98.4
16-69	193	11829	2.1	13.1987	1.9	1.8587	2.8	0.1779	2.0	1088.9	38.0	96.9
16-17	38	19204	1.0	13.1462	2.8	1.8636	3.3	0.1777	1.7	1096.8	56.0	96.1
16-62	180	40736	4.9	13.1138	1.1	1.9892	2.3	0.1892	2.0	1101.8	22.6	101.4
16-104	58	36078	0.9	13.0300	1.7	1.9324	2.0	0.1826	1.2	1114.6	33.8	97.0
16-28	46	34147	2.0	12.9315	3.2	2.0043	3.3	0.1880	0.9	1129.7	62.9	98.3
16-34	27	5723	1.6	12.8738	6.9	1.6660	7.3	0.1555	2.6	1138.7	136.5	81.9
16-66	48	16566	2.3	12.8554	2.8	2.0684	3.8	0.1929	2.5	1141.5	56.0	99.6
16-23	88	86773	3.2	12.7908	1.3	2.0648	1.5	0.1915	0.8	1151.5	25.4	98.1
16-103	88	13945	1.2	12.7194	5.4	2.0082	5.5	0.1853	0.7	1162.6	107.7	94.2
16-84	120	62162	1.7	12.6503	0.5	2.1381	2.4	0.1962	2.3	1173.4	9.5	98.4
16-38	117	107778	2.1	12.5981	1.0	2.1539	1.6	0.1968	1.2	1181.6	19.7	98.0
16-9	179	98164	0.5	12.5787	0.8	2.1838	1.4	0.1992	1.1	1184.6	16.6	98.9
16-87	91	109247	2.6	12.5520	1.0	2.1790	1.8	0.1984	1.5	1188.8	20.0	98.1
16-68	64	43969	1.8	12.5350	3.2	2.3059	3.4	0.2096	1.1	1191.5	63.4	103.0
16-81	40	56183	1.3	12.3883	2.9	2.3242	3.0	0.2088	0.8	1214.7	57.1	100.6
16-37	77	55645	2.5	12.3404	1.6	2.3032	2.0	0.2061	1.2	1222.3	30.9	98.9
16-71	175	197807	4.5	12.2700	0.9	2.4076	1.7	0.2143	1.4	1233.5	18.6	101.5
16-39	260	76943	2.7	12.2280	0.3	2.3711	1.2	0.2103	1.2	1240.2	5.1	99.2
16-43	221	80232	1.2	12.2089	0.7	2.3395	1.1	0.2072	0.9	1243.3	12.9	97.6
16-33	100	92476	1.6	12.1970	1.5	2.3381	3.1	0.2068	2.8	1245.2	29.5	97.3
16-15	56	31433	1.6	11.6585	2.1	2.7000	5.4	0.2283	5.0	1333.1	40.0	99.4
16-22	67	60346	1.0	11.1189	1.4	3.0473	1.7	0.2457	0.9	1424.2	27.6	99.5
16-53	65	42872	1.1	11.0491	1.0	3.1199	2.0	0.2500	1.8	1436.2	19.0	100.2

Grain No.	U (ppm)	$^{206}Pb/^{204}Pb$	U/Th	$^{206}Pb^{*}/^{207}Pb^{*}$	Error (±%)	$^{207}Pb^{*}/^{235}U^{*}$	Error (±%)	$^{206}Pb^{*}/^{238}U$	Error (±%)	Best Age (Ma)	Error (± Ma)	Concordance (%)
16-41	83	88564	1.2	11.0363	1.4	3.0098	3.4	0.2409	3.1	1438.4	26.3	96.7
16-1	53	76000	1.2	10.8911	1.7	3.1397	2.6	0.2480	2.0	1463.6	33.1	97.6
16-19	31	30556	0.4	10.8283	2.2	3.1965	2.9	0.2510	1.8	1474.6	42.6	97.9
16-100	72	3114	0.7	10.7120	2.5	3.2161	2.6	0.2499	0.6	1495.0	47.4	96.2
16-72	79	94322	4.6	10.4128	1.4	3.0163	5.5	0.2278	5.4	1548.5	26.7	85.4
16-82	269	11989	1.1	10.0244	0.9	3.7562	1.7	0.2731	1.5	1619.5	16.2	96.1
16-24	28	26585	0.7	9.9072	3.5	3.9590	3.9	0.2845	1.8	1641.4	64.3	98.3
16-52	44	24422	1.4	9.8778	2.2	4.0814	2.8	0.2924	1.7	1646.9	41.5	100.4
16-27	105	78205	2.6	9.8596	0.7	4.0519	1.4	0.2897	1.3	1650.3	12.7	99.4
16-99	51	33983	1.1	9.7362	1.1	4.1327	1.6	0.2918	1.1	1673.6	20.8	98.6
16-93	65	57746	0.8	9.7067	1.4	4.2424	1.6	0.2987	0.8	1679.2	25.8	100.3
16-44	47	74782	0.8	9.5912	1.6	4.1857	2.0	0.2912	1.2	1701.3	30.0	96.8
16-35	63	103778	2.9	9.5725	2.0	4.2425	2.1	0.2945	0.8	1704.9	36.0	97.6
16-47	151	109352	1.8	9.5112	0.5	4.3464	2.1	0.2998	2.1	1716.7	8.3	98.5
16-30	76	67415	1.0	9.4752	0.5	4.4360	3.1	0.3048	3.0	1723.7	8.9	99.5
16-49	150	124033	1.2	9.4709	0.5	4.4421	0.9	0.3051	0.8	1724.5	8.9	99.5
16-14	51	63998	2.3	9.4402	0.9	4.4528	2.6	0.3049	2.4	1730.5	16.5	99.1
16-86	33	26253	4.9	9.3864	2.1	4.5269	2.5	0.3082	1.4	1741.0	38.9	99.5
16-88	182	250684	3.2	9.3515	0.3	4.6095	0.6	0.3126	0.5	1747.8	5.4	100.3
16-36	75	95791	1.0	9.0959	0.4	4.8988	2.0	0.3232	1.9	1798.4	6.9	100.4
16-101	21	14740	0.8	8.5246	2.2	5.5275	2.4	0.3417	0.8	1915.6	40.1	98.9
16-29	106	90946	1.2	8.5074	0.5	5.6077	1.4	0.3460	1.3	1919.2	8.1	99.8
16-10	92	136985	0.7	6.0107	0.9	9.9133	2.7	0.4322	2.6	2521.4	15.5	91.8
16-91	171	190409	0.6	5.8104	0.1	11.6636	0.7	0.4915	0.7	2578.2	2.3	100.0
16-65	203	289706	0.6	5.6214	0.1	12.3312	1.1	0.5027	1.1	2633.3	1.8	99.7
16-11	64	151408	1.0	5.4979	0.3	12.7502	2.1	0.5084	2.1	2670.1	4.7	99.2
16-90	25	12413	0.7	5.3863	0.5	13.4262	1.0	0.5245	0.9	2704.0	8.4	100.5
16-12	242	469781	0.7	5.3576	0.2	13.2543	2.3	0.5150	2.3	2712.9	4.0	98.7
16-54	141	7275	1.2	5.2213	0.3	14.2987	2.5	0.5415	2.5	2755.3	4.8	101.2
16-3	211	422665	1.3	5.1790	0.6	14.3719	2.0	0.5398	1.9	2768.6	10.0	100.5
16-48	23	44108	0.5	4.9530	0.8	15.0529	1.4	0.5407	1.1	2841.6	13.6	98.1

SAMPLE 17- Atmore Landfill, AL

Grain No.	U (ppm)	^{206}Pb/ ^{204}Pb	U/Th	^{206}Pb*/ ^{207}Pb*	Error (±%)	^{207}Pb*/ ^{235}U*	Error (±%)	^{206}Pb*/ ^{238}U	Error (±%)	Best Age (Ma)	Error (± Ma)	Concordance (%)
17-11	74	13193	52.1	18.6601	7.1	0.3949	7.7	0.0534	2.9	335.6	9.4	NA
17-23	37	6151	0.7	18.6758	10.0	0.4245	10.1	0.0575	1.9	360.4	6.6	NA
17-24	41	9334	0.7	17.9850	9.9	0.4412	10.5	0.0575	3.4	360.7	12.1	NA
17-100	84	856	0.6	18.2311	17.3	0.4586	18.5	0.0606	6.5	379.5	24.1	NA
17-43	189	32812	1.1	18.6408	2.8	0.4556	3.2	0.0616	1.6	385.3	5.9	NA
17-14	132	26628	5.8	18.2498	6.2	0.4979	6.5	0.0659	2.1	411.4	8.2	101.9
17-49	139	25886	1.2	17.7510	2.3	0.5407	3.7	0.0696	2.9	433.8	12.2	93.2
17-18	72	12459	0.8	19.1477	5.7	0.5076	6.0	0.0705	1.7	439.1	7.4	148.7
17-92	282	75478	1.2	18.0825	1.6	0.5443	1.8	0.0714	1.0	444.5	4.2	104.7
17-87	172	67349	1.2	18.0018	4.0	0.5496	4.3	0.0718	1.7	446.7	7.2	102.8
17-48	309	51647	1.6	17.5953	2.3	0.5750	2.5	0.0734	0.8	456.5	3.4	94.1
17-69	274	75191	20.2	18.0150	1.9	0.5670	2.1	0.0741	0.7	460.7	3.1	106.4
17-46	165	23798	3.2	18.0289	2.9	0.5733	3.8	0.0750	2.4	466.0	11.0	108.1
17-77	213	46323	2.7	17.9720	2.5	0.5825	3.6	0.0759	2.6	471.8	11.8	107.7
17-81	522	44860	5.2	16.0694	1.1	0.9517	1.3	0.1109	0.7	678.1	4.6	99.4
17-51	122	35487	2.1	14.6719	1.6	1.1472	3.0	0.1221	2.5	742.5	17.6	85.0
17-35	100	33522	1.7	14.2559	1.3	1.5362	1.9	0.1588	1.4	932.6	27.4	101.9
17-19	68	31014	2.0	14.1377	2.8	1.6005	3.0	0.1641	1.2	949.7	56.9	103.1
17-67	57	20720	2.6	14.1163	2.0	1.6125	2.7	0.1651	1.9	952.8	40.1	103.4
17-10	242	29574	2.2	14.0398	0.9	1.4892	1.9	0.1516	1.7	963.9	17.8	94.4
17-70	50	48831	2.1	14.0331	2.3	1.6538	2.5	0.1683	1.0	964.9	47.0	103.9
17-73	39	32631	0.4	13.9850	3.7	1.5683	3.8	0.1591	0.8	971.9	76.5	97.9
17-6	180	75510	1.0	13.8941	0.8	1.6623	1.7	0.1675	1.4	985.2	17.2	101.3
17-75	63	70675	1.8	13.8561	2.8	1.6859	3.0	0.1694	0.9	990.8	57.7	101.8
17-60	36	13543	2.5	13.8341	3.4	1.7057	3.8	0.1711	1.8	994.0	68.5	102.5
17-97	242	269996	2.9	13.8276	1.0	1.7001	1.3	0.1705	0.9	994.9	20.3	102.0
17-21	97	43831	2.3	13.7895	1.5	1.7270	4.6	0.1727	4.4	1000.5	30.1	102.7
17-55	159	99789	2.0	13.7559	1.0	1.6922	3.0	0.1688	2.9	1005.5	20.9	100.0
17-103	112	129084	1.6	13.7044	0.7	1.6735	1.2	0.1663	1.0	1013.1	13.7	97.9
17-15	93	80947	1.3	13.6759	1.9	1.7533	2.2	0.1739	1.1	1017.3	39.4	101.6
17-72	27	9518	1.9	13.6679	7.8	1.7042	8.0	0.1689	1.7	1018.5	158.3	98.8
17-84	77	58137	2.5	13.6613	1.9	1.6958	2.2	0.1680	1.1	1019.5	38.2	98.2

Grain No.	U (ppm)	$^{206}Pb/^{204}Pb$	U/Th	$^{206}Pb^*/^{207}Pb^*$	Error (±%)	$^{207}Pb^*/^{235}U^*$	Error (±%)	$^{206}Pb^*/^{238}U$	Error (±%)	Best Age (Ma)	Error (± Ma)	Concordance (%)
17-45	59	26683	1.7	13.6159	2.2	1.7503	2.6	0.1728	1.2	1026.2	45.4	100.2
17-2	291	191175	1.9	13.5932	0.5	1.7828	1.1	0.1758	1.0	1029.6	9.5	101.4
17-78	160	179445	2.1	13.5859	1.2	1.7781	1.4	0.1752	0.7	1030.7	24.0	101.0
17-71	197	86920	0.8	13.5623	0.8	1.7722	1.1	0.1743	0.8	1034.2	16.2	100.2
17-4	50	40604	1.8	13.5618	2.6	1.7287	3.0	0.1700	1.3	1034.2	53.3	97.9
17-41	133	51035	1.5	13.5590	1.3	1.7487	1.5	0.1720	0.8	1034.7	26.2	98.9
17-5	162	62942	2.9	13.5487	1.0	1.8350	1.8	0.1803	1.5	1036.2	19.3	103.1
17-82	149	95347	2.1	13.4910	0.8	1.7565	1.8	0.1719	1.6	1044.8	16.5	97.9
17-79	62	9366	1.2	13.4783	1.5	1.7024	2.7	0.1664	2.2	1046.7	29.6	94.8
17-58	528	32077	3.0	13.4688	0.2	1.8751	1.4	0.1832	1.4	1048.2	4.9	103.4
17-29	149	151438	1.0	13.4192	0.8	1.8605	1.9	0.1811	1.8	1055.6	16.0	101.6
17-96	369	118836	2.3	13.4147	0.5	1.8332	2.4	0.1784	2.3	1056.3	10.5	100.2
17-59	63	9043	1.6	13.3737	4.1	1.7500	4.2	0.1697	0.9	1062.4	83.3	95.1
17-76	48	23356	0.7	13.3453	4.7	1.8445	4.7	0.1785	0.7	1066.7	94.2	99.3
17-32	167	76797	2.2	13.3306	1.2	1.8843	1.7	0.1822	1.2	1068.9	25.1	100.9
17-17	287	207007	1.6	13.3078	0.2	1.8861	1.1	0.1820	1.1	1072.4	4.1	100.5
17-28	38	27826	1.8	13.2821	3.2	1.9352	4.5	0.1864	3.1	1076.3	65.2	102.4
17-57	151	123770	3.6	13.0765	1.0	1.9704	1.6	0.1869	1.2	1107.5	19.2	99.7
17-88	28	9518	1.4	13.0457	4.9	2.0736	5.5	0.1962	2.3	1112.2	98.8	103.8
17-90	49	23215	1.5	13.0034	2.0	1.9553	2.7	0.1844	1.8	1118.7	39.8	97.5
17-39	247	92432	1.4	12.9636	1.3	1.8783	6.9	0.1766	6.7	1124.8	25.1	93.2
17-105	128	295176	2.1	12.9556	1.5	2.0367	2.5	0.1914	2.0	1126.0	29.5	100.2
17-8	74	6029	1.4	12.9442	5.9	1.8905	6.0	0.1775	1.1	1127.8	117.0	93.4
17-101	22	13343	2.0	12.9119	4.2	2.1131	4.3	0.1979	1.0	1132.7	83.9	102.8
17-16	50	14857	2.4	12.8836	2.1	2.1273	2.6	0.1988	1.5	1137.1	42.0	102.8
17-83	213	80631	2.4	12.8628	0.5	2.1063	2.7	0.1965	2.7	1140.3	9.9	101.4
17-94	43	22162	0.8	12.8493	3.5	2.1184	3.8	0.1974	1.4	1142.4	70.3	101.7
17-7	69	26897	1.5	12.8403	1.3	2.1468	1.8	0.1999	1.2	1143.8	26.2	102.7
17-85	121	267840	1.8	12.8343	0.8	2.0295	1.5	0.1889	1.2	1144.7	15.2	97.4
17-68	190	76012	1.8	12.8245	1.9	1.6576	7.8	0.1542	7.6	1146.3	38.6	80.6
17-27	62	4221	1.4	12.8156	5.3	2.0963	5.7	0.1949	2.2	1147.6	105.4	100.0
17-50	153	65392	1.6	12.8156	0.7	2.1029	1.4	0.1955	1.2	1147.6	13.8	100.3
17-3	253	167161	4.9	12.7894	0.5	2.1098	0.9	0.1957	0.7	1151.7	10.6	100.0

Grain No.	U (ppm)	$^{206}Pb/^{204}Pb$	U/Th	$^{206}Pb^*/^{207}Pb^*$	Error (±%)	$^{207}Pb^*/^{235}U^*$	Error (±%)	$^{206}Pb^*/^{238}U$	Error (±%)	Best Age (Ma)	Error (± Ma)	Concordance (%)
17-52	283	184926	4.0	12.7110	0.6	2.1086	2.0	0.1944	2.0	1163.9	11.5	98.4
17-99	160	173542	1.8	12.7076	0.7	2.1526	1.2	0.1984	1.0	1164.4	13.4	100.2
17-74	210	160885	1.1	12.6835	0.4	2.2133	1.0	0.2036	0.9	1168.2	8.8	102.3
17-54	63	24107	1.6	12.6605	2.4	2.1350	2.8	0.1960	1.4	1171.8	46.8	98.5
17-33	133	137285	2.3	12.6453	1.1	2.1859	1.7	0.2005	1.4	1174.2	21.2	100.3
17-31	241	205442	3.4	12.6219	0.5	2.1887	1.1	0.2004	1.0	1177.8	9.2	100.0
17-34	116	45732	13.7	12.5525	1.7	2.3350	3.4	0.2126	3.0	1188.7	33.2	104.5
17-1	82	56452	2.4	12.5500	1.6	2.1570	1.9	0.1963	1.0	1189.1	31.2	97.2
17-47	354	24770	2.1	12.5431	0.8	2.2083	1.0	0.2009	0.7	1190.2	15.0	99.2
17-66	219	76815	1.4	12.4917	0.7	2.1190	1.9	0.1920	1.8	1198.3	13.3	94.5
17-64	87	72164	4.7	12.4728	1.4	2.1785	2.2	0.1971	1.7	1201.3	27.1	96.5
17-104	99	41456	1.9	12.3990	1.0	2.3646	1.4	0.2126	0.9	1213.0	19.5	102.5
17-61	84	60642	2.6	12.2639	1.3	2.4150	1.8	0.2148	1.2	1234.5	24.7	101.6
17-22	156	98402	3.0	12.2583	0.6	2.3883	1.5	0.2123	1.4	1235.4	12.6	100.5
17-62	78	9024	1.8	12.2478	1.8	2.1032	7.0	0.1868	6.7	1237.1	35.9	89.3
17-26	115	61766	2.3	12.1795	1.1	2.3259	2.2	0.2055	1.9	1248.0	21.6	96.5
17-36	56	80239	2.2	12.1079	2.2	2.5072	4.0	0.2202	3.3	1259.5	43.2	101.8
17-37	270	40683	2.6	12.0819	0.3	2.4982	1.4	0.2189	1.3	1263.8	6.1	101.0
17-93	55	26580	1.6	11.8149	1.9	2.6967	2.5	0.2311	1.6	1307.3	37.3	102.5
17-53	155	104774	1.5	11.7170	0.8	2.7128	1.7	0.2305	1.5	1323.4	14.7	101.1
17-12	65	21219	1.6	11.6323	1.7	2.6164	2.9	0.2207	2.4	1337.4	33.6	96.1
17-44	60	24005	1.9	11.4029	1.5	2.8616	2.9	0.2367	2.5	1375.8	28.4	99.5
17-20	131	89179	2.4	11.3574	0.6	2.9249	1.1	0.2409	0.9	1383.5	11.5	100.6
17-98	237	15912	2.4	11.2961	1.1	2.7768	2.1	0.2275	1.8	1393.9	21.4	94.8
17-65	89	38174	2.0	11.2711	1.2	2.7940	3.2	0.2284	3.0	1398.2	22.8	94.8
17-95	96	39387	2.1	11.2164	1.7	2.6480	4.7	0.2154	4.4	1407.5	32.1	89.4
17-86	21	14223	1.5	11.1742	3.7	2.9088	4.5	0.2357	2.6	1414.7	70.0	96.5
17-30	132	109969	0.9	10.9232	1.0	2.9077	6.0	0.2304	5.9	1458.0	18.2	91.7
17-91	188	155626	2.1	10.8795	0.4	3.0773	1.1	0.2428	1.1	1465.6	7.5	95.6
17-102	64	29941	2.4	10.8647	1.2	3.2345	1.8	0.2549	1.4	1468.2	21.9	99.7
17-38	142	118902	2.7	10.7665	0.5	3.3654	1.2	0.2628	1.1	1485.4	9.7	101.3
17-42	556	250046	16.9	9.9404	0.2	3.9834	0.9	0.2872	0.9	1635.2	4.6	99.5
17-9	99	93483	1.0	8.1976	0.4	6.1487	1.4	0.3656	1.4	1985.5	6.5	101.2

Grain No.	U (ppm)	$^{206}Pb/^{204}Pb$	U/Th	$^{206}Pb^*/^{207}Pb^*$	Error (±%)	$^{207}Pb^*/^{235}U^*$	Error (±%)	$^{206}Pb^*/^{238}U$	Error (±%)	Best Age (Ma)	Error (± Ma)	Concordance (%)
17-40	136	59276	1.6	5.1617	0.4	13.7609	1.0	0.5152	1.0	2774.1	6.5	96.6

SAMPLE 18- N of Jackson, AL												
Grain No.	U (ppm)	$^{206}Pb/^{204}Pb$	U/Th	$^{206}Pb^*/^{207}Pb^*$	Error (±%)	$^{207}Pb^*/^{235}U^*$	Error (±%)	$^{206}Pb^*/^{238}U$	Error (±%)	Best Age (Ma)	Error (± Ma)	Concordance (%)
18-95	335	8377	2.0	19.9555	17.5	0.0601	18.0	0.0087	4.3	55.8	2.4	NA
18-49	85	8463	1.4	21.0206	10.8	0.2103	11.5	0.0321	3.8	203.5	7.6	NA
18-72	273	37556	1.9	17.5992	2.7	0.5227	3.4	0.0667	2.0	416.3	8.3	85.9
18-78	75	13081	2.3	18.9689	7.7	0.4910	7.9	0.0675	1.8	421.4	7.3	133.1
18-5	152	32095	1.8	17.6825	4.2	0.5673	4.4	0.0728	1.4	452.7	5.9	95.5
18-8	284	117014	7.8	17.8639	1.7	0.5663	2.0	0.0734	0.9	456.5	4.1	101.1
18-84	144	20792	3.5	17.4507	3.3	0.5811	3.4	0.0735	0.9	457.5	3.9	90.9
18-43	63	35171	1.4	16.9855	9.9	0.6043	10.9	0.0744	4.5	462.9	20.1	82.3
18-89	191	45201	4.8	14.8595	4.1	0.7417	4.8	0.0799	2.3	495.7	11.2	58.5
18-58	55	10891	0.7	17.6124	6.1	0.6771	6.2	0.0865	1.3	534.8	6.5	110.7
18-16	191	83377	1.1	16.9777	2.1	0.7084	2.1	0.0872	0.6	539.1	3.0	95.7
18-17	279	64320	3.3	16.4811	1.4	0.7696	1.5	0.0920	0.5	567.3	2.5	90.4
18-90	77	24986	1.4	15.0477	4.0	1.1701	4.2	0.1277	1.2	774.7	8.8	94.4
18-96	137	63286	2.8	14.3271	2.2	1.2781	2.9	0.1328	1.9	803.9	14.4	87.1
18-93	20	13350	0.6	14.3281	9.6	1.5137	9.7	0.1573	1.3	922.3	198.0	102.1
18-103	48	15685	1.3	14.2269	3.2	1.4497	4.1	0.1496	2.7	936.8	65.4	95.9
18-34	91	38093	2.1	14.1009	1.2	1.6369	1.5	0.1674	0.9	955.0	25.1	104.5
18-23	118	131175	7.1	14.0564	1.4	1.4957	1.8	0.1525	1.2	961.5	28.1	95.2
18-6	77	56291	1.1	13.9755	1.9	1.5742	2.2	0.1596	1.0	973.3	39.6	98.1
18-86	191	78568	2.8	13.9324	1.0	1.6273	2.2	0.1644	2.0	979.5	20.0	100.2
18-53	67	57679	2.5	13.9263	2.6	1.6535	2.7	0.1670	0.7	980.4	52.2	101.5
18-87	99	29570	1.0	13.8259	2.1	1.6512	2.7	0.1656	1.7	995.2	42.1	99.2
18-92	153	98483	5.7	13.7151	0.7	1.7381	1.1	0.1729	0.8	1011.5	14.2	101.6
18-19	91	81683	1.8	13.7141	2.3	1.7088	2.7	0.1700	1.4	1011.6	46.8	100.0
18-28	72	46642	2.2	13.7049	2.2	1.7084	2.4	0.1698	0.9	1013.0	44.9	99.8
18-32	83	94146	1.4	13.6972	1.6	1.7329	1.8	0.1721	0.9	1014.1	31.5	101.0
18-101	92	61948	1.8	13.6887	2.5	1.7237	2.8	0.1711	1.3	1015.4	50.4	100.3
18-46	21	22191	421.4	13.6848	9.8	1.7451	10.9	0.1732	4.9	1016.0	198.1	101.4
18-36	150	83434	6.3	13.6149	0.8	1.6165	1.5	0.1596	1.2	1026.4	16.1	93.0
18-12	159	59954	7.1	13.5929	1.1	1.7108	1.3	0.1687	0.7	1029.6	21.5	97.6
18-9	20	13397	3.0	13.5639	10.0	1.7458	10.3	0.1717	2.5	1033.9	202.6	98.8
18-63	177	91136	2.5	13.5385	1.4	1.7419	2.4	0.1710	2.0	1037.7	29.0	98.1

Grain No.	U (ppm)	$^{206}Pb/^{204}Pb$	U/Th	$^{206}Pb^{*}/^{207}Pb^{*}$	Error (±%)	$^{207}Pb^{*}/^{235}U^{*}$	Error (±%)	$^{206}Pb^{*}/^{238}U$	Error (±%)	Best Age (Ma)	Error (± Ma)	Concordance (%)
18-30	48	12178	1.9	13.5383	2.2	1.8076	2.2	0.1775	0.4	1037.7	44.4	101.5
18-48	111	37680	0.6	13.5310	1.7	1.7576	4.9	0.1725	4.6	1038.8	34.6	98.7
18-51	127	85230	1.5	13.5250	0.8	1.7466	1.3	0.1713	1.0	1039.7	16.7	98.0
18-60	25	22287	1.8	13.5166	4.7	1.7120	5.2	0.1678	2.2	1041.0	94.6	96.1
18-100	118	57812	3.2	13.5069	2.1	1.7213	2.3	0.1686	1.0	1042.4	42.0	96.4
18-33	82	37086	2.7	13.4835	2.2	1.8788	3.1	0.1837	2.2	1046.0	43.4	104.0
18-71	113	109625	1.9	13.4610	1.6	1.7705	3.1	0.1728	2.7	1049.3	32.7	97.9
18-4	84	74595	1.4	13.4197	2.5	1.7058	3.0	0.1660	1.6	1055.5	51.2	93.8
18-57	212	83966	2.2	13.4157	1.0	1.7702	1.1	0.1722	0.5	1056.1	20.5	97.0
18-56	36	15884	0.9	13.4150	5.0	1.6245	5.1	0.1581	1.4	1056.2	99.8	89.6
18-88	174	132239	2.2	13.4035	0.9	1.8207	1.2	0.1770	0.8	1058.0	18.4	99.3
18-102	44	26982	2.0	13.3982	7.3	1.7933	7.4	0.1743	1.3	1058.8	146.4	97.8
18-2	58	24217	1.6	13.3820	2.3	1.8830	2.5	0.1828	0.9	1061.2	47.0	102.0
18-25	119	52707	0.6	13.3509	1.6	1.8523	1.7	0.1794	0.6	1065.9	32.2	99.8
18-41	124	56686	2.6	13.3284	1.6	1.8176	2.5	0.1757	2.0	1069.3	31.2	97.6
18-99	104	47978	1.5	13.3198	1.3	1.8477	2.0	0.1785	1.5	1070.6	25.4	98.9
18-74	186	94663	2.3	13.3034	0.8	1.8591	1.5	0.1794	1.2	1073.0	16.4	99.1
18-10	64	45862	1.3	13.2822	3.7	1.8166	4.0	0.1750	1.6	1076.2	73.6	96.6
18-44	129	114957	1.9	13.2411	1.4	1.8929	2.6	0.1818	2.2	1082.4	28.7	99.5
18-24	98	27784	2.3	13.2386	3.5	1.8263	4.4	0.1754	2.7	1082.8	70.3	96.2
18-31	218	161755	6.5	13.2089	0.7	1.9129	3.8	0.1833	3.7	1087.3	14.9	99.8
18-98	82	50999	2.0	13.1835	2.2	1.8962	2.5	0.1813	1.4	1091.2	43.1	98.4
18-68	125	78868	2.5	13.0803	1.7	1.8968	2.8	0.1799	2.2	1106.9	34.9	96.4
18-83	38	37189	1.4	12.9557	3.0	2.0858	3.5	0.1960	1.7	1126.0	60.1	102.5
18-75	303	386008	26.1	12.9498	0.7	2.0160	1.8	0.1893	1.7	1126.9	13.3	99.2
18-50	94	40531	1.5	12.9277	2.3	2.1103	3.2	0.1979	2.3	1130.3	45.1	103.0
18-104	97	26591	3.0	12.9055	2.2	1.6144	3.0	0.1511	2.1	1133.7	42.9	80.0
18-64	303	52462	1.0	12.8850	0.7	2.0724	1.3	0.1937	1.1	1136.9	13.3	100.4
18-40	49	23863	1.8	12.8716	3.9	2.1099	4.4	0.1970	2.1	1139.0	77.0	101.8
18-67	30	23213	1.2	12.8588	2.7	2.0247	3.6	0.1888	2.3	1140.9	53.8	97.7
18-52	222	226777	1.1	12.7793	0.7	2.0308	1.6	0.1882	1.5	1153.3	14.6	96.4
18-47	265	141140	2.0	12.7233	0.6	2.0543	0.8	0.1896	0.5	1162.0	11.5	96.3
18-39	151	61238	1.8	12.6960	1.0	2.1313	1.3	0.1963	0.8	1166.2	19.9	99.1
18-97	286	63926	1.4	12.6902	0.5	2.0731	1.9	0.1908	1.8	1167.1	10.4	96.5
18-1	175	147179	1.8	12.6619	0.8	2.1393	1.0	0.1965	0.5	1171.6	16.1	98.7

Grain No.	U (ppm)	$^{206}Pb/^{204}Pb$	U/Th	$^{206}Pb^*/^{207}Pb^*$	Error (±%)	$^{207}Pb^*/^{235}U^*$	Error (±%)	$^{206}Pb^*/^{238}U$	Error (±%)	Best Age (Ma)	Error (± Ma)	Concordance (%)
18-38	47	18565	2.6	12.6532	2.3	2.1300	3.5	0.1955	2.7	1172.9	44.9	98.1
18-7	67	22929	1.8	12.6365	2.1	2.1301	2.6	0.1952	1.5	1175.6	41.7	97.8
18-26	85	36064	1.8	12.6345	1.7	2.2259	1.8	0.2040	0.6	1175.9	33.0	101.8
18-91	139	205774	2.6	12.6069	0.9	2.1413	1.1	0.1958	0.5	1180.2	18.4	97.7
18-55	171	7549	0.8	12.5761	2.2	2.0587	3.0	0.1878	2.1	1185.0	43.1	93.6
18-82	39	38601	1.7	12.4243	4.6	2.3282	5.0	0.2098	2.2	1209.0	89.8	101.6
18-105	56	49938	2.4	12.3623	4.2	2.0856	4.4	0.1870	1.4	1218.8	81.8	90.7
18-54	82	143824	1.3	12.3387	0.9	2.2166	2.9	0.1984	2.8	1222.5	18.2	95.4
18-35	375	401458	4.8	12.2662	0.5	2.4005	1.5	0.2136	1.4	1234.1	9.1	101.1
18-61	60	23399	5.9	12.2525	2.5	2.1948	2.9	0.1950	1.3	1236.3	49.8	92.9
18-3	30	18550	1.2	12.2118	6.2	2.2269	6.5	0.1972	2.0	1242.9	120.8	93.4
18-65	141	46504	1.3	11.9402	1.5	2.3481	2.2	0.2033	1.5	1286.8	29.3	92.7
18-14	209	49149	1.5	11.8447	2.0	2.4361	2.1	0.2093	0.6	1302.4	38.7	94.1
18-22	66	73133	1.3	11.7668	1.3	2.6759	1.7	0.2284	1.2	1315.2	24.7	100.8
18-77	68	51033	2.3	11.6650	1.5	2.7207	2.7	0.2302	2.2	1332.0	29.9	100.3
18-11	73	12905	1.2	11.6404	1.9	2.2415	3.3	0.1892	2.7	1336.1	36.9	83.6
18-18	140	115669	1.8	11.5040	0.6	2.6783	1.2	0.2235	1.0	1358.8	12.1	95.7
18-69	125	61690	1.9	11.4053	0.9	2.8811	1.1	0.2383	0.6	1375.4	18.2	100.2
18-73	54	36015	0.8	11.3863	1.9	2.9209	2.0	0.2412	0.7	1378.6	36.8	101.0
18-59	250	73405	1.4	11.3559	0.5	2.7967	0.8	0.2303	0.6	1383.8	9.9	96.6
18-45	57	45985	2.1	10.9193	1.6	3.1636	1.8	0.2505	0.8	1458.7	30.2	98.8
18-85	310	208579	1.5	10.8950	0.5	3.0754	0.8	0.2430	0.6	1462.9	9.2	95.9
18-94	134	78791	1.5	10.8505	1.0	3.2059	1.7	0.2523	1.4	1470.7	19.5	98.6
18-42	268	168606	4.7	10.3062	1.1	3.4602	2.5	0.2586	2.3	1567.8	20.3	94.6
18-76	53	47044	0.7	8.6482	0.8	5.5389	2.5	0.3474	2.4	1889.7	13.9	101.7
18-21	96	69713	0.9	8.4690	0.8	5.6497	1.0	0.3470	0.5	1927.3	15.1	99.6
18-29	131	210382	1.3	6.2907	0.4	10.0621	4.2	0.4591	4.1	2444.7	7.2	99.6
18-62	89	119428	1.1	5.3894	0.2	13.2752	0.7	0.5189	0.7	2703.1	4.1	99.7

SAMPLE 19- Citronelle, AL

Grain No.	U (ppm)	$^{206}Pb/^{204}Pb$	U/Th	$^{206}Pb^{*}/^{207}Pb^{*}$	Error (±%)	$^{207}Pb^{*}/^{235}U^{*}$	Error (±%)	$^{206}Pb^{*}/^{238}U$	Error (±%)	Best Age (Ma)	Error (± Ma)	Concordance (%)
19-36	354	5148	2.8	23.2638	21.2	0.0362	21.5	0.0061	3.7	39.3	1.5	NA
19-54	237	52264	1.1	18.3844	2.8	0.4707	3.0	0.0628	1.1	392.4	4.4	NA
19-23	109	14337	1.3	17.4534	1.8	0.5599	2.1	0.0709	1.1	441.4	4.8	87.8
19-10	198	37092	1.4	17.6200	2.0	0.5846	2.9	0.0747	2.1	464.4	9.3	96.4
19-73	95	21463	1.3	17.8200	2.4	0.5798	3.1	0.0749	1.8	465.8	8.3	101.9
19-52	148	235251	1.6	17.3401	3.3	0.6924	4.0	0.0871	2.3	538.2	11.9	104.1
19-78	27	6401	2.3	16.5898	10.6	0.7546	10.9	0.0908	2.3	560.3	12.3	91.3
19-83	228	79118	2.8	16.0916	1.9	0.8307	3.0	0.0969	2.3	596.5	13.2	87.8
19-70	73	23931	2.2	14.4144	2.2	1.4747	2.3	0.1542	0.5	909.9	45.9	101.6
19-75	53	26727	1.4	14.1581	4.1	1.6065	4.3	0.1650	1.1	946.8	84.2	104.0
19-29	28	28017	1.2	13.8578	6.9	1.7396	7.1	0.1748	1.8	990.5	139.8	104.9
19-85	65	29748	1.5	13.8341	2.9	1.6424	3.2	0.1648	1.2	994.0	59.8	98.9
19-5	109	48571	3.0	13.8123	1.6	1.7263	2.3	0.1729	1.6	997.2	33.3	103.1
19-58	171	143187	1.7	13.7666	1.4	1.6977	1.8	0.1695	1.2	1003.9	28.4	100.5
19-105	19	8175	1.6	13.7387	5.7	1.7671	7.5	0.1761	4.8	1008.0	116.5	103.7
19-34	42	19351	2.2	13.7066	4.8	1.7225	5.1	0.1712	1.7	1012.8	97.6	100.6
19-8	251	108194	1.7	13.6677	0.5	1.6569	1.4	0.1642	1.4	1018.5	9.3	96.2
19-93	66	26168	0.9	13.6438	1.3	1.7339	2.5	0.1716	2.2	1022.1	26.4	99.9
19-92	106	71280	2.4	13.6354	1.3	1.7174	2.2	0.1698	1.8	1023.3	26.8	98.8
19-33	108	80470	1.5	13.6293	1.4	1.8231	1.6	0.1802	0.7	1024.2	29.3	104.3
19-87	114	33270	3.8	13.6159	1.6	1.7112	2.2	0.1690	1.5	1026.2	32.0	98.1
19-86	235	130424	5.2	13.5874	0.8	1.7616	1.0	0.1736	0.6	1030.4	17.1	100.1
19-31	76	117213	2.6	13.5500	1.8	1.7436	1.9	0.1713	0.5	1036.0	36.0	98.4
19-47	139	112615	2.5	13.5484	1.1	1.6952	2.6	0.1666	2.3	1036.2	21.7	95.8
19-69	120	49954	2.0	13.5455	1.9	1.7983	2.0	0.1767	0.4	1036.7	38.9	101.2
19-59	134	71416	1.1	13.5336	1.6	1.7804	1.8	0.1748	0.9	1038.5	33.0	100.0
19-4	108	74115	3.2	13.4838	1.2	1.7666	1.7	0.1728	1.2	1045.9	24.0	98.2
19-66	107	49581	4.7	13.4832	1.3	1.7980	1.5	0.1758	0.7	1046.0	27.0	99.8
19-46	65	52341	2.1	13.4816	3.0	1.7945	3.2	0.1755	1.3	1046.3	60.4	99.6
19-40	300	235665	2.3	13.4804	0.6	1.8148	0.8	0.1774	0.6	1046.4	12.7	100.6
19-65	71	36039	1.3	13.4711	2.3	1.8363	3.6	0.1794	2.8	1047.8	47.2	101.5
19-72	52	38022	2.2	13.4622	4.6	1.7639	4.7	0.1722	0.8	1049.2	92.7	97.6

Grain No.	U (ppm)	$^{206}Pb/^{204}Pb$	U/Th	$^{206}Pb^*/^{207}Pb^*$	Error (±%)	$^{207}Pb^*/^{235}U^*$	Error (±%)	$^{206}Pb^*/^{238}U$	Error (±%)	Best Age (Ma)	Error (± Ma)	Concordance (%)
19-95	466	355613	5.4	13.4514	0.5	1.8116	0.8	0.1767	0.6	1050.8	11.0	99.8
19-56	79	56897	1.6	13.4496	1.0	1.8550	2.6	0.1809	2.4	1051.0	20.3	102.0
19-77	39	8319	2.6	13.4376	4.6	1.6041	6.0	0.1563	3.9	1052.9	92.0	88.9
19-12	735	23499	5.4	13.4292	0.9	1.7578	2.2	0.1712	2.0	1054.1	17.8	96.6
19-16	68	41890	2.5	13.3683	3.7	1.8128	4.6	0.1758	2.9	1063.3	73.7	98.2
19-55	67	29598	2.6	13.3418	2.4	1.8407	2.5	0.1781	0.7	1067.2	49.2	99.0
19-57	58	36845	2.5	13.3130	2.9	1.8279	3.2	0.1765	1.5	1071.6	57.5	97.8
19-79	18	3841	2.0	13.3102	8.6	1.7711	8.8	0.1710	2.0	1072.0	173.3	94.9
19-51	88	39044	1.5	13.3039	1.6	1.9015	1.9	0.1835	1.0	1073.0	32.6	101.2
19-62	78	43551	0.7	13.2961	2.7	1.8305	3.2	0.1765	1.7	1074.1	53.9	97.6
19-76	62	62559	2.6	13.2804	2.7	1.8643	3.0	0.1796	1.4	1076.5	54.4	98.9
19-2	604	182973	1.9	13.2587	0.3	1.9030	0.9	0.1830	0.8	1079.8	6.3	100.3
19-38	122	104475	2.2	13.2492	1.3	1.8326	2.2	0.1761	1.8	1081.2	26.4	96.7
19-1	109	44391	0.7	13.2163	1.2	1.9331	2.4	0.1853	2.1	1086.2	23.9	100.9
19-91	97	104265	2.2	13.1707	2.0	1.8813	2.4	0.1797	1.4	1093.1	40.4	97.5
19-71	81	43579	0.9	13.1670	1.7	1.9268	1.9	0.1840	0.8	1093.7	35.0	99.6
19-18	18	9288	2.2	13.1601	4.9	1.8463	6.7	0.1762	4.6	1094.8	97.8	95.6
19-21	84	53328	3.3	13.1385	1.1	1.7441	5.3	0.1662	5.2	1098.0	23.0	90.3
19-6	350	107271	6.1	13.1302	0.4	1.9466	1.6	0.1854	1.6	1099.3	8.9	99.7
19-9	133	2512	1.6	13.1228	1.9	1.7701	4.1	0.1685	3.6	1100.4	37.2	91.2
19-82	32	34931	1.6	13.0906	2.1	1.8147	3.0	0.1723	2.1	1105.3	42.3	92.7
19-89	28	15637	1.9	13.0807	7.0	1.8172	7.3	0.1724	1.9	1106.9	140.1	92.6
19-103	173	71621	3.2	13.0622	0.7	1.9899	3.5	0.1885	3.4	1109.6	13.7	100.3
19-90	46	27443	1.5	12.9471	2.7	2.0116	2.9	0.1889	1.0	1127.3	53.2	98.9
19-30	273	147824	2.9	12.9256	0.8	2.0922	2.2	0.1961	2.0	1130.6	16.4	102.1
19-11	241	156236	2.9	12.9233	0.5	2.0468	1.6	0.1918	1.6	1131.0	9.1	100.0
19-53	370	29507	6.5	12.9092	0.7	1.7718	2.1	0.1659	2.0	1133.1	14.9	87.3
19-20	535	201327	5.0	12.8868	0.5	2.0590	0.8	0.1924	0.6	1136.6	9.2	99.8
19-37	240	73998	4.6	12.8234	0.7	2.0425	1.3	0.1900	1.1	1146.4	14.7	97.8
19-60	49	67586	1.9	12.8223	3.3	2.1132	3.5	0.1965	1.2	1146.6	64.7	100.9
19-94	26	13667	1.8	12.8011	4.3	2.2157	4.6	0.2057	1.7	1149.9	86.1	104.9
19-15	74	34033	3.4	12.7238	2.1	2.1722	3.6	0.2005	2.9	1161.9	40.7	101.4
19-45	95	49897	0.6	12.7190	0.7	2.0784	2.5	0.1917	2.4	1162.6	13.8	97.3

Grain No.	U (ppm)	$^{206}Pb/^{204}Pb$	U/Th	$^{206}Pb^*/^{207}Pb^*$	Error (±%)	$^{207}Pb^*/^{235}U^*$	Error (±%)	$^{206}Pb^*/^{238}U$	Error (±%)	Best Age (Ma)	Error (± Ma)	Concordance (%)
19-61	573	29138	2.7	12.6720	0.4	2.0958	0.8	0.1926	0.8	1170.0	7.5	97.1
19-88	129	19544	2.8	12.6680	3.2	1.9428	4.5	0.1785	3.1	1170.6	63.6	90.4
19-48	346	137970	1.8	12.6679	0.5	2.1786	0.7	0.2002	0.4	1170.6	10.3	100.5
19-102	27	18517	0.8	12.6581	4.3	1.8944	4.7	0.1739	1.8	1172.2	85.4	88.2
19-32	77	68907	2.4	12.6060	2.4	2.2136	2.8	0.2024	1.4	1180.3	48.0	100.7
19-100	41	17321	1.9	12.5168	2.6	2.3636	3.6	0.2146	2.5	1194.3	50.7	104.9
19-101	66	29229	2.8	12.4653	1.8	2.2349	3.9	0.2020	3.4	1202.5	36.3	98.7
19-74	212	66534	4.0	12.4506	0.9	2.1085	1.9	0.1904	1.7	1204.8	18.2	93.3
19-19	138	78125	2.0	12.4427	1.1	2.1428	2.4	0.1934	2.1	1206.0	22.1	94.5
19-104	238	137738	1.9	12.4204	0.5	2.3175	4.5	0.2088	4.5	1209.6	9.2	101.0
19-7	86	65963	1.0	12.4033	1.3	2.3157	2.1	0.2083	1.6	1212.3	25.9	100.6
19-17	78	36673	2.6	12.3644	1.7	2.3820	2.5	0.2136	1.8	1218.4	33.8	102.4
19-80	127	130662	2.4	12.3271	0.8	2.3237	1.1	0.2077	0.7	1224.4	15.8	99.4
19-99	14	20680	1.2	12.0091	8.0	2.3726	8.7	0.2066	3.4	1275.5	157.0	94.9
19-24	85	49057	2.2	11.9894	1.5	2.5081	1.7	0.2181	0.9	1278.7	29.2	99.5
19-13	384	131844	3.6	11.7534	0.3	2.4509	2.6	0.2089	2.6	1317.4	5.2	92.8
19-14	176	87138	2.0	11.7532	1.0	2.7002	2.0	0.2302	1.8	1317.4	18.5	101.4
19-43	42	41368	5.0	11.7391	2.8	2.7823	4.0	0.2369	2.8	1319.8	53.6	103.8
19-35	39	49768	0.7	11.6510	2.0	2.8176	2.3	0.2381	1.3	1334.3	38.1	103.2
19-42	152	74604	3.0	11.5530	0.4	2.7929	0.7	0.2340	0.6	1350.6	7.4	100.4
19-49	33	22808	2.3	11.4130	2.8	2.9432	3.2	0.2436	1.6	1374.1	54.0	102.3
19-50	88	85834	1.8	11.3789	1.2	2.8582	1.5	0.2359	0.9	1379.9	22.1	98.9
19-84	251	191890	2.1	11.2103	0.7	2.7937	1.2	0.2271	1.0	1408.5	12.8	93.7
19-26	52	75179	1.6	10.7854	1.8	3.2988	2.2	0.2580	1.4	1482.1	33.4	99.8
19-3	267	19214	1.0	9.8510	0.5	4.0187	0.8	0.2871	0.5	1651.9	10.0	98.5
19-25	82	92732	1.0	9.2873	0.8	4.4743	3.0	0.3014	2.9	1760.4	14.5	96.5
19-22	85	64814	2.1	8.8009	0.8	5.2533	1.2	0.3353	0.9	1858.2	13.8	100.3
19-44	98	85282	1.6	8.2845	0.5	5.9594	0.6	0.3581	0.3	1966.7	9.2	100.3

SAMPLE 20- Alum Bluff, FL

Grain No.	U (ppm)	$^{206}Pb/^{204}Pb$	U/Th	$^{206}Pb^*/^{207}Pb^*$	Error (±%)	$^{207}Pb^*/^{235}U^*$	Error (±%)	$^{206}Pb^*/^{238}U$	Error (±%)	Best Age (Ma)	Error (± Ma)	Concordance (%)
20-52	208	64475	0.9	19.0305	4.8	0.3684	4.9	0.0508	0.9	319.7	2.7	NA
20-36	294	32529	3.4	18.7735	2.2	0.3826	2.3	0.0521	0.8	327.3	2.6	NA
20-77	213	34737	14.5	18.8663	2.3	0.4009	2.4	0.0549	0.8	344.3	2.6	NA
20-22	306	4439	1.7	17.9725	2.0	0.4315	4.7	0.0562	4.2	352.8	14.5	NA
20-56	248	45082	7.3	18.5329	2.4	0.4275	2.7	0.0575	1.3	360.1	4.4	NA
20-24	97	9670	1.0	18.6471	5.0	0.4371	5.7	0.0591	2.8	370.3	10.0	NA
20-80	245	43805	8.6	18.4872	2.2	0.4813	2.4	0.0645	1.1	403.1	4.3	107.5
20-46	84	16074	3.2	18.2202	5.1	0.5002	5.5	0.0661	2.1	412.6	8.3	101.3
20-57	153	72029	0.9	17.6538	5.8	0.5259	5.9	0.0673	1.0	420.1	4.1	87.9
20-47	87	11763	1.1	18.6510	8.7	0.5112	8.8	0.0691	1.5	431.0	6.2	121.4
20-48	325	37654	0.5	17.6978	1.8	0.5394	2.5	0.0692	1.8	431.6	7.5	91.4
20-9	151	43751	0.6	18.4594	3.6	0.5180	4.0	0.0693	1.7	432.2	7.2	114.3
20-21	56	26370	0.8	18.6960	12.3	0.5124	12.6	0.0695	2.9	433.0	12.3	123.9
20-94	412	138471	0.8	17.9781	0.7	0.5357	1.0	0.0698	0.8	435.2	3.4	99.5
20-96	93	19982	2.3	19.0448	6.0	0.5181	6.4	0.0716	2.5	445.6	10.6	144.9
20-64	54	13771	0.8	18.8071	9.9	0.5275	10.0	0.0720	1.5	447.9	6.6	133.3
20-66	114	45310	1.4	18.1072	5.8	0.5786	5.9	0.0760	0.8	472.1	3.6	112.0
20-61	56	21954	3.6	14.2279	3.2	1.5454	3.5	0.1595	1.3	936.7	66.3	101.8
20-76	22	8216	1.0	14.0979	9.7	1.5768	9.9	0.1612	2.1	955.5	198.0	100.8
20-15	77	45758	1.9	14.0525	2.7	1.5089	4.2	0.1538	3.2	962.1	55.4	95.8
20-63	293	157218	2.0	14.0408	0.7	1.4775	1.3	0.1505	1.0	963.8	14.6	93.7
20-7	33	12285	1.0	14.0341	5.3	1.5679	5.5	0.1596	1.3	964.8	109.0	98.9
20-8	155	4034	2.3	13.9644	3.6	1.4832	3.7	0.1502	0.9	974.9	73.1	92.5
20-40	101	61310	2.3	13.9352	1.8	1.5643	2.5	0.1581	1.8	979.1	35.7	96.6
20-104	363	82973	10.0	13.9057	0.6	1.5607	0.9	0.1574	0.6	983.5	12.5	95.8
20-32	119	82175	2.2	13.8801	1.6	1.4737	2.1	0.1484	1.5	987.2	31.7	90.3
20-11	248	82832	4.0	13.8483	0.8	1.5837	3.4	0.1591	3.3	991.9	15.6	95.9
20-13	331	128803	3.7	13.7846	0.8	1.5363	1.5	0.1536	1.3	1001.2	15.3	92.0
20-105	174	126020	1.9	13.7474	1.9	1.6573	2.1	0.1652	1.0	1006.7	37.9	97.9
20-72	1024	317842	15.7	13.7441	0.4	1.5323	1.2	0.1527	1.1	1007.2	8.7	91.0
20-98	46	24496	1.0	13.7292	2.8	1.7638	3.2	0.1756	1.6	1009.4	57.2	103.3
20-12	1289	134670	16.8	13.7227	0.3	1.5874	1.3	0.1580	1.3	1010.4	6.3	93.6

Grain No.	U (ppm)	$^{206}Pb/^{204}Pb$	U/Th	$^{206}Pb^{*}/^{207}Pb^{*}$	Error (±%)	$^{207}Pb^{*}/^{235}U^{*}$	Error (±%)	$^{206}Pb^{*}/^{238}U$	Error (±%)	Best Age (Ma)	Error (± Ma)	Concordance (%)
20-93	552	554483	2.2	13.7021	0.3	1.6591	0.8	0.1649	0.7	1013.4	7.1	97.1
20-95	154	45418	2.4	13.7014	1.1	1.6752	2.0	0.1665	1.7	1013.5	22.7	97.9
20-34	293	106778	2.7	13.6700	0.8	1.6869	1.5	0.1672	1.2	1018.2	16.2	97.9
20-60	434	470936	3.4	13.6568	0.3	1.6750	1.1	0.1659	1.1	1020.1	6.0	97.0
20-30	61	27964	1.5	13.6561	2.4	1.7202	2.9	0.1704	1.6	1020.2	49.2	99.4
20-84	74	38055	1.0	13.6553	2.6	1.5233	5.7	0.1509	5.1	1020.4	52.9	88.8
20-39	36	20477	1.5	13.6428	4.5	1.8228	4.7	0.1804	1.4	1022.2	91.6	104.6
20-5	117	70262	1.6	13.6383	1.4	1.6898	2.2	0.1672	1.6	1022.9	28.9	97.4
20-29	140	45575	1.9	13.6364	1.3	1.7017	2.8	0.1683	2.5	1023.2	27.1	98.0
20-67	124	48706	1.4	13.6293	1.1	1.7575	1.8	0.1737	1.5	1024.2	21.7	100.8
20-91	156	62677	2.7	13.6235	1.1	1.7439	1.7	0.1723	1.3	1025.1	22.0	100.0
20-1	101	87921	4.1	13.6098	2.3	1.6592	2.6	0.1638	1.1	1027.1	47.2	95.2
20-81	121	57516	2.5	13.6095	1.0	1.7176	1.6	0.1695	1.2	1027.2	19.8	98.3
20-55	30	36182	1.0	13.6064	6.4	1.6989	6.6	0.1677	1.3	1027.6	130.1	97.2
20-88	70	32461	1.2	13.5988	2.1	1.7604	2.6	0.1736	1.5	1028.7	41.8	100.3
20-4	124	33588	2.8	13.5872	2.0	1.5302	3.7	0.1508	3.1	1030.5	39.7	87.9
20-89	268	124514	6.3	13.5759	0.8	1.7464	2.1	0.1720	1.9	1032.2	15.8	99.1
20-78	131	62929	2.0	13.5705	0.9	1.6930	2.0	0.1666	1.7	1032.9	19.1	96.2
20-45	150	84131	1.1	13.5503	1.1	1.8132	1.7	0.1782	1.3	1036.0	22.4	102.0
20-79	131	87629	2.2	13.5465	1.1	1.6901	1.6	0.1661	1.1	1036.5	22.8	95.5
20-70	139	76222	1.8	13.5325	1.0	1.7419	1.8	0.1710	1.4	1038.6	20.4	98.0
20-68	408	244152	5.3	13.5292	0.8	1.7784	1.0	0.1745	0.7	1039.1	15.8	99.8
20-73	342	182671	3.5	13.5178	0.5	1.6815	1.1	0.1649	1.0	1040.8	10.1	94.5
20-6	60	41534	1.8	13.4954	2.9	1.7586	3.1	0.1721	1.1	1044.2	59.0	98.1
20-44	60	43981	1.1	13.4729	2.5	1.8611	2.7	0.1819	1.1	1047.6	50.5	102.8
20-103	207	74583	3.4	13.4546	0.9	1.6610	1.6	0.1621	1.3	1050.3	18.7	92.2
20-71	75	27209	2.1	13.4510	1.4	1.7284	2.1	0.1686	1.6	1050.8	27.3	95.6
20-14	87	39809	2.5	13.4385	2.1	1.6986	3.1	0.1656	2.2	1052.7	43.0	93.8
20-42	207	173504	2.4	13.4081	0.4	1.7881	1.9	0.1739	1.8	1057.3	8.3	97.7
20-25	47	23706	0.9	13.4045	3.6	1.8192	4.8	0.1769	3.2	1057.8	73.5	99.2
20-75	235	132650	3.2	13.3923	0.7	1.7553	2.5	0.1705	2.4	1059.7	14.3	95.8
20-50	32	14116	0.9	13.3682	4.3	1.7603	4.5	0.1707	1.4	1063.3	86.2	95.5
20-35	140	104506	3.6	13.3601	0.6	1.7807	2.3	0.1725	2.2	1064.5	12.5	96.4

Grain No.	U (ppm)	$^{206}Pb/^{204}Pb$	U/Th	$^{206}Pb^*/^{207}Pb^*$	Error (±%)	$^{207}Pb^*/^{235}U^*$	Error (±%)	$^{206}Pb^*/^{238}U$	Error (±%)	Best Age (Ma)	Error (± Ma)	Concordance (%)
20-43	36	17636	1.0	13.3159	4.3	1.8963	4.5	0.1831	1.5	1071.1	85.5	101.2
20-23	35	14138	1.0	13.2486	4.2	1.8596	5.4	0.1787	3.5	1081.3	83.3	98.0
20-102	25	17158	0.8	13.1107	5.9	1.7253	6.2	0.1641	1.8	1102.3	118.0	88.8
20-18	59	60673	2.5	13.0141	1.8	2.0734	2.2	0.1957	1.4	1117.1	34.9	103.1
20-38	46	35435	1.1	12.9791	2.3	2.0478	2.6	0.1928	1.3	1122.4	46.0	101.2
20-17	115	216375	2.9	12.9471	1.2	1.9699	3.0	0.1850	2.7	1127.3	23.6	97.1
20-19	251	83835	2.5	12.9439	0.7	2.0223	3.9	0.1898	3.8	1127.8	13.2	99.4
20-49	632	283164	1.8	12.9025	0.7	2.0533	3.9	0.1921	3.8	1134.2	13.0	99.9
20-59	20	15187	1.0	12.8958	6.6	1.7538	7.6	0.1640	3.7	1135.2	132.3	86.3
20-87	124	46655	2.1	12.8482	1.3	2.0680	1.7	0.1927	1.1	1142.6	26.0	99.4
20-53	218	112703	2.0	12.8307	0.7	2.0642	2.2	0.1921	2.0	1145.3	14.7	98.9
20-69	104	38094	1.0	12.7946	1.2	2.1083	1.4	0.1956	0.8	1150.9	23.3	100.1
20-51	142	216599	3.1	12.7786	1.1	2.0875	2.0	0.1935	1.6	1153.4	21.4	98.9
20-28	249	195763	1.5	12.7290	0.4	2.1227	1.7	0.1960	1.6	1161.1	8.9	99.4
20-31	486	224602	2.3	12.7177	0.2	2.1102	0.7	0.1946	0.6	1162.8	4.8	98.6
20-54	376	125581	2.6	12.7107	0.3	2.0980	1.3	0.1934	1.2	1163.9	6.0	97.9
20-82	134	40634	1.9	12.6900	1.2	1.9868	1.9	0.1829	1.5	1167.2	24.1	92.8
20-65	510	35506	1.3	12.6874	1.2	2.1195	1.8	0.1950	1.3	1167.6	23.5	98.4
20-100	197	368570	1.3	12.5944	0.8	2.1949	1.5	0.2005	1.2	1182.1	16.3	99.6
20-37	168	72322	2.8	12.5436	0.6	2.1775	2.0	0.1981	1.9	1190.1	12.2	97.9
20-101	133	24332	1.6	12.3213	0.7	2.2420	2.1	0.2004	1.9	1225.3	13.0	96.1
20-83	144	137327	2.3	12.1895	1.0	2.3637	2.1	0.2090	1.8	1246.4	19.1	98.1
20-97	28	24805	1.2	12.0050	4.6	2.3845	4.8	0.2076	1.0	1276.2	90.5	95.3
20-20	53	31904	1.1	11.8583	2.6	2.5978	4.8	0.2234	4.1	1300.1	50.0	100.0
20-85	118	159764	4.2	11.3884	0.5	2.6831	0.9	0.2216	0.7	1378.3	9.5	93.6
20-41	27	19493	2.4	10.8437	3.5	3.3247	4.4	0.2615	2.6	1471.9	66.7	101.7
20-92	305	220375	1.3	9.7506	0.3	3.7324	1.8	0.2639	1.8	1670.9	5.2	90.4

APPENDIX II

CONCORDIA ($^{206}Pb/^{238}U$ vs. $^{207}Pb/^{235}U$) PLOTS OF DETRITAL ZIRCON SAMPLES

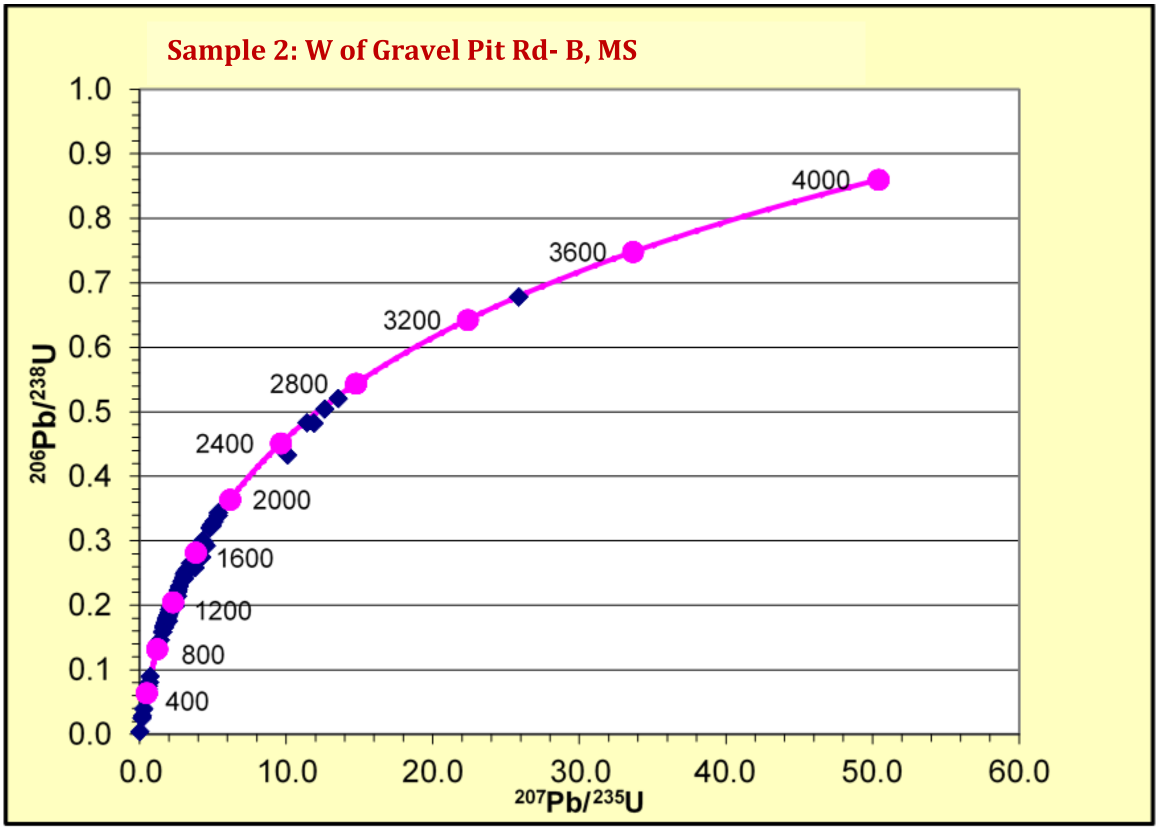
Sample 2: W of Gravel Pit Rd- B, MS
4000
3600
3200
2800
2400
2000
1600
1200
800
400
1.0
0.9
0.8
0.7
0.6
0.5
0.4
0.3
0.2
0.1
0.0
0.0
10.0
20.0
30.0
40.0
50.0
60.0
206Pb/238U
207Pb/235U

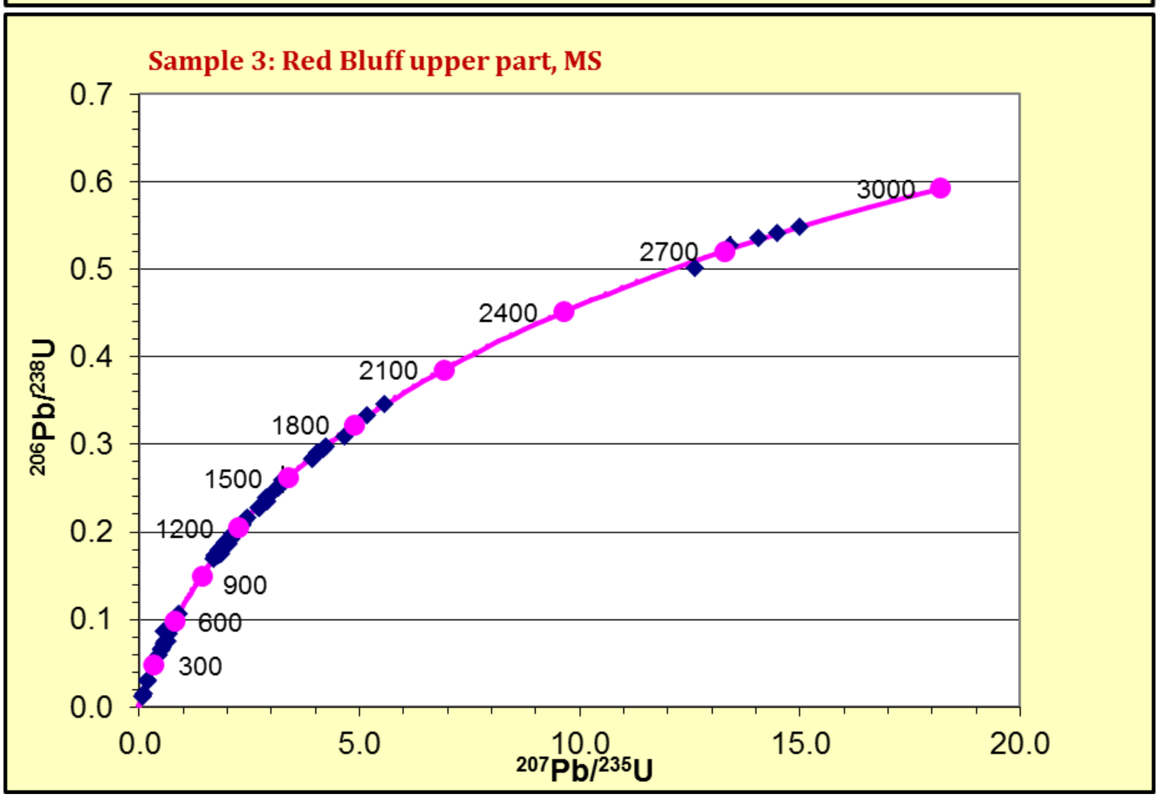
Sample 3: Red Bluff upper part, MS
3000
2700
2400
2100
1800
1500
1200
900
600
300
0.7
0.6
0.5
0.4
0.3
0.2
0.1
0.0
0.0
5.0
10.0
15.0
20.0
206Pb/238U
207Pb/235U

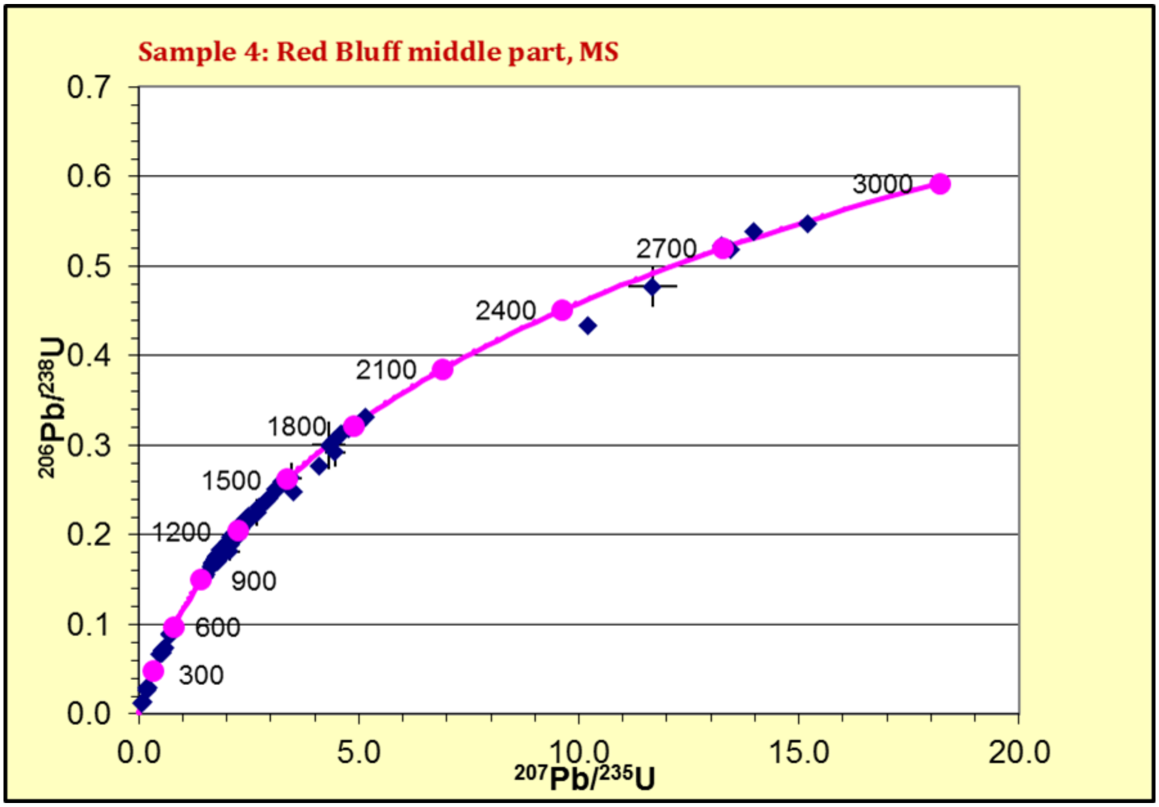
Sample 4: Red Bluff middle part, MS
0.7
0.6
0.5
0.4
0.3
0.2
0.1
0.0
$^{206}Pb/^{238}U$
0.0
5.0
10.0
15.0
20.0
$^{207}Pb/^{235}U$
300
600
900
1200
1500
1800
2100
2400
2700
3000

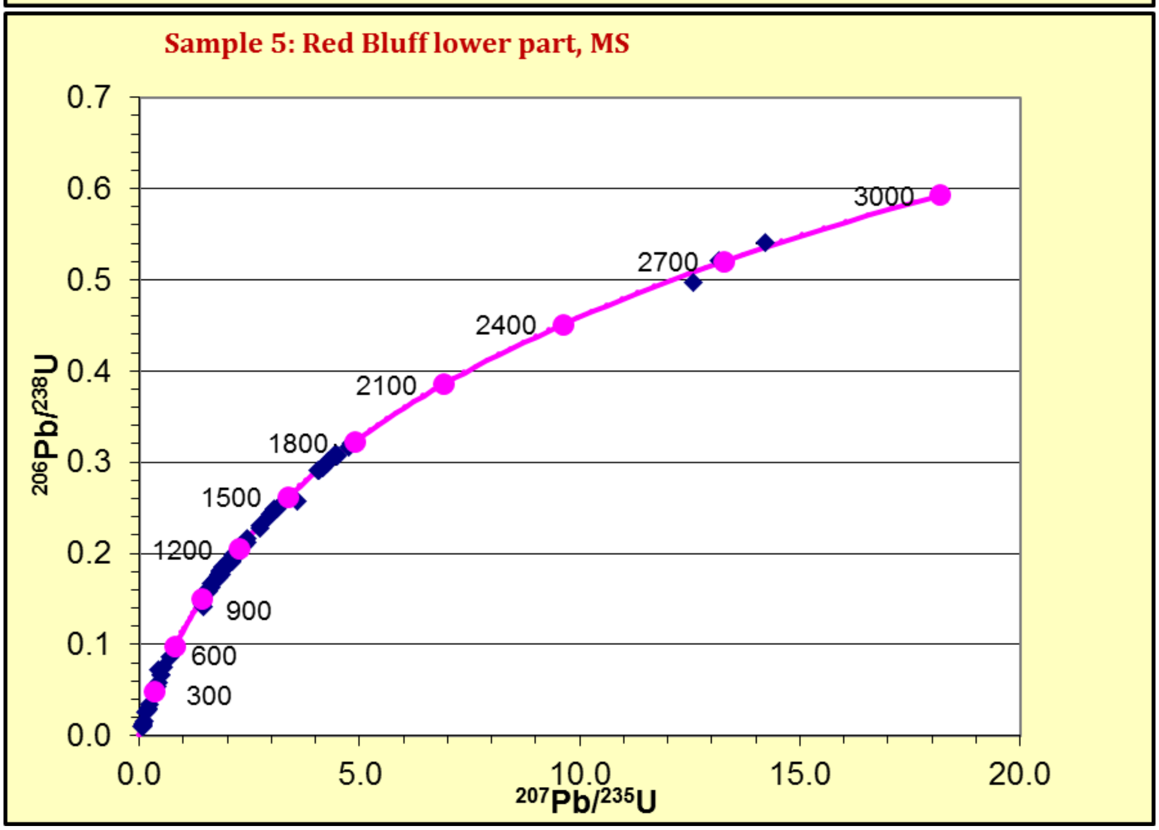
Sample 5: Red Bluff lower part, MS
0.7
0.6
0.5
0.4
0.3
0.2
0.1
0.0
$^{206}Pb/^{238}U$
0.0
5.0
10.0
15.0
20.0
$^{207}Pb/^{235}U$
300
600
900
1200
1500
1800
2100
2400
2700
3000

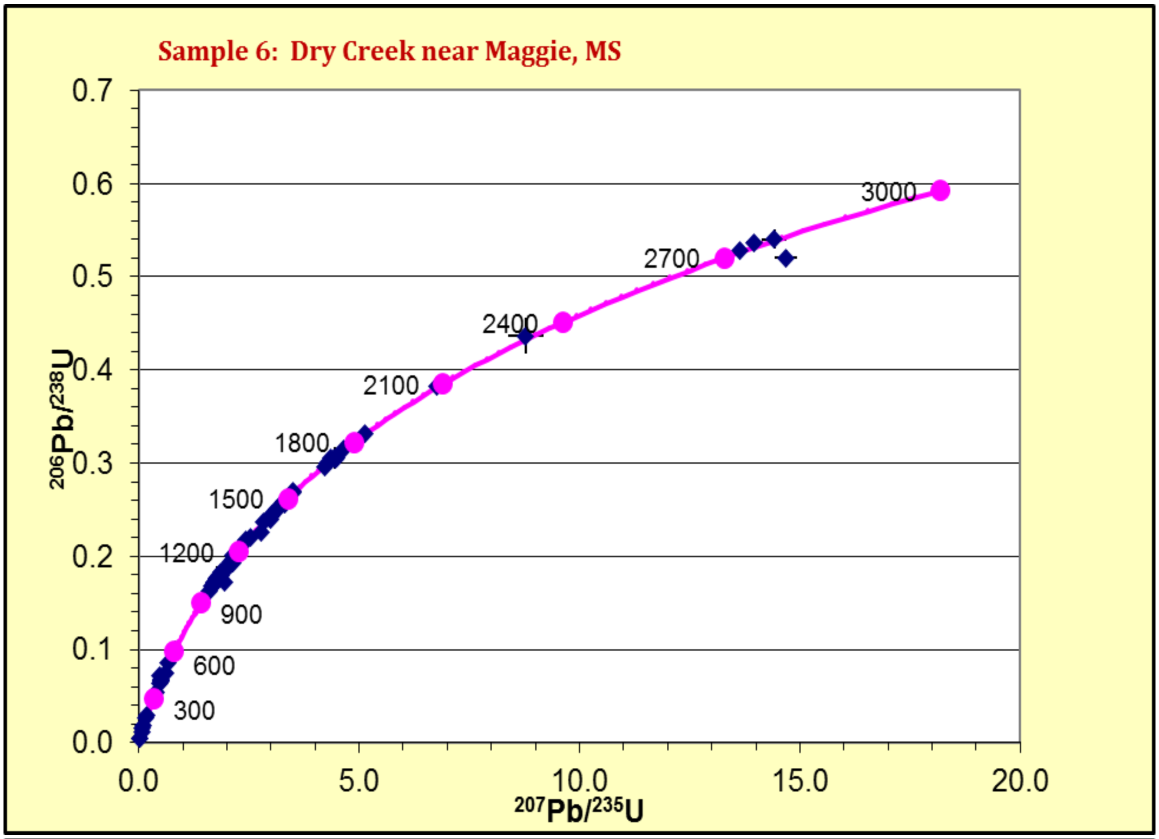
Sample 6: Dry Creek near Maggie, MS
0.7
0.6
0.5
0.4
0.3
0.2
0.1
0.0
^{206}Pb/^{238}U
3000
2700
2400
2100
1800
1500
1200
900
600
300
0.0
5.0
10.0
15.0
20.0
^{207}Pb/^{235}U

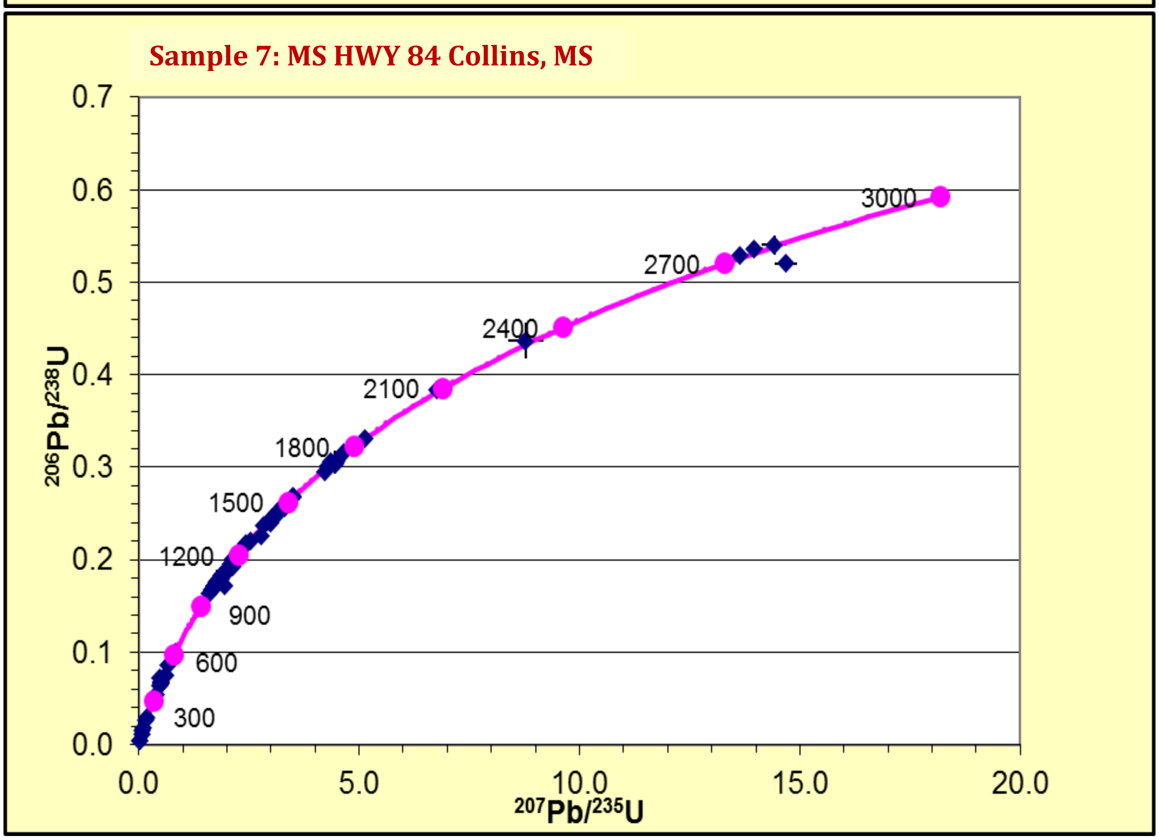
Sample 7: MS HWY 84 Collins, MS
0.7
0.6
0.5
0.4
0.3
0.2
0.1
0.0
^{206}Pb/^{238}U
3000
2700
2400
2100
1800
1500
1200
900
600
300
0.0
5.0
10.0
15.0
20.0
^{207}Pb/^{235}U

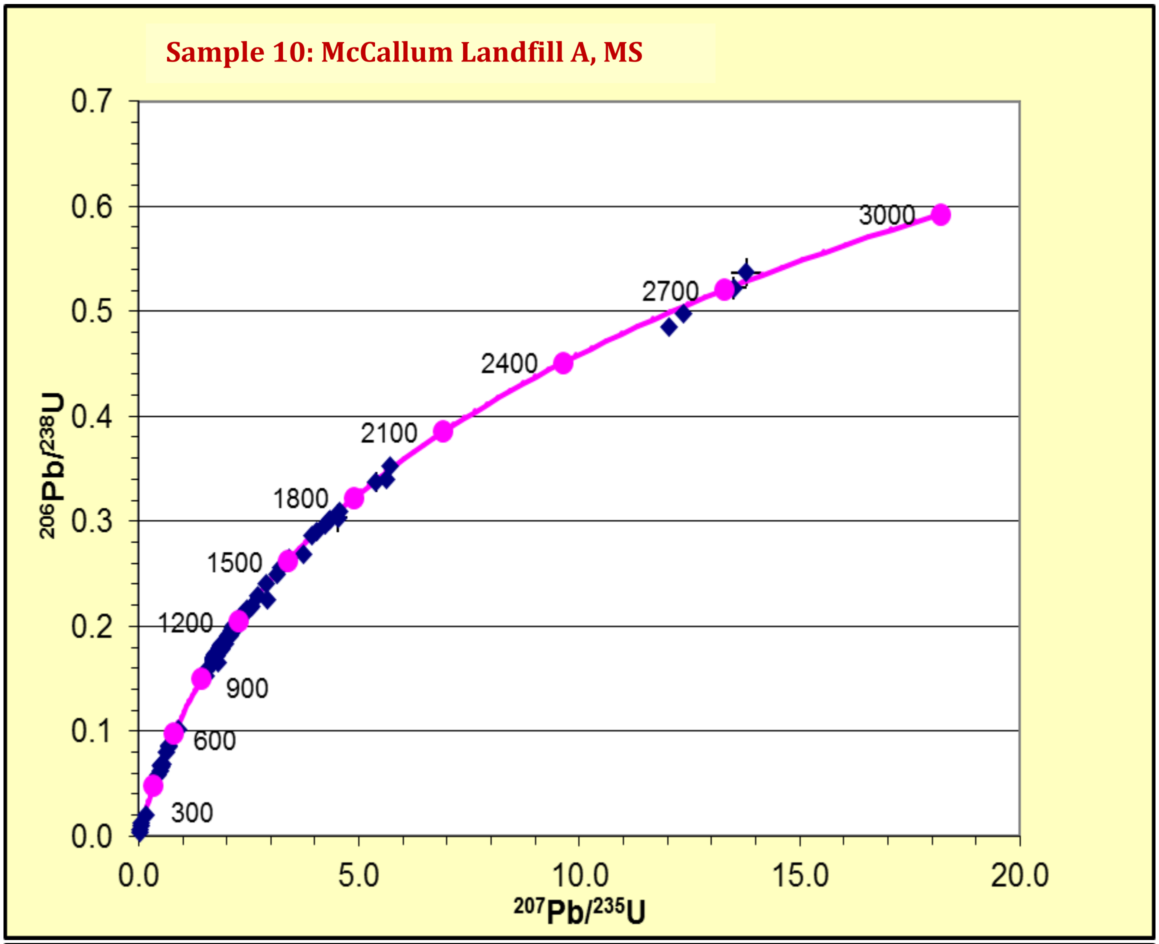
Sample 10: McCallum Landfill A, MS
0.7
0.6
0.5
0.4
0.3
0.2
0.1
0.0
$^{206}Pb/^{238}U$
3000
2700
2400
2100
1800
1500
1200
900
600
300
0.0
5.0
10.0
15.0
20.0
$^{207}Pb/^{235}U$

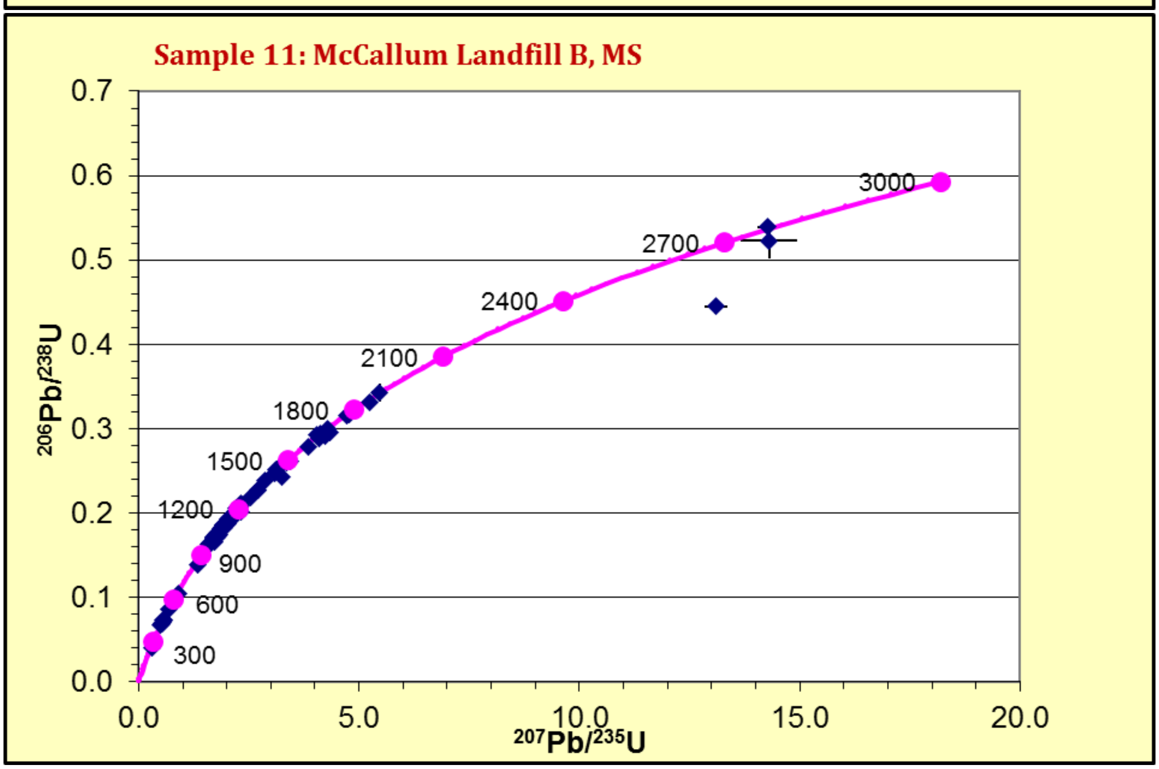
Sample 11: McCallum Landfill B, MS
0.7
0.6
0.5
0.4
0.3
0.2
0.1
0.0
$^{206}Pb/^{238}U$
3000
2700
2400
2100
1800
1500
1200
900
600
300
0.0
5.0
10.0
15.0
20.0
$^{207}Pb/^{235}U$

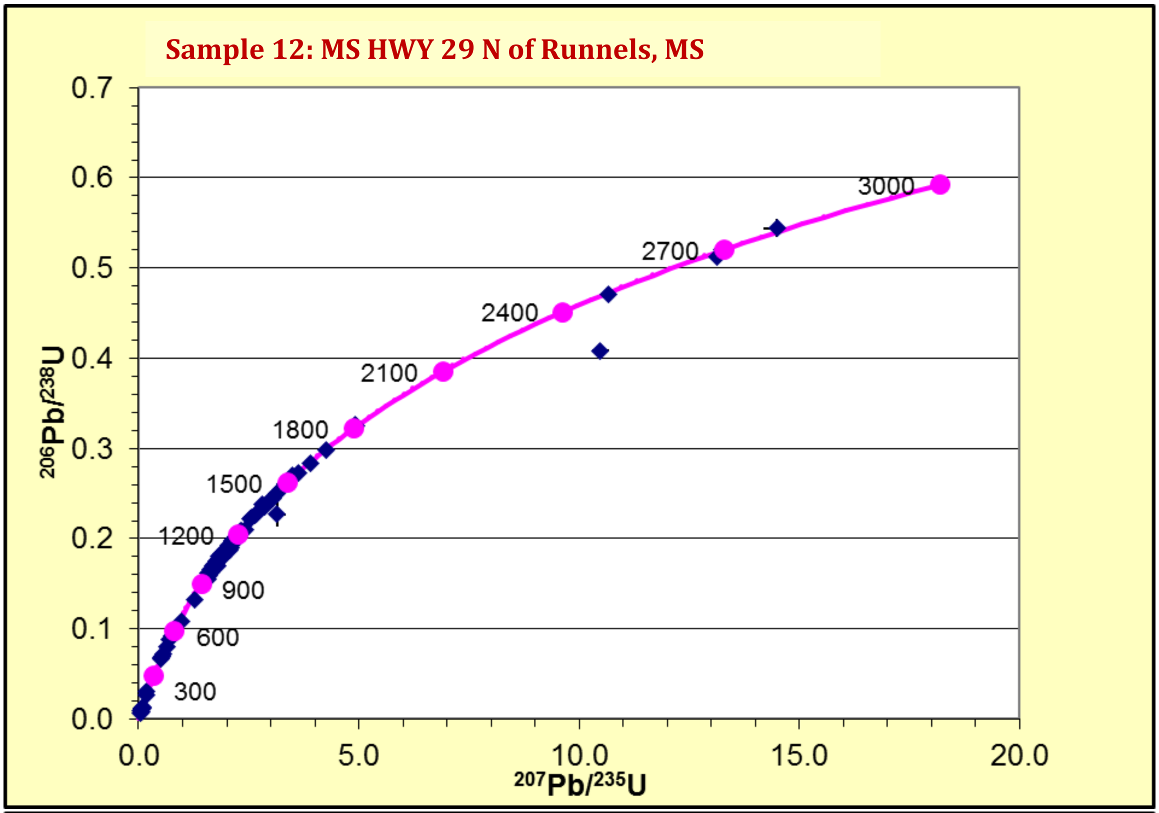
Sample 12: MS HWY 29 N of Runnels, MS
0.7
0.6
0.5
0.4
0.3
0.2
0.1
0.0
$^{206}Pb/^{238}U$
3000
2700
2400
2100
1800
1500
1200
900
600
300
0.0
5.0
10.0
15.0
20.0
$^{207}Pb/^{235}U$

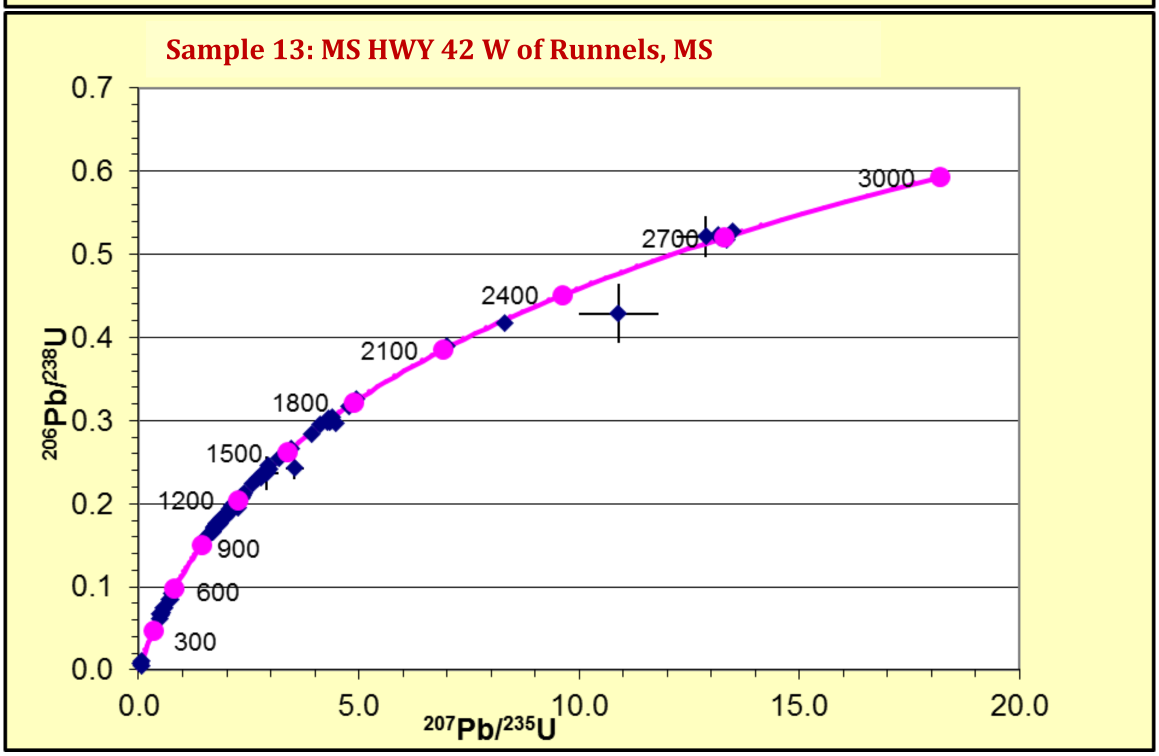
Sample 13: MS HWY 42 W of Runnels, MS
0.7
0.6
0.5
0.4
0.3
0.2
0.1
0.0
$^{206}Pb/^{238}U$
3000
2700
2400
2100
1800
1500
1200
900
600
300
0.0
5.0
10.0
15.0
20.0
$^{207}Pb/^{235}U$

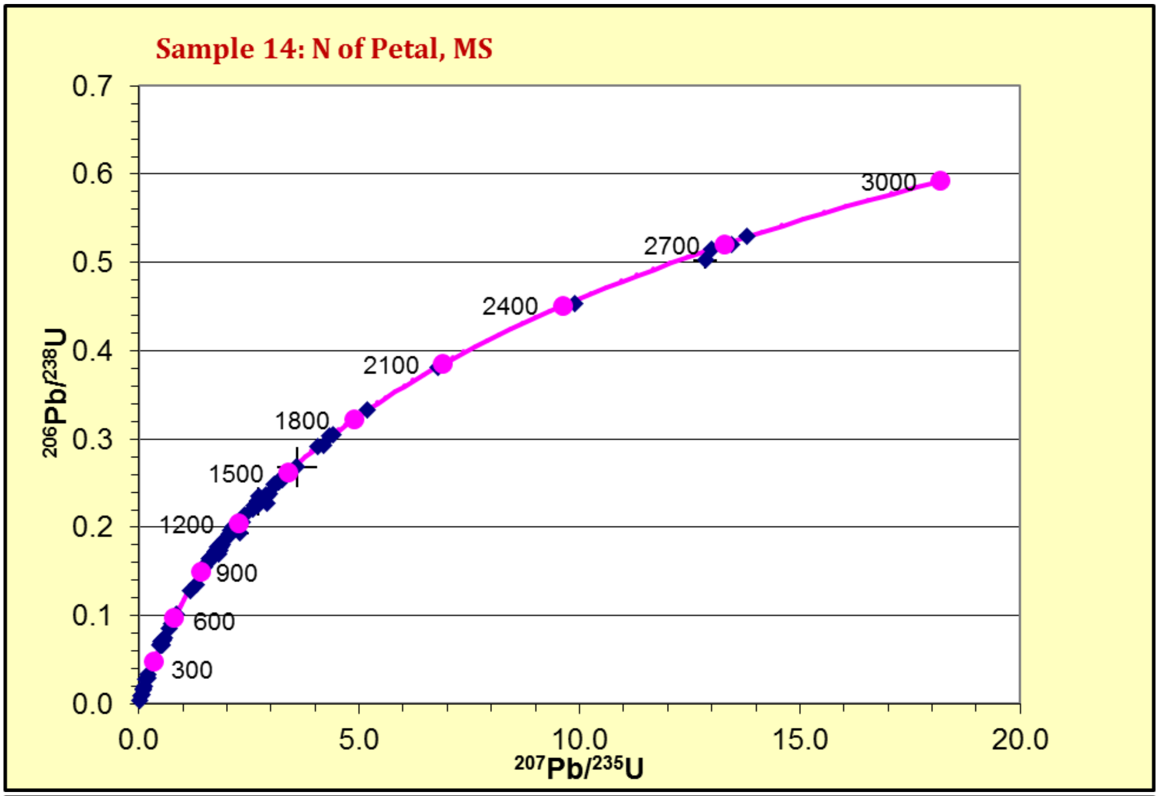
Sample 14: N of Petal, MS
0.7
0.6
0.5
0.4
0.3
0.2
0.1
0.0
206Pb/238U
3000
2700
2400
2100
1800
1500
1200
900
600
300
0.0
5.0
10.0
15.0
20.0
207Pb/235U

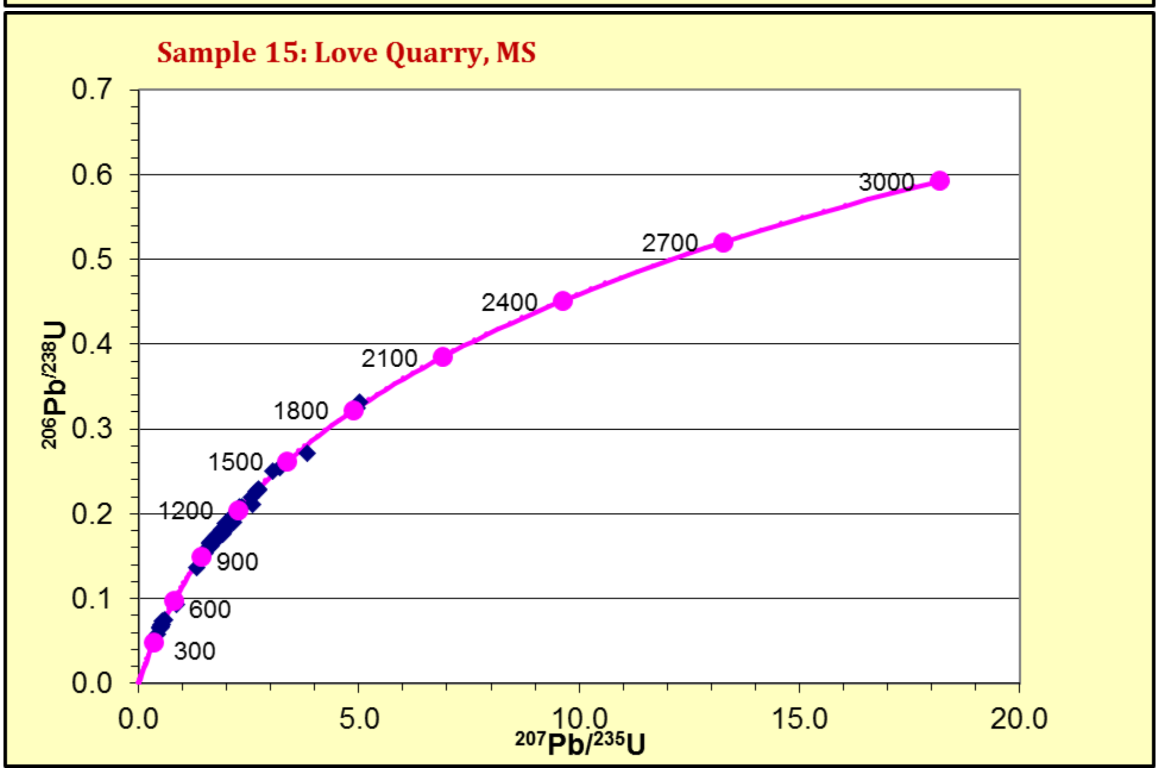
Sample 15: Love Quarry, MS
0.7
0.6
0.5
0.4
0.3
0.2
0.1
0.0
206Pb/238U
3000
2700
2400
2100
1800
1500
1200
900
600
300
0.0
5.0
10.0
15.0
20.0
207Pb/235U

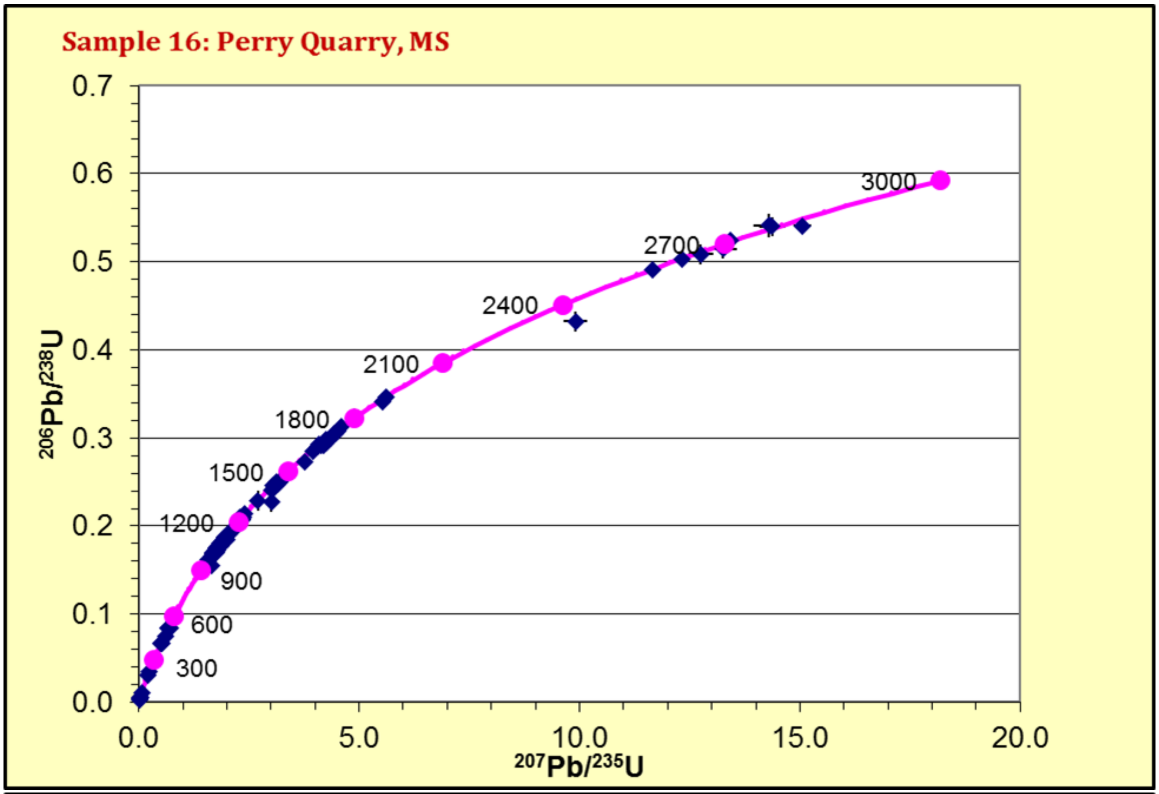
Sample 16: Perry Quarry, MS
0.7
0.6
0.5
0.4
0.3
0.2
0.1
0.0
3000
2700
2400
2100
1800
1500
1200
900
600
300
0.0
5.0
10.0
15.0
20.0
206Pb/238U
207Pb/235U

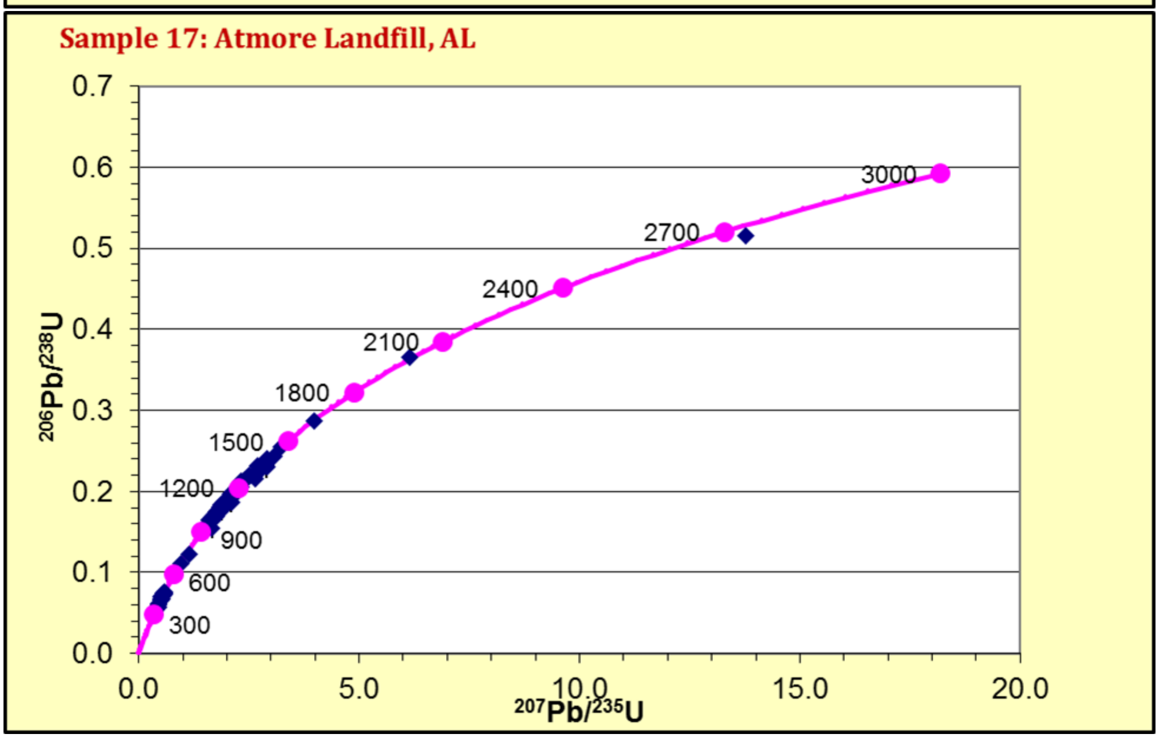
Sample 17: Atmore Landfill, AL
0.7
0.6
0.5
0.4
0.3
0.2
0.1
0.0
3000
2700
2400
2100
1800
1500
1200
900
600
300
0.0
5.0
10.0
15.0
20.0
206Pb/238U
207Pb/235U

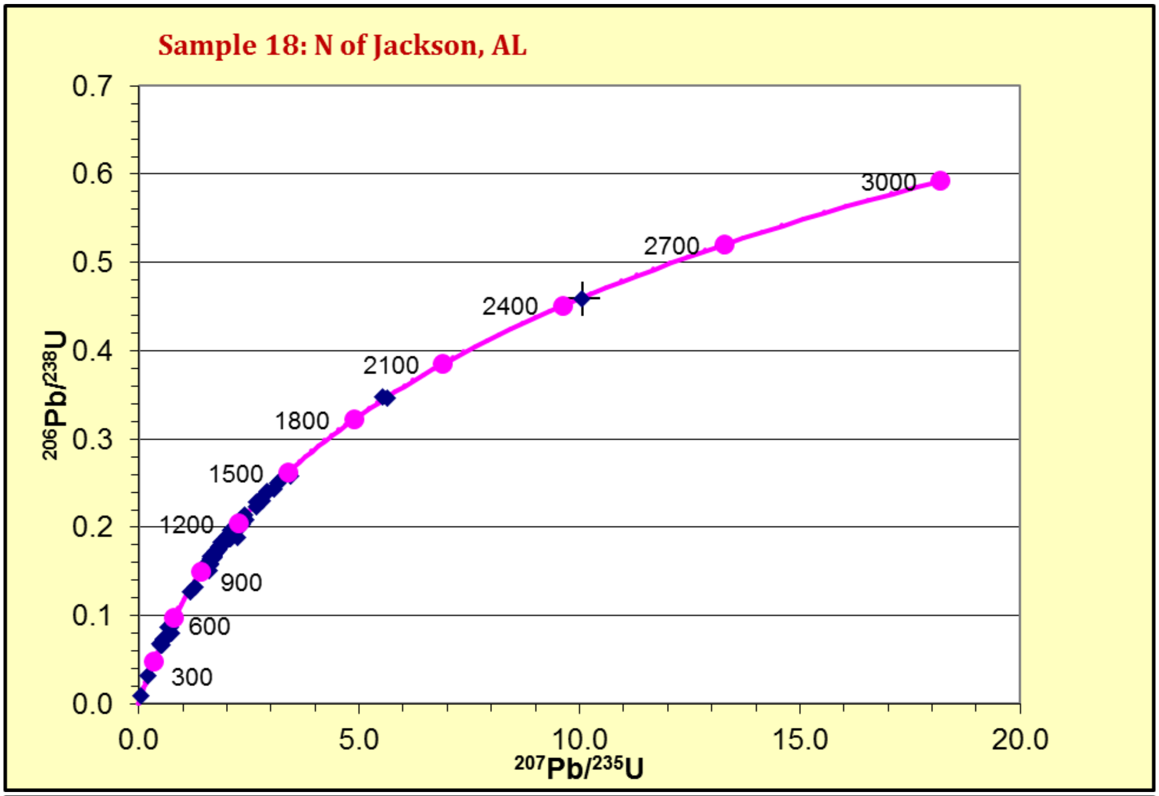
Sample 18: N of Jackson, AL
0.7
0.6
0.5
0.4
0.3
0.2
0.1
0.0
0.0
5.0
10.0
15.0
20.0
206Pb/238U
207Pb/235U
3000
2700
2400
2100
1800
1500
1200
900
600
300

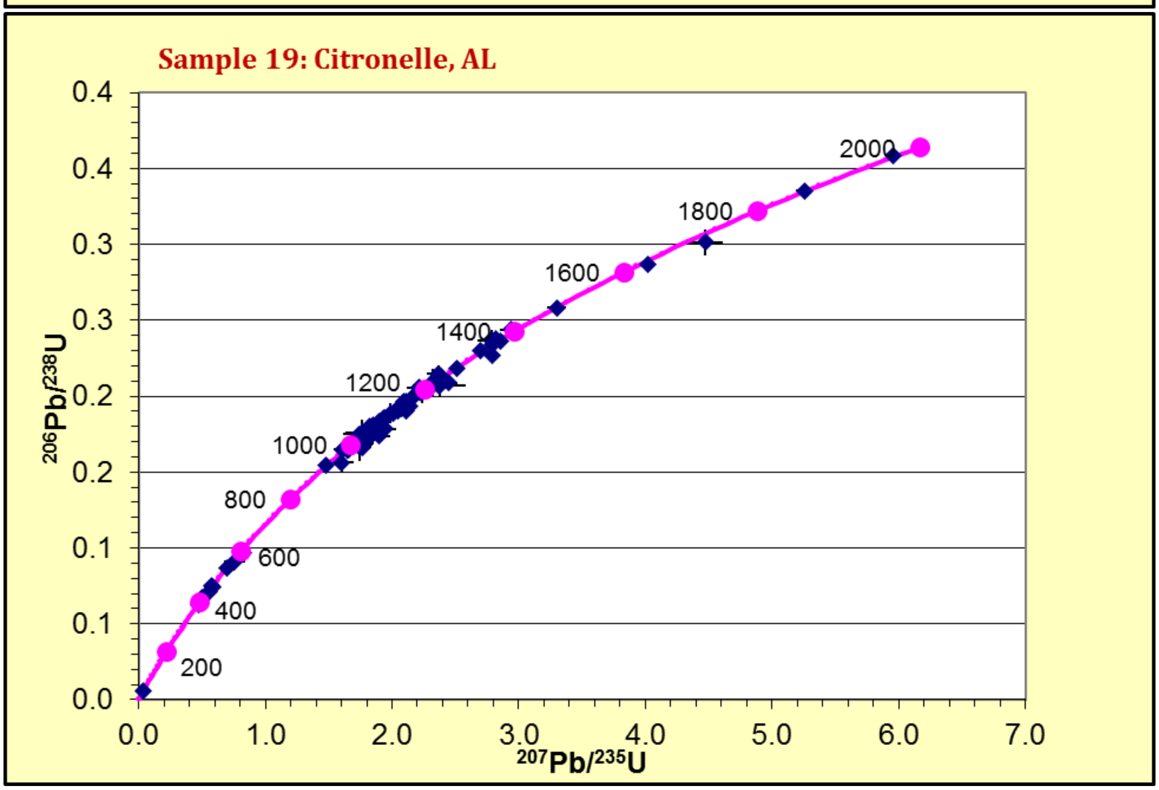
Sample 19: Citronelle, AL
0.4
0.4
0.3
0.3
0.2
0.2
0.1
0.1
0.0
0.0
1.0
2.0
3.0
4.0
5.0
6.0
7.0
206Pb/238U
207Pb/235U
2000
1800
1600
1400
1200
1000
800
600
400
200

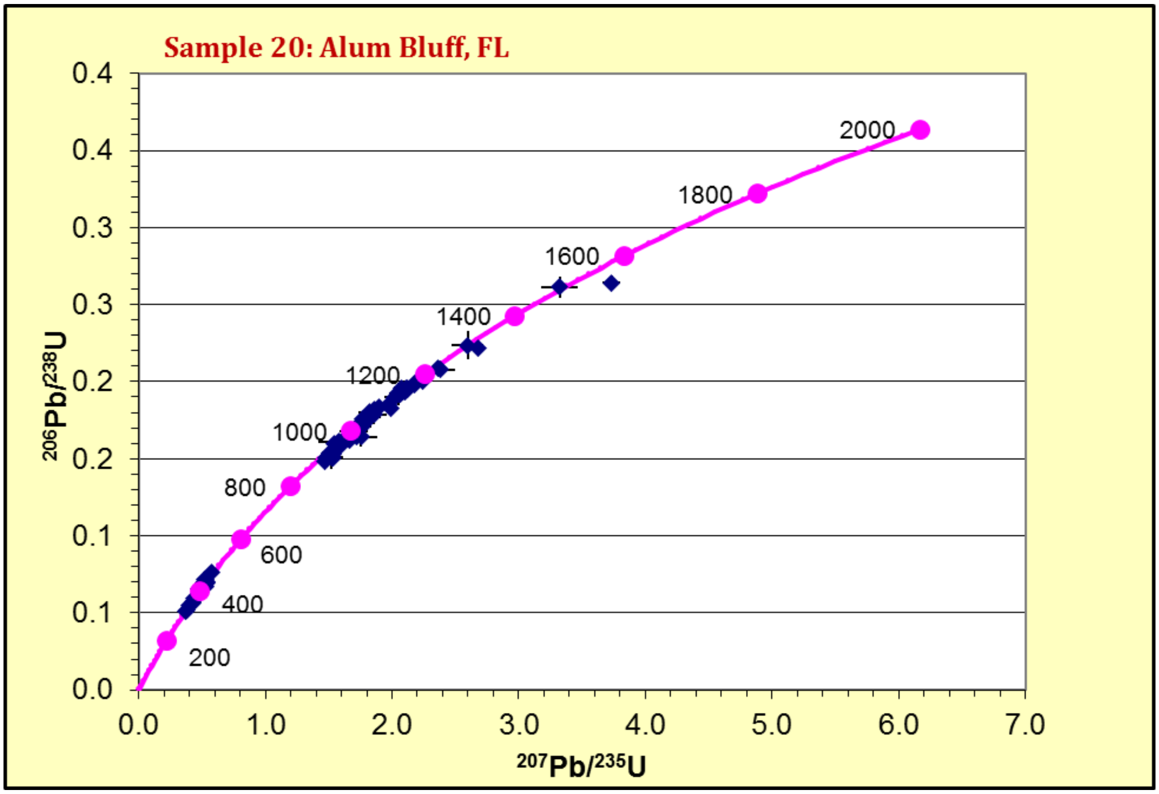
Sample 20: Alum Bluff, FL
0.4
0.4
0.3
0.3
0.2
0.2
0.1
0.1
0.0
2000
1800
1600
1400
1200
1000
800
600
400
200
0.0
1.0
2.0
3.0
4.0
5.0
6.0
7.0
206Pb/238U
207Pb/235U

APPENDIX III

FREQUENCY HISTOGRAM AND PROBABILITY DENSITY PLOT OF DETRITAL ZIRCON SAMPLES

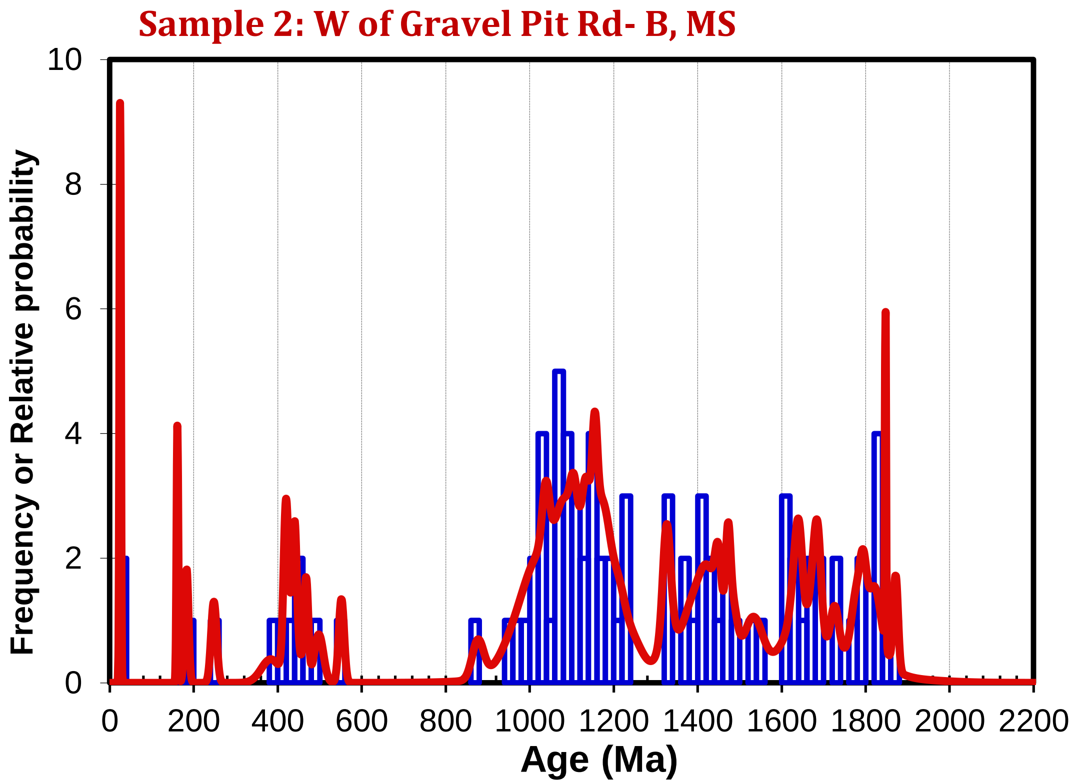

Sample 2: W of Gravel Pit Rd- B, MS
Frequency or Relative probability
0
2
4
6
8
10
0
200
400
600
800
1000
1200
1400
1600
1800
2000
2200
Age (Ma)

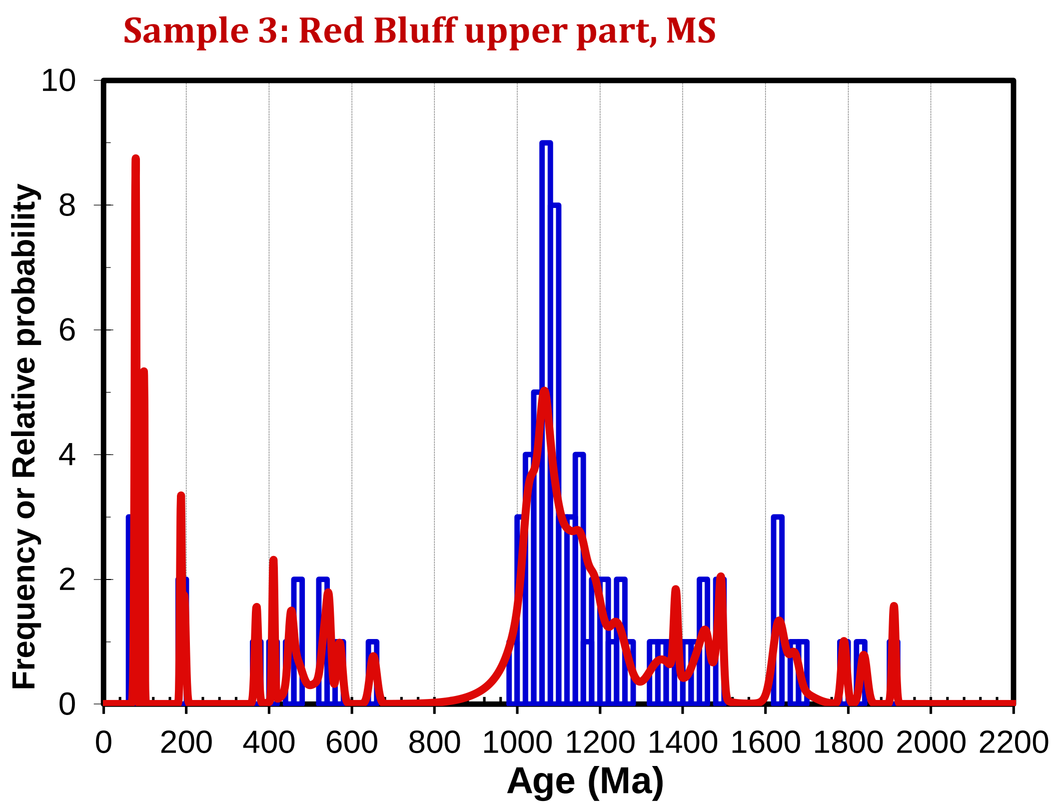

Sample 3: Red Bluff upper part, MS
Frequency or Relative probability
0
2
4
6
8
10
0
200
400
600
800
1000
1200
1400
1600
1800
2000
2200
Age (Ma)

Sample 4: Red Bluff middle part, MS

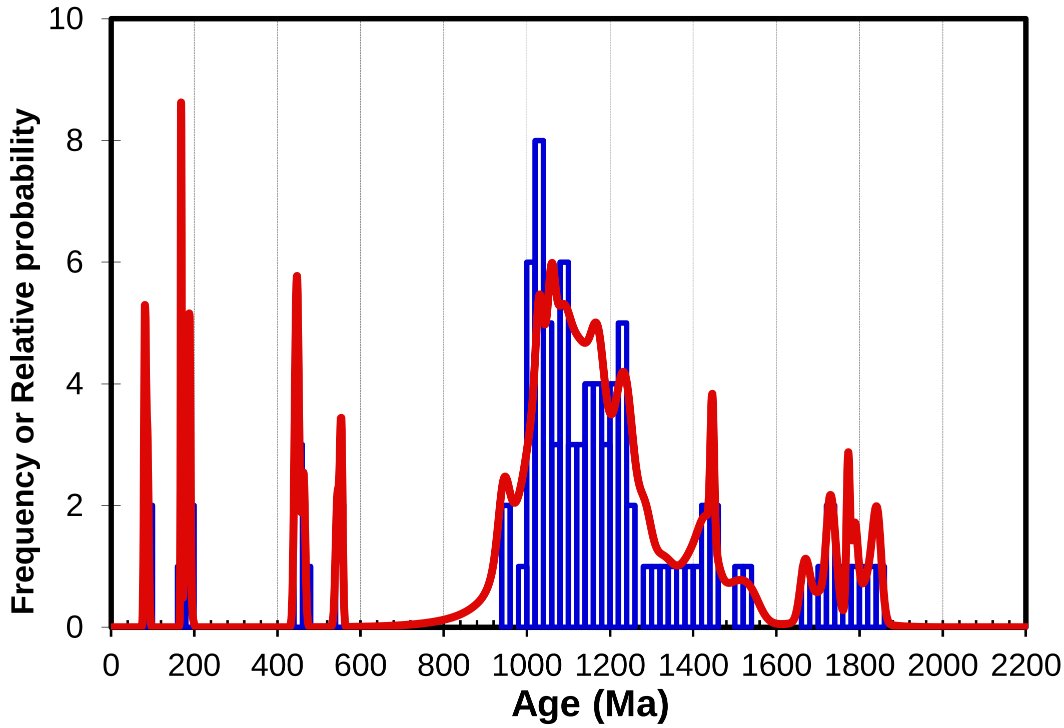

Sample 5:Red Bluff lower part, MS

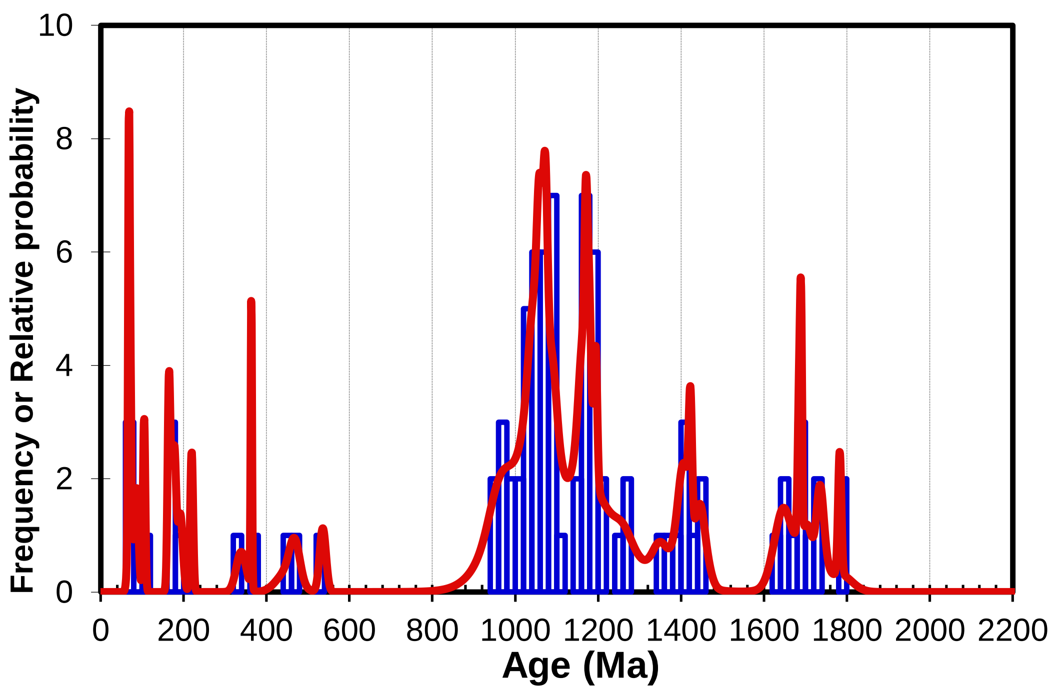

Sample 6: Dry Creek near Maggie, MS

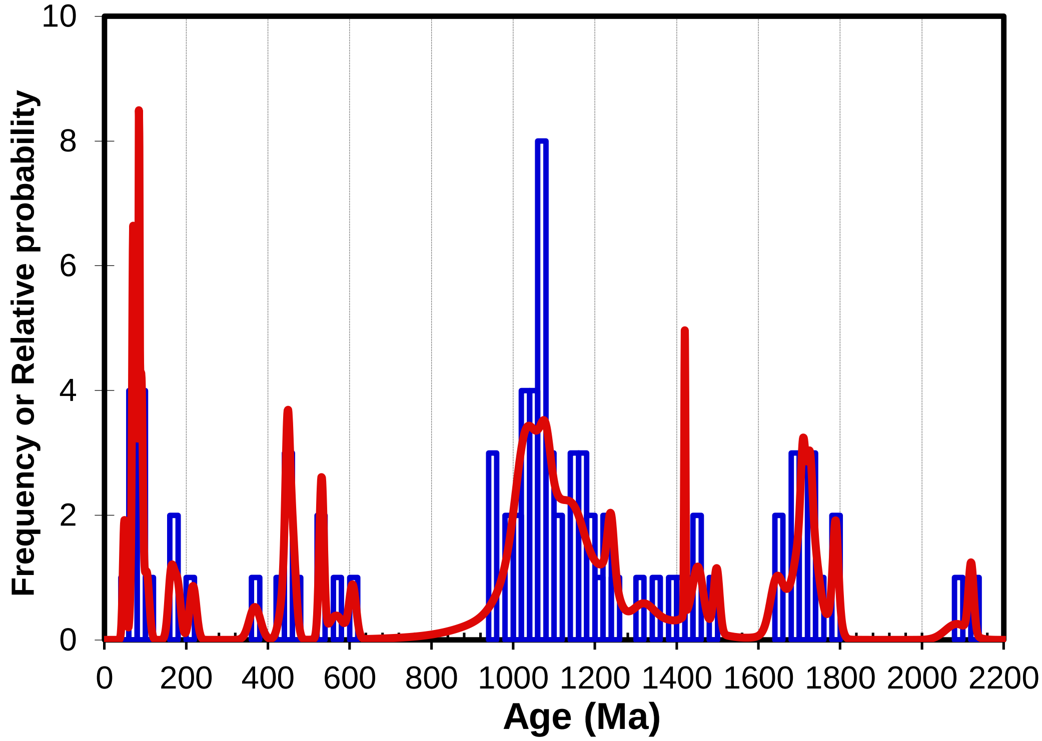

Sample 7: MS HWY 84 Collins, MS

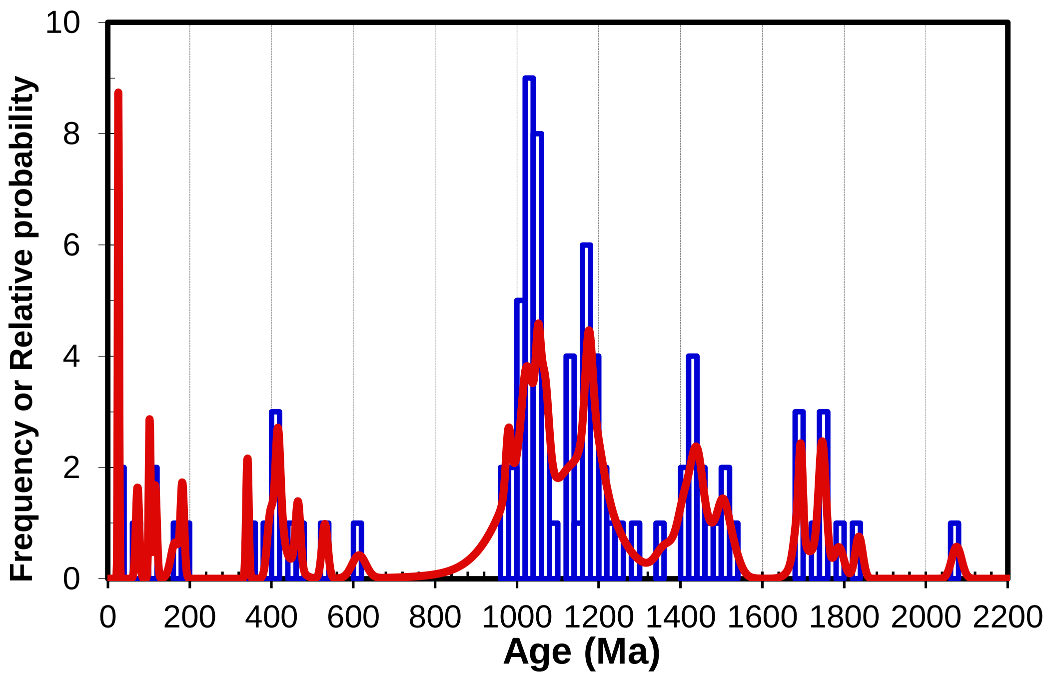

Sample 10: McCallum Landfill A, MS

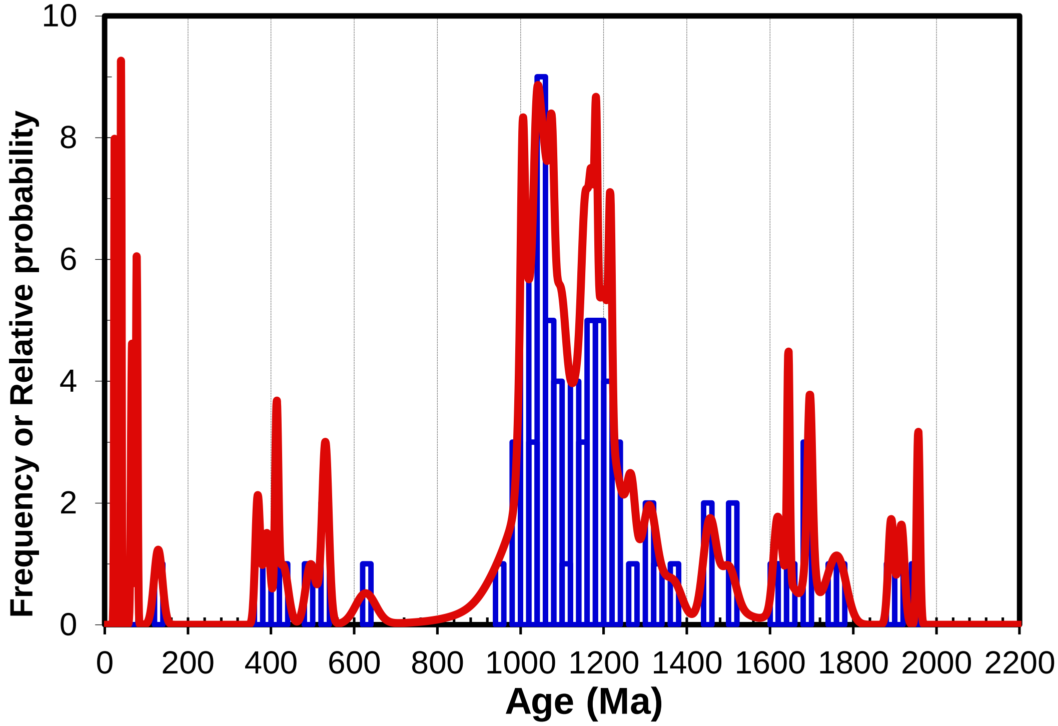

Sample 11: McCallum Landfill B, MS

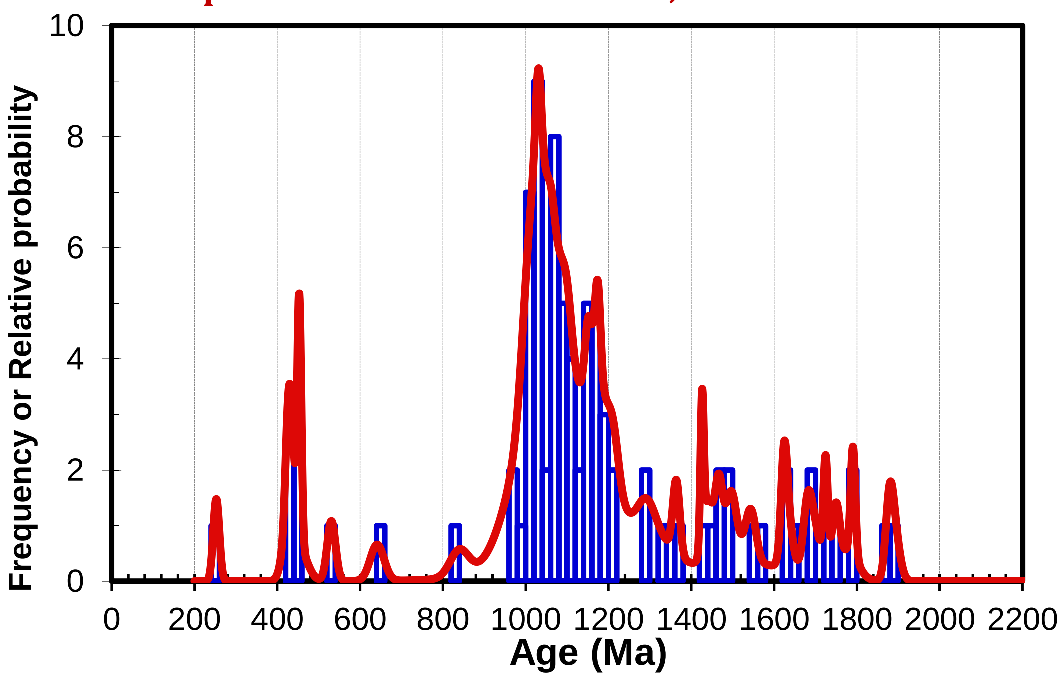

Sample 12: MS HWY 29 N of Runnels, MS

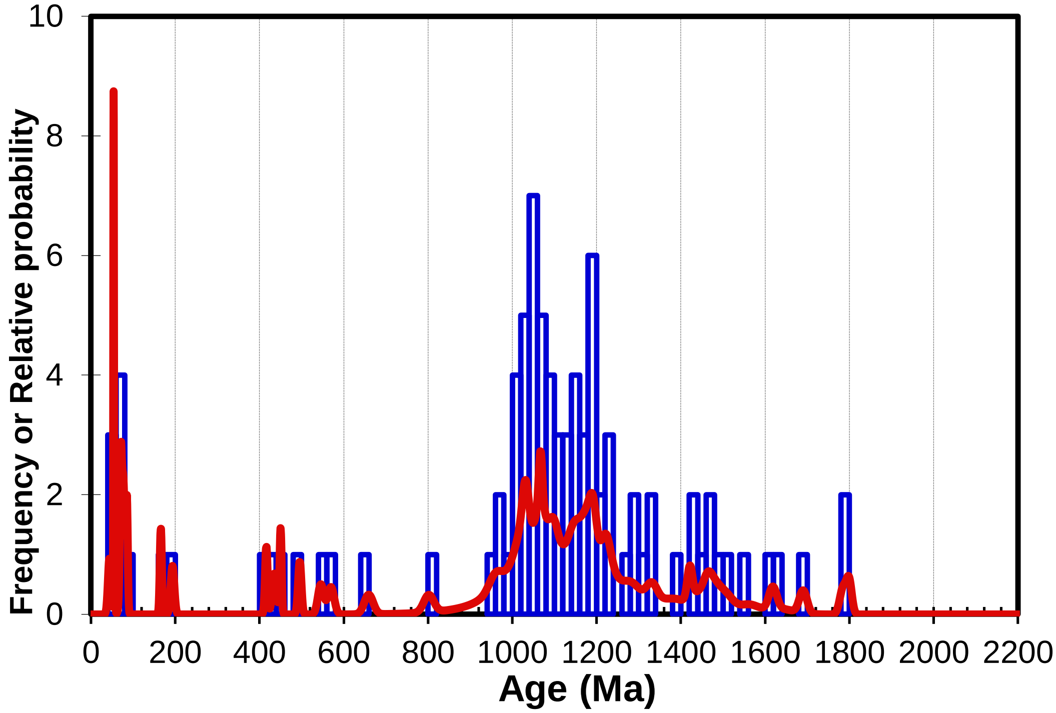

Sample 13: MS HWY 42 W of Runnels, MS

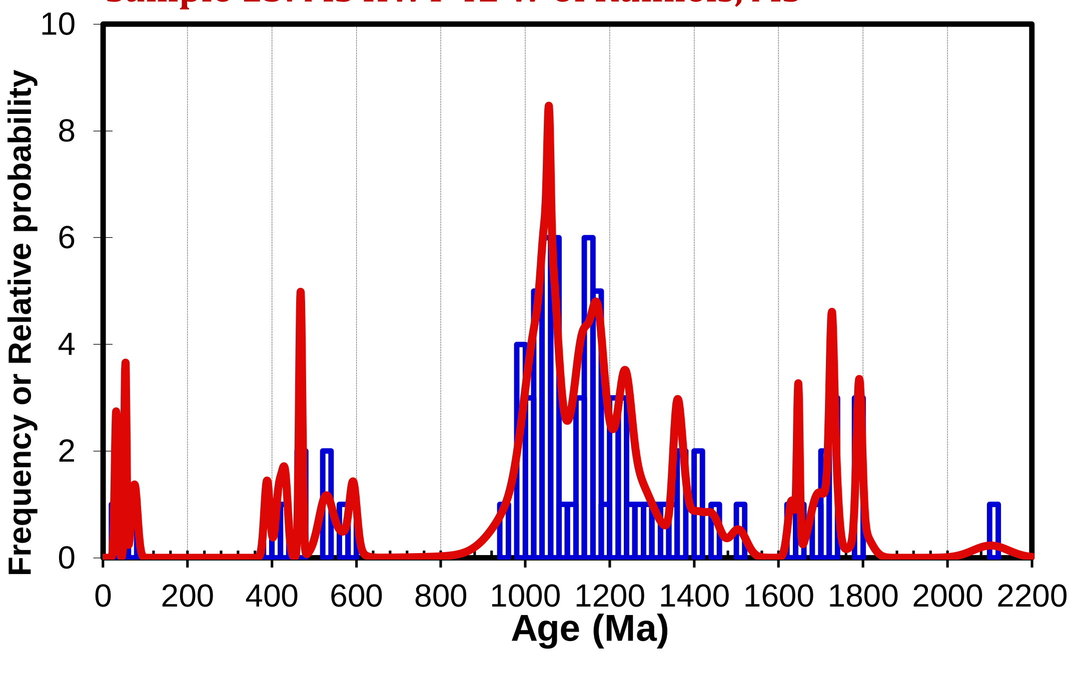

Sample 14: N of Petal, MS

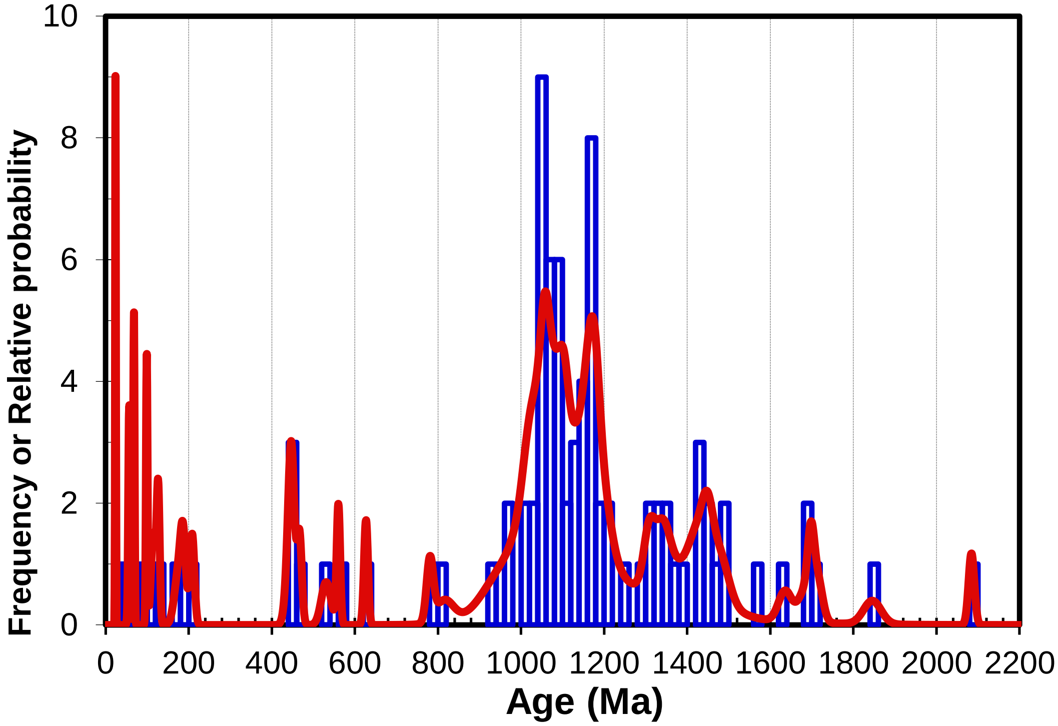

Sample 15: Love Quarry, MS

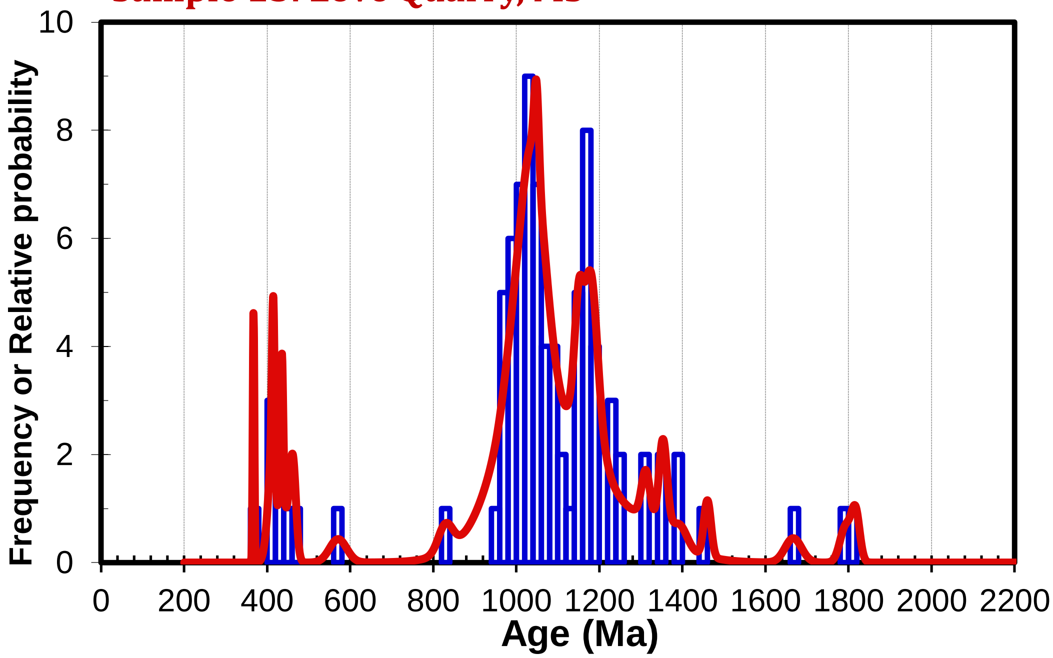

Sample 16: Perry Quarry, MS

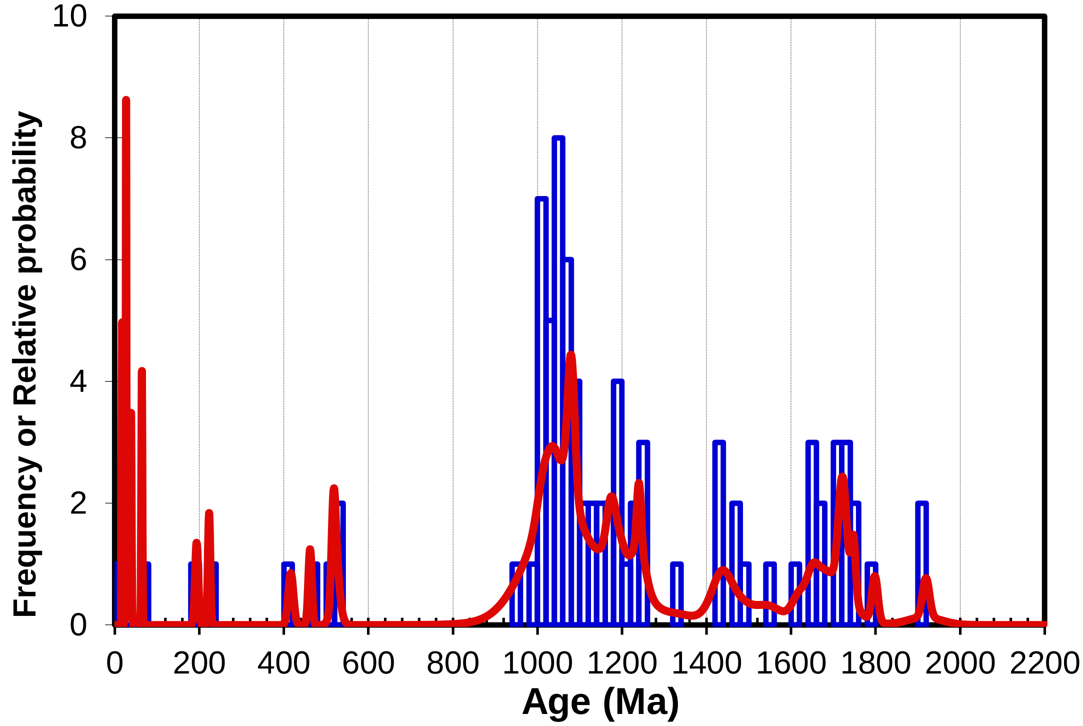

Sample 17: Atmore Landfill, AL

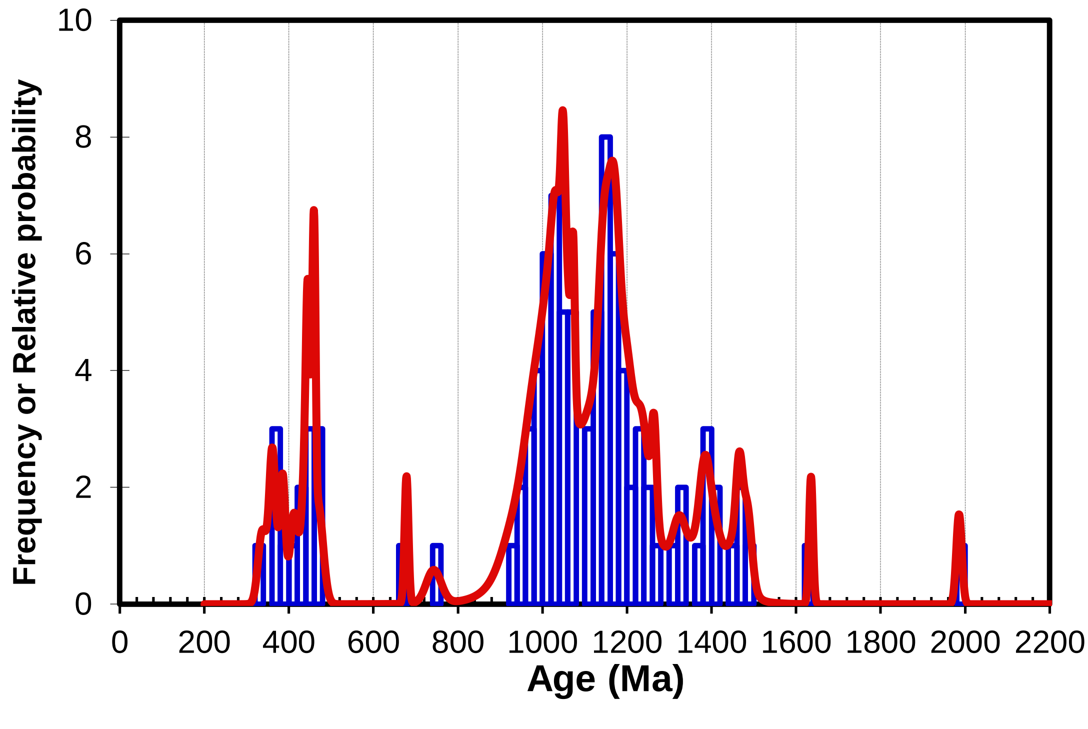

Sample 18: N of Jackson, AL

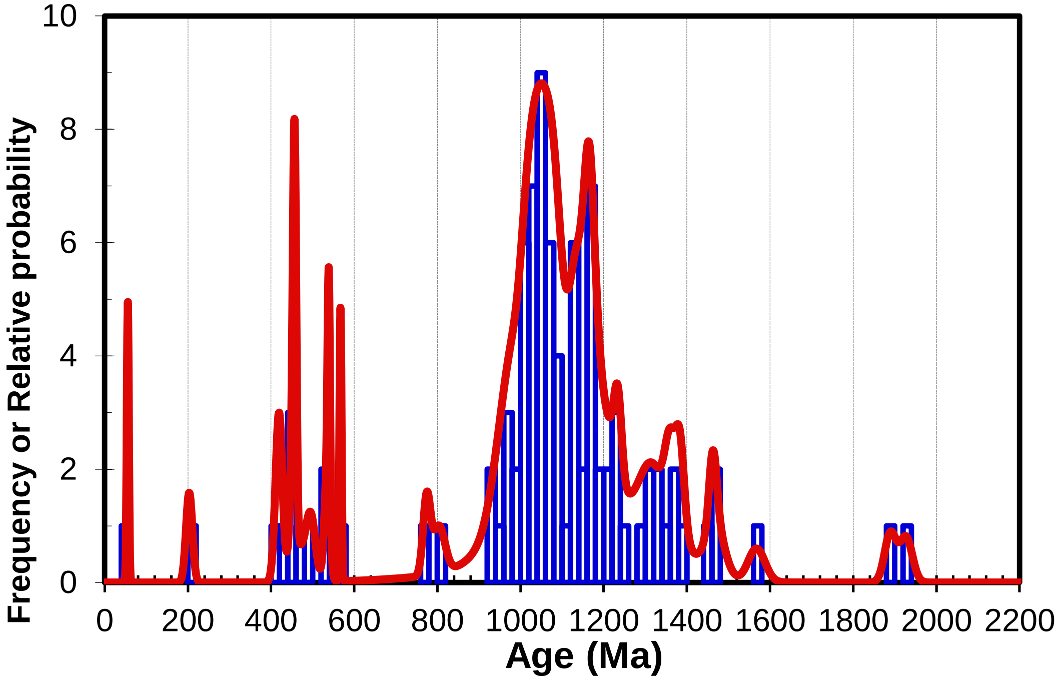

Sample 19: Citronelle, AL

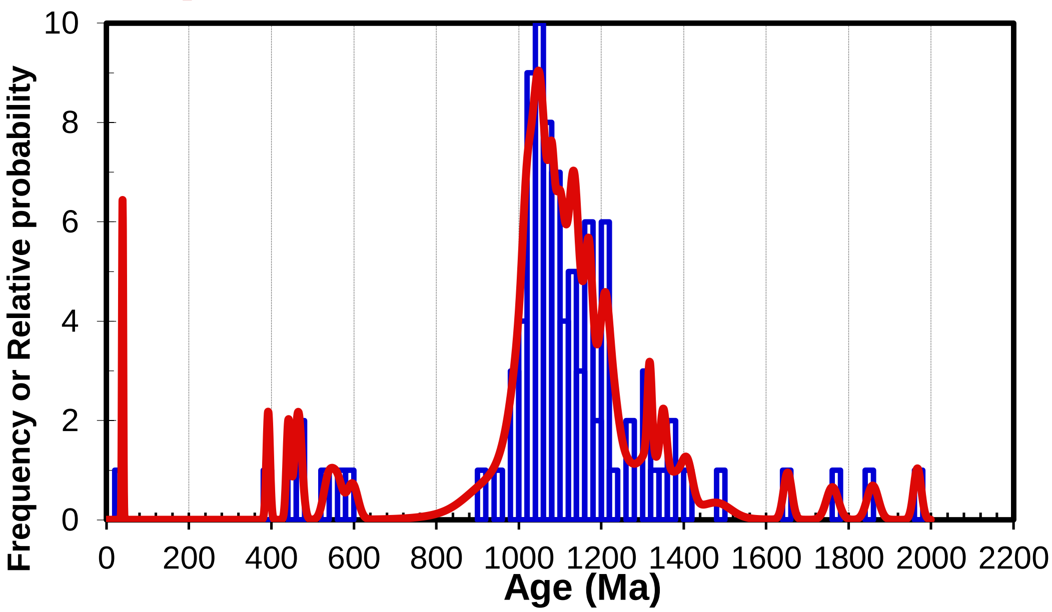

Sample 20: Alum Bluff, FL

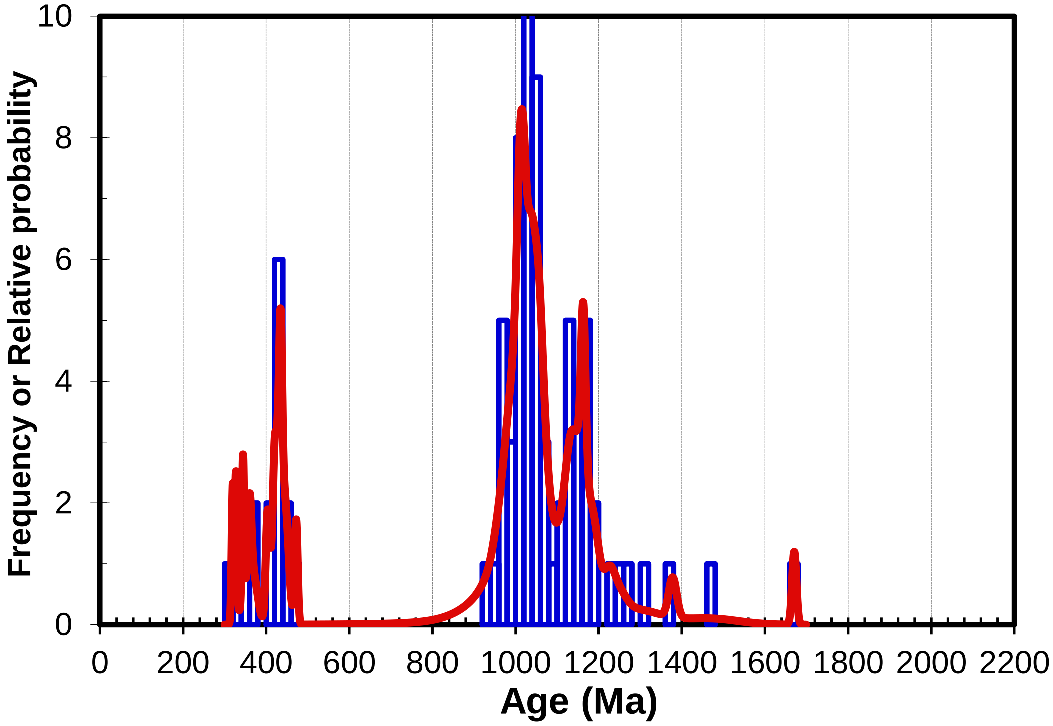

VITA

Mary Sheela Biswal was born in Orissa, India, to Sanjukta and Tapas Biswal. She grew up in Mumbai, India and most of her early years were spent travelling and discovering her interests. She entered the St. Xavier's College, Mumbai in 2005 and majored in geology. She was admitted to the prestigious Indian Institute of Technology, Bombay, in 2008 and completed her Master's in geology. During an indecisive period after her degree, she started to work for a Mining Company as a geologist. Within a couple of years of her work, she realized her inclination towards research and applied for a Ph.D. program outside of India. She started her graduate program in year 2012 under the supervision of Dr. Robert D. Hatcher, Jr., at the University of Tennessee. She defended her thesis to earn a second Master's degree during fall, 2015. She intends to digress into a broader entrepreneurship field where she can use her knowledge of geology and possibly work with science- and technology-based industry.